



University  
of Glasgow

Bhutta, Musab Saeed (2014) *Investigating the role of the ESCRT proteins in cytokinesis*. PhD thesis.

<http://theses.gla.ac.uk/4958/>

Copyright and moral rights for this thesis are retained by the author

A copy can be downloaded for personal non-commercial research or study, without prior permission or charge

This thesis cannot be reproduced or quoted extensively from without first obtaining permission in writing from the Author

The content must not be changed in any way or sold commercially in any format or medium without the formal permission of the Author

When referring to this work, full bibliographic details including the author, title, awarding institution and date of the thesis must be given



University of Glasgow | College of Medical,  
Veterinary & Life Sciences

# Investigating the role of the ESCRT proteins in cytokinesis

**Musab Saeed Bhutta B.Sc. (Hons)**

Thesis submitted in fulfilment of the requirements for the Degree of  
Doctor of Philosophy

February 2014

Institute of Molecular, Cell and Systems Biology

College of Medical, Veterinary and Life Sciences

University of Glasgow

© Musab Saeed Bhutta, February 2014

## Summary

Endosomal sorting complex required for transport (ESCRT) proteins are conserved between Archaea, yeast and mammalian cells. ESCRT proteins mediate membrane scission events in the downregulation of ubiquitin-labelled receptors via the multivesicular body (MVB) pathway and HIV budding from host cells. In addition, ESCRT proteins have an established role in the final stage of cytokinesis, abscission, although the functional mechanisms by which they mediate daughter cell separation have yet to be demonstrated biochemically *in vivo*.

The ESCRT machinery is composed of four subunits: ESCRT-0, -I, -II and -III; and the modular composition of the ESCRT machinery is reflected in its various functions. ESCRT proteins are recruited sequentially to the endosomal membrane for MVB formation: first, ESCRT-0 sequesters ubiquitylated cargo destined for degradation; second, ESCRT-I and II deform the peripheral membrane to produce a bud; and third, ESCRT-III constricts the bud neck to form an intraluminal vesicle. Thereafter, AAA-ATPase Vps4 redistributes ESCRT-III subunits back into the cytoplasm to mediate further MVB formation; it is the association of ESCRT-III and Vps4 that forms the conserved membrane scission machinery in all ESCRT functions.

At a precise time during late cytokinesis, ESCRT-I protein TSG101 and ESCRT-associated protein ALIX are recruited to the midbody where they localise to both sides of the dense proteinaceous Flemming body through interactions with CEP55; TSG101 and ALIX in turn recruit ESCRT-III components. Immediately before abscission, ESCRT-III redistributes outwards from the Flemming body to the abscission site; microtubules are severed and the daughter cells separate. Thereafter, ESCRT-III appears on the opposite side of the Flemming body and the process is repeated to produce the midbody remnant. How this selective and specific redistribution of ESCRT proteins is regulated in space and time remains unsolved.

To this end, polo kinase and Cdc14 phosphatase were identified as potential regulators of ESCRT function, due to their significant functions in regulating cytokinesis. Homologues in the fission yeast *Schizosaccharomyces pombe*, Plo1p

and Clp1p, are required for either formation or stabilisation of the contractile ring that drives cytoplasmic cleavage. Furthermore, human polo-like kinase, Plk1, maintains CEP55 in a phosphorylated state to negatively regulate its localisation to the midbody; and although Plk1 proteolysis facilitates abscission complex assembly, Plk1 re-emerges at the midbody late during cytokinesis. It was hypothesised, therefore, that polo kinase and Cdc14 phosphatase regulate members of the ESCRT machinery to mediate cytokinetic abscission.

To address this, fission yeast was used to study interactions between Plo1p, Clp1p and ESCRT proteins. Initially, ESCRT function in fission yeast cytokinesis was examined by characterising formation of the specialised medial cell wall, the septum, in individual ESCRT deletion strains. ESCRT genes were shown to be required for cytokinesis and cell separation in fission yeast, implying a role for the ESCRT proteins in this process.

A yeast genetics approach was then employed to investigate genetic interactions between ESCRT genes and *plo1*<sup>+</sup> and *clp1*<sup>+</sup>. Double mutants were produced from crosses between ESCRT deletion strains and mutants of *plo1* and *clp1*. Synthetic defective growth rates were observed in double mutants, indicating genetic interactions between *plo1*<sup>+</sup>, *clp1*<sup>+</sup> and ESCRT genes. The effect of single ESCRT deletions on vacuolar sorting in fission yeast was characterised. Single mutants of *plo1* and *clp1* were also shown to affect vacuolar sorting, indicating novel roles for these proteins in fission yeast. Analysis of vacuolar sorting in double mutants provided further characterisation of observed genetic interactions: *plo1*<sup>+</sup> was regarded to function upstream of ESCRT genes, and *clp1*<sup>+</sup> downstream.

The yeast two-hybrid assay was used to further analyse interactions. Physical interactions were observed between Plo1p and Sst4p (human HRS, ESCRT-0), Vps28p (VPS28, ESCRT-I), Vps25p (EAP20, ESCRT-II), Vps20p (CHMP6, ESCRT-III) and Vps32p (CHMP4, ESCRT-III). Clp1p was also shown to interact with Vps28p.

Interactions were then investigated between human homologues of these proteins in HEK293 cells. Immunoprecipitation and co-immunoprecipitation methods revealed interactions between Plk1 and CHMP6, CHMP4B, CHMP3 and CHMP2A (all ESCRT-III). Furthermore, interactions were demonstrated between CDC14A and CHMP4B and CHMP2A.

These results indicate that polo kinase and Cdc14 phosphatase have conserved roles in regulating ESCRT components. Characterising the nature and functional significance of this regulation may inform future approaches in disease prevention.

# Table of Contents

Summary .....	2
Table of Contents .....	5
List of Tables.....	9
List of Figures .....	10
Acknowledgements .....	12
Author's Declaration .....	13
List of Abbreviations.....	14
<b>Chapter 1 Introduction.....</b>	<b>17</b>
<b>1.1 Cell division is a well-regulated network of events .....</b>	<b>17</b>
1.1.1 Cell division consists of nuclear and cytoplasmic divisions .....	17
1.1.2 Cell cycle control by cyclin-dependent kinases .....	18
<b>1.2 <i>Schizosaccharomyces pombe</i> as a model organism for cytokinesis.....</b>	<b>20</b>
1.2.1 Fission yeast facilitates rapid genetic and protein analysis .....	20
1.2.2 Cytokinesis proceeds by the assembly and constriction of an actomyosin contractile ring .....	20
1.2.3 Fission yeast septation is analogous to cytokinesis in higher eukaryotes .....	21
<b>1.3 Polo kinase is a key regulator of cytokinesis .....</b>	<b>23</b>
1.3.1 Polo kinase functions are well-conserved between species.....	23
1.3.2 Fission yeast Plo1p controls cytokinesis and septation .....	23
1.3.3 Human Plk1 controls cytokinesis .....	24
1.3.4 Polo kinase function is subject to spatiotemporal control .....	25
<b>1.4 Cdc14 phosphatase is a key regulator of cytokinesis .....</b>	<b>27</b>
1.4.1 Cdc14 functions are well-conserved between species .....	27
1.4.2 Clp1p maintains orderly M/G1 progression .....	28
1.4.3 Temporal control of Clp1p activation is required for M/G1 progression .....	29
1.4.4 Clp1p regulates ring stability and contraction.....	29
1.4.5 Clp1p controls M/G1 gene expression .....	30
1.4.6 The role of human CDC14 in mitosis and cytokinesis is less well characterised.....	30
<b>1.5 Abcission is mediated by the ESCRT proteins .....</b>	<b>32</b>
1.5.1 Abcission occurs at the midbody in mammalian cells.....	32
1.5.2 Vesicular trafficking is required for secondary ingression.....	32
1.5.3 ESCRT proteins form a conserved membrane scission machinery .....	33
1.5.4 ESCRT function has diverged between species.....	34
1.5.5 A division of labour exists among the ESCRT machinery .....	35
1.5.6 ESCRT-III is recruited to the midbody by TSG101/ESCRT-I and ALIX.....	36
1.5.7 ESCRT-III performs the final scission step of cytokinesis .....	37
1.5.8 How is the ESCRT machinery regulated in cytokinesis?.....	40
<b>1.6 The present study.....</b>	<b>42</b>
1.6.1 Hypotheses .....	42
1.6.2 Approach and principal findings .....	42
<b>Chapter 2 Materials and methods .....</b>	<b>44</b>
<b>2.1 Materials.....</b>	<b>44</b>
2.1.1 Media.....	44
2.1.1.1 <i>E. coli</i> media .....	44

2.1.1.2	<i>S. cerevisiae</i> media .....	44
2.1.1.3	<i>S. pombe</i> media .....	44
2.1.2	Oligonucleotide primers .....	45
2.1.3	Plasmid sources .....	48
2.1.4	Antibodies .....	50
2.1.4.1	Primary antibodies .....	50
2.1.4.2	Secondary antibodies .....	51
2.1.5	Standard solutions .....	51
<b>2.2</b>	<b>Yeast methods .....</b>	<b>54</b>
2.2.1	General yeast methods .....	54
2.2.2	Septal defect analysis in <i>S. pombe</i> .....	54
2.2.3	<i>S. pombe</i> mating and tetrad dissection .....	54
2.2.4	Selection of double mutants .....	55
2.2.4.1	Genotypic screening .....	55
2.2.4.2	Mating type determination .....	55
2.2.5	Growth rate comparison .....	55
2.2.6	FM 4-64 staining of <i>S. pombe</i> vacuoles for confocal microscopy .....	56
2.2.7	Cell imaging via confocal microscopy .....	56
2.2.8	Cloning events for yeast two-hybrid analysis .....	56
2.2.9	Transformation of <i>S. pombe</i> and <i>S. cerevisiae</i> .....	57
2.2.10	X-Gal overlay assay .....	58
<b>2.3</b>	<b>Mammalian methods .....</b>	<b>59</b>
2.3.1	Cell culture .....	59
2.3.1.1	General cell culture maintenance .....	59
2.3.1.2	Culturing cells from frozen stocks .....	59
2.3.1.3	HeLa cell culture maintenance .....	59
2.3.1.4	HEK293 cell culture maintenance .....	59
2.3.2	Amplification of the plasmids containing ESCRT genes .....	60
2.3.3	Transfecting HeLa and HEK293 cells for lysate preparation .....	60
2.3.4	HeLa cell synchronisation and lysate preparation .....	60
2.3.4.1	HeLa cell synchronisation to metaphase and telophase .....	60
2.3.4.2	Plk1 inhibition in HeLa cells .....	61
2.3.4.3	Lysate preparation .....	61
2.3.5	Protein quantification .....	61
2.3.6	Immunoprecipitation from HeLa or HEK293 lysates .....	62
2.3.6.1	Immunoprecipitation of Plk1 from non-transfected HeLa or HEK293 lysates .....	62
2.3.6.2	Immunoprecipitation of FOXM1, ESCRT proteins and various epitopes .....	62
2.3.7	SDS-PAGE .....	63
2.3.8	Immunoblotting .....	63
2.3.8.1	Transfer to nitrocellulose membrane .....	63
2.3.8.2	Membrane blocking and protein probing .....	63
2.3.8.3	Immunodetection of proteins via enhanced chemiluminescence (ECL) .....	64

<b>Chapter 3</b>	<b><i>Plo1p</i> kinase and <i>Clp1p</i> (<i>Cdc14</i>) phosphatase interact with ESCRT proteins to control cell division in <i>S. pombe</i> .....</b>	<b>65</b>
<b>3.1</b>	<b>Introduction .....</b>	<b>65</b>
3.1.1	Fission yeast is an appropriate model organism for studying cell division .....	65
3.1.2	Aims .....	65
<b>3.2</b>	<b>Results .....</b>	<b>67</b>
3.2.1	The ESCRT proteins have a role in cell division in fission yeast .....	67
3.2.2	Cell division defects observed in ESCRT mutants are exacerbated when combined with mutants of <i>plo1</i> , <i>clp1</i> , <i>mid1</i> and <i>ark1</i> .....	71
3.2.3	<i>plo1</i> <sup>+</sup> and <i>clp1</i> <sup>+</sup> interact genetically with ESCRT genes .....	72
3.2.4	<i>Plo1p</i> and <i>Clp1p</i> affect ESCRT-mediated vesicular trafficking .....	77
3.2.5	<i>Plo1p</i> and <i>Clp1p</i> interact physically with ESCRT proteins .....	85

<b>3.3 Concluding remarks</b> .....	<b>101</b>
3.3.1 Principal findings .....	101
3.3.2 Summary.....	101
<b>Chapter 4 Plk1 kinase and CDC14A phosphatase interact with ESCRT proteins in humans</b> .....	<b>102</b>
<b>4.1 Introduction</b> .....	<b>102</b>
4.1.1 Fission yeast shares a high degree of conservation with higher eukaryotes.....	102
4.1.2 Aims and key findings .....	102
<b>4.2 Results</b> .....	<b>104</b>
4.2.1 Investigating interactions between Plk1 and ESCRT proteins in HeLa cells.....	104
4.2.1.1 Interactions between Plk1 and FOXM1 were detected in metaphase-arrested cells.....	104
4.2.1.2 Immunoprecipitation of VPS28 did not yield detection of Plk1 .....	108
4.2.2 Investigating interactions between Plk1 and over-expressed ESCRT proteins in HEK293 cells .....	111
4.2.2.1 Plk1 interacts with CHMP6 (fission yeast Vps20p, ESCRT-III) .....	111
4.2.2.2 Plk1 interacts with CHMP6 (Vps20p, ESCRT-III), CHMP4B (Vps32p, ESCRT-III), CHMP3 (Vps24p, ESCRT-III) and CHMP2A (Vps2p, ESCRT-III).....	113
4.2.2.3 Sequential immunoprecipitation of Plk1 depletes the co-immunoprecipitation of CHMP6, CHMP4B, CHMP3 and CHMP2A .....	115
4.2.2.4 Plk1-ESCRT interactions remained after increasing the detergent in assay conditions..	119
4.2.2.5 Immunoprecipitation of ESCRT proteins did not result in the co-immunoprecipitation of endogenous or over-expressed Plk1 .....	122
4.2.2.6 Immunoprecipitation of Plk1-YFP did not result in co-immunoprecipitation of ESCRT proteins.....	125
4.2.2.7 Immunoprecipitation of ESCRT proteins did not result in detection of Plk1.K82R-YFP ..	128
4.2.3 Investigating interactions between Plk1 and over-expressed ESCRT proteins in HeLa cells.....	129
4.2.3.1 Over-expression of ESCRT proteins in HeLa cells was not robust and did not yield observable interactions.....	129
4.2.3.2 Immunoprecipitation of over-expressed ESCRT proteins did not yield detection of Plk1.....	129
4.2.4 Investigating an ESCRT protein phospho-mobility shift in the presence of Plk1 kinase inhibition .....	130
4.2.5 Investigating interactions between CDC14A and ESCRT proteins on over-expressing both in HEK293 cells.....	132
4.2.5.1 CDC14A phosphatase interacts with CHMP4B (Vps32p, ESCRT-III).....	132
4.2.5.2 CDC14A interacts with CHMP4B (Vps32p, ESCRT-III) and CHMP2A (Vps2p, ESCRT-III)...	134
4.2.5.3 Phosphatase-dead CDC14A.C278S interacts with CHMP4B and CHMP2A.....	136
4.2.5.4 Immunoprecipitation of ESCRT proteins yields detection of CDC14A .....	138
4.2.5.5 Immunoprecipitation of ESCRT proteins did not yield detection of phosphatase-dead CDC14A.C278S .....	140
4.2.6 Concluding remarks .....	143
4.2.6.1 Principal findings .....	143
4.2.6.2 Summary .....	144
<b>Chapter 5 Discussion</b> .....	<b>145</b>
<b>5.1 Plo1p kinase and Clp1 (Cdc14) phosphatase interact with ESCRT proteins in fission yeast</b> 145	
5.1.1 Analysis of the key findings .....	145
5.1.2 A model for ESCRT regulation by Plo1p and Clp1p.....	149
<b>5.2 Plk1 kinase and CDC14A phosphatase interact with ESCRT proteins in humans</b> .....	<b>151</b>
5.2.1 Analysis of the key findings .....	151
5.2.2 Refining the model .....	155
<b>5.3 Future work</b> .....	<b>157</b>

5.4	Conclusion.....	160
<b>Chapter 6</b>	<b>Appendices .....</b>	<b>161</b>
6.1	Strains list .....	161
6.1.1	<i>Schizosaccharomyces pombe</i> strains .....	161
6.1.2	<i>Saccharomyces cerevisiae</i> strains .....	166
6.2	Septation defects in mutants of <i>plo1</i> , <i>clp1</i> , <i>mid1</i> and <i>ark1</i> .....	170
6.2.1	Single mutants <i>plo1-ts35</i> , <i>clp1Δ</i> , <i>mid1Δ</i> , <i>ark1-T8</i> and <i>ark1-T11</i> exhibit septation defects	170
6.2.2	Septation defects in <i>plo1-ts35</i> double mutants .....	172
6.2.3	Septation defects in <i>clp1Δ</i> double mutants.....	174
6.2.4	Septation defects in <i>mid1Δ</i> double mutants .....	176
6.2.5	Septation defects in <i>ark1ts</i> double mutants .....	178
6.2.5.1	Septation defects in <i>ark1-T8</i> double mutants.....	178
6.2.5.2	Septation defects in <i>ark1-T11</i> double mutants.....	180
	<b>List of References .....</b>	<b>182</b>

## List of Tables

### Chapter 3

Table 3.1: Synthetic growth phenotypes of mutations in <i>plo1</i> , <i>clp1</i> and ESCRT genes. ....	76
Table 3.2: A summary of synthetic growth phenotypes of mutations in <i>plo1</i> , <i>clp1</i> and ESCRT genes. ....	76
Table 3.3: A summary of the vacuolar sorting epistasis data in double mutants of ESCRT genes and <i>plo1</i> or <i>clp1</i> . ....	85
Table 3.4: A summary of blue yeast observation in yeast two-hybrid analysis of Plo1p and the ESCRT proteins. ....	92
Table 3.5: A summary of blue yeast observation in yeast two-hybrid analysis of Clp1p and the ESCRT proteins. ....	99
Table 3.6: A summary of physical interactions between the ESCRT proteins and Plo1p and Clp1p.....	100

### Chapter 5

Table 5.1: Genetic and physical interactions were observed between ESCRT proteins, polo kinase and Cdc14 phosphatase in fission yeast and humans. ....	156
--	-----

# List of Figures

## Chapter 1

Figure 1.1: Feedback loops within fission yeast signalling contribute to Cdc2p downregulation. ....	28
Figure 1.2: Multivesicular body biogenesis is mediated by sequential function of ESCRT subunits. ....	36
Figure 1.3: A model for ESCRT-mediated cytokinetic abscission. ....	38

## Chapter 3

Figure 3.1: ESCRT proteins are required for septation in fission yeast. ....	70
Figure 3.2: Fission yeast double mutants were generated by ascus dissection. .	73
Figure 3.3: <i>plo1-ts35</i> shows synthetic growth phenotypes with <i>vps28Δ</i> . ....	74
Figure 3.4: Defective vacuolar sorting is observed in fission yeast with individual chromosomal deletions of ESCRT genes. ....	79
Figure 3.5: Mutants of <i>plo1</i> and <i>clp1</i> cause defective vacuolar sorting in fission yeast. ....	81
Figure 3.6: Genetic interactions between <i>plo1-ts35</i> and ESCRT deletions in controlling cell sorting. ....	83
Figure 3.7: Genetic interactions between <i>clp1Δ</i> and ESCRT deletions in controlling cell sorting. ....	85
Figure 3.8: Vps28p, Vps20p and Vps32p physically interact with wild-type Plo1p. ....	88
Figure 3.9: Sst4p and Vps25p physically interact with kinase-dead Plo1p. ....	89
Figure 3.10: Sst6p, Vps36p, Vps2p and Vps4p do not exhibit physical interactions with Plo1p. ....	91
Figure 3.11: ESCRT proteins do not definitively exhibit physical interactions with Clp1p. ....	97
Figure 3.12: Vps28p and Clp1aa.1-371 results in a negative yeast two-hybrid assay. ....	97

## Chapter 4

Figure 4.1: FOXM1 did not co-immunoprecipitate with Plk1 from asynchronous HeLa cell lysates. ....	105
Figure 4.2: FOXM1 co-immunoprecipitated with Plk1 from metaphase-arrested cell lysates. ....	107
Figure 4.3: Plk1 did not co-immunoprecipitate with VPS28 from asynchronous or arrested HeLa cell lysates. ....	109
Figure 4.4: Over-expressed CHMP6 co-immunoprecipitates with Plk1 from HEK293 cell lysates. ....	112
Figure 4.5: Over-expressed CHMP6, CHMP4B, CHMP3 and CHMP2A co-immunoprecipitate with Plk1 from HEK293 cell lysates. ....	114
Figure 4.6: Sequential immunoprecipitation of Plk1 depletes detection of over-expressed ESCRT proteins from anti-Plk1 immunoprecipitations. ....	118
Figure 4.7: CHMP6, CHMP4B, CHMP3 and CHMP2A co-immunoprecipitate with Plk1 in the presence of increased detergent conditions. ....	121
Figure 4.8: Plk1 was not detected on immunoprecipitation of ESCRT proteins. ....	124

Figure 4.9: Anti-GFP immunoprecipitation of Plk1-YFP did not result in co-immunoprecipitation of ESCRT proteins. ....	127
Figure 4.10: A phospho-mobility shift in the position of CHMP6 was not detected on inhibition of Plk1. ....	131
Figure 4.11: CHMP4B co-immunoprecipitates with CDC14A from HEK293 cell lysates. ....	133
Figure 4.12: CHMP4B and CHMP2A co-immunoprecipitate with CDC14A from HEK293 cell lysates. ....	135
Figure 4.13: CHMP4B and CHMP2A co-immunoprecipitate with phosphatase-dead CDC14A.C278S from HEK293 cell lysates. ....	137
Figure 4.14: CDC14A co-immunoprecipitates with CHMP4B and CHMP2A. ....	139
Figure 4.15: CDC14A.C278S was not detected on immunoprecipitation of VPS28, CHMP4B or CHMP2A. ....	141

## Chapter 5

Figure 5.1: Plo1p and Clp1p interact with members of the ESCRT machinery in fission yeast. ....	150
Figure 5.2: Plk1 and CDC14A interact with members of the ESCRT machinery in human cells. ....	155

## Chapter 6

Figure 6.1: Fission yeast with mutants in <i>plo1</i> , <i>ark1</i> , <i>clp1</i> and <i>mid1</i> exhibit septal defects. ....	171
Figure 6.2: Double mutants of ESCRT deletions and <i>plo1-ts35</i> exhibit septation defects in fission yeast. ....	173
Figure 6.3: Double mutants of ESCRT deletions and <i>clp1</i> $\Delta$ exhibit septation defects in fission yeast. ....	175
Figure 6.4: Double mutants of ESCRT deletions and <i>mid1</i> $\Delta$ exhibit septation defects in fission yeast. ....	177
Figure 6.5: Double mutants of ESCRT deletions and <i>ark1-T8</i> exhibit septation defects in fission yeast. ....	179
Figure 6.6: Double mutants of ESCRT deletions and <i>ark1-T11</i> exhibit septation defects in fission yeast. ....	181

## Acknowledgements

All praise and thanks are due to Almighty God, Who fashioned us, and appointed for us hearing, sight and intellects, that we may be grateful to Him.

I must express thanks first and foremost to my family. I dedicate this thesis to the two greatest blessings in my life - my mother and father. They have sacrificed everything for my brothers and me and have gone above and beyond to allow me to pursue my PhD. I am also profoundly grateful to my wife Saira for her encouragement and fantastic help in producing many of the figures in this thesis.

It has been my honour to be the student of two excellent scientists, Dr Christopher McInerny and Prof Gwyn Gould. Their complementary styles of guidance, nurture and encouragement over the past four years have made this entire process so much more enjoyable. I thank them both from the bottom of my heart.

I thank Prof Nia Bryant, Dr Joe Gray and Prof Hugh Nimmo for their advice and encouragement throughout my project.

I am immensely grateful to Dr Jennifer Roccisana for her patient instruction, commenting on my thesis, and for being a good friend. I also owe a debt of gratitude to Steph Evans for her help and friendship throughout my PhD. I would like to thank Dr Sue Krause, Dr Hélia Neto and Dr Louse Collins for guiding me through various techniques and aspects of my research. I would also like to thank Josie McGhie, Clare Miller, Brinta Roy and past and present members of Labs 217 and 241.

Finally, I thank the Biotechnology and Biological Sciences Research Council for funding this research.

## **Author's Declaration**

I declare that the work presented in this thesis is my own, unless otherwise stated. It is entirely of my own composition and has not, in whole or in part, been submitted for any other degree.

Musab Saeed Bhutta

September 2013

## List of Abbreviations

AAA-ATPase	-	ATPase associated with diverse cellular activities
ALIX	-	Apoptosis-linked gene 2-interacting protein
APC/C	-	Anaphase promoting complex/cyclosome
ATP	-	Adenosine triphosphate
BSA	-	Bovine serum albumin
Cdc	-	Cell division cycle
Cdk	-	Cyclin-dependent kinase
CEP55	-	Centrosomal protein of 55 kDa
CHMP	-	Charged multivesicular body protein
Clp1	-	Cdc14-like phosphatase
DAPI	-	4'6-diamidino-2-phenylindole, dihydrochloride
DMEM	-	Dulbecco's Modified Eagle Medium
DMSO	-	Dimethyl sulfoxide
DTT	-	Dithiothreitol
EDTA	-	Ethylenediaminetetraacetic acid
EGTA	-	Ethylene glycol-bis(2-aminoethylether)-N,N,NJ,NJ-tetraacetic acid
EMM	-	Edinburgh minimal medium
ESCRT	-	Endosomal sorting complex required for transport

FCS EU	-	Foetal calf serum (European Union)
FIP3	-	Family of Rab11-interacting proteins
GAPDH	-	Glyceraldehyde 3-phosphate dehydrogenase
GFP	-	Green fluorescent protein
HA	-	Haemagglutinin
HEK	-	Human embryonic kidney
HIV	-	Human immunodeficiency virus
IgG	-	Immunoglobulin G
ILV	-	Intraluminal vesicle
kb	-	Kilobase
kDa	-	Kilo Dalton
LSB	-	Laemmli sample buffer
ME	-	Malt extract
MEN	-	Mitotic exit network
MVB	-	Multivesicular body
<i>nmt</i>	-	not-made-in-thiamine
PBF	-	PCB-binding factor
PBS	-	Phosphate-buffered saline
PBST	-	Phosphate-buffered saline + Triton X-100

PCB	-	Pombe cell cycle box
PCR	-	Polymerase chain reaction
Plk	-	Polo-like kinase
RFP	-	Red fluorescent protein
SDS	-	Sodium dodecyl sulphate
SDS-PAGE	-	SDS-polyacrylamide gel electrophoresis
SIN	-	Septation initiation network
TBS	-	Tris-buffered saline
TBST	-	Tris-buffered saline + Tween-20
TSG101	-	Tumour susceptibility gene 101
Ub-GFP- <i>SpCPS</i>	-	Ubiquitin-GFP-labelled <i>S. pombe</i> carboxypeptidase S
Vps	-	Vacuolar protein sorting
X-Gal	-	5-bromo-4-chloro-3-indolyl- $\beta$ -D-galactopyranoside
YE	-	Yeast extract
YFP	-	Yellow fluorescent protein

# Chapter 1 Introduction

## 1.1 Cell division is a well-regulated network of events

### 1.1.1 Cell division consists of nuclear and cytoplasmic divisions

From self-serving single-celled organisms to the most complex sentient beings to walk this planet, every life form is required to multiply - or else make way for another to thrive in its place. To this end, cells of all branches of life have developed intricate mechanisms to multiply their genetic material and effectively divide it among offspring. Cell division consists of two processes: nuclear division, mitosis, and cytoplasmic division, cytokinesis (Balasubramanian et al. 2004).

Following the successful replication of DNA in interphase, cells enter mitosis. The first stage is prophase, wherein the chromosomes condense and the duplicated centrosomes generate the mitotic spindle. In prometaphase, the nuclear membrane breaks down and chromosomes attach to the spindle. In metaphase, chromosomes are arranged along the equator of the spindle, and then separate and move towards opposite poles during anaphase. By telophase, the chromosomes have reached opposite poles and the nuclear envelope reforms for each of the new daughter nuclei. Cytokinesis begins early in anaphase with the assembly of the actomyosin contractile ring. The actomyosin ring then constricts to rapidly ingress the plasma membrane and divide the cytoplasm in two; membrane fusion events then resolve the membrane to separate the two daughter cells. Regulatory mechanisms are required to temporally restrict DNA replication, mitosis and cytokinesis in a manner that ensures chromosome segregation follows duplication, and that cytokinesis is halted in the event that the requirements of a checkpoint are not met (Balasubramanian et al. 2004).

The events of the cell cycle can be described within the parameters of four successive phases: G1, S, G2 and M (Forsburg and Nurse 1991). S phase refers to the period in which genetic material is duplicated, and M in which this material is separated between progeny. G1 and G2 represent gap phases in which the cell grows, and various checks are made prior to DNA synthesis and mitosis, respectively. In higher eukaryotes, such as humans, incorrect regulation of the

cell cycle is a major cause of disease, most prominently cancer. Therefore, cell cycle control is crucial to maintain the fidelity and proper timing of events. These checks and balances, therefore, preserve the genetic integrity of offspring and ensure that they receive sufficient provisions for life.

### 1.1.2 Cell cycle control by cyclin-dependent kinases

The key inducer of mitosis among several eukaryotes is the well-conserved family of cyclin-dependent kinases (Cdks), a class of serine/threonine kinases. Human cells possess four Cdk homologues, of which Cdk1 is the master regulator of S phase and mitosis. The budding yeast *Saccharomyces cerevisiae* and the fission yeast *Schizosaccharomyces pombe* possess one unique Cdk each, Cdc28 and Cdc2p, respectively. Cdks regulate the cell cycle by phosphorylating substrates in a cell cycle-dependent manner to mediate functions including initiation of DNA replication, chromosome condensation, nuclear envelope breakdown and cytoskeletal reorganisation. Due to their diverse and important functions, Cdk activity is tightly regulated throughout the cell cycle. Cdk activity is mediated by various mechanisms, including modification of its phosphorylation state and cell cycle-specific associations with either stimulatory or inhibitory subunits (Morgan 1995).

Cdks are named for their association with cyclin to form an active heterodimer. Eukaryotic cells possess distinct cyclin subunits that differentially associate with Cdks for their activation at different stages of the cell cycle. Cellular levels of cyclins oscillate according to expression levels and targeted proteolysis (Koepp et al. 1999). In mammalian cells, Cyclin B associates with Cdk1 to drive mitosis. Cdk is inactive as a monomer, thus controlling cyclin levels in cells provides an elaborate method of controlling Cdk activity. Four cyclin subunits exist in fission yeast, of which only Cdc13p is essential for cell survival, due to its association with fission yeast Cdk, Cdc2p, to drive mitosis and inhibit re-initiation of S phase (Hayles et al. 1994). Cdc2p activity must be abolished for mitotic exit, and among the methods fission yeast employs to decrease Cdc2p activity is by directing Cdc13p for ubiquitin-dependent degradation according to its N-terminal 'destruction box' motif (Yamano et al. 2000). Cdk functions in fission yeast and human cells will be mentioned further in *Sections 1.3* and *1.4*.

The research topic of this study is the conserved requirement and regulation of a multi-protein complex in cytokinesis. This introductory chapter will begin with a brief discussion on the effectiveness of using fission yeast as a model organism for cytokinesis. Thereafter, with relevance to this thesis, the key regulators of cytokinesis, polo kinase and Cdc14 phosphatase, will be described. Focus will then turn to the multi-protein complex, the ESCRT proteins. Finally, the predominant models of mammalian abscission will be outlined, with particular emphasis on the role of ESCRT proteins.

## **1.2 *Schizosaccharomyces pombe* as a model organism for cytokinesis**

### **1.2.1 Fission yeast facilitates rapid genetic and protein analysis**

Fission yeast are rod-shaped cells that divide by fission following formation of a medial cell wall, termed *septation*. Fission yeast provides an attractive model organism in which to study cytokinesis due to the ease by which it may be genetically manipulated and phenotypically characterised, including by microscopy. It is also, with respect to mammalian cells, simple and inexpensive to handle, and crucially, the genes used for cytokinesis have been well conserved among eukaryotes. This can be illustrated in fission yeast lacking the major cell cycle regulator *cdc2*<sup>+</sup>, as function can be rescued in such mutants by incorporating its human homologue (Lee & Nurse 1987). Furthermore, studies in fission yeast cytokinesis have uncovered a greater catalogue of knowledge regarding contractile ring assembly, constriction and disassembly than in any other organism (Pollard & Wu 2010).

### **1.2.2 Cytokinesis proceeds by the assembly and constriction of an actomyosin contractile ring**

As in humans, fission yeast cytokinesis proceeds with the assembly, maturation and constriction of an actomyosin contractile ring, although this process begins earlier in fission yeast than in animal cells (Burgess & Chang 2005). Many aspects of this system are conserved among higher eukaryotes, including the basic composition of the actomyosin ring. However, unlike fission yeast, which marks the division plane by the position of the nucleus, human cells determine the division plane by the position of the mitotic apparatus. The purpose of cytokinesis is to produce two daughter cells with identical nuclei, therefore correct positioning and timely contraction of the actomyosin ring is absolutely crucial.

Studies in fission yeast revealed the existence of precursors to the contractile ring, membrane-associated interphase nodes, which together with the nucleus determine the division site (Vavylonis et al. 2008). Polo kinase, Plo1p, releases Mid1p from the nucleus, which matures the interphase nodes into cytokinesis nodes by the addition of myosin-II and proteins required for actin assembly and

ring stability (Pollard & Wu 2010). Mid1p is required for correct ring positioning, and mutations in *mid1*<sup>+</sup> lead to aberrant ring positioning and septation (Sohrmann et al. 1996). Fluorescence recovery after photobleaching of myosin-II light chain revealed rapid recovery, indicative of highly dynamic protein exchanges during maturation of nodes (Vavylonis et al. 2008). Nucleated actin forms a network between nodes, which initiates myosin-II-mediated movement of nodes to bundle in order to establish a contractile ring attached to the plasma membrane. Ring contraction then proceeds via interactions between actin and myosin-II, possibly in the same sliding mechanism known to occur in striated muscle; although unlike in muscle, actin is lost as the ring contracts (Pollard & Wu 2010).

Well-coordinated timing of chromosome segregation and ring constriction is crucial, and part of this requirement is the downregulation of Cdc2p, whose activity inhibits cytokinesis (Krapp et al. 2004). The septation initiation network (SIN) is responsible for downregulating Cdc2p, and this signalling cascade is further responsible for plasma membrane ingression with deposition of a specialised cell wall, the septum (Jin et al. 2006).

### **1.2.3 Fission yeast septation is analogous to cytokinesis in higher eukaryotes**

The septation initiation network is a signalling cascade consisting of protein kinases and a GTPase, Spg1p. SIN components assemble at the spindle pole bodies via interactions with scaffolding proteins Sid4p and Cdc11p and are required for actomyosin ring maturation and contraction, as well as septal deposition (Krapp et al. 2004). Plo1p kinase associates with Sid4p to promote the Spg1p active state, making Plo1p a key regulator of cytokinesis in fission yeast (Krapp et al. 2004).

SIN signalling is not required for formation of the contractile ring, as rings have been shown to form in fission yeast with mutations in SIN genes; however, rings fail to contract, and are subsequently disassembled (Jin et al. 2006). Although the processes by which ring stability is achieved by the SIN pathway are not fully understood, it is known that SIN signalling is required for phosphorylation of Cdc14-like phosphatase 1, Clp1p, which is then retained in the cytosol and

anchored to the actomyosin ring by Mid1p (Hachet & Simanis 2008; Chen et al. 2008; Clifford et al. 2008). In its free and active state, Clp1p is able to dephosphorylate Cdc15p, a component of mature cytokinesis nodes, which in turn contributes to ring stability (Pollard & Wu 2010).

The final step of fission yeast cell division is medial fission by formation of a multi-layered septum, composed of one primary septum at the site of constriction, and two secondary septa that subsequently form the new ends of the daughter cells (Johnson et al. 1973). Centripetal primary septal deposition occurs simultaneously with constriction of the actomyosin ring (Liu et al. 1999). The processes required for the dissolution of the primary septum still remain unclear, although it has been noted that lessons learned from fission yeast septation may enhance our understanding of cytokinesis in mammalian cells (Jin et al. 2006; Pollard & Wu 2010).

## 1.3 Polo kinase is a key regulator of cytokinesis

### 1.3.1 Polo kinase functions are well-conserved between species

Polo kinase was first identified in *Drosophila melanogaster*, in which mutants resulted in monopolar spindles and condensed chromosomes (Sunkel & Glover 1988). Homologues have since been identified in humans, budding and fission yeasts, and several other organisms. DNA and protein analyses have since identified sequences and motifs of interest, principally, a highly conserved N-terminal kinase domain and two regulatory polo box regions at the C-terminus. Structural and functional studies have shown that polo boxes act as a single functional domain for phosphopeptide recognition; thus, polo kinase preferentially selects substrates that have been previously phosphorylated, particularly by Cdk (Elia et al. 2003). Polo box domains also mediate substrate interactions and polo kinase subcellular localisation (Reynolds & Ohkura 2003). Furthermore, polo box domains function to maintain the inactive form of human polo, Plk1, as polo box and kinase domains have been shown to associate with each other; stimulatory phosphorylation by Aurora A on Thr210 relieves the inhibitory effect of polo box association (Jang et al. 2002; Seki et al. 2008).

Polo kinases are key regulators of mitotic events and cytokinesis, with well-conserved functions between eukaryotes, from amplifying Cdk activity to induce mitosis, to promoting chromatid separation (Toyoshima-Morimoto et al. 2001; Sumara et al. 2002). A number of these functions in fission yeast and human cells will be explored.

### 1.3.2 Fission yeast Plo1p controls cytokinesis and septation

Mutants of fission yeast *plo1<sup>+</sup>* provided the first evidence of a role for Plo1p in cytokinesis. Ohkura et al. (1995) conducted several experiments using various mutant and over-expressing strains to demonstrate the significance of *plo1<sup>+</sup>* in mitotic progression and septal formation. By switching off *plo1<sup>+</sup>* expression, they characterised three phenotypes: cells with a cluster of over-condensed chromosomes, and unseptated cells with either two clusters of over-condensed chromosomes or two uncondensed interphase nuclei. By repressing transcription of *plo1<sup>+</sup>* using an *nmt* (not-made-in-thiamine) promoter (Maundrell 1993), they characterised a further phenotype whereby the cells failed to form a septum but

still underwent one or two nuclear divisions, the result of which being unseptated cells with multiple nuclei (Ohkura et al. 1995). This was confirmed by fluorescence microscopy of cells stained with Calcofluor and DAPI. The *nmt* repression was also utilised to demonstrate that *plo1*<sup>+</sup> is involved in the formation of the contractile ring. Shortly after the daughter cells separate, actin is localised at the newly divided end of the cell. It then localises to both poles of the cell during interphase and subsequently forms a ring around the circumference in a plane determined by the location of the nucleus. However, on repressing *plo1*<sup>+</sup> activity, less than 20% of cells formed the actin ring.

A series of over-expression experiments were also described which revealed cells with over-condensed chromosomes, or an interphase nucleus compressed or displaced by one or more septa (Ohkura et al. 1995). These experiments further demonstrated that Plo1p is a key regulator of septal formation as over-expression in G1 or G2 cells gave rise to the septum. However, Plo1p regulates septal formation via the SIN pathway (*Section 1.2.3*), so spontaneous septal formation is only apparent in cells with a functional SIN pathway (Tanaka et al. 2001). Although human cells lack septa, it has been noted that the influence Plo1p exerts on septation may have consequences for cytokinesis in higher eukaryotes (Ohkura et al. 1995).

Plo1p phosphorylates Mid1p, which is required for correct positioning of the actomyosin contractile ring (*Section 1.2.2*). Mid1p resides predominantly in the nucleus during interphase and Plo1p is required for Mid1p nuclear exit during early mitosis; *plo1*<sup>+</sup> over-expression leads to premature exit of Mid1p from the nucleus (Bähler et al. 1998). Furthermore, Plo1p phosphorylates multiple residues in the Mid1p N-terminus; phosphorylation of these residues is indirectly required for myosin-II recruitment (Almonacid et al. 2011). Plo1p, therefore, couples mitotic onset with contractile ring assembly.

### **1.3.3 Human Plk1 controls cytokinesis**

Similar to its yeast counterparts, human Plk1 is required for the rapid amplification of Cdk1 activity to induce mitotic entry; Plk1 achieves this by multiple means. Firstly, Plk1 phosphorylates CDC25C, the activating phosphatase of Cdk1-Cyclin B; Plk1 phosphorylation of CDC25C in a nuclear export signal

sequence activates CDC25C and causes translocation to the nucleus (Toyoshima-Morimoto et al. 2002). Secondly, Plk1 phosphorylates Cdk1-Cyclin B inhibitory kinases, Wee1 and Myt1; in the case of Wee1, Plk1 phosphorylation leads to proteolysis (Watanabe et al. 2004; Nakajima et al. 2003). Additionally, Plk1 phosphorylates Cyclin B at centrosomes, which may cause nuclear translocation of Cdk1-Cyclin B (Toyoshima-Morimoto et al. 2001). It is by these mechanisms that Plk1 triggers the activation of Cdk1-Cyclin B, and thus mitosis, in human cells.

The dynamic control of cytokinesis by Plk1 is reflected in dynamic localisation of Plk1 at specific structures throughout mitosis and cytokinesis. Plk1 localisation is diffuse during interphase and then targeted to centrosomes late in G2 phase. Plk1 persists at centrosomes and kinetochores throughout mitosis, although a significant sub-population translocates to the midbody during cytokinesis (Golsteyn et al. 1995; Taniguchi et al. 2002). Plk1 is recruited to the midbody by PRC1, the microtubule-associated protein regulating cytokinesis 1, and Plk1 itself primes PRC1 for secondary phosphorylation post-anaphase. To prevent early recruitment to the midbody during prophase or prometaphase, PRC1 exists in a phosphorylated state, thus inhibiting untimely midbody formation (Neef et al. 2003; Hu et al. 2012). Plk1 localisation to the midbody is essential for cytokinesis, as Plk1 initiates actomyosin ring formation by recruiting guanine nucleotide exchange factor ECT2 to activate GTPase RhoA, which in turn drives actin polymerisation and myosin activation (Petronczki et al. 2007). Furthermore, Plk1 downregulation is required for translocation of CEP55 to the midbody for assembly of the abscission machinery (*Section 1.5.6*); however, Plk1 levels peak again late in cytokinesis (Hu et al. 2012), which may reveal further functions for Plk1 in cytokinesis.

### **1.3.4 Polo kinase function is subject to spatiotemporal control**

Temporal activation of polo kinase is essential for the temporal control of cytokinesis. Polo kinase activity is subject to various levels of control, including transcriptional activation, subcellular localisation, and substrate selectivity by phospho-priming.

In addition to dynamic localisation of Plk1 during mitosis (*Section 1.3.3*), Plk1 is controlled by dynamic gene expression, as expression levels peak during G2 and M phase, as a result of directed transcription followed by proteolysis (Laoukili et al. 2005; Lindon & Pines 2004). Fission yeast mRNA analysis has revealed that *plp1<sup>+</sup>* is one of approximately 40 genes that are transcribed in a wave at the M/G1 interval (Ng et al. 2006). Many of these genes, including *plp1<sup>+</sup>*, share an upstream activating sequence known as the *pombe cell cycle box* (PCB); this is upregulated by a complex of proteins termed the PCB-binding factor (PBF) (Anderson et al. 2002). Plo1p itself has been shown to phosphorylate Mbx1p, a member of the PBF, thus contributing to its own regulation (Papadopoulou et al. 2010). Homologues of this system, termed *forkhead homologue-dependent transcription factor* (FKH-TF), have been found in budding yeast and humans. Interestingly, the human forkhead transcription factor, FOXM1, has been shown to drive G2/M-specific *PLK1<sup>+</sup>* transcription and is itself a substrate for Plk1 phosphorylation (Laoukili et al. 2005; Fu et al. 2008). Therefore, similar to the Mbx1p-directed Plo1p positive feedback loop observed in fission yeast, Plk1 drives activation of its own gene expression by phospho-activation of FOXM1.

The two C-terminal polo-box regions conserved among all polo kinases fold to form one functional polo box domain, which then binds phosphorylated peptides (*Section 1.3.1*). Therefore, Plk1 function can be restricted and directed to particular phospho-primed substrates; Cdk1 or even Plk1 itself may conduct this priming phosphorylation (Park et al. 2010).

Polo kinases are subject to tight regulation for the orderly completion of mitosis and cytokinesis. By increasing expression of polo kinase at particular times in the cell cycle, and targeting its functions towards specific substrates, cells are able to spatially and temporally control polo kinase for maximum effect.

## 1.4 Cdc14 phosphatase is a key regulator of cytokinesis

### 1.4.1 Cdc14 functions are well-conserved between species

Cdc14 was first identified in budding yeast as a phosphatase responsible for downregulation of Cdk activity and mitotic exit. Homologues have since been identified in fission yeast, mammalian cells and other organisms. This highly conserved protein-tyrosine phosphatase family have important functions in conducting dephosphorylation events required for mitotic exit and have roles in cytokinesis (Mocciaro & Schiebel 2010).

Budding yeast Cdc14 is localised in the nucleolus during interphase, but is released via the mitotic exit network (MEN) and causes the downregulation of Cdc28 via the proteolysis of Clb, homologous to human Cdk1-Cyclin B (Trautmann et al. 2001). MEN signalling facilitates the full release of Cdc14 from the nucleolus via a positive feedback loop driven by Cdc14 itself. Furthermore, a negative feedback loop incorporating Cdc28 drives Cdc14 release from the nucleolus during anaphase via the disruption of the interaction between Cdc14 and its competitive inhibitor, Net1/Cfi1 (Visintin et al. 1999). This interaction has proven to be temporally significant as disruption during any stage of the cell cycle leads to downregulation of Cdc28.

Cdc14 is retained in the cytoplasm by the MEN and conducts dephosphorylation events at the kinetochores, spindle body and contractile ring that antagonise Cdc28 activity to drive mitotic exit, as Cdc14 phosphatases have been revealed to elicit preferential binding to substrates of proline-directed kinases, such as Cdk (Wolfe et al. 2006; Clifford et al. 2008; Lanzetti et al. 2007). Cdc28 is needed for mitotic entry, but its activity must be downregulated for mitotic exit and cytokinesis (Trautmann et al. 2001; *Section 1.1.2*). Cdc14 drives Clb cyclin proteolysis by dephosphorylating Cdh1, which activates APC/C-mediated proteolysis of Clb (Schwab et al. 1997). Furthermore, Cdc14 activates by dephosphorylation the Cdc28 inhibitor Sic1, as well as its transcription factor, Swi5; this contributes to stable expression of Sic1 and thus deactivation of Cdc28 (Visintin et al. 1998). Similar transcription factor activation has been noted in *Caenorhabditis elegans* but appears absent in fission yeast (Saito et al. 2004; Lanzetti et al. 2007).

### 1.4.2 Clp1p maintains orderly M/G1 progression

Unlike its budding yeast homologue, fission yeast Clp1p is not required for mitotic exit, but is required for synchronising cytokinesis with the next cell cycle. Deletion mutants of *clp1* result in defects in chromosome segregation and cytokinesis (Trautmann et al. 2004). Clp1p is released early in mitosis from the nucleolus; however, the fission yeast homologue of the MEN, the SIN, is not required for this process, but is required to retain Clp1p in the cytoplasm (Trautmann et al. 2001). Clp1p then antagonises Cdk Cdc2p, which leads to SIN activation. This coordinates cytokinesis and septation with the next cell cycle, in which Cdc2p plays a major role. Fission yeast Clp1p-mediated downregulation of Cdc2p activity is more direct than that of Cdc14 upon Cdc28 in budding yeast (Figure 1.1).

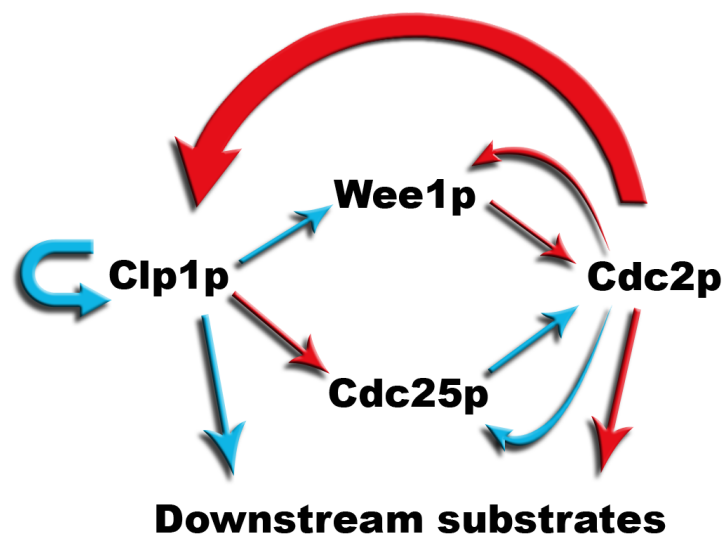


**Figure 1.1: Feedback loops within fission yeast signalling contribute to Cdc2p downregulation.**

Clp1p downregulates Cdc2p by dephosphorylating an inhibitory kinase, Wee1p, and an activating phosphatase, Cdc25p. Cdc2p exerts kinase downregulation on Clp1p, which is capable of auto-dephosphorylation. Both Clp1p and Cdc2p control common substrates via their phosphorylation status. Blue, activation; red, inhibition.

Cdc2p self-regulates by the phosphorylation of its activator and inhibitor (Trautmann et al. 2001). Wee1p is a protein kinase that phosphorylates Cdc2p to inhibit its function and Cdc25p is a phosphatase that acts in opposition to Wee1p, thus activating Cdc2p. Clp1p, therefore, downregulates Cdc2p activity in a direct manner by dephosphorylating both its activator and inhibitor. Clp1p further antagonises Cdc2p activity by reversing inhibitory Cdc2p-dependent

phosphorylation events. For instance, Sid1p is a component of the SIN whose localisation is inhibited by Cdc2p; it is possible that this inhibition is relieved not only by the downregulation of Cdc2p, as mediated by Clp1p, but that Clp1p reverses the phosphorylation of Sid1p, thus activating the SIN in a direct manner.

### **1.4.3 Temporal control of Clp1p activation is required for M/G1 progression**

Regulation of Clp1p differs from the regulation of Cdc14 in budding yeast, which is primarily at the level of control of localisation (Wolfe et al. 2006). Clp1p is released from the nucleolus at the start of mitosis and concentrates at the kinetochores and contractile ring; however, despite being capable of binding substrates, it does not conduct dephosphorylation events until mitotic exit. It must therefore follow that Clp1p is otherwise regulated. It has been suggested that following release from the nucleolus, Clp1p is phosphorylated by Cdc2p, but then auto-dephosphorylates during anaphase to activate SIN signalling (Wolfe et al. 2006). This auto-dephosphorylation in the presence of substrates may elicit a temporal activation of Clp1p substrates, as they would therefore bind in order of affinity.

### **1.4.4 Clp1p regulates ring stability and contraction**

Mutants of *clp1* reveal negative genetic interactions with several cytokinetic genes, including those required for assembly of the actomyosin ring and septal formation. Mid1p is required for proper assembly and orientation of the contractile ring (*Section 1.2.2*). Mid1p plays a scaffolding role at the contractile ring and Clp1p is included in its list of substrates (Clifford et al. 2008). Clp1p may play several important roles at the contractile ring, including regulating the mobility of Cdc15p, which is required for ring stability, and myosin-II, which is required for contraction with actin. Disruption of the Mid1p-Clp1p interaction has particularly deleterious effects on cytokinesis in fission yeast strains already compensating for otherwise silent mutations in actomyosin ring components, thus confirming an important role for Mid1p recruitment to the cytokinetic machinery. Clp1p remains at the ring until the end of cytokinesis and then returns to the nucleolus.

### 1.4.5 Clp1p controls M/G1 gene expression

Clp1p has also emerged as a mediator of cell cycle-specific gene expression via the PBF-PCB complex (Papadopoulou et al. 2010; *Section 1.3.4*). Mbx1p, a member of the PBF, is phosphorylated and activated by both Plo1p and Cdc2p; Cdc2p phosphorylation is reversed by Clp1p to attenuate gene expression. In fission yeast with *clp1Δ* null mutation, gene expression occurs throughout the cell cycle, therefore, Clp1p serves to temporally restrict gene expression to the M/G1 interval. This direct involvement of Clp1p in gene expression is not conserved in budding yeast Cdc14 function, although Cdc14 does dephosphorylate transcription factors to allow them to enter the nucleus (*Section 1.4.1*), thus upregulating transcription, as opposed to Clp1p which downregulates.

### 1.4.6 The role of human CDC14 in mitosis and cytokinesis is less well characterised

Human cells possess two Cdc14 homologues, CDC14A and CDC14B, sharing between them approximately 50% sequence homology, predominantly in the N-terminal region encompassing the protein-tyrosine phosphatase catalytic domain (Lanzetti et al. 2007). Although human CDC14 is less well characterised than its yeast counterparts, mutants of *CDC14A* result in cytokinetic defects (Kaiser et al. 2002).

Human CDC14 isoforms exhibit differential subcellular localisation and functions. CDC14A localises to the centrosomes during interphase and at the spindle midzone and midbody during mitosis and cytokinesis. On the other hand, CDC14B is found predominantly in the nucleolus of interphase cells, and then at the spindle apparatus of mitotic cells (Kaiser et al. 2002). CDC14A depletion results in delayed centrosome separation and chromosome segregation, and defects in cytokinesis (Mailand et al. 2002; Lanzetti et al. 2007). Furthermore, and related to its budding yeast homologue (*Section 1.4.1*), CDC14A has been shown to phosphorylate CDH1 *in vitro*, which lead to reconstitution of the APC/C-CDH1 proteolytic module. This suggests a mechanism similar to budding yeast by which CDC14A may degrade cyclin subunits in human cells (Bembenek & Yu 2001).

Less is known about CDC14B function, although stabilising activities related to microtubules may suggest a role in regulating spindle dynamics in mitosis (Asakawa & Toh-e 2002).

## **1.5 Abscission is mediated by the ESCRT proteins**

### **1.5.1 Abscission occurs at the midbody in mammalian cells**

Actomyosin ring constriction and furrow ingression in mammalian cells results in the formation of the midbody bridge connecting two daughter cells. At the centre of the midbody resides the Flemming body, a dense proteinaceous ring surrounding the interlocking ends of anti-parallel microtubule arrays. Abscission occurs at the midbody bridge and is mediated by signals from the Flemming body (Neto & Gould 2011; Schiel & Prekeris 2010). Abscission can be divided into two broad mechanisms: first, the formation of the abscission zone, and second, microtubule severing and membrane scission mediated by the endosomal sorting complex required for transport (ESCRT) proteins.

### **1.5.2 Vesicular trafficking is required for secondary ingression**

At the completion of furrowing, an intercellular bridge connects daughter cells. Present models suggest that a further ingression, so-called *secondary ingression*, is required to thin the bridge diameter prior to the membrane scission event, as the diameter of the bridge at the Flemming body is too great for membrane remodelling machinery such as the ESCRT proteins (Elia et al. 2011). Hence, membrane scission is conducted at secondary ingression sites located approximately 1  $\mu\text{m}$  from the centre of the Flemming body. The fusion of membrane vesicles with each other and the plasma membrane in the intercellular bridge mediates the formation of secondary ingression sites, a process that involves the trafficking of Rab GTPase-positive secretory and endosomal vesicles (Schiel et al. 2011; Wilson et al. 2005; Goss & Toomre 2008). Such extensive vesicular recruitment to the midbody requires machinery for spatial targeting and tethering to the plasma membrane, and as such, the exocyst has been implicated in mammalian cytokinesis. The exocyst is a multimeric protein complex with roles in membrane tethering to the plasma membrane; fission yeast with mutated exocyst components are unable to cleave following septum formation, and defects have also been noted in plant cytokinesis (Sztul & Lupashin 2006; Martín-Cuadrado et al. 2005; Fendrych et al. 2010). Furthermore, exocyst components have been shown to interact with

known regulators of abscission, such as endosomal GTPases Rab11 and Arf6 (Fielding et al. 2005; Cascone et al. 2008).

Rab11 and its effector FIP3 are implicated in cytokinetic membrane trafficking (Neto et al. 2011). Rab11 recruits FIP3 to vesicles of the recycling endosomes, and interaction with a motor protein facilitates the delivery of these vesicles to the cleavage furrow, where the interaction of Rab11/FIP3 with Arf6 and the exocyst complex facilitates the tethering of vesicles to the plasma membrane (Wilson et al. 2005). Accumulation of intracellular vesicles by the exocyst, therefore, is a necessary step in membrane thinning and formation of secondary ingression zones (Gromley et al. 2005). However, vesicular trafficking to the midbody may serve a second important role - that of assembling the abscission machinery (Gould & Lippincott-Schwartz 2009).

McDonald and Martin-Serrano (2009) have presented a model for abscission that includes Rab-GTPase-mediated trafficking of endosome-derived vesicles to the midbody. This model describes abscission in three stages. First, Rab GTPases mediate the transport of post-Golgi and endosome-derived vesicles to the midbody, where they are targeted to specific sites on the plasma membrane by the exocyst. Assemblies of septin filaments are proposed to outline compartments in the plasma membrane to restrict movement of the exocyst, thereby promoting targeted vesicle delivery to the abscission site (Estey et al. 2010). In the second stage, vesicle fusion with the plasma membrane is mediated by the interaction of SNARE proteins endobrevin and syntaxin-2. Finally, CEP55 recruits late-acting fission complex proteins for ESCRT-mediated membrane scission (McDonald & Martin-Serrano 2009; *Section 1.5.6*).

### **1.5.3 ESCRT proteins form a conserved membrane scission machinery**

ESCRT proteins were identified in budding yeast as Class E *vps* gene products and are known to have important roles in several processes, such as sorting during downregulation of ubiquitin-labelled receptors via the formation of multivesicular bodies (MVB) and in HIV budding from host cells (Raymond et al. 1992; McDonald & Martin-Serrano 2009).

Ubiquitin-labelled receptors are trafficked to the endosome where MVBs are formed by invagination of the endosomal membrane; MVBs then fuse with the lysosome to mediate protein degradation. The ESCRT proteins are essential to the formation of MVBs (Wollert & Hurley 2010). The ESCRT machinery consists of four main subunits assembled sequentially on the endosomal membrane: ESCRT-0, -I, -II and -III, and AAA-ATPase Vps4 disassembles the machinery (Teis et al. 2009).

ESCRT proteins are required for multivesicular body biogenesis and HIV virion egress. Both events require the internal resolution of a cytoplasm-filled membrane tubule; such an event is topologically opposed to that mediated by dynamin, but is similar to the final scission step of cytokinesis (Hinshaw 2000; Hurley & Hanson 2010). ESCRT-III has been identified as the primary driving force in ESCRT-mediated membrane scission events, with Vps4 required to redistribute ESCRT-III subunits back into the cytoplasm (Wollert et al. 2009; Lin et al. 2005; Babst et al. 1998). Vps4 is necessary for all ESCRT-mediated processes (Morita et al. 2010; Neto & Gould 2011).

#### **1.5.4 ESCRT function has diverged between species**

Despite first being characterised in *S. cerevisiae*, neither ESCRT localisation at bud necks nor a direct requirement for ESCRT proteins in abscission has been identified (McMurray et al. 2011). In contrast, filaments of GTP-binding septin proteins are required for deposition of new cell wall material, which is in turn required to drive plasma membrane ingression (Bi 2001). However, budding yeast mutants of ESCRT-III gene *SNF7*<sup>+</sup> (fission yeast *vps32*<sup>+</sup>, human *CHMP4*<sup>+</sup>), resulted in cytokinetic failure and increased DNA content (McMurray et al. 2011). Furthermore, genetic studies in budding yeast mutants with cytokinesis-sensitised backgrounds due to impaired septin function have suggested a role for ESCRT proteins in recycling key enzymes required for cytokinesis (McMurray et al. 2011).

Fission yeast requires ESCRT proteins for MVB formation and cytokinesis, while human cells utilise ESCRT machinery for MVB formation, cytokinesis and HIV budding from host cells (McDonald & Martin-Serrano 2009). These observations imply divergent functions for ESCRT proteins between organisms. Interestingly,

studies in Archaea have revealed roles for ESCRT-III and VPS4 in cell division and potentially viral budding (Samson & Bell 2009). This observation is particularly significant because Archaea lack endomembrane structures, thus strengthening the view that ESCRT proteins have a well-conserved function in the scission aspect of cytokinesis, rather than endosomal sorting for vesicular fusion (McDonald & Martin-Serrano 2009).

### **1.5.5 A division of labour exists among the ESCRT machinery**

The modular nature of ESCRT components suggests divergent functions, both within particular cells, but further, between organisms and even branches of evolution. Emphasis has been placed on understanding the mechanisms of ESCRT-III as the principal engine of membrane deformation. ESCRT classes 0-II, therefore, are regarded as being auxiliary to ESCRT-III. In fact, studies in Archaea indicate a lack of ESCRT-0-II homologues, but underpin the conservation of the ESCRT-III interaction with VPS4 (Samson & Bell 2009).

ESCRT proteins function sequentially in the formation of MVBs (Teis et al. 2009). Wollert & Hurley (2010) described an *in vitro* model of ESCRT assembly and function whereby ESCRT-0 self-assembles and, together with clathrin, forms large domains on the endosomal membrane. One significant finding with regard to membrane budding was the discovery that it is performed by a super-complex of ESCRT-I and -II (Wollert & Hurley 2010), as opposed to the previously-held position that membrane budding was mediated by ESCRT-III (Teis et al. 2008). Although the mechanisms by which ESCRT-I/II forms membrane invaginations are unclear, it is possible that they hold the membrane open via rigid superstructures, allowing ESCRT-III to perform the scission step (Figure 1.2; Wollert & Hurley 2010).

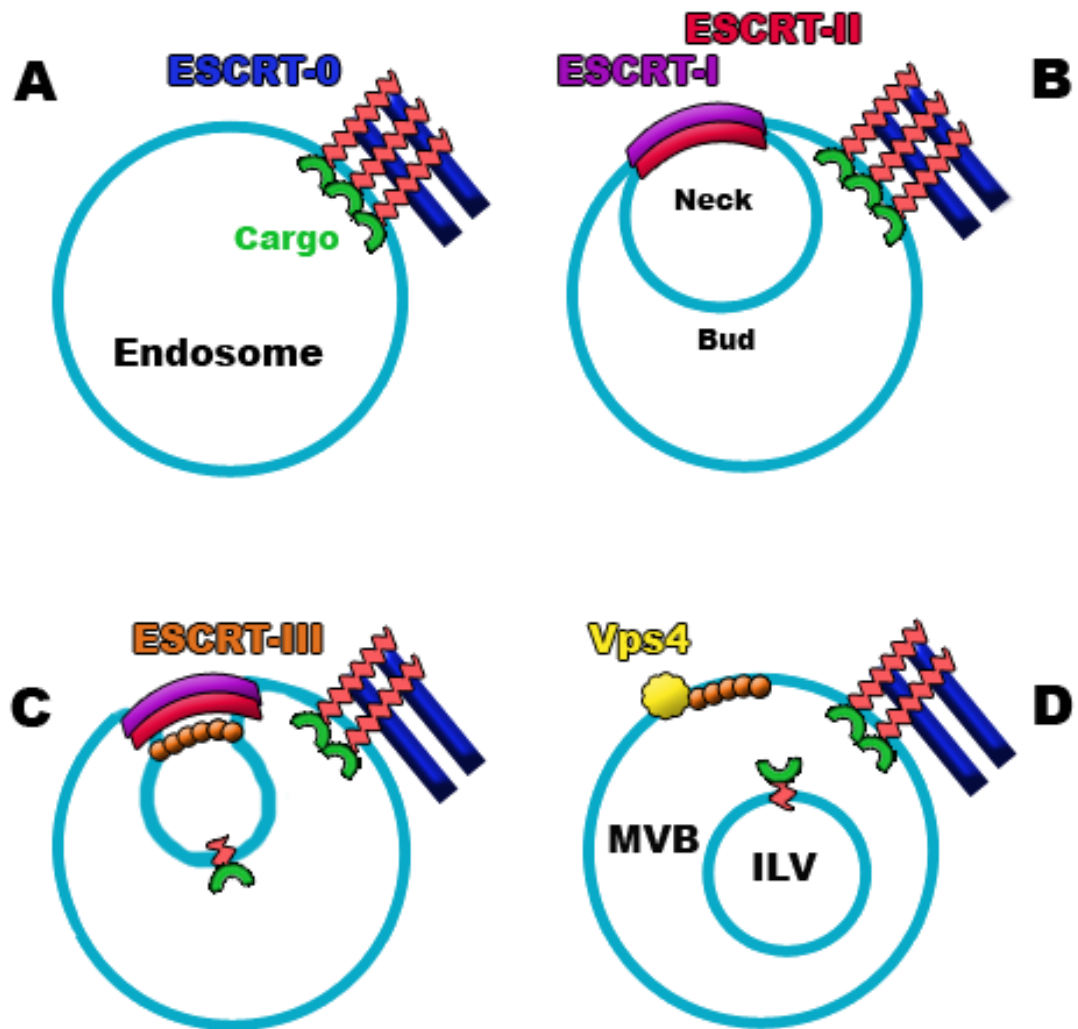


**Figure 1.2: Multivesicular body biogenesis is mediated by sequential function of ESCRT subunits.**

(A) ESCRT-0 sequesters ubiquitylated cargo to endosomal membranes destined for degradation in the lysosome. (B) ESCRT-I and -II form rigid stalks that deform the peripheral membrane, resulting in inward budding. (C) ESCRT-III polymerises and constricts the bud neck. (D) Critical proximity results in membrane fusion and formation of an intraluminal vesicle (ILV) within a multivesicular body (MVB). Vps4 recycles ESCRT-III back into the cytoplasm. Adapted from (Wollert & Hurley 2010).

ESCRT proteins are not lost in the process of membrane remodelling; rather, ESCRT-III remains on the periphery of the MVB membrane until Vps4 recycles it back into the cytoplasm to mediate the formation of further MVBs (Wollert & Hurley 2010).

### 1.5.6 ESCRT-III is recruited to the midbody by TSG101/ESCRT-I and ALIX

Centrosomal protein of 55 kDa (CEP55) is recruited to the midbody by centralspindlin component MKLP1 following mitotic degradation of Plk1, the negative phospho-regulator of CEP55 midbody recruitment (Bastos & Barr 2010).

CEP55 has several important roles in cytokinesis, including organising the Flemming body by recruiting late-acting proteins for abscission (Skop et al. 2004; Zhao et al. 2006). Tumour susceptibility gene 101 protein (TSG101), an ESCRT-I component, and apoptosis-linked gene 2-interacting protein (ALIX) are recruited to the midbody from centrosomes by CEP55 (Morita et al. 2007). Both TSG101 and ALIX have established early roles in MVB biogenesis (Hurley & Emr 2006; Martin-Serrano et al. 2003), HIV egress (Morita & Sundquist 2004) and abscission (Morita et al. 2007). TSG101 and ALIX have sometimes interchangeable roles (Fisher et al. 2007), and both function with downstream ESCRT pathways members in protein sorting and membrane fission (Morita et al. 2007). CEP55 localises to the Flemming body itself, whereas TSG101 and ALIX localise to either side (Elia et al. 2011). TSG101 localises as membrane-associated rings either side of the Flemming body; it is at these sites that ESCRT-III assembles in a TSG101/ALIX-dependent manner (Elia et al. 2011). Indeed, ALIX mutations unable to bind CEP55 or ESCRT-III, as well as depletion of either TSG101 or ALIX, inhibit abscission (Morita et al. 2007).

### **1.5.7 ESCRT-III performs the final scission step of cytokinesis**

ESCRT-III has been proposed to assemble sequentially during intraluminal vesicle scission: first by recruitment of CHMP6, then CHMP4, which polymerises into a spiral, then CHMP3 and CHMP2 which terminate the spiral and recruit VPS4 for ESCRT redistribution (Wollert et al. 2009; Hurley & Hanson 2010). During cytokinesis, ESCRT proteins are recruited to the midbody and have a direct role in abscission, as demonstrated by resultant multinucleate cells on ESCRT depletion (Morita et al. 2007). CHMP4B localises to the Flemming body peripheries in a series of cortical rings exhibiting significant overlap with TSG101/ESCRT-I; along with CHMP2A, both have been shown to localise to secondary ingression zones immediately prior to abscission (Elia et al. 2011; Guizetti et al. 2011). A model for ESCRT-mediated abscission is demonstrated in Figure 1.3.

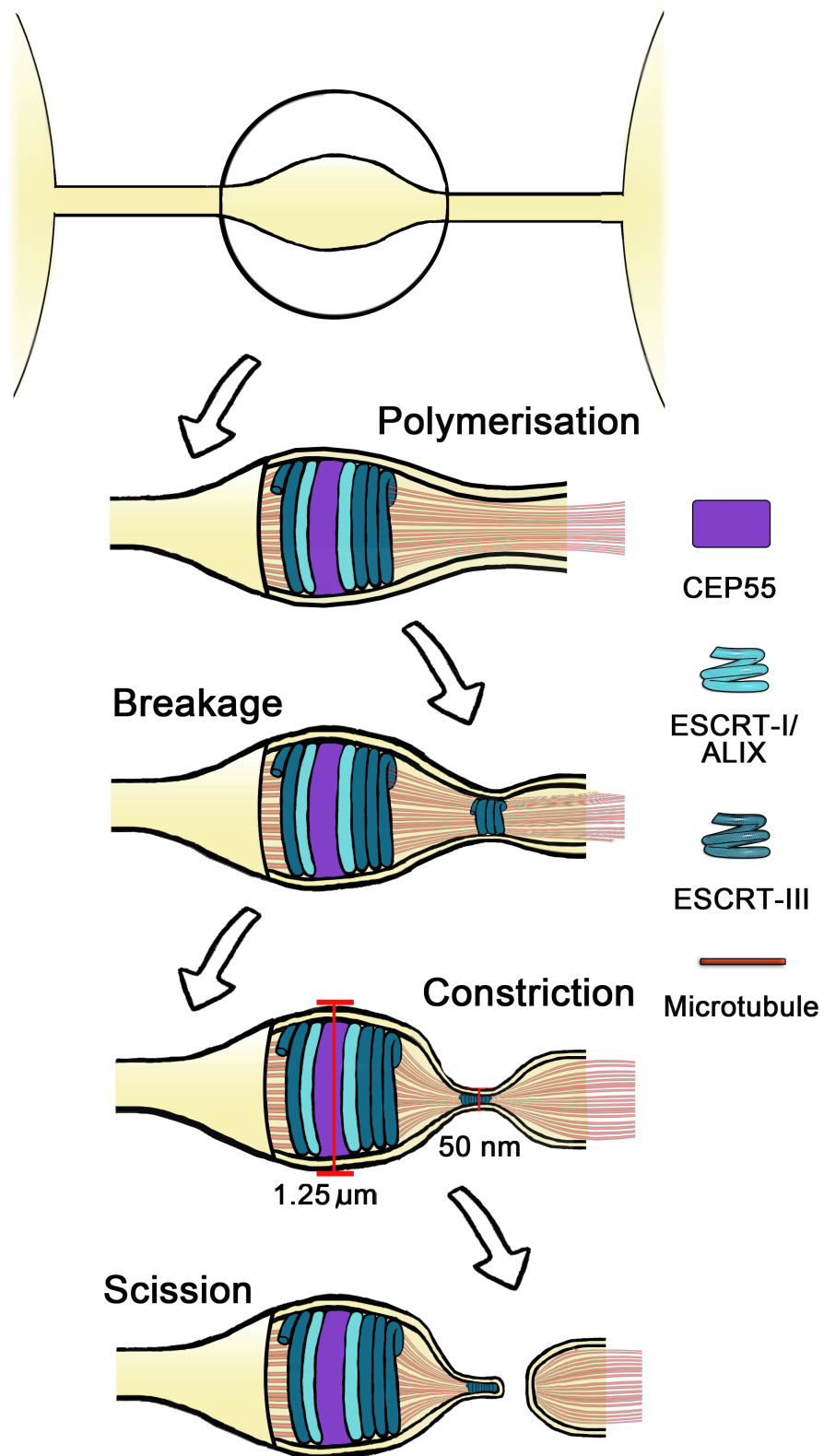


**Figure 1.3: A model for ESCRT-mediated cytokinetic abscission.**

CEP55 localises to the Flemming body and recruits TSG101/ESCRT-I and ALIX to the Flemming body peripheries in ring formations, which in turn recruit ESCRT-III component CHMP4B, also in membrane-associated ring formations. Nucleation sets CHMP4B in motion away from the Flemming body, and breakage by VPS4 facilitates localisation towards the secondary ingressions. Finally, microtubule severing, perhaps by spastin, allows CHMP4B to constrict the membrane bridge to within critical proximity for fusion. Adapted from (Elia et al. 2012).

Abscission occurs sequentially at the secondary ingression zones either side of the midbody. CHMP4B localises in low levels during early cytokinesis as two cortical rings; however, a second pool of CHMP4B localises approximately 1  $\mu\text{m}$  from the centre of the Flemming body, representing the abscission site (Elia et al. 2011). Guizetti et al (2011) reported membrane ripples corresponding to the abscission site; these ripples were absent in CHMP2A-depleted cells, indicating that ESCRT-III is necessary for cortical constriction (Guizetti et al. 2011).

Timing studies indicate that abscission takes place in the last 20 minutes of cytokinesis, during which time, one side of the Flemming body acutely narrows and microtubules break before membrane scission. Consistent with this observation, CHMP4B localises to the abscission site 20 minutes before abscission, which triggers an acute decrease in microtubule diameter, coincidental with a much greater abundance of membrane-severing spastin on the midbody arm where abscission occurs (Elia et al. 2011). Spastin depletion was shown to delay abscission, but rippled constriction zones were still present (Yang et al. 2008; Guizetti et al. 2011). VPS4 co-localises with CHMP4B at the constriction site and abscission occurs 10 minutes later (Elia et al. 2011). Following the first abscission event, CHMP4B localises to the second abscission site, microtubules bundle and sever, and abscission occurs to produce the midbody remnant.

Live cell imaging revealed that the second CHMP4B pool emanates from the first (Elia et al. 2011), which is evidence for a model for CHMP4B redistribution from the Flemming body to the abscission site. This model suggests that CHMP4B is nucleated by an as-yet-unknown factor, but then a second pool arises from polymer breakage, presumably by VPS4, and proceeds to the site of constriction. Consistent with this is the observation that ATP depletion inhibits CHMP4B breakage, resulting in a continuous polymer extending a significant distance from the Flemming body. Computational modelling suggests that equilibrium of elastic forces may drive the ESCRT-III fission complex to the constriction site. This model is consistent with the observation that ESCRT-III mediates membrane scission of much smaller diameters than that present at the midbody, as the constriction site is a more manageable 50 nm. Scission then occurs due to constrictive force of fission complex attachment to the plasma membrane, consistent with the observation that ESCRT-III proteins assemble into spiral

filaments *in vitro* with exposed membrane interactions sites (Elia et al. 2011; Lata et al. 2008).

### 1.5.8 How is the ESCRT machinery regulated in cytokinesis?

Although the model presented (Elia et al. 2012; *Section 1.5.7*) aptly describes a mechanism for ESCRT-mediated abscission, there are still several issues that require elucidation, perhaps most notably, the mechanism of CHMP4B nucleation. Elia et al (2012) suggest the involvement of lipid interactions, due to the proposed role of membrane trafficking in secondary ingression formation (Neto et al. 2011) and the *in vitro* preference of ESCRT-III for acidic membranes (Muziol et al. 2006). They therefore propose that attractive forces mediated by the lipid bilayer composition may drive ESCRT-III to the constriction site (Elia et al. 2012). Guizetti et al (2011) reported an absence of endocytic vesicles at the constriction site; however, their analysis did not preclude the presence of vesicles of other origins. It is worth noting, however, that ESCRT components may bind lipid bilayers in MVB formation and HIV budding due to interactions with phosphatidylinositol 3-phosphate or cholesterol-rich lipid raft domains, respectively (Guizetti & Gerlich 2010; Whitley et al. 2003; Lin et al. 2005; Yorikawa et al. 2005); such enriched domains have been reported to accumulate in the midbody (Neto et al. 2011). Although an interesting proposition, it seems unlikely that lipid composition alone could mediate ESCRT-III nucleation, though it may aid ESCRT-III translocation coincidentally with nucleation by another factor.

Furthermore, biochemical analysis has yet to confirm that the cortical rings reported at constriction sites (Guizetti et al. 2011) are actually ESCRT proteins; it is possible that the rings are in fact septin-based, as septin-7 and -9 are also essential components of cytokinesis (Estey et al. 2010; Hu et al. 2012; Neto & Gould 2011; *Sections 1.5.2 and 1.5.4*).

The precise role and regulation of the ESCRT machinery in abscission has yet to be solved. ESCRT components are phosphoproteins, so kinases and phosphatases are likely candidates for ESCRT regulation. For instance, CEP55 depletion results in failed accumulation of late-acting abscission factors at the midbody, including ESCRT proteins, Aurora B kinase and Plk1 (Morita et al. 2007). Aurora B has been

shown to phosphorylate CHMP4C to delay abscission and prevent the accumulation of DNA damage (Carlton et al. 2012); indeed budding yeast Aurora B localises to the anaphase spindle due to the phosphatase activity of Cdc14 (Pereira & Schiebel 2003). In addition, human CDC14A is required for Rab5-mediated endocytic trafficking (Lanzetti et al. 2007); it is possible that such an association may provide a role for CDC14A in trafficking to the midbody during cytokinesis. Furthermore, although Plk1 downregulation is required for CEP55 midbody localisation, and thus ESCRT localisation, Plk1 reappears on late midbodies (Hu et al. 2012). These observations make phospho-regulation of ESCRT proteins an attractive direction of investigation.

## 1.6 The present study

### 1.6.1 Hypotheses

In this study, the role of ESCRT proteins in cytokinesis was investigated. It was hypothesised that polo kinase and Cdc14 phosphatase regulate ESCRT components in fission yeast and that these interactions are conserved in human cells. Furthermore, it was hypothesised that interactions with the ESCRT proteins are required for controlling phosphorylation status, and that this in turn mediates ESCRT function in cytokinesis.

### 1.6.2 Approach and principal findings

Fission yeast was used as a model organism to test interactions between Plo1p, Clp1p and the ESCRT proteins. Initially, septation phenotypes among wild-type and fission yeast strains with individual deletions in ESCRT genes were characterised. ESCRT genes were shown to be required for cell division in fission yeast, implying a role for the ESCRT proteins in this process.

A yeast genetics approach was employed to investigate genetic interactions between ESCRT genes and *plo1*<sup>+</sup> and *clp1*<sup>+</sup>. Double mutants were produced from crosses between ESCRT deletion strains and mutants of *plo1* and *clp1*. Defective growth rates were observed in double mutants, indicating genetic interactions between *plo1*<sup>+</sup>, *clp1*<sup>+</sup> and ESCRT genes.

The effect of single ESCRT deletions on vacuolar sorting in fission yeast was characterised. Single mutants of *plo1* and *clp1* were also shown to affect vacuolar sorting, although phenotypes were dissimilar to those observed in ESCRT deletion strains. Analysis of the vacuolar sorting in double mutants provided further characterisation of observed genetic interactions; and *plo1*<sup>+</sup> was regarded to function upstream of ESCRT genes, and *clp1*<sup>+</sup> downstream.

The yeast two-hybrid assay was used to analyse protein-protein interactions. Physical interactions were observed between Plo1p and Sst4p (human HRS, ESCRT-0), Vps28p (VPS28, ESCRT-I), Vps25p (EAP20, ESCRT-II), Vps20p (CHMP6, ESCRT-III) and Vps32p (CHMP4, ESCRT-III). Clp1p was also shown to interact with Vps28p.

Interactions were then investigated between human homologues of these proteins. Immunoprecipitation and co-immunoprecipitation methods in mitotic HeLa cells demonstrated interactions between Plk1 and known binding partner FOXM1 (Fu et al. 2008). Interactions were not detected between Plk1 and ESCRT proteins, so HEK293 cells were used to over-express ESCRT proteins.

Plk1 co-immunoprecipitated over-expressed CHMP6 (fission yeast Vps20p), CHMP4B (Vps32p), CHMP3 (Vps24p) and CHMP2A (Vps2p, all ESCRT-III). Furthermore, immunoprecipitation and co-immunoprecipitation methods demonstrated interactions between CDC14A and CHMP4B and CHMP2A in HEK293 cells.

## Chapter 2 Materials and methods

### 2.1 Materials

#### 2.1.1 Media

All measurements for the production of media given below refer to dissolving in one litre of distilled water. All media was autoclaved prior to use. To produce solid media, 20 g/l bacto agar (BD Biosciences) was added prior to autoclaving.

##### 2.1.1.1 *E. coli* media

Bacteria were cultured and maintained as described (Sambrook et al. 2001).

Luria broth (LB): 20 g/l Lennox L broth (Sigma).

To select for ampicillin or kanamycin resistance in bacterial growth, antibiotics were added to cooled media at a working concentration of 50 µg/ml.

##### 2.1.1.2 *S. cerevisiae* media

*S. cerevisiae* were cultured and maintained as described (Sambrook et al. 2001).

Synthetic dropout (SD): 20 g D-glucose, 6.7 g Difco yeast nitrogen bases w/o amino acids (BD Biosciences) and 0.64 g CSM-Leu-Trp (Bio101 Systems).

Yeast extract/peptone/dextrose (YPD): 50 g/l YPD (BD Biosciences).

##### 2.1.1.3 *S. pombe* media

*S. pombe* were cultured and maintained as described (Moreno et al. 1991).

Edinburgh minimal media (EMM): 20 g D-glucose, 5 g ammonium chloride, 0.1 g sodium sulphate, 0.1 g magnesium chloride, 15 mg calcium chloride, 3 g potassium hydrogen phthalate, 1.8 g disodium hydrogen orthophosphate, 1 ml vitamins (per litre: 10 g inositol, 10 g nicotinic acid, 1 g calcium pantothenate and 10 mg biotin) and 0.1 ml trace (per litre: 5 g boric acid, 5.2 g manganese sulphate, 4 g zinc sulphate, 2 g ferric chloride, 1.44 g molybdic acid, 0.4 g copper sulphate, 10 g citric acid and 0.1 g potassium iodide).

EMM was supplemented appropriately with (per litre EMM) 375 mg adenine or uracil, or 187.5 mg leucine or histidine.

Malt extract (ME): 30 g bacto malt extract.

Yeast extract (YE): 30 g D-glucose, 5 g bacto yeast extract, 225 mg adenine and 225 mg uracil.

### 2.1.2 Oligonucleotide primers

Lab No. (GO)	Primer annotation	Species	Description	Sequence
744	sst4+R	<i>S. pombe</i>	Reverse primer to amplify <i>sst4</i> <sup>+</sup> from <i>S. pombe</i> genomic DNA	GCG CGC GTC GAC CTA AAG CTC GAT TAA AGA TGC TTC TTG AAC TTC
746	sst6.aa20-487R	<i>S. pombe</i>	Reverse primer to amplify <i>sst6</i> <sup>+</sup> from <i>S. pombe</i> genomic DNA	GCG CGC GTC GAC TTA AGA GTA TTG AAG CAT TTC GTC CCG TAT TAA
748	vps20+R	<i>S. pombe</i>	Reverse primer to amplify <i>vps20</i> <sup>+</sup> from <i>S. pombe</i> genomic DNA	GCG CGC GTC GAC TTA TCC CAG GAC TGG ATC TTT TCG AAG TTC T
750	vps36+R	<i>S. pombe</i>	Reverse primer to amplify <i>vps36</i> <sup>+</sup> from <i>S. pombe</i> genomic DNA	GCG CGC CTC GAG CTA TGA TTC ATC AAA CCA TTT AGT CAA TTC TTC T
751	sst4+F	<i>S. pombe</i>	Forward primer to amplify <i>sst4</i> <sup>+</sup> from <i>S. pombe</i> genomic DNA	CGC GCG TGG ATC CGA ATG TCT CGG TGG TGG AAT TCC AAT TCT CAG
752	sst6.aa20-487F	<i>S. pombe</i>	Forward primer to amplify <i>sst6</i> intron-free from <i>S. pombe</i> genomic DNA	CGC GCG TGG ATC CGA ATT AGA TTT TGG AAG AAT GGA CTT GCT GAA

753	vps20+F	<i>S. pombe</i>	Forward primer to amplify <i>vps20</i> <sup>+</sup> from <i>S. pombe</i> genomic DNA	CGC GCG TGG ATC CGA ATG GGG GTT AAC AGT AGT AAA ATT AAT GAT
754	vps36+F	<i>S. pombe</i>	Forward primer to amplify <i>vps36</i> <sup>+</sup> from <i>S. pombe</i> genomic DNA	GCG CGC CCC CCG GGG ATG GCC TTT TAT TTA GAA ACA ACC CCT TCT
757	vps28+F	<i>S. pombe</i>	Forward primer to amplify <i>vps28</i> <sup>+</sup> from <i>S. pombe</i> genomic DNA	CGC GCG TGG ATC CGA ATG ACT GAA TAC TAC GAT CTG AAC CTT TTA
758	vps28+R	<i>S. pombe</i>	Reverse primer to amplify <i>vps28</i> <sup>+</sup> from <i>S. pombe</i> genomic DNA	CGC GCG TGG ATC CGA ATG ACT GAA TAC TAC GAT CTG AAC CTT TTA
759	sst4+F (internal)	<i>S. pombe</i>	Forward primer to amplify a central region of <i>sst4</i> <sup>+</sup> from <i>S. pombe</i> genomic DNA	TTG GTA TCT ATT CTA CGA TCT CCT GC
760	sst4+R (internal)	<i>S. pombe</i>	Reverse primer to amplify a central region of <i>sst4</i> <sup>+</sup> from <i>S. pombe</i> genomic DNA	GAG TTC CTG TAG CTG ATA TTC CGT
761	vps2+F	<i>S. pombe</i>	Forward primer to amplify <i>vps2</i> <sup>+</sup> from <i>S. pombe</i> genomic DNA	CGC GCG TGG ATC CGA ATG GGC TTA ACT TCT TGG CTA TTT GGA GGG
762	vps2+R	<i>S. pombe</i>	Reverse primer to amplify <i>vps2</i> <sup>+</sup> from <i>S. pombe</i> genomic DNA	CGC GCG TGG ATC CGA ATG GGC TTA ACT TCT TGG CTA TTT GGA GGG
763	vps4+F	<i>S. pombe</i>	Forward primer to amplify <i>vps4</i> <sup>+</sup> from <i>S. pombe</i> genomic DNA	CGC GCG TGG ATC CGA ATG TCC AAT CCA GAT TGT TTA AGT AAA GCA

764	vps4+R	<i>S. pombe</i>	Reverse primer to amplify <i>vps4</i> <sup>+</sup> from <i>S. pombe</i> genomic DNA	CGC GCG TGG ATC CGA ATG TCC AAT CCA GAT TGT TTA AGT AAA GCA
765	vps25+F	<i>S. pombe</i>	Forward primer to amplify <i>vps25</i> <sup>+</sup> from <i>S. pombe</i> genomic DNA	CGC GCG TGG ATC CGA ATG CGT GTT CCA TCC ATT TAT AAC TTT CCT
766	vps25+R	<i>S. pombe</i>	Reverse primer to amplify <i>vps25</i> <sup>+</sup> from <i>S. pombe</i> genomic DNA	GCG CGC CTC GAG TTA AGC TTT CAG TAC CTT GAA CCC GCT
768	vps32+F	<i>S. pombe</i>	Forward primer to amplify <i>vps32</i> <sup>+</sup> from <i>S. pombe</i> genomic DNA	CGC GCG TGG ATC CGA ATG TCT GGA TTT TTA AGA TGG TTT GGG GGC
769	vps32+R	<i>S. pombe</i>	Reverse primer to amplify <i>vps32</i> <sup>+</sup> from <i>S. pombe</i> genomic DNA	GCG CGC CTC GAG TTA AAG AGA GAA TTC AGC CTG TAG TTT TCG
770	plk1+F (pGBKT7)	Human	Forward primer to amplify <i>PLK1</i> <sup>+</sup> from vector template to clone into pGBKT7	CGC GCG CAT ATG ATG AGT GCT GCA GTG ACT GCA GGG AAG CTG
771	plk1+R (pGBKT7)	Human	Reverse primer to amplify <i>PLK1</i> <sup>+</sup> from vector template to clone into pGBKT7	GCG CGC GAA TTC TTA GGA GGC CTT GAG ACG GTT GCT GGC CGA
772	plk1+F (pHB18)	Human	Forward primer to amplify <i>PLK1</i> <sup>+</sup> from vector template to clone into pHB18	CGC GCG GAA TTC ATG AGT GCT GCA GTG ACT GCA GGG AAG CTG
773	plk1+R (pHB18)	Human	Reverse primer to amplify <i>PLK1</i> <sup>+</sup> from vector template to clone into pHB18	GCG CGC CTC GAG TTA GGA GGC CTT GAG ACG GTT GCT GGC CGA

774	cdc14a2+F (pGBKT7 and pHB18)	Human	Forward primer to amplify <i>CDC14A</i> <sup>+</sup> from vector template to clone into pGBKT7 and pHB18	GCG CGC GAA TTC ATG GCA GCG GAG TCA GGG GAA CTA ATC GGG
775	cdc14a2+R (pGBKT7 and pHB18)	Human	Reverse primer to amplify <i>CDC14A</i> <sup>+</sup> from vector template to clone into pGBKT7 and pHB18	GCG CGC GGA TCC TCA GAA GGC TTC CTT GGC ACT ATT AAA TTT
776	vps4F (exons 3&4)	<i>S. pombe</i>	Forward primer to amplify exons 3 and 4 of vps4 <sup>+</sup> from <i>S. pombe</i> genomic DNA	CGC GCG TGG ATC CGA ATG TCC AAT CCA GAT TGT TTA AGT AAA GCA

### 2.1.3 Plasmid sources

Lab No. (GB)	Gene product	Species	Description	Plasmid	Source
331	Gal4 activation domain	<i>S. Cerevisiae</i>	Yeast two-hybrid activation domain	pACT2	(Reynolds & Ohkura 2003)
332	Gal4 DNA- binding domain	<i>S. Cerevisiae</i>	Yeast two-hybrid DNA-binding domain	pBTM116	(Reynolds & Ohkura 2003)
586	Gal4 DNA- binding domain	<i>S. Cerevisiae</i>	Yeast two-hybrid DNA-binding domain	pGBT9	(Clifford et al. 2008)
620	Ub-GFP- SpCPS	<i>S. pombe</i>	Ubiquitin-GFP- labelled CPS to characterise vacuolar sorting in <i>S. pombe</i>	pREP41	(Iwaki et al. 2007)

664	Plk1-YFP	Human	YFP-labelled Plk1	pCMX	(Lindon & Pines 2004)
676	Gal4 activation domain	Human	Yeast two-hybrid activation domain	pHB18	(Agromayor & Martin-Serrano 2006)
677	Gal4 DNA-binding domain	Human	Yeast two-hybrid DNA-binding domain	pGBKT7	(Agromayor & Martin-Serrano 2006)
678	CHMP3-myc	Human	Myc-tagged CHMP3	pcDNA3	Katherine Bowers, University College London
680	CHMP4B-myc	Human	Myc-tagged CHMP4B	pcDNA3	Katherine Bowers, University College London
682	CHMP6-HA	Human	HA-tagged CHMP6	pIRESneo2	Katherine Bowers, University College London
684	CDC14A-myc	Human	Myc-tagged CDC14A	pcDNA3	(Lanzetti et al. 2007)
685	CDC14A.C278S-myc	Human	Myc-tagged CDC14A.C278S	pcDNA3	(Lanzetti et al. 2007)
686	Plk1.K82R-YFP	Human	YFP-labelled Plk1.K82R	pEYFP-C3	(Lindon & Pines 2004)
715	CHMP4B-YFP	Human	YFP-labelled CHMP4B	pCR3.1	(Carlton et al. 2012)
716	CHMP2A-GFP	Human	GFP-labelled CHMP2A	pmEGFP	Addgene plasmid 31805 (Guizetti et al. 2011)

717	CHMP6-GFP	Human	GFP-labelled CHMP6	pmEGFP	Addgene plasmid 31806 (Guizetti et al. 2011)
754	VPS28-V5	Human	V5-tagged VPS28	pcDNA5-V5	Philip Woodman, The University of Manchester

## 2.1.4 Antibodies

### 2.1.4.1 Primary antibodies

For immunoblotting, all antibodies were incubated overnight at 4°C, unless otherwise stated.

Epitope	Clonality	Host species	Dilution	Diluent	Source (catalogue no.)
CHMP2	Polyclonal	Goat	1:1000	5% BSA-PBST	Santa Cruz Biotechnology (C-17)
CHMP3	Monoclonal	Mouse	1:750	5% BSA-PBST	Santa Cruz Biotechnology (F-1)
CHMP4A	Polyclonal	Goat	1:1000	5% BSA-PBST	Santa Cruz Biotechnology (P-16)
CHMP6	Polyclonal	Rabbit	1:1000	3% BSA-PBST	Abcam (ab76929)
Cyclin B1	Polyclonal	Rabbit	1:1000	3% BSA-PBST	Abcam (ab2096-100)
FOXM1	Monoclonal	Mouse	1:200	5% BSA-TBST	Santa Cruz Biotechnology (263C2a)
GFP	Polyclonal	Rabbit	1:1000	5% BSA-PBST	Abcam (ab290)
HA.11	Monoclonal	Mouse	1:1000	5% milk-PBST	Covance/Cambridge Biosciences (MMS-101P)

Myc	Polyclonal	Rabbit	1:1000	5% BSA-PBST	Abcam (ab9106)
Plk1 (two nights)	Monoclonal	Rabbit	1:750	5% BSA-TBST	Cell Signaling (208G4)
TSG101	Monoclonal	Mouse	1:1000	3% BSA-PBST	Abcam (ab4A10)
VPS28	Monoclonal	Mouse	1:250	5% BSA-PBST	Santa Cruz Biotechnology (E-7)

#### 2.1.4.2 Secondary antibodies

For immunoblotting, all horseradish peroxidase-linked secondary antibodies were diluted in 1% milk-PBST/TBST and incubated at room temperature for two hours.

Epitope	Host species	Dilution	Source (catalogue no.)
Goat IgG	Swine	1:2000	Caltag (G50007)
Mouse IgG	Sheep	1:1000	GE Healthcare (NA931)
Rabbit IgG	Goat	1:80,000	Sigma (A9169)

#### 2.1.5 Standard solutions

Unless stated otherwise, all buffers and reagents were prepared in distilled water.

##### Enhanced chemiluminescence (ECL) detection reagents

Solution 1: 0.1 M Tris-HCl, pH 8.5, 450 mg/l luminol (Sigma) in 2% (v/v) DMSO and 130 mg/l Coumaric acid (Sigma) in 1% (v/v) DMSO

Solution 2: 0.1 M Tris-HCl, pH 8.5 and 0.02% (v/v) H<sub>2</sub>O<sub>2</sub>

Immunoprecipitation wash buffer 1 (pH 7.5)

20 mM Hepes, 100 mM KCl and 1mM DTT

Immunoprecipitation wash buffer 2 (pH 7.5)

20 mM Hepes, 250 mM NaCl, 1% (v/v) Triton X-100 and 1mM DTT

Laemmli sample buffer (4X LSB)

200mM Tris-HCl, pH 6.8, 8% (w/v) SDS, 40% (v/v) glycerol, 0.4% (w/v) bromophenol blue and 400 mM DTT

Lysis buffer

50 mM Tris-HCl, 50 mM NaF, 1 mM Na<sub>4</sub>PPi, 1 mM EGTA and 1 mM EDTA. The following were added on day of use: 10% (v/v) glycerol, 0.01% (v/v) Triton X-100, 0.5% Igepal (Nonidet P-40 substitute), 1 mM DTT, 1 mM activated vanadate, 1 μM microcystin and one Complete mini EDTA-free protease inhibitor tablet

Phosphate-buffered saline (PBS) (pH 7.2)

85 mM NaCl, 1.7 mM KCl, 5 mM Na<sub>2</sub>HPO<sub>4</sub> and 0.9 mM KH<sub>2</sub>PO<sub>4</sub>

Phosphate-buffered saline + Triton X-100 (PBST)

PBS and 0.01% (v/v) Triton X-100. 250 mM NaCl was added to produce high-salt PBST

Ponceau S stain

0.2% (w/v) Ponceau S and 1% (v/v) acetic acid

SDS-PAGE running buffer

25 mM Tris-HCl, 250 mM glycine and 0.1% (w/v) SDS

Transfer buffer

25 mM Tris-HCl, 192 mM glycine and 20% (v/v) ethanol

Tris-buffered saline (TBS) (pH 7.5)

20 mM Tris-HCl, pH 7.5, 137 mM NaCl

Tris-buffered saline + Tween-20 (TBST)

TBS and 0.1% (v/v) Tween-20. 250 mM NaCl was added to produce high-salt TBST

## 2.2 Yeast methods

### 2.2.1 General yeast methods

The general molecular methods of Sambrook et al. (2001) were employed. Yeast strains were obtained from glycerol stocks frozen at  $-70^{\circ}\text{C}$ , or by mating strains from frozen stocks. *S. cerevisiae* strains were grown on solid rich medium (YPD) or minimal synthetic dropout medium (*Section 2.1.1.2*). *S. pombe* strains were grown on solid yeast extract (YE), mated on solid malt extract (ME) and genotypically screened on solid Edinburgh minimal medium (EMM) (*Section 2.1.1.3*). All strains were assigned a laboratory number, 'GGBY' for *S. cerevisiae* and 'GG' for *S. pombe*, in accordance with the laboratory collection (*Appendix 6.1*).

### 2.2.2 Septal defect analysis in *S. pombe*

*S. pombe* septa were visualised using Calcofluor stain and fluorescent microscopy as described (Mitchison & Nurse 1985). Cells were cultured overnight in liquid YE and 1 ml was transferred to a microcentrifuge tube (if the cells were too confluent, they were diluted as appropriate in YE). 50  $\mu\text{l}$  Calcofluor stain (Sigma) was added; cells were inverted and then incubated at room temperature for five minutes. Cells were then centrifuged at 4,000 rpm for one minute and washed three times with distilled  $\text{H}_2\text{O}$ . The pellet was resuspended in 20-50  $\mu\text{l}$  distilled  $\text{H}_2\text{O}$  and visualised using the brightfield and DAPI filters of a Zeiss Axiovert 135 fluorescent microscope equipped with a Zeiss 63X Plan-APOCHROMAT oil-immersion objective lens. The images were collected and processed using Microsoft PowerPoint.

### 2.2.3 *S. pombe* mating and tetrad dissection

Parent yeast strains were freshly grown at  $30^{\circ}\text{C}$ , having been recovered from  $-70^{\circ}\text{C}$  stocks three days earlier, or re-plated from  $20^{\circ}\text{C}$  (room temperature) one day earlier. Temperature-sensitive strains were incubated at  $25^{\circ}\text{C}$ , and so were afforded an additional day incubation. Mating of strains was performed by mixing approximately equal amounts of two parent strains on solid ME medium with an arbitrary volume of distilled water (approximately 10  $\mu\text{l}$ ). The mating

mixture was incubated at 25°C for two days and a sample was observed under a standard light microscope to confirm ascus formation.

A small number of cells were spread onto solid YE medium and tetrads were selected using a Singer MSM Ascus Dissector. Tetrads were incubated at 37°C for 4-6 hours to allow the ascus membranes to degrade. The four spores were separated and then incubated at 30°C for three days, or 25°C for five days, to permit growth.

## **2.2.4 Selection of double mutants**

### **2.2.4.1 Genotypic screening**

Once spores had developed into colonies, they were genetically screened by replica plating onto selective media: supplemented EMM, supplemented YE (G418, Sigma), or YE at different temperatures. After two days of incubation at 30°C, double mutants were identified and streaked onto fresh solid YE. These were incubated at 30°C for two days and then stored in 30% sterile glycerol frozen at -70°C.

Once dissected, the crosses with a temperature-sensitive parent were incubated at 25°C for five days. Genotypes were confirmed by replica plating; usually analysed after three days of growth at 25°C, except for those grown on solid YE medium incubated at 36°C, which were observed microscopically after only one day. Double mutants were identified and incubated at 25°C on fresh solid medium for three days before storage in 30% sterile glycerol frozen at -70°C.

### **2.2.4.2 Mating type determination**

To determine mating types of new strains, double mutants were re-plated onto solid ME and mated with standard  $h^+$  and  $h^-$  strains. Tetrad formation was then scored microscopically after two days.

## **2.2.5 Growth rate comparison**

Growth rates of double mutants were compared to their parents by streaking to single colonies two or three isolates of a double mutant and each of its parent

strains on YE and supplemented EMM solid medium. These were then grown at 25 °C, 30 °C or 36 °C for 2-4 days.

### **2.2.6 FM 4-64 staining of *S. pombe* vacuoles for confocal microscopy**

*S. pombe* cells were cultured in 100 ml liquid EMM, supplemented appropriately, including 10 µM thiamine to repress gene expression under *nmt1*<sup>+</sup> control (Maundrell 1993), and incubated overnight at the appropriate temperature. 16-20 hours before microscopy, the culture was centrifuged at 3,000 rpm for five minutes; the pellet was washed twice in EMM and resuspended in 25 ml EMM. Up to 10 ml of this resuspension was cultured in a final volume of 100 ml supplemented EMM lacking thiamine to induce gene expression under *nmt1*<sup>+</sup> control. After incubating for 16-20 hours at the appropriate temperature, the culture was centrifuged at 3,000 rpm for five minutes and resuspended in 500 µl in a microcentrifuge tube. 10 µM FM 4-64 (Invitrogen) was added and the cells were incubated shaking for 30 minutes (Iwaki et al. 2007). The culture was then centrifuged at 4,000 rpm for one minute and washed twice in EMM. The pellet was resuspended in 500 µl EMM and incubated shaking for 90 minutes. 5 µl was placed on a chamber designed for liquid cultures (Lab-Tek II Chamber 155379) and confocal microscopy was performed (Section 2.2.7).

### **2.2.7 Cell imaging via confocal microscopy**

Confocal microscopy was performed using a Carl Zeiss LSM 5 Exciter microscope fitted with a He/Ne and Ag laser system, and using a 63X high NA objective lens. The images were collected using Zeiss Pascal software and processed using Microsoft PowerPoint.

### **2.2.8 Cloning events for yeast two-hybrid analysis**

*plo1*<sup>+</sup> and *clp1*<sup>+</sup> were previously cloned into the bait vector used for yeast two-hybrid (Papadopoulou et al 2008); therefore, ESCRT genes were cloned into the equivalent prey vector, pACT2 (Clontech). Oligonucleotides were designed containing restriction sites (York Bioscience), and *S. pombe* genomic DNA was used as the template for PCR. PCR was performed using the Stratagene RoboCycler Gradient 96 machine to allow easy identification of the most

appropriate annealing temperature. The presence of DNA product was confirmed by ethidium bromide staining and agarose gel electrophoresis; the product was then cloned using the StrataClone Blunt PCR Cloning Kit. Correct ligation was confirmed by an *EcoRI* digestion and agarose gel electrophoresis, and positive vector DNA was sequenced (University of Dundee). On sequence confirmation (using software Vector NTI, Invitrogen), the gene was excised from the StrataClone vector and ligated into pACT2; this was confirmed by restriction digestion.

### **2.2.9 Transformation of *S. pombe* and *S. cerevisiae***

Lithium acetate transformation of *S. pombe* and *S. cerevisiae* were performed as described (Okazaki et al. 1990). Appropriate yeast strains lacking reporter plasmid genes were grown overnight in 10 ml rich liquid medium. Cells were harvested by centrifugation for five minutes at 3,000 rpm and washed in 30 ml sterile H<sub>2</sub>O. The cells were resuspended in 1 ml sterile H<sub>2</sub>O and transferred to a microcentrifuge tube. The cells were next centrifuged for one minute at 4,000 rpm, washed once with 1 ml TE/LiAc (10 mM Tris-Cl, 1 mM EDTA, 1 mM lithium acetate, pH 7.5) and then resuspended in 500 µl TE/LiAc. 100 µl of cells were then transferred to individual microcentrifuge tubes for transformation, and 2 µl salmon sperm DNA (10 mg/ml) and 10 µl transforming DNA were added. After ten minutes at room temperature, 260 µl PEG/TE/LiAc (40% (w/v) polyethylene glycol in TE/LiAc) was added and the cells were incubated for 30-60 minutes at 30°C; cells were inverted several times during the incubation period. After the incubation, 43 µl dimethyl sulfoxide was added and the cells were incubated at 42°C for five minutes. The cells were then centrifuged at 4,000 rpm for minute, with the pellet washed once with distilled H<sub>2</sub>O before being resuspended in 500 µl distilled H<sub>2</sub>O and transferred to the appropriate selective solid medium. Transformed cells were then incubated at 30°C for 3-5 days. Single colonies were selected and streaked onto fresh solid medium and grown for three days; from these, single colonies were selected and master plates were prepared. After three days, the colonies from master plates were frozen in 30% glycerol at -70°C.

### 2.2.10 X-Gal overlay assay

Yeast two-hybrid analysis was performed as described (Reynolds & Ohkura 2003). *S. cerevisiae* strains carrying bait and prey plasmids were cultured on solid synthetic dropout media lacking leucine and tryptophan and grown for three days at 30°C. The plates were scanned prior to the assay. A solution of 9.3 ml 0.5 M potassium phosphate buffer (19.5% (v/v) 1 M KH<sub>2</sub>PO<sub>4</sub>, 30.5% (v/v) 1 M K<sub>2</sub>HPO<sub>4</sub> in distilled H<sub>2</sub>O), 0.6 ml dimethyl formamide and 0.1 ml 10% SDS was mixed with 80 mg low-melting agarose (SeaPlaque GTG Agarose) and melted using a microwave oven. The solution was incubated at room temperature for 2-3 minutes before 30 µl X-Gal (40 mg/ml stock solution in dimethyl formamide) and 6 µl β-mercaptoethanol were added with gentle mixing. In a fume hood, the mixture was poured over the surface of the *S. cerevisiae* colonies and to allowed to cool before cultures were incubated at 30°C. Cells were reviewed for colour development every second hour over the next six to eight hours and then incubated overnight. Colour reactions were recorded by scanning typically 12-36 hours after the assay was performed.

## **2.3 Mammalian methods**

### **2.3.1 Cell culture**

#### **2.3.1.1 General cell culture maintenance**

Human cell lines were cultured in Corning T75 flasks, 6-well plates or Falcon 10 cm dishes. Both HeLa and HEK293 cells (cultured from stocks obtained from the American Tissue Culture Collection) were incubated at 37°C in a humidified atmosphere containing 5% CO<sub>2</sub>. To passage the cells into fresh medium, the medium was aspirated from cultures 70-80% confluent and 5 ml trypsin (0.05% (v/v) in EDTA) was added to each culture and incubated for 5 minutes. 10 ml fresh medium was added to each suspension and 3 ml was transferred to 9 ml medium in each subsequent flask.

#### **2.3.1.2 Culturing cells from frozen stocks**

Cryogenic vials containing frozen cell stocks were thawed from liquid nitrogen storage and diluted into 12 ml fresh, pre-warmed medium in a Corning T75 flask. The culture was incubated at 37°C with the medium being aspirated and replaced after 24 hours.

#### **2.3.1.3 HeLa cell culture maintenance**

HeLa cell cultures were maintained in DMEM (Gibco) supplemented with 10% (v/v) FCS EU (Gibco), 1% (v/v) glutamine (Gibco) and 1% (v/v) penicillin/streptomycin antibiotic (Gibco). HeLa cells were passaged into fresh medium three times weekly, and in the absence of antibiotics prior to transfection.

#### **2.3.1.4 HEK293 cell culture maintenance**

HEK293 cell cultures were maintained in MEM (Gibco) supplemented with 10% (v/v) FCS EU, 1% (v/v) glutamine, 1% (v/v) penicillin/streptomycin and 1% (v/v) sodium pyruvate. HEK293 cells were passaged into fresh medium twice weekly, and in the absence of antibiotics prior to transfection.

### **2.3.2 Amplification of the plasmids containing ESCRT genes**

*E. coli* transformations were performed using the Invitrogen One Shot TOP10 Chemically Competent *E. coli* kit. Colonies were selected and transferred to 3 ml LB supplemented with ampicillin or kanamycin and incubated for 16 hours at 37°C with rotation. 100 ml LB supplemented with ampicillin or kanamycin was inoculated with 100 µl of the bacterial culture. Plasmids were then purified using the QIAfilter Plasmid Purification for Maxi kit (Qiagen). Spectrophotometry was performed to quantify the concentration of DNA purified.

### **2.3.3 Transfecting HeLa and HEK293 cells**

HeLa or HEK293 cells were split in medium lacking antibiotics and plated in 6-well plates (or for immunofluorescence, onto ethanol-washed coverslips in 12-well plates) one day prior to transfection. After 24 hours, master mixes of DNA, Lipofectamine 2000 (Invitrogen) and Opti-MEM (Gibco) were prepared to allow each well to receive the stipulated amount of DNA and half the volume of Lipofectamine 2000 as per the Lipofectamine 2000 protocol. In the no-DNA controls, additional Opti-MEM was used in place of DNA. Master mixes were incubated for 20 minutes at room temperature. Medium was aspirated and replaced with fresh antibiotic-free medium, and then master mixes were added. Cells were then incubated at 37°C, 5% CO<sub>2</sub> for 48 hours; the medium was aspirated and replaced the following day with antibiotic-free medium.

### **2.3.4 Cell fixation and DAPI staining for immunofluorescence**

Cells were washed three times with PBS, fixed with 3% paraformaldehyde for 20 minutes and then washed twice with PBS. Cells were then permeabilised in 0.1% (v/v) Triton X-100/PBS for 2 minutes. 1 µg/ml DAPI in 0.1% Triton X-100/PBS was added to cells for 10 minutes before a final three washes with PBS. Coverslips were fixed to glass slides with mounting medium and left overnight to dry.

### **2.3.5 HeLa cell synchronisation and lysate preparation**

#### **2.3.5.1 HeLa cell synchronisation to metaphase and telophase**

HeLa cells were synchronised as described (Harper 2005). 5 mM thymidine was added to 24 flasks of HeLa cells (approximately 60% confluency); cells were

incubated for 16 hours, after which they were washed twice with cold PBS and twice with warm DMEM. Cells were then given 12 ml fresh DMEM and incubated for eight hours, at which point 100 ng/ml nocodazole was added to the cultures. 16 hours later, the medium was gently aspirated and the flasks vigorously agitated to dislodge the cells. The cells from all 24 flasks were collected in 20 ml PBS and centrifuged for five minutes at 1,000 rpm. The cells were washed twice with cold sterile PBS and thrice with warm DMEM. The cells were resuspended in 30 ml DMEM and transferred to two 10 cm plates. Metaphase-arrested cells were incubated for 45 minutes and telophase-arrested cells were incubated for 90 minutes.

### **2.3.5.2 Plk1 inhibition in HeLa cells**

To inhibit Plk1 kinase, cells were cultured and synchronised (*Section 2.3.5.1*) and 60 µl BI 2536 was added along with nocodazole.

### **2.3.5.3 Lysate preparation**

100 µl lysis buffer (*Section 2.1.5*) was added to each well of a 6-well plate and cells were incubated on ice for five minutes. Cells were then scraped into centrifuge tubes. Mitosis-arrested cells were scraped into a centrifuge tube and pelleted for five minutes at 2,000 rpm, 4°C. Cells were resuspended in 2 ml lysis buffer.

Cells were then passed 10 times through a 26-gauge needle, rested on ice for 20 minutes and then again passed 10 times through the needle. The homogenised mix was transferred to microcentrifuge tubes and centrifuged for 15 minutes at 15,000 x g, 4°C. The supernatants were retained and quantified before storing at -80°C.

### **2.3.6 Protein quantification**

The Micro BCA Protein Assay Kit (Pierce) and FLUOstar OPTIMA (BMG Labtech) were used to quantify protein concentrations from cell lysate preparations. Briefly, standard protein concentrations, 0-12 mg/ml, were prepared from bovine serum albumin (BSA) and pipetted in duplicate on a Corning 96-well plate. The protein samples were pipetted in duplicate in both 1:1 and 1:10

dilutions. 100 µl of the Micro BCA buffer mix (50% A, 48% B and 2% C) was added to each well and the plate was incubated at 37°C for 30 minutes. The dilutions were then analysed using FLUOstar OPTIMA; a standard curve was established from which the protein concentrations of the samples were extrapolated.

### **2.3.7 Immunoprecipitation from HeLa or HEK293 lysates**

#### **2.3.7.1 Immunoprecipitation of Plk1 from non-transfected HeLa or HEK293 lysates**

Immunoprecipitations were modified from (Fielding et al. 2005) and (Fu et al. 2008). One mg of cell lysate, brought up to 500 µl in lysis buffer, was incubated overnight at 4°C with rotation with 7.5 µl (HeLa cell lysates) or 10 µl (HEK293 cell lysates) anti-Plk1 antibody. Various negative controls were performed as follows: 50 ng IgG from rabbit serum (I5006, Sigma) was incubated with lysate, anti-Plk1 was incubated with 500 µl lysis buffer, and to perform a beads-only IP, lysate was incubated overnight without any addition. After incubation, 30 µl Protein A sepharose beads (GE Healthcare Life Sciences), pre-washed twice and resuspended in cold lysis buffer, was added and lysate mixtures were again incubated with rotation at 4°C for two hours. After incubation, mixtures were centrifuged at 4°C for 25 seconds and the supernatant was retained. Beads were washed twice in IP wash buffer 1 and thrice in IP wash buffer 2. Beads were then resuspended in 75 µl 1X LSB, mixed vigorously using a vortex and heated to 65°C for ten minutes. Beads were centrifuged for five minutes and the supernatant was retained. Samples were either analysed immediately using SDS-PAGE or stored at -80°C.

#### **2.3.7.2 Immunoprecipitation of FOXM1, ESCRT proteins and various epitopes**

To immunoprecipitate FOXM1, ESCRT proteins or other proteins via epitopes, the method described (*Section 2.3.7.1*) was followed with different antibody and beads combinations. The following antibodies were captured using Protein A sepharose beads: anti-CHMP6, anti-GFP and anti-myc antibodies. The following antibodies were captured using Protein G sepharose beads: anti-FOXM1, anti-HA, anti-TSG101 and anti-VPS28 antibodies.

### 2.3.8 SDS-PAGE

Protein samples were mixed 3:1 with 4X LSB, heated to 65°C for ten minutes and loaded on a 10-15% 1.5 mm Tris-HCl SDS gel. The gels were cast using Bio-Rad mini-Protean III gel casting units and comprised 30% (w/v) acrylamide (Severn Biotech), 10% SDS, 10% ammonium persulphate and tetramethylethylenediamine (TEMED). To determine molecular weight, Bio-Rad Precision Plus Protein Standards All Blue (161-0373) was run in at least one lane of the gel. Gels were run in SDS-PAGE running buffer (*Section 2.1.5*) at 80 V constant voltage during the stacking portion of the gel and then 120 V, using the Bio-Rad Protean III system.

### 2.3.9 Immunoblotting

#### 2.3.9.1 Transfer to nitrocellulose membrane

Following SDS-PAGE, proteins were transferred to nitrocellulose membrane using the Bio-Rad mini Protean III trans-blot system. Transfer cassettes were assembled with sponges, filter paper (Whatman 3MM blotting paper), SDS gel and nitrocellulose membrane (Pall Corporation), all pre-soaked in transfer buffer (*Section 2.1.5*). Transfer was performed using a constant current of 200 mA for two hours or 50 mA overnight.

#### 2.3.9.2 Membrane blocking and protein probing

Following transfer, membranes were washed in PBS or TBS and briefly stained with Ponceau S to confirm that proteins had successfully transferred. Membranes were washed again and non-specific sites were blocked in 1% (w/v) milk (Marvel) in PBS/TBS, incubating with rotation for one hour at room temperature. Membranes were then washed in PBS/TBS and incubated rotating in a solution of primary antibody in the appropriate concentration of BSA (Sigma) in PBST/TBST at 4°C for one or two nights (*Section 2.1.4.1*). Membranes were then washed several times in PBST/TBST and incubated with rotation in a solution of appropriate horseradish peroxidase (HRP)-conjugated secondary antibody diluted in 1% (w/v) milk-PBST/TBST for two hours at room temperature (*Section 2.1.4.2*). Membranes were then washed several times in PBST/TBST or high salt solutions as necessary.

### **2.3.9.3 Immunodetection of proteins via enhanced chemiluminescence (ECL)**

Membranes were rotated at room temperature for one minute in a 1:1 solution of ECL 1 and 2 (*Section 2.1.5*). Membranes were then fixed between plastic film in a developing box. In a dark room, Kodak Medical X-ray films were exposed to the membranes and then developed in a Kodak X-OMAT 2000 Processor.

## **Chapter 3 Plo1p kinase and Clp1p (Cdc14) phosphatase interact with ESCRT proteins to control cell division in *S. pombe***

### **3.1 Introduction**

The ESCRT proteins have a role in cytokinesis in humans (Morita et al. 2007). However, the regulation of these proteins remains largely unresolved. One of the most widespread methods of protein regulation is activation/deactivation via phosphorylation status. The fission yeast *Schizosaccharomyces pombe* ESCRT proteins all have amino acid residues that are potentially regulated by phosphorylation ([www.pombase.org](http://www.pombase.org)). Thus, two candidate regulators were identified in fission yeast on the basis of their significant roles in cytokinesis: Plo1p kinase and Clp1p (Cdc14p) phosphatase (Barr et al. 2004; Trautmann et al. 2001).

#### **3.1.1 Fission yeast is an appropriate model organism for studying cell division**

Fission yeast cell division progresses in a manner similar to animals, primarily by cytoplasmic cleavage furrowing driven by constriction of an actomyosin ring. In excess of 100 cytokinesis genes have been identified in fission yeast, and it has been noted that significant overlap exists between human cytokinesis genes and their yeast homologues (Wu et al. 2003). Therefore, understanding cytokinesis in fission yeast should generate findings applicable to higher eukaryotes, including humans (Pollard & Wu 2010).

#### **3.1.2 Aims**

Genetic interactions between ESCRT genes and *plo1*<sup>+</sup> and *clp1*<sup>+</sup> were investigated using a three-pronged approach. Initially, the effect of deleting chromosomal copies of individual ESCRT genes upon fission yeast cytokinesis and cell separation was characterised through observed effects on septation. Further, due to the established role of ESCRT proteins in vacuolar sorting (Hurley & Emr 2006), the effect of mutations in *plo1* and *clp1* on vacuolar sorting was analysed via the distribution of a GFP-labelled receptor and vacuolar staining in cells.

Finally, the genetic interactions between ESCRT genes and *plo1* and *clp1* mutants were investigated by growth rate analysis.

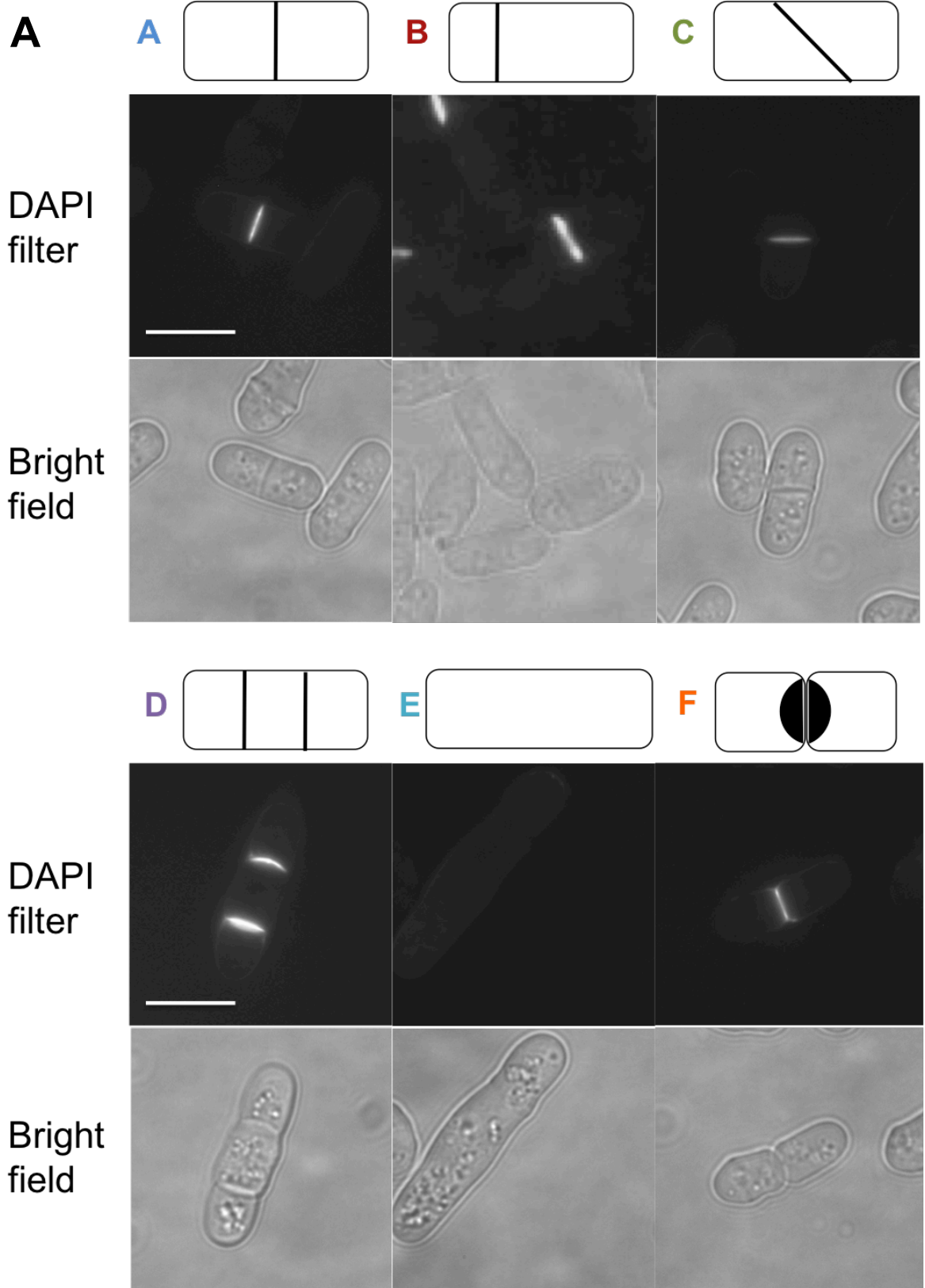
The yeast two-hybrid assay was then employed to extend the genetic interactions observed into detectable protein-protein interactions between ESCRT proteins and Plo1p and Clp1p.

## 3.2 Results

### 3.2.1 The ESCRT proteins have a role in cell division in fission yeast

Central to this investigation is the observation that ESCRT proteins are involved in cytokinesis in human cells (Morita et al. 2007). To this end, the effect of ESCRT proteins on cell separation in *S. pombe* was first investigated. Fission yeast cell separation proceeds by mitosis, followed by the physical division of the cells, so-called *septation* (Sohrmann et al. 1996). Thus, septation in fission yeast was analysed as it serves as an analogous system to mammalian cytokinesis.

To study septation in fission yeast, cells were cultured in rich liquid medium and then exposed to Calcofluor stain (*Materials and Methods 2.2.2*), which specifically stains newly deposited cell wall. The septa of dividing cells were then visualised using fluorescence microscopy. Initially, the unperturbed septation phenotypes in wild-type cells were characterised. Phenotypes were then characterised in cells containing individual ESCRT chromosomal deletions (Iwaki et al. 2007) (Figure 3.1A). The relative frequencies of these phenotypes were then quantified in mutants and compared to wild-type (Figure 3.1B). A list of the strains used and produced in this study is shown in *Appendix 6.1*.



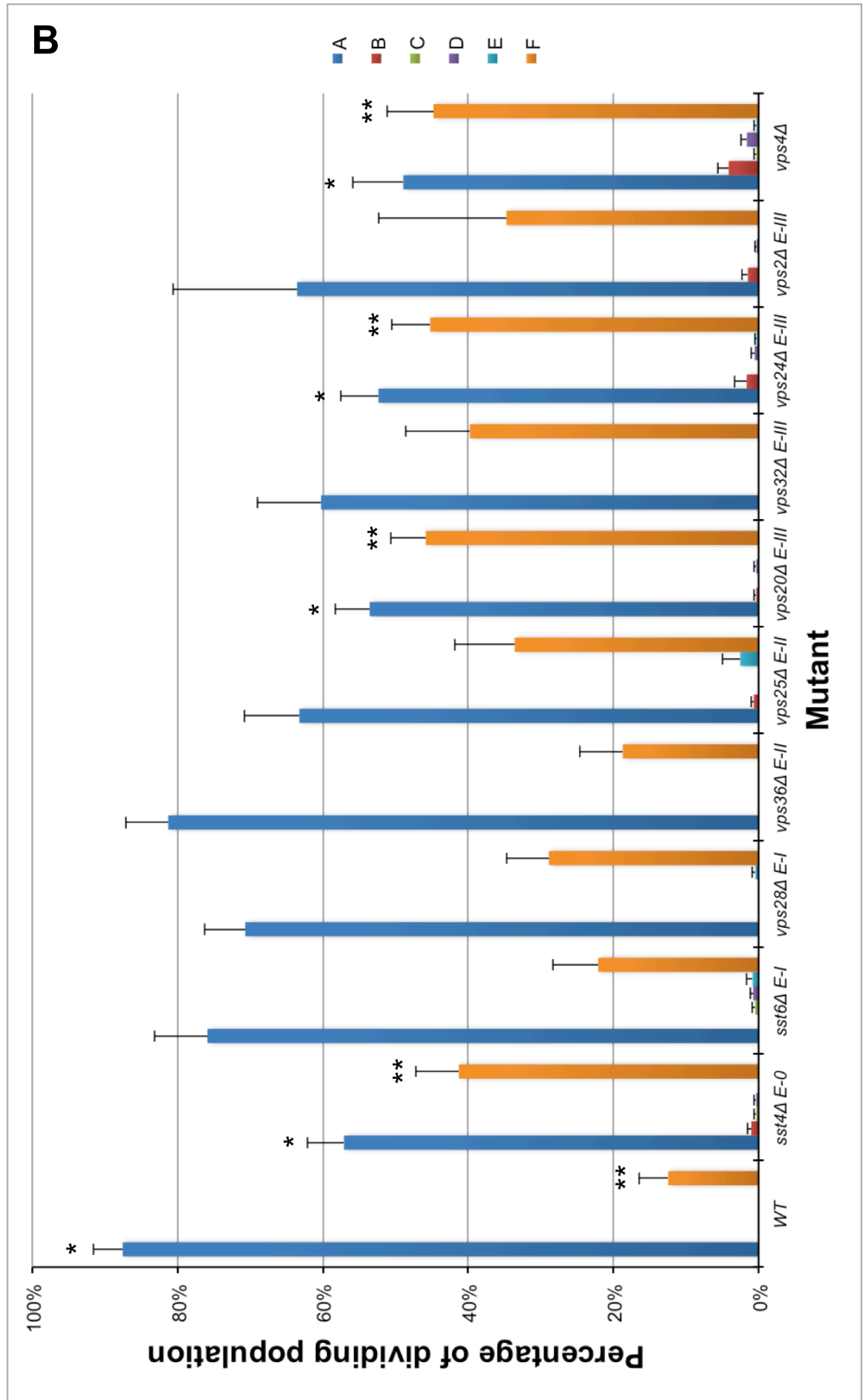


**Figure 3.1: ESCRT proteins are required for septation in fission yeast.**

Wild-type fission yeast, and strains containing individual chromosomal deletions of ESCRT genes were grown in rich liquid medium to mid-exponential phase and harvested. Cells were stained with Calcofluor white and visualised by fluorescence microscopy. Images were captured of both fluorescence via a DAPI filter and bright field. (A) Panels A-F indicate the observed septation phenotypes across various yeast strains. Diagrams above panels represent each phenotype: (A) a normal septum, (B) a misaligned septum, (C) a non-perpendicular septum, (D) multiple septa, (E) no septal formation, and (F) failed separation of daughter cells following septation. Scale bars – 10 microns. (B) Statistical analysis of the frequency of septation phenotypes A-F among ESCRT-deleted yeast strains, in comparison to the wild-type frequencies (400 cells, n=3; \* $p < 0.05$ ). Each of the ESCRT genes labels is accompanied by its respective ESCRT subunit (E-0-III).

Characterising septation in wild-type cells revealed two prevalent phenotypes: cells dividing normally and cells with delayed separation following septation. Characterising ESCRT-deleted strains revealed an increased proportion of cells with various septal defects, such as misaligned and non-perpendicular septa. There was also an increase in the proportion of cells with multiple septa, or even the complete absence of a septum. The latter was identified due to the length of the cell in comparison to the rest of the population: cells with failed septal formation would reach approximately double, or even three times the length of other cells.

However, the largest proportion of septal defects was in the identified *F phenotype*. This phenotype presented as two small joined cells with their contact edges stained (Figure 3.1A, panel F) and was thus described as two daughter cells that had failed to separate efficiently following septation. Although fission yeast do not immediately separate following division (Mitchison & Nurse 1985), an increased prevalence was observed of this phenotype relative to wild-type. To quantify the frequency of these phenotypes, 400 cells were counted in triplicate for wild-type and each ESCRT-deleted strain. Each phenotype was represented as a percentage of the total dividing population before being compared to the wild-type phenotype in the application of a Student's t-Test (with a two-tailed distribution, processed using Microsoft Excel). Statistical analysis by this means revealed a significant ( $p < 0.05$ ) increase in the failed separation *F phenotype* for chromosomal deletions of four ESCRT genes: *sst4*, *vps20*, *vps24* and *vps4* (Figure 3.1B).

These data show that the absence of ESCRT genes leads to defective septation in fission yeast; in some cells, this defect manifested as delayed septation, in other

cells as defective septation. These data imply that ESCRT proteins, particularly ESCRT-0, -III and Vps4p, are required for cell division in fission yeast.

### **3.2.2 Cell division defects observed in ESCRT mutants are exacerbated when combined with mutants of *plo1*, *clp1*, *mid1* and *ark1***

To identify fission yeast proteins that may regulate ESCRT protein function during cell division, septation phenotypes were examined in strains that contained double mutants of ESCRT deletions combined with mutants in genes *plo1*, *clp1*, *mid1* and *ark1*. These preliminary data were produced by graduate student Brinta Roy, whom I supervised, and are shown in *Appendix 6.2*. In each case, double mutants were produced by tetrad analysis (*Materials and Methods 2.2.3*), and the septation phenotypes characterised by Calcofluor staining (*Section 3.2.1*). A list of the strains used and produced in this study is shown in *Appendix 6.1*.

Cells with a temperature-sensitive mutant of *plo1* exhibited an increased proportion of *phenotypes C-F*. An increased proportion of the *C* and *F phenotypes* was observed in cells containing a *clp1* null mutation. Interestingly, both *plo1* and *clp1* mutants when combined with individual mutations in ESCRT genes frequently revealed a decreased proportion of the *F phenotype*; this may indicate phenotypic rescue and the interaction of these genes within a shared pathway. Both sets of double mutants also exhibited increases in aberrant phenotypes *B-E*, particularly double mutants with *clp1Δ*.

The observation of misaligned and non-perpendicular septa is similar to that reported in cells containing mutations in *mid1* (Sohrmann et al. 1996), which is required for actin ring formation in fission yeast (Ng et al. 2006). Thus, cells with a *mid1* null mutation were characterised, and an increased proportion of all aberrant *B-E phenotypes* was noted (Figure 3.1A). In addition, a further dividing phenotype of branched cells, sometimes with multiple septa, was identified. Double mutants of *mid1Δ* and ESCRT genes revealed an increased proportion of, in particular, *C phenotypes*, as well as the branched phenotype, designated *G phenotype*.

Ark1p is the fission yeast homologue of Aurora kinase, which has an established role in late stages of the cell cycle (Petersen & Hagan 2003). Thus, in light of the data collected in this study, it was investigated whether two temperature-sensitive mutants of *ark1*, *ark1-T8* and *ark1-T11* (Koch et al. 2011), exacerbate the septation phenotypes observed in ESCRT mutant strains. Single mutants were revealed to have an increased proportion of *C*, *E* and *F* phenotypes, and analysis of double mutants with ESCRT genes revealed a higher prevalence of *B-E* phenotypes in particular.

These observations indicate that ESCRT proteins mediate cell separation in fission yeast and that Plo1p, Clp1p, Mid1p and Ark1p potentially regulate ESCRT proteins in cell division.

### 3.2.3 *plo1*<sup>+</sup> and *clp1*<sup>+</sup> interact genetically with ESCRT genes

To test the hypothesis that Plo1p and Clp1p regulate ESCRT protein function, a yeast genetic approach was employed. This method allowed for the rapid analysis of a large number of genetic interactions between *plo1*<sup>+</sup>, *clp1*<sup>+</sup> and eight ESCRT genes.

Double mutants were produced by crossing yeast strains containing individual deletions of ESCRT genes (Iwaki et al. 2007) with various mutant strains of *plo1* and *clp1*. Progeny were characterised by tetrad analysis (*Materials and Methods* 2.2.3), an example of which is shown in Figure 3.2. A temperature-sensitive mutant of *plo1*, *plo1-ts35* (Anderson et al. 2002), and three different mutations of *clp1* were used: chromosomal deletion *clp1Δ* (Trautmann et al. 2001), phosphatase-dead *clp1.D257A* and *clp1.3A*, a gain-of-function mutant with reduced phosphorylation by Cdc2p (Wolfe et al. 2006). A list of the strains used and produced in this study is shown in *Appendix 6.1*.



**Figure 3.2: Fission yeast double mutants were generated by ascus dissection.**

Yeast strains were mated on solid ME medium and then transferred to solid YE medium for ascus dissection using a Singer MSM Ascus Dissector. This particular cross was incubated at 25°C, then replica plated to four selective solid media: YE grown at 36°C, YE with the addition of G418 (kanamycin), EMM lacking leucine and EMM lacking adenine. The double mutant is boxed in blue.

A strong indication of a genetic interaction between two genes is the generation of a synthetic lethal offspring, where two viable single mutants produce a non-viable double mutant. In this scenario, synthetic lethality may indicate a direct relationship between gene products, such that the combination of their activities is necessary for the survival of the organism (*Future work 5.3*). However, it may equally demonstrate the involvement of the respective gene products in distinct pathways, both of which are required for cell survival. None of the crosses between ESCRT deletions and *plo1* or *clp1* mutants produced such a synthetic lethal phenotype. However, more subtle genetic interactions may be inferred from impaired growth rates. To search for the presence of such phenotypes, parent and offspring strains were streaked to single colonies on rich and minimal solid media at various temperatures (*Materials and Methods 2.2.5*). As *plo1-ts35* is a temperature-sensitive strain with a permissive temperature of 25°C and a restrictive temperature of 36°C, it was hypothesised that combining this with mutations in ESCRT genes may result in the reduction of the restrictive temperature. Therefore, yeast strains were also grown at 25°C and 30°C to search for growth differences. Figure 3.3 illustrates the identification of just such a synthetic growth phenotype in double mutant *vps28Δ plo1-ts35* grown at 30°C.

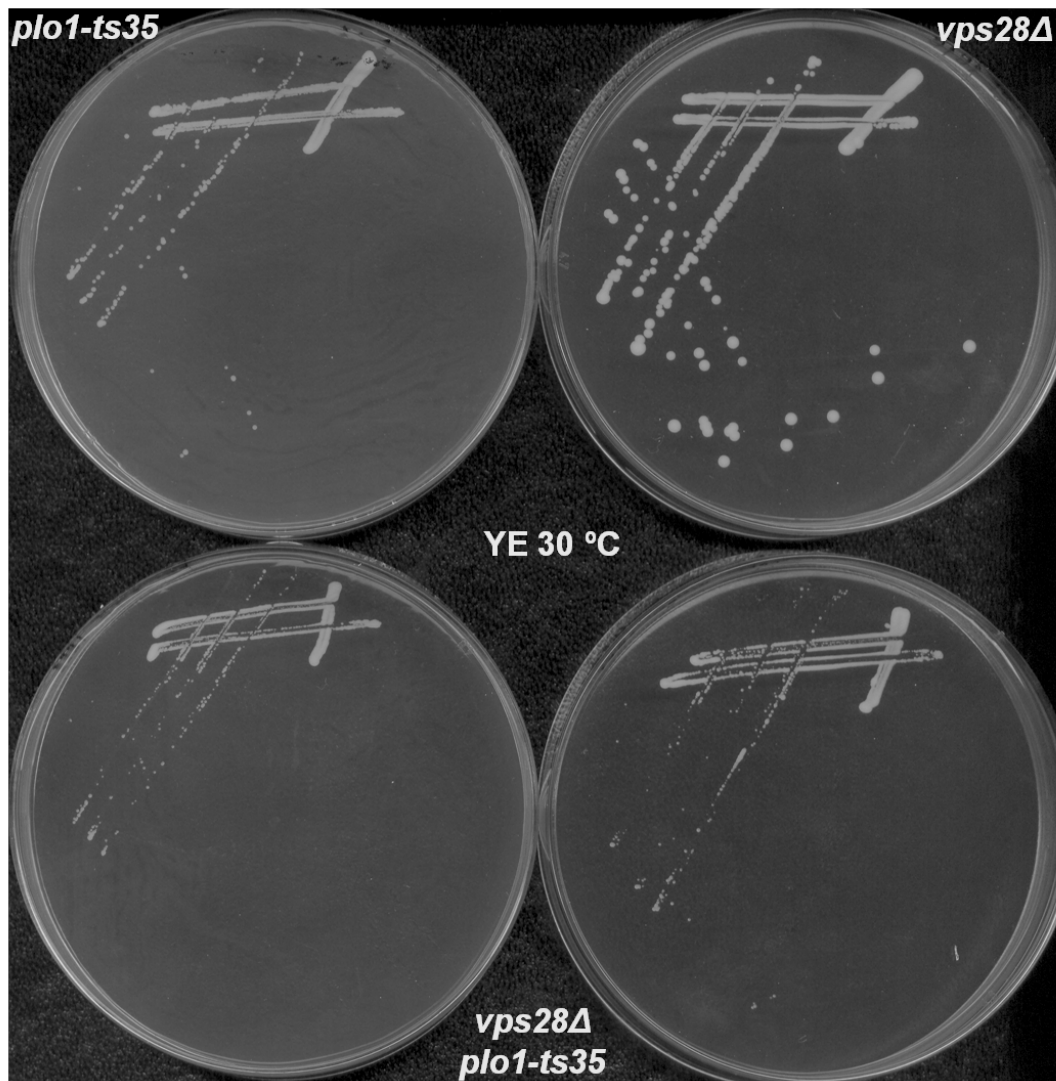


**Figure 3.3: *plo1-ts35* shows synthetic growth phenotypes with *vps28Δ*.**

Single and double mutants of *plo1-ts35* and *vps28Δ* were streaked to single colonies on solid YE medium. Images were captured after three days of growth at 30°C.

The results of the growth rate studies of all the ESCRT deletion strains with *plo1-ts35* and the three *clp1* mutant strains are shown in Table 3.1 and summarised in Table 3.2. Excitingly, it was observed that *plo1-ts35* and mutants of *clp1* showed genetic interactions with several ESCRT deletions, as they exhibited synthetic phenotypes at one or more of the temperatures and media investigated.

<i>ESCRTΔ</i>	Media	Temp	<i>plo1-ts35</i>	<i>clp1Δ</i>	<i>clp1.D257A</i>	<i>clp1.3A</i>
<i>sst4Δ</i> <i>E-0</i>	YE	25°C	X	X	X	X
		30°C	✓	X	X	X
		36°C	X	✓	✓	X
	EMM	25°C	X	X	X	X
		30°C	X	X	X	X
		36°C	X	X	X	X
<i>sst6Δ</i> <i>E-I</i>	YE	25°C	X			
		30°C	X			
		36°C	X			
	EMM	25°C	X			
		30°C	X			
		36°C	X			
<i>vps28Δ</i> <i>E-I</i>	YE	25°C	X	X	X	X
		30°C	✓	X	X	X
		36°C	X	✓	X	✓
	EMM	25°C	X	X	X	X
		30°C	X	X	X	X
		36°C	X	X	X	X
<i>vps36Δ</i> <i>E-II</i>	YE	25°C	X	X	X	X
		30°C	X	X	X	X
		36°C	X	✓	X	✓
	EMM	25°C	X	X	X	X
		30°C	X	X	X	X
		36°C	X	X	X	X
<i>vps25Δ</i> <i>E-II</i>	YE	25°C	X	X	X	X
		30°C	✓	X	X	X
		36°C	X	X	X	X
	EMM	25°C	X	X	X	X
		30°C	X	X	X	X
		36°C	X	X	X	X
<i>vps20Δ</i> <i>E-III</i>	YE	25°C	X	X	X	X
		30°C	✓	X	X	X
		36°C	✓	✓	✓	✓
	EMM	25°C	X	X	X	X
		30°C	X	X	X	X
		36°C	X	X	X	X
<i>vps2Δ</i> <i>E-III</i>	YE	25°C	X	X	X	X
		30°C	X	X	X	X
		36°C	✓	✓	X	X
	EMM	25°C	X	X	X	X
		30°C	X	X	X	X
		36°C	X	X	X	X
<i>vps4Δ</i>	YE	25°C	✓	X	X	X
		30°C	✓	X	X	X
		36°C	✓	✓	✓	✓
	EMM	25°C	X	X	X	X
		30°C	X	X	X	X
		36°C	X	X	X	X

**Table 3.1: Synthetic growth phenotypes of mutations in *plo1*, *clp1* and ESCRT genes.**

The table summarises growth rate analysis data, such as illustrated in Figure 3.3. Double mutants of *plo1-ts35* or mutant *clp1* with ESCRT mutants that resulted in synthetic growth phenotypes are indicated by ticks. Three temperatures were investigated on both rich (YE) and supplemented minimal (EMM) media. Double mutants could not be readily generated from *sst6Δ* and *clp1* as the genes are tightly linked, being less than 4.2 kb apart on the same chromosome ([www.pombase.org](http://www.pombase.org)).

The genetic interactions observed in crosses between ESCRT deletion strains and *plo1-ts35* and *clp1* mutant strains are summarised in Table 3.2. This shows a global perspective of the genetic interactions observed between these strains, as the represented genetic interactions may refer to one or more observations of a synthetic phenotype in the six conditions analysed for each genetic cross (rich and minimal media, and three temperatures).

<b>ESCRTΔ</b>	<b><i>plo1-ts35</i></b>	<b><i>clp1Δ</i></b>	<b><i>clp1.D257A</i></b>	<b><i>clp1.3A</i></b>
<b><i>sst4Δ E-0</i></b>	✓	✓	✓	X
<b><i>sst6Δ E-I</i></b>	✓	Genes are tightly linked		
<b><i>vps28Δ E-I</i></b>	✓	✓	X	✓
<b><i>vps36Δ E-II</i></b>	X	✓	X	✓
<b><i>vps25Δ E-II</i></b>	✓	X	X	X
<b><i>vps20Δ E-III</i></b>	✓	✓	✓	✓
<b><i>vps2Δ E-III</i></b>	✓	✓	X	X
<b><i>vps4Δ</i></b>	✓	✓	✓	✓

**Table 3.2: A summary of synthetic growth phenotypes of mutations in *plo1*, *clp1* and ESCRT genes.**

The table summarises the growth rate analysis data presented in Table 3.1. Double mutants of *plo1-ts35* or *clp1Δ* with ESCRT mutants that resulted in synthetic growth phenotypes are indicated by ticks. Double mutants could not be readily generated from *sst6Δ* and *clp1* as the genes are tightly linked, being less than 4.2 kb apart on the same chromosome ([www.pombase.org](http://www.pombase.org)).

These synthetic phenotypes indicate genetic interactions, which in turn suggest that ESCRT proteins interact with Plo1p and Clp1p.

### 3.2.4 Plo1p and Clp1p affect ESCRT-mediated vesicular trafficking

To augment the genetic data indicating interactions between *plo1*<sup>+</sup>, *clp1*<sup>+</sup> and ESCRT genes, a parallel study was performed analysing the effect of *plo1* and *clp1* mutants upon sorting during downregulation of ubiquitin-labelled receptors. The basis of this study is the observation that ESCRT proteins have roles in cell sorting (Iwaki et al. 2007). The hypothesis that Plo1p and Clp1p regulate ESCRT components leads to the current hypothesis that genetic mutants of *plo1* and *clp1* will affect vesicular trafficking in an ESCRT-dependent manner. Iwaki et al (2007) demonstrated the principle of this experiment by generating a ubiquitin-GFP-labelled receptor (Ub-GFP-*SpCPS*) that localised to vacuoles in wild-type fission yeast cells. They then showed that in ESCRT-null strains, the pattern of fluorescence changed from vacuolar to endosomal, indicating defective sorting. This finding supports the observation that ESCRT proteins have roles in vacuolar sorting.

To examine receptor localisation in fission yeast, the Ub-GFP-*SpCPS* construct (Iwaki et al. 2007) was transformed into wild-type fission yeast and strains with individual deletions in ESCRT genes. FM 4-64, a stain for yeast vacuolar membranes, was used to identify the vacuoles, and the cells were visualised by confocal fluorescence microscopy (*Materials and Methods* 2.2.6). Similar to reported descriptions (Iwaki et al. 2007), wild-type cells exhibited a largely vacuolar pattern of sorting (Figure 3.4). This was identified by the overlap in fluorescence between Ub-GFP-*SpCPS* and the FM 4-64-stained vacuoles. However, the ESCRT-deleted yeast strains, with one ESCRT mutant chosen from each ESCRT class, exhibited a punctate pattern of fluorescence associated with Ub-GFP-*SpCPS* (Figure 3.4). Iwaki et al (2007) identified this as endosomal, via the localisation of RFP-labelled phosphatidylinositol-(3,4,5)-triphosphate, which has previously been shown to accumulate on the endosome (Mitra et al. 2004). Cells with a *vps4Δ* deletion exhibited a sorting pattern similar to wild-type cells.

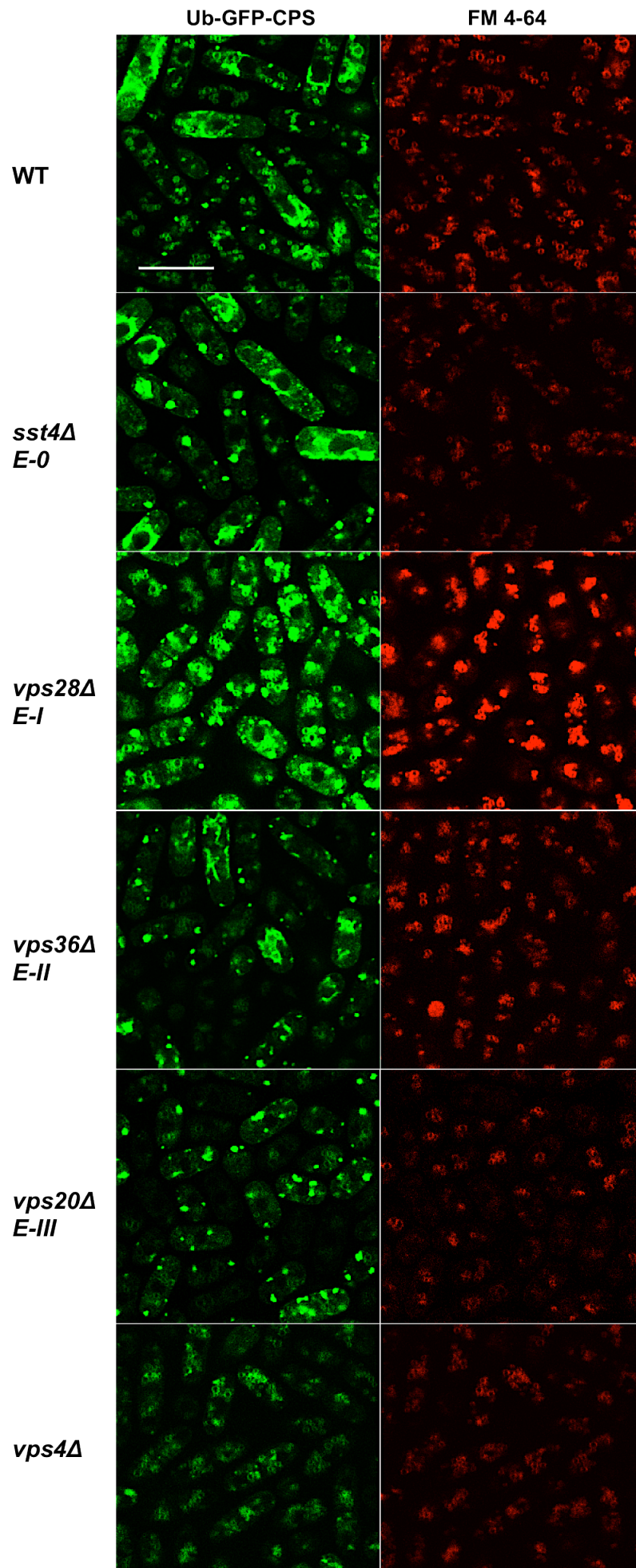
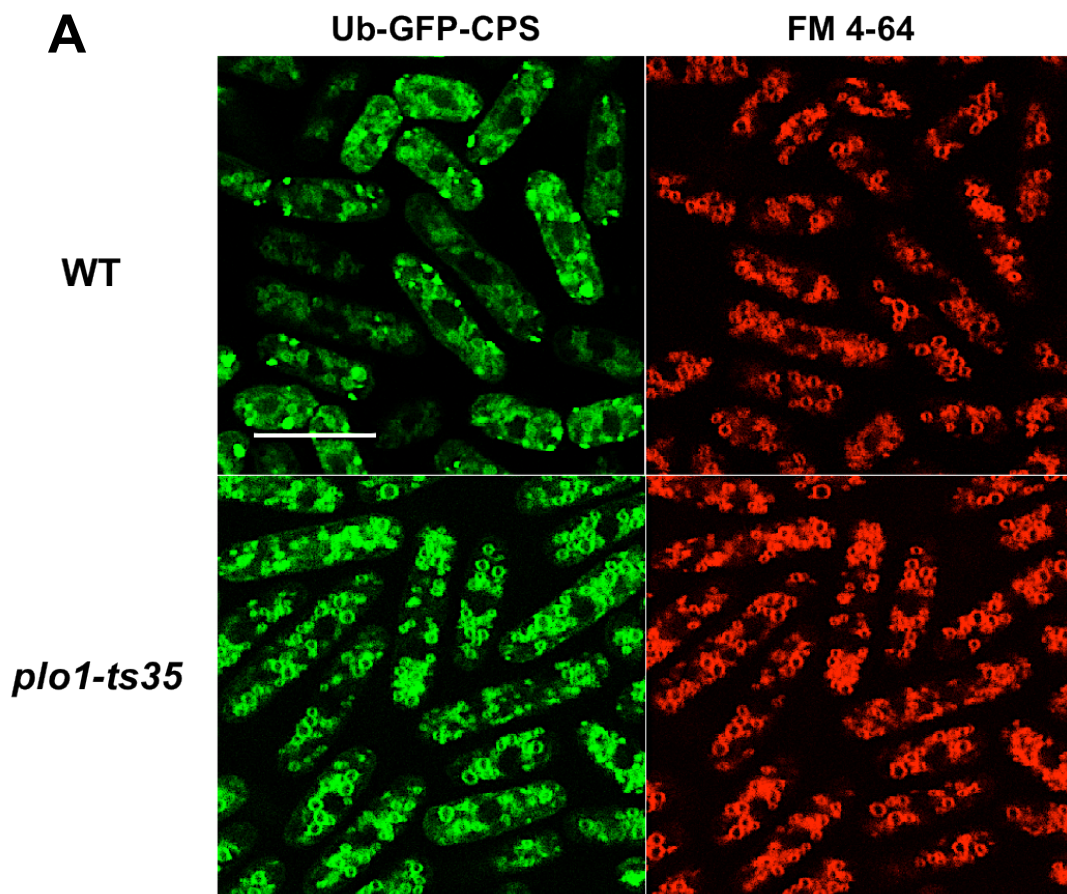


**Figure 3.4: Defective vacuolar sorting is observed in fission yeast with individual chromosomal deletions of ESCRT genes.**

Wild-type and ESCRT-deleted fission yeast strains, transformed with Ub-GFP-*SpCPS*, were cultured in liquid minimal medium, stained with FM 4-64 and visualised using a confocal microscope. Strains were cultured at 30°C, although similar profiles were noted in strains cultured at 25°C. Scale bar – 10 microns.

The wild-type phenotype presented here differs from the luminal GFP distribution reported (Iwaki et al. 2007); this may be due to the culturing of these strains, as nutrient stress may contribute to differences in the observed phenotypes. Nevertheless, once a reproducible phenotype for the wild-type and ESCRT-deleted strains was achieved, the Ub-GFP-*SpCPS* and vacuolar distribution in *plo1-ts35* and *clp1* mutant cells was characterised (Figure 3.5). Distinct vacuolar profiles were noted in these strains, particularly in *plo1-ts35* cells, which exhibited a uniform array of vacuoles that precisely co-localised with the Ub-GFP-*SpCPS* construct (Figure 3.5A). In contrast, Ub-GFP-*SpCPS* tended to localise to the lumina of *clp1*Δ cells (Figure 3.5B). The *clp1* mutant, *clp1.D257A*, revealed a phenotype closer to wild-type cells. The *clp1.3A* mutant revealed a phenotype similar to the reported wild-type phenotype (Iwaki et al. 2007), which is, according to these data presented, more similar to the phenotype observed in *plo1-ts35* cells.

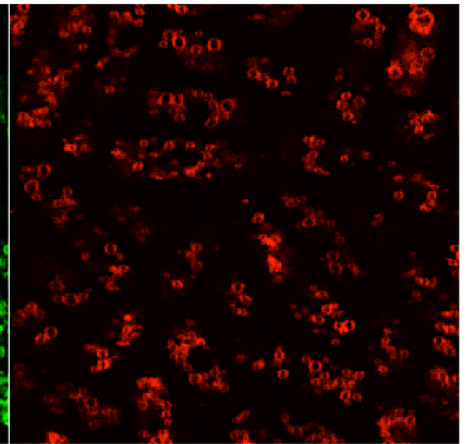
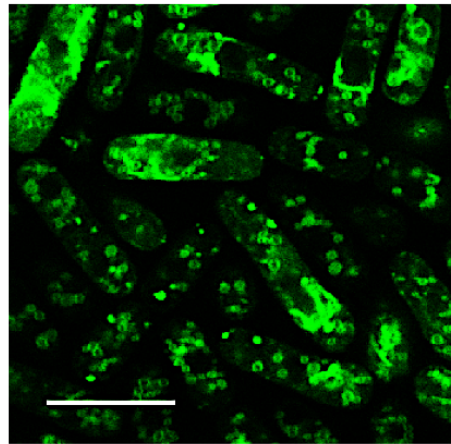
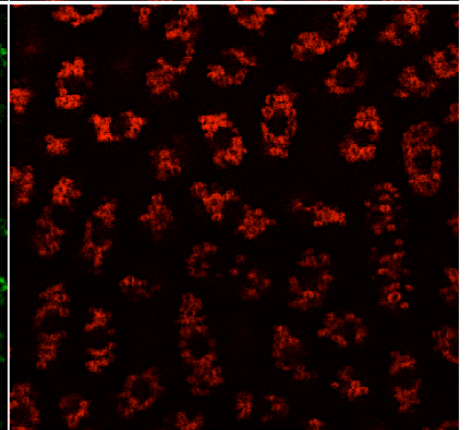
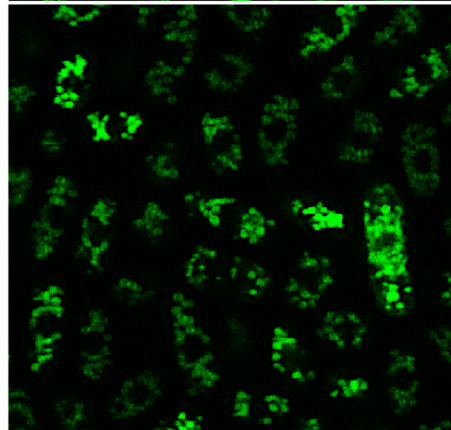
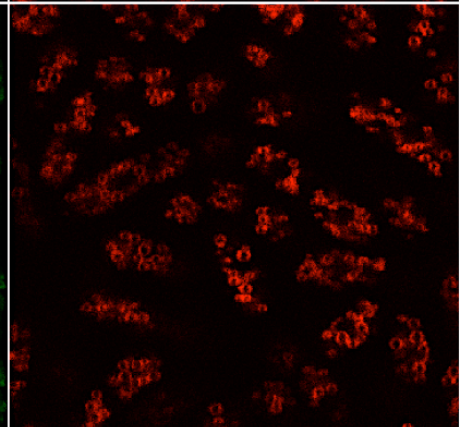
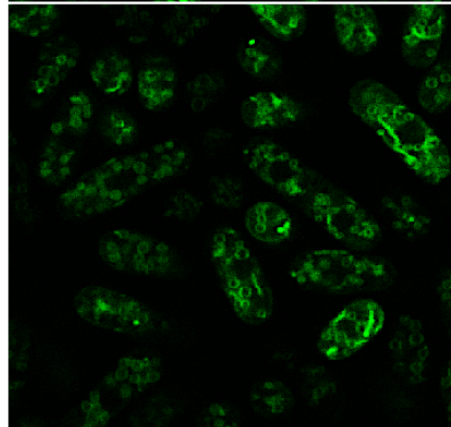
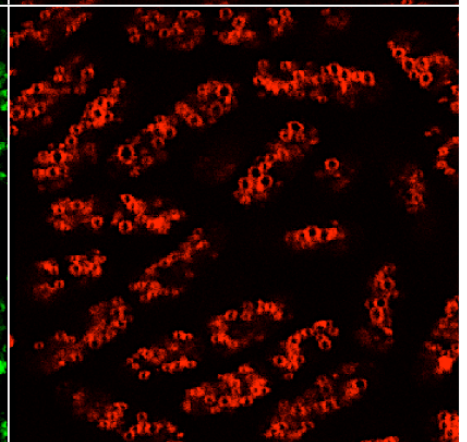
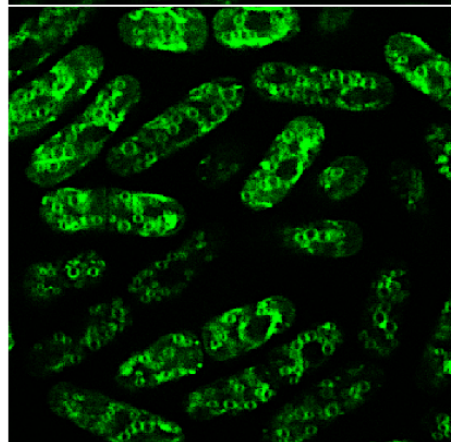


**B**

Ub-GFP-CPS

FM 4-64

WT

*clp1Δ**clp1.D257A**clp1.3A*

**Figure 3.5: Mutants of *plo1* and *clp1* cause defective vacuolar sorting in fission yeast.**

Wild-type and ESCRT-deleted fission yeast strains, transformed with Ub-GFP-*SpCPS*, were cultured in liquid minimal medium, stained with FM 4-64 and visualised using a confocal microscope. Strains were cultured at (A) 25°C or (B) 30°C. Scale bar – 10 microns.

One way to infer a role for Plo1p and Clp1p in regulating ESCRT protein function would be to observe similar patterns of Ub-GFP-*SpCPS* and vacuolar distribution in cells containing mutations in their genes. However, this was not observed. One possible explanation for this may be linked to the observation that Plo1p and Clp1p are active late in the cell cycle (Ng et al. 2006; Papadopoulou et al. 2010); thus their regulation of the ESCRT proteins may be restricted to ESCRT functions in cytokinesis. This would be consistent with the hypothesis of this study that Plo1p and Clp1p regulate ESCRT proteins in cytokinesis.

Nevertheless, *plo1-ts35* and *clp1Δ* did present striking profiles of vacuolar morphology, albeit distinct to that observed in ESCRT deletion strains. These observations prompted an epistasis experiment, whereby the Ub-GFP-*SpCPS* construct was transformed into double mutants of ESCRT deletions and *plo1-ts35* and *clp1Δ*; one representative of each ESCRT class was selected. This allowed the qualitative analysis of the Ub-GFP-*SpCPS* and vacuolar distributions in double mutants compared to each parent. Such analysis might allow inferences to be made as to the possible dependency of ESCRT genes on *plo1*<sup>+</sup> and *clp1*<sup>+</sup> to control the cell sorting function.

The images produced from such an epistatic analysis revealed that all but one of the *plo1-ts35* ESCRT double mutants exhibited a phenotype closer to their *plo1-ts35* parent (Figure 3.6). In contrast, all of the *clp1Δ* ESCRT double mutants exhibited a phenotype closer to their ESCRT parent (Figure 3.7). The results of these experiments are summarised in Table 3.3.

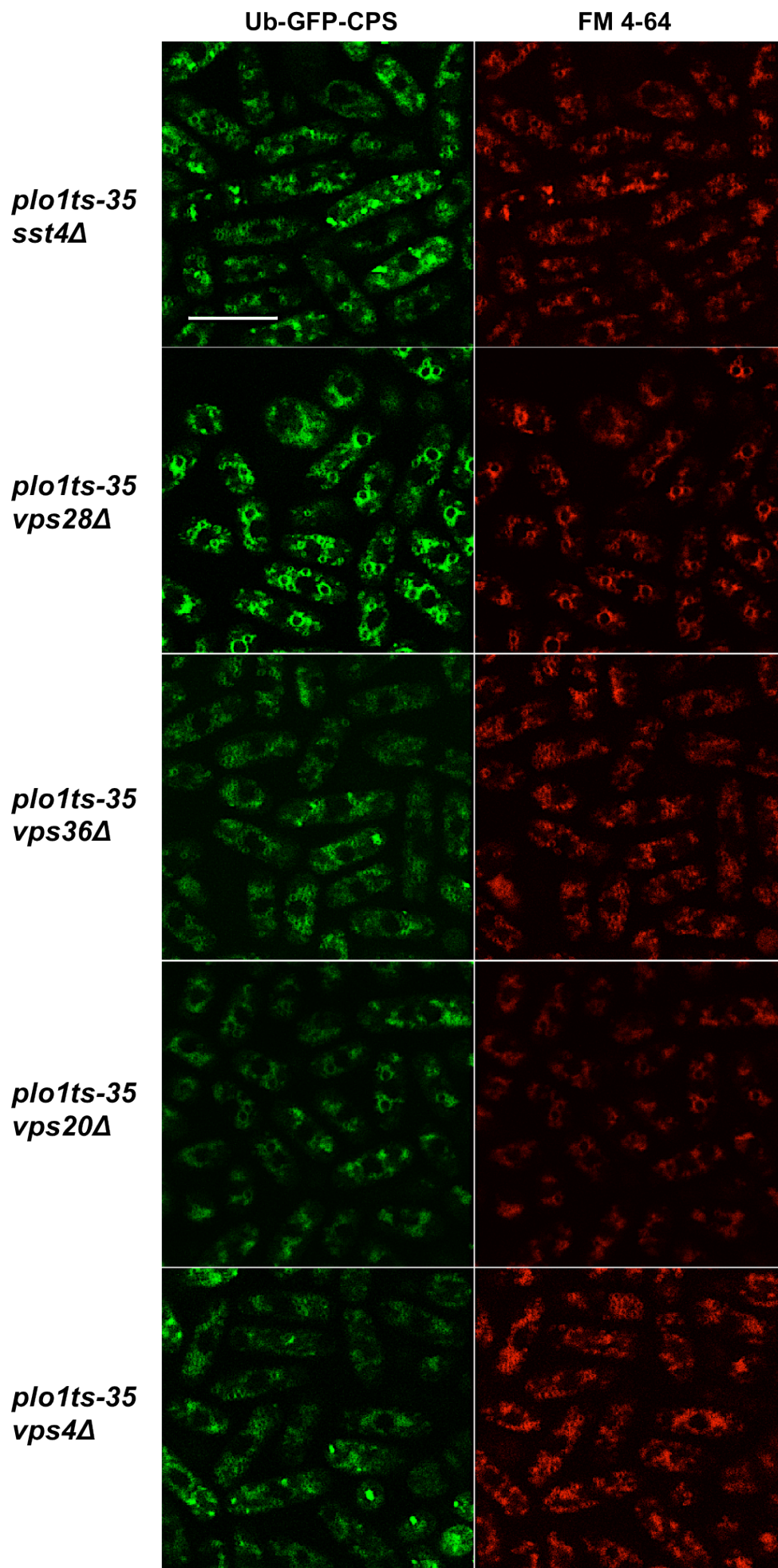


**Figure 3.6: Genetic interactions between *plp1-ts35* and ESCRT deletions in controlling cell sorting.**

Double mutants of *plp1-ts35* and ESCRT deletions, transformed with Ub-GFP-*SpCPS*, were cultured in liquid minimal medium at 25°C, stained with FM 4-64 and visualised using a confocal microscope. Scale bar – 10 microns.

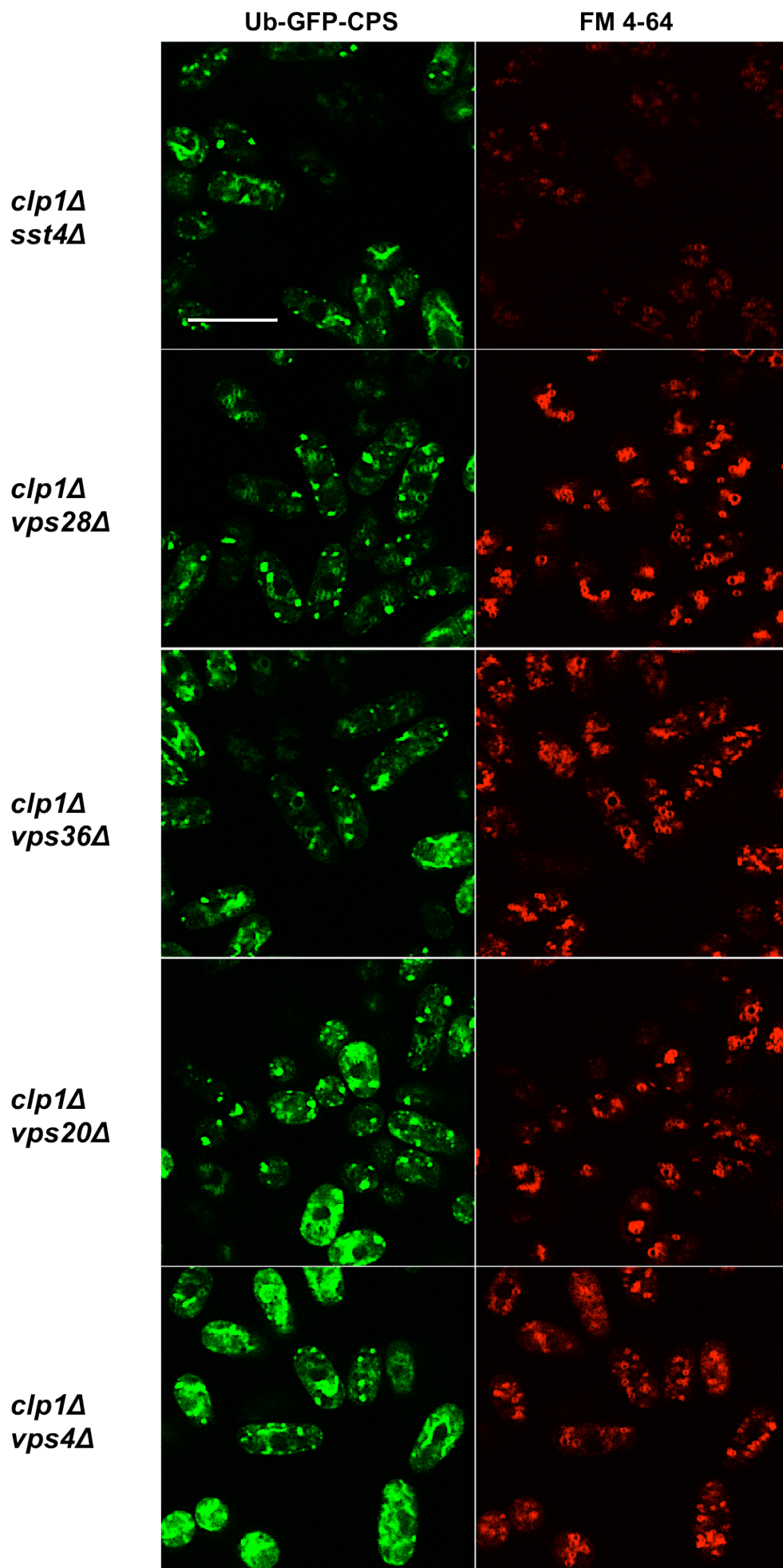


**Figure 3.7: Genetic interactions between *clp1Δ* and ESCRT deletions in controlling cell sorting.**

Double mutants of *clp1Δ* and ESCRT deletions, transformed with Ub-GFP-*SpCPS*, were cultured in liquid minimal medium at 25°C, stained with FM 4-64 and visualised using a confocal microscope. Scale bar – 10 microns.

<b><i>ESCRTΔ</i></b>	<b><i>plo1-ts35</i></b>	<b><i>clp1Δ</i></b>
<b><i>sst4Δ E-0</i></b>	<i>plo1-ts35</i>	<i>sst4Δ</i>
<b><i>vps28Δ E-I</i></b>	<i>plo1-ts35</i>	<i>vps28Δ</i>
<b><i>vps36Δ E-II</i></b>	<i>plo1-ts35</i>	<i>vps36Δ</i>
<b><i>vps20Δ E-III</i></b>	<i>plo1-ts35</i>	<i>vps20Δ</i>
<b><i>vps4Δ</i></b>	<i>vps4Δ</i>	<i>vps4Δ</i>

**Table 3.3: A summary of the vacuolar sorting epistasis data in double mutants of ESCRT genes and *plo1* or *clp1*.**

The table summarises the epistasis data collected in double mutants of *plo1-ts35* or *clp1Δ* with ESCRT genes. The mutants named in the body of the table indicate which parent the double mutants resembled.

Qualitatively, the *plo1-ts35* double mutants with *sst4Δ*, *vps28Δ*, *vps36Δ* and *vps20Δ* more closely resembled the *plo1-ts35* single mutant, whereas the *plo1-ts35 vps4Δ* double mutant more closely resembled its *vps4Δ* parent. However, all of the *clp1Δ* double mutants more closely resembled their respective ESCRT deletion parent. These epistasis data suggest that *plo1*<sup>+</sup> functions upstream of the ESCRT genes, and *clp1*<sup>+</sup> downstream, in controlling cell sorting in fission yeast.

### 3.2.5 Plo1p and Clp1p interact physically with ESCRT proteins

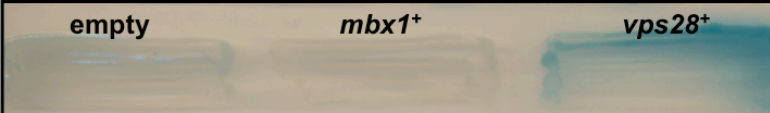
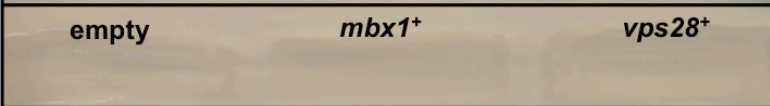
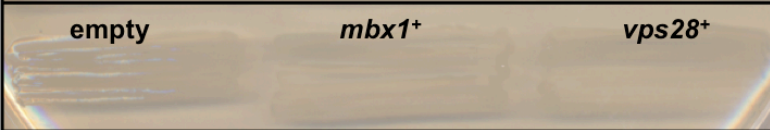
The observations presented in Sections 3.2.2 to 3.2.4 suggest genetic interactions between *plo1*<sup>+</sup>, *clp1*<sup>+</sup> and ESCRT genes. The simplest explanation for these genetic interactions is that the encoded proteins physically interact. This was tested using the yeast two-hybrid method (Fields & Song 1989). Plo1p or Clp1p fused to the DNA-binding domain of the GAL4 transcription factor in the so-called *bait* vector (Reynolds & Ohkura 2003; Papadopoulou et al. 2010) were co-transformed into budding yeast cells with individual ESCRT proteins fused to the DNA-activation domain in the *prey* vector. Transcriptional readout from the *gal4* promoter linked to the reporter gene in these yeast cells, as shown by the

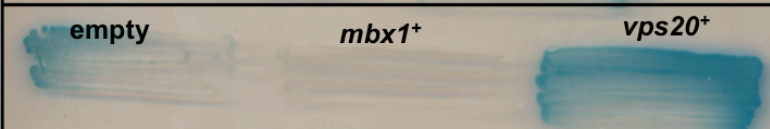
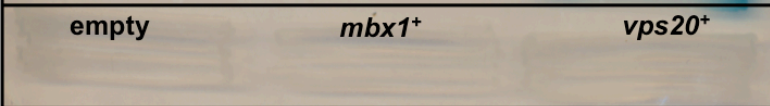
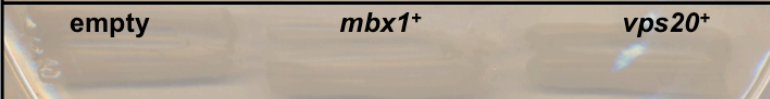
production of a blue pigment from substrate X-Gal, indicates that the proteins interact *in vivo*.

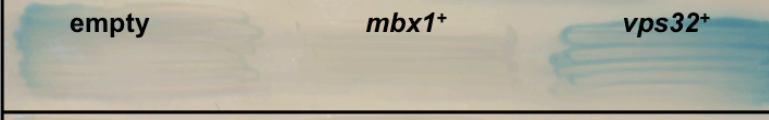
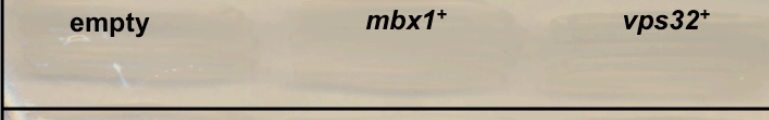
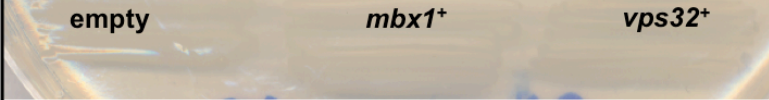
To facilitate cloning the ESCRT genes, the StrataClone Blunt PCR Cloning kit was employed (*Materials and Methods 2.2.8*). Genes were amplified using suitable oligonucleotides (*Materials and Methods 2.1.2*) and proof-reading *Pfu* polymerase for PCR and then cloned into the StrataClone vector. Once the integrity of cloned genes was confirmed by sequencing, they were sub-cloned into the prey vector, pACT2. Constructs were then transformed into budding yeast strains GGBY 138 or 171. A list of the strains used and produced in this study is shown in *Appendix 6.1*.

Transformed yeast strains were grown on solid minimal medium alongside appropriate controls for three days at 30°C. To test for interactions with Plo1p, each of the ESCRT proteins was interrogated for interactions with wild-type Plo1p, a kinase-dead mutant (Plo1.K69R) and two mutants in the polo-box domain, which is required for substrate binding (Plo1.472-684 and Plo1.DHK625AAA) (Reynolds & Ohkura 2003). The interaction of Plo1p with Mbx1p was used as the positive control for the assay (Papadopoulou et al. 2008). The X-Gal overlay assay was performed (*Materials and Methods 2.2.10*) and images were captured both approximately 12 hours later, and after 1-2 days, depending on the strength of the interaction.

A number of the ESCRT proteins exhibited interactions with wild-type Plo1p and inactive Plo1p (Plo1.K69R). These are shown in Figure 3.8, which is summarised in Table 3.4, and were Vps28p (ESCRT-I), Vps20p (ESCRT-III) and Vps32p (ESCRT-III).

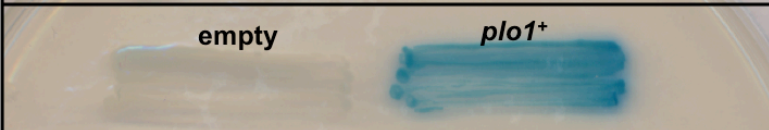
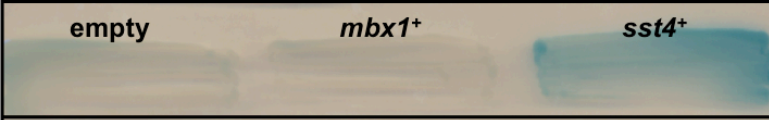
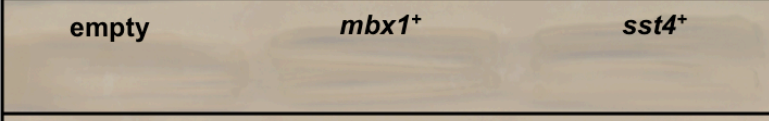
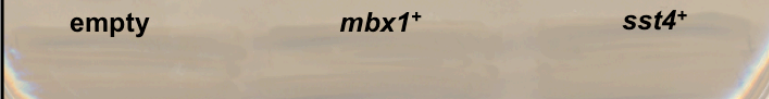
	empty	<i>plo1</i> <sup>+</sup>	empty	
	empty	<i>plo1</i> <sup>+</sup>	<i>mbx1</i> <sup>+</sup>	
	empty	<i>plo1</i> <sup>+</sup>	<i>vps28</i> <sup>+</sup>	
	empty	<i>mbx1</i> <sup>+</sup>	<i>vps28</i> <sup>+</sup>	<i>plo1.K69R</i>
	empty	<i>mbx1</i> <sup>+</sup>	<i>vps28</i> <sup>+</sup>	<i>plo1.472-684</i>
	empty	<i>mbx1</i> <sup>+</sup>	<i>vps28</i> <sup>+</sup>	<i>plo1.DHK625AAA</i>

	empty	<i>plo1</i> <sup>+</sup>	empty	
	empty	<i>plo1</i> <sup>+</sup>	<i>mbx1</i> <sup>+</sup>	
	empty	<i>plo1</i> <sup>+</sup>	<i>vps20</i> <sup>+</sup>	
	empty	<i>mbx1</i> <sup>+</sup>	<i>vps20</i> <sup>+</sup>	<i>plo1.K69R</i>
	empty	<i>mbx1</i> <sup>+</sup>	<i>vps20</i> <sup>+</sup>	<i>plo1.472-684</i>
	empty	<i>mbx1</i> <sup>+</sup>	<i>vps20</i> <sup>+</sup>	<i>plo1.DHK625AAA</i>

	empty	<i>plo1</i> <sup>+</sup>	empty	
	empty	<i>mbx1</i> <sup>+</sup>	<i>mbx1</i> <sup>+</sup>	
	empty	<i>vps32</i> <sup>+</sup>	<i>vps32</i> <sup>+</sup>	
	empty	<i>mbx1</i> <sup>+</sup>	<i>vps32</i> <sup>+</sup>	<i>plo1.K69R</i>
	empty	<i>mbx1</i> <sup>+</sup>	<i>vps32</i> <sup>+</sup>	<i>plo1.472-684</i>
	empty	<i>mbx1</i> <sup>+</sup>	<i>vps32</i> <sup>+</sup>	<i>plo1.DHK625AAA</i>

**Figure 3.8: Vps28p, Vps20p and Vps32p physically interact with wild-type Plo1p.** Budding yeast strains were transformed with the yeast two-hybrid bait and prey plasmid constructs indicated. The ESCRT proteins were fused to the prey domain of the GAL4 transcription factor; however, for ease of identification, the bait and prey plasmids have not been labelled consistently. The strains were grown for three days on selective medium when the X-Gal overlay assay was performed.

However, other ESCRT proteins exhibited interactions with inactive Plo1p, yet not wild-type; these are shown in Figure 3.9 and summarised in Table 3.4, and were Sst4p (ESCRT-0) and Vps25p (ESCRT-II).

	empty	<i>plo1</i> <sup>+</sup>	empty	
	empty	<i>mbx1</i> <sup>+</sup>	<i>mbx1</i> <sup>+</sup>	
	empty	<i>sst4</i> <sup>+</sup>	<i>sst4</i> <sup>+</sup>	
	empty	<i>mbx1</i> <sup>+</sup>	<i>sst4</i> <sup>+</sup>	<i>plo1.K69R</i>
	empty	<i>mbx1</i> <sup>+</sup>	<i>sst4</i> <sup>+</sup>	<i>plo1.472-684</i>
	empty	<i>mbx1</i> <sup>+</sup>	<i>sst4</i> <sup>+</sup>	<i>plo1.DHK625AAA</i>

empty	<i>plo1<sup>+</sup></i>		empty
empty	<i>plo1<sup>+</sup></i>		<i>mbx1<sup>+</sup></i>
empty	<i>plo1<sup>+</sup></i>		<i>vps25<sup>+</sup></i>
empty	<i>mbx1<sup>+</sup></i>	<i>vps25<sup>+</sup></i>	<i>plo1.K69R</i>
empty	<i>mbx1<sup>+</sup></i>	<i>vps25<sup>+</sup></i>	<i>plo1.472-684</i>
empty	<i>mbx1<sup>+</sup></i>	<i>vps25<sup>+</sup></i>	<i>plo1.DHK625AAA</i>

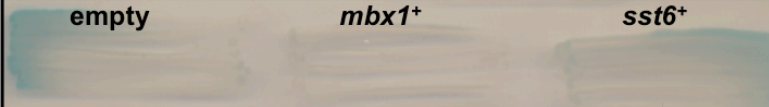
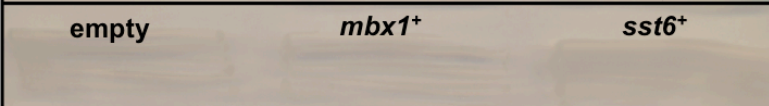
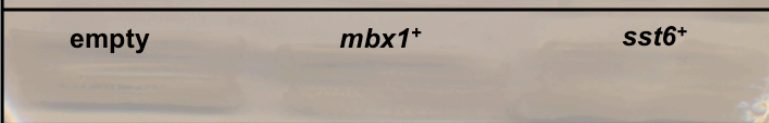
**Figure 3.9: Sst4p and Vps25p physically interact with kinase-dead Plo1p.**

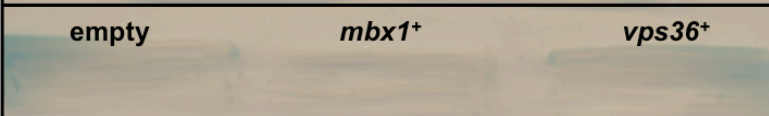
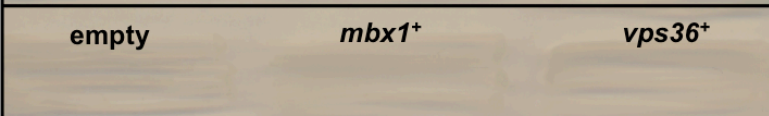
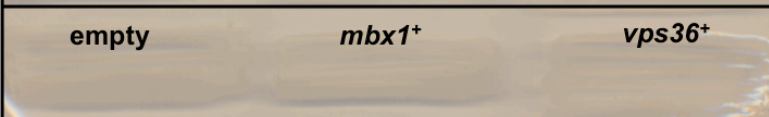
Budding yeast strains were transformed with the yeast two-hybrid bait and prey plasmid constructs indicated. The ESCRT proteins were fused to the prey domain of the GAL4 transcription factor; however, for ease of identification, the bait and prey plasmids have not been labelled consistently. The strains were grown for three days on selective medium when the X-Gal overlay assay was performed.

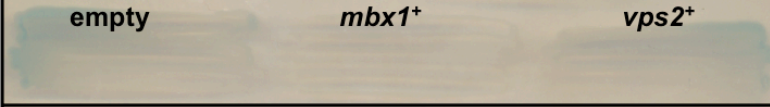
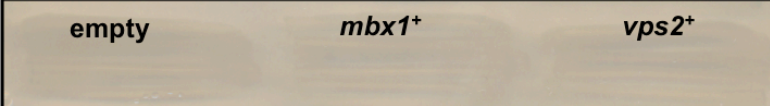
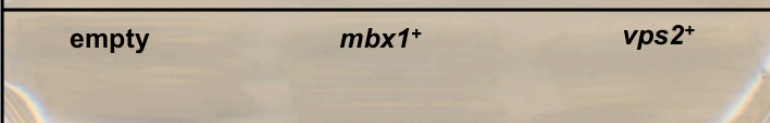
One possible explanation for interactions with Sst4p and Vps25p only being detected with a catalytically inactive version of Plo1p is that wild-type Plo1p normally only interacts transiently with these proteins, which is not detected by this two-hybrid assay. Possibly, the catalytically inactive version of Plo1p ‘traps’ Sst4p and Vps25p, resulting in a more stable interaction, which is, in contrast, detected.

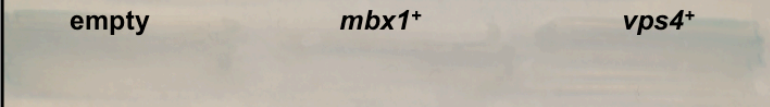
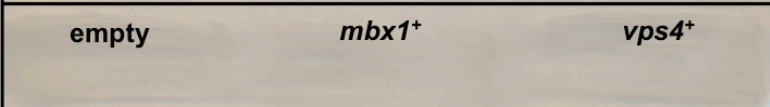
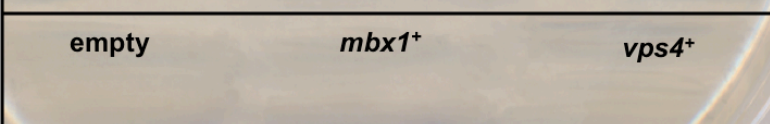
Those ESCRT proteins that exhibited no interaction with Plo1p are shown in Figure 3.10 and summarised in Table 3.4. These were Sst6aa.20-487, a form of Sst6p that omitted a short, early intron (ESCRT-I), Vps36p (ESCRT-II), Vps2p (ESCRT-III) and Vps4p.

Finally, none of the ESCRT proteins exhibited interactions with the Plo1 mutants of the polo-box domain, which is consistent with this domain’s role in substrate binding (Reynolds & Ohkura 2003).

	empty	<i>plo1</i> <sup>+</sup>	empty	
	empty	<i>plo1</i> <sup>+</sup>	<i>mbx1</i> <sup>+</sup>	
	empty	<i>plo1</i> <sup>+</sup>	<i>sst6</i> <sup>+</sup>	
	empty	<i>mbx1</i> <sup>+</sup>	<i>sst6</i> <sup>+</sup>	<i>plo1.K69R</i>
	empty	<i>mbx1</i> <sup>+</sup>	<i>sst6</i> <sup>+</sup>	<i>plo1.472-684</i>
	empty	<i>mbx1</i> <sup>+</sup>	<i>sst6</i> <sup>+</sup>	<i>plo1.DHK625AAA</i>

	empty	<i>plo1</i> <sup>+</sup>	empty	
	empty	<i>plo1</i> <sup>+</sup>	<i>mbx1</i> <sup>+</sup>	
	empty	<i>plo1</i> <sup>+</sup>	<i>vps36</i> <sup>+</sup>	
	empty	<i>mbx1</i> <sup>+</sup>	<i>vps36</i> <sup>+</sup>	<i>plo1.K69R</i>
	empty	<i>mbx1</i> <sup>+</sup>	<i>vps36</i> <sup>+</sup>	<i>plo1.472-684</i>
	empty	<i>mbx1</i> <sup>+</sup>	<i>vps36</i> <sup>+</sup>	<i>plo1.DHK625AAA</i>

	<b>empty</b>	<b><i>plo1<sup>+</sup></i></b>	<b>empty</b>	
	<b>empty</b>	<b><i>plo1<sup>+</sup></i></b>	<b><i>mbx1<sup>+</sup></i></b>	
	<b>empty</b>	<b><i>plo1<sup>+</sup></i></b>	<b><i>vps2<sup>+</sup></i></b>	
	<b>empty</b>	<b><i>mbx1<sup>+</sup></i></b>	<b><i>vps2<sup>+</sup></i></b>	<b><i>plo1.K69R</i></b>
	<b>empty</b>	<b><i>mbx1<sup>+</sup></i></b>	<b><i>vps2<sup>+</sup></i></b>	<b><i>plo1.472-684</i></b>
	<b>empty</b>	<b><i>mbx1<sup>+</sup></i></b>	<b><i>vps2<sup>+</sup></i></b>	<b><i>plo1.DHK625AAA</i></b>

	<b>empty</b>	<b><i>plo1<sup>+</sup></i></b>	<b>empty</b>	
	<b>empty</b>	<b><i>plo1<sup>+</sup></i></b>	<b><i>mbx1<sup>+</sup></i></b>	
	<b>empty</b>	<b><i>plo1<sup>+</sup></i></b>	<b><i>vps4<sup>+</sup></i></b>	
	<b>empty</b>	<b><i>mbx1<sup>+</sup></i></b>	<b><i>vps4<sup>+</sup></i></b>	<b><i>plo1.K69R</i></b>
	<b>empty</b>	<b><i>mbx1<sup>+</sup></i></b>	<b><i>vps4<sup>+</sup></i></b>	<b><i>plo1.472-684</i></b>
	<b>empty</b>	<b><i>mbx1<sup>+</sup></i></b>	<b><i>vps4<sup>+</sup></i></b>	<b><i>plo1.DHK625AAA</i></b>

**Figure 3.10: Sst6p, Vps36p, Vps2p and Vps4p do not exhibit physical interactions with Plo1p.**

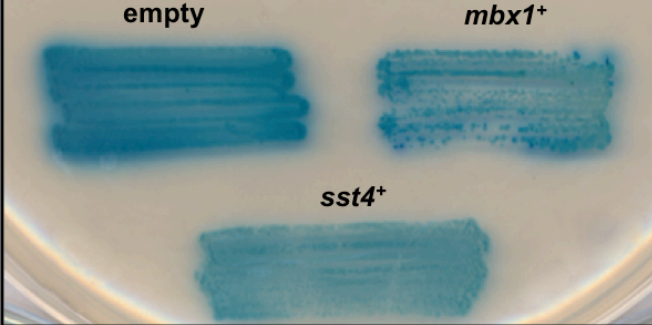
Budding yeast strains were transformed with the yeast two-hybrid bait and prey plasmid constructs indicated. The ESCRT proteins were fused to the prey domain of the GAL4 transcription factor; however, for ease of identification, the bait and prey plasmids have not been labelled consistently. The strains were grown for three days on selective medium when the X-Gal overlay assay was performed.

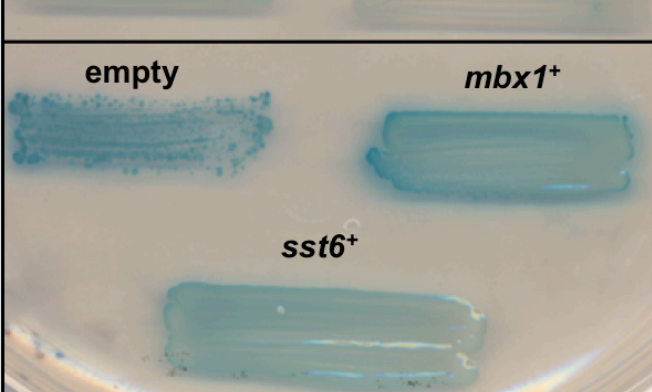
ESCRT	Plo1p	Plo1.K69R	Plo1.472-684	Plo1.DHK625AAA
Sst4p E-0	X	✓	X	X
Sst6aa.20-487 E-I	X	X	X	X
Vps28p E-I	✓	✓	X	X
Vps36p E-II	X	X	X	X
Vps25p E-II	X	✓	X	X
Vps20p E-III	✓	✓	X	X
Vps32p E-III	✓	✓	X	X
Vps2p E-III	X	X	X	X
Vps4p	X	X	X	X

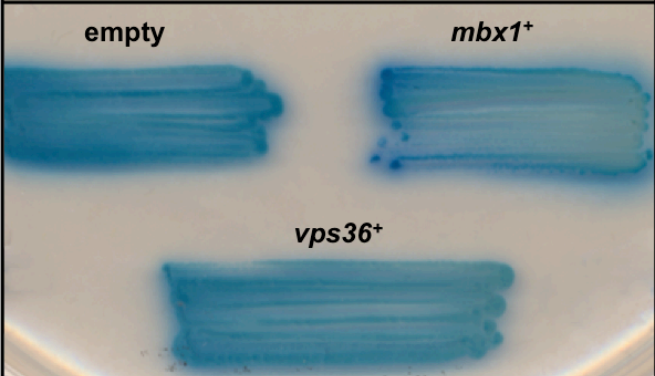
**Table 3.4: A summary of blue yeast observation in yeast two-hybrid analysis of Plo1p and the ESCRT proteins.**

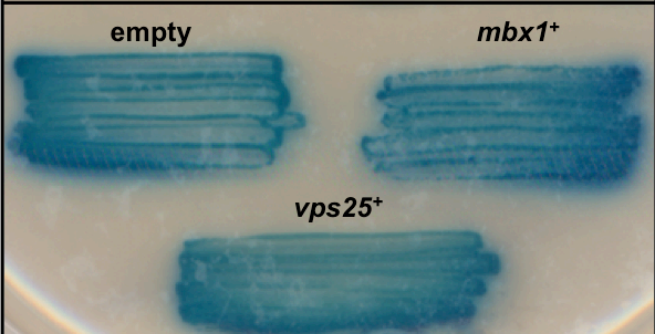
The table summarises the presence or absence of yeast cells showing blue colour when each of the ESCRT proteins was assayed with various versions of Plo1p by yeast two-hybrid analysis.

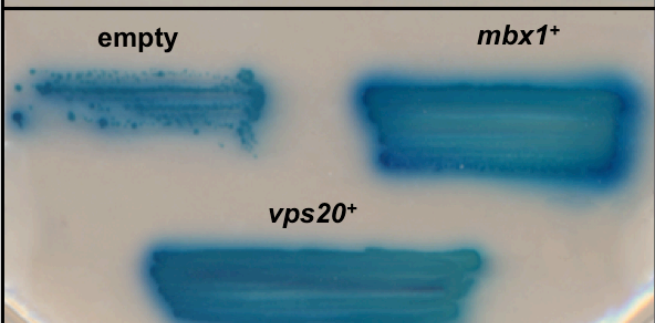
Yeast two-hybrid analysis with Clp1p yielded more ambiguous results (Figure 3.11), and thus some interpretation was required. In this instance, ESCRT proteins were tested for interactions with wild-type Clp1p and a truncated form of Clp1p (Clp1aa.1-371, a gift from K. Gould, Vanderbilt University).

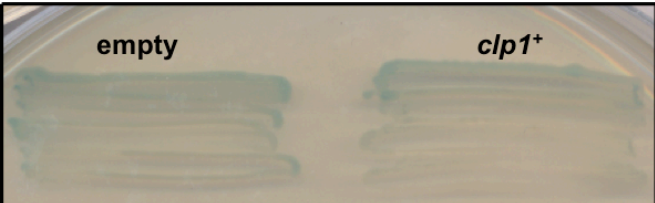
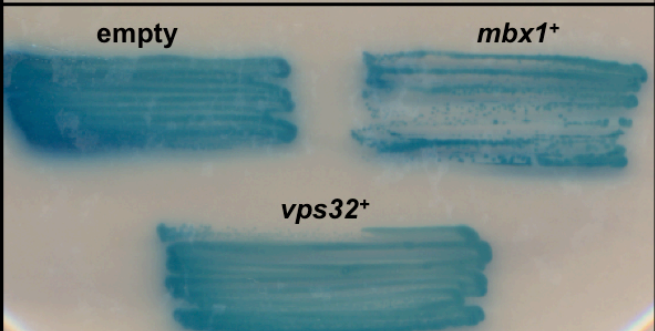
 <p>empty <i>clp1<sup>+</sup></i></p>	<b>empty</b>
 <p>empty <i>clp1<sup>+</sup></i></p>	<b><i>mbx1<sup>+</sup></i></b>
 <p>empty <i>clp1<sup>+</sup></i></p>	<b><i>sst4<sup>+</sup></i></b>
 <p>empty <i>mbx1<sup>+</sup></i> <i>sst4<sup>+</sup></i></p>	<b><i>clp1aa.1-371</i></b>

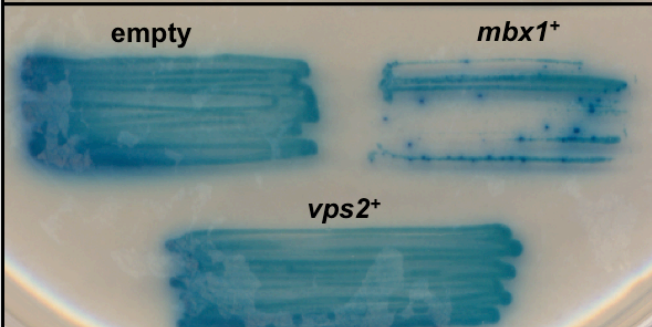
 <p>empty <i>clp1<sup>+</sup></i></p>	<b>empty</b>
 <p>empty <i>clp1<sup>+</sup></i></p>	<b><i>mbx1<sup>+</sup></i></b>
 <p>empty <i>clp1<sup>+</sup></i></p>	<b><i>sst6<sup>+</sup></i></b>
 <p>empty <i>mbx1<sup>+</sup></i> <i>sst6<sup>+</sup></i></p>	<b><i>clp1aa.1-371</i></b>

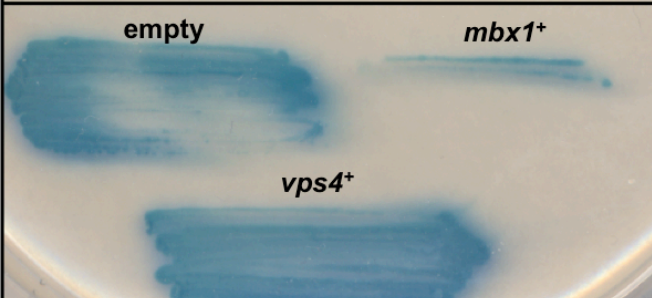
 <p>empty <i>clp1<sup>+</sup></i></p>	empty
 <p>empty <i>clp1<sup>+</sup></i></p>	<i>mbx1<sup>+</sup></i>
 <p>empty <i>clp1<sup>+</sup></i></p>	<i>vps36<sup>+</sup></i>
 <p>empty <i>mbx1<sup>+</sup></i> <i>vps36<sup>+</sup></i></p>	<i>clp1aa.1-371</i>

 <p>empty <i>clp1<sup>+</sup></i></p>	empty
 <p>empty <i>clp1<sup>+</sup></i></p>	<i>mbx1<sup>+</sup></i>
 <p>empty <i>clp1<sup>+</sup></i></p>	<i>vps25<sup>+</sup></i>
 <p>empty <i>mbx1<sup>+</sup></i> <i>vps25<sup>+</sup></i></p>	<i>clp1aa.1-371</i>

	empty
	<i>mbx1</i> <sup>+</sup>
	<i>vps20</i> <sup>+</sup>
	<i>clp1aa.1-371</i>

	empty
	<i>mbx1</i> <sup>+</sup>
	<i>vps32</i> <sup>+</sup>
	<i>clp1aa.1-371</i>

	<b>empty</b>	<b><i>clp1</i><sup>+</sup></b>	<b>empty</b>
	<b>empty</b>	<b><i>clp1</i><sup>+</sup></b>	<b><i>mbx1</i><sup>+</sup></b>
	<b>empty</b>	<b><i>clp1</i><sup>+</sup></b>	<b><i>vps2</i><sup>+</sup></b>
	<b>empty</b>	<b><i>mbx1</i><sup>+</sup></b>	<b><i>clp1aa.1-371</i></b>
		<b><i>vps2</i><sup>+</sup></b>	

	<b>empty</b>	<b><i>clp1</i><sup>+</sup></b>	<b>empty</b>
	<b>empty</b>	<b><i>clp1</i><sup>+</sup></b>	<b><i>mbx1</i><sup>+</sup></b>
	<b>empty</b>	<b><i>clp1</i><sup>+</sup></b>	<b><i>vps4</i><sup>+</sup></b>
	<b>empty</b>	<b><i>mbx1</i><sup>+</sup></b>	<b><i>clp1aa.1-371</i></b>
		<b><i>vps4</i><sup>+</sup></b>	

**Figure 3.11: ESCRT proteins do not definitively exhibit physical interactions with Clp1p.**

Budding yeast strains were transformed with the yeast two-hybrid bait and prey plasmid constructs indicated. The ESCRT proteins were fused to the prey domain of the GAL4 transcription factor; however, for ease of identification, the bait and prey plasmids have not been labelled consistently. The strains were grown for three days on selective medium when the X-Gal overlay assay was performed.

Experiments with Clp1p using yeast two-hybrid are more difficult to interpret than Plo1p, as the positive control, Clp1p-Mbx1p (Papadopoulou et al. 2008), did not result in yeast cells that were deep blue, which would indicate a strong physical interaction. However, one interesting observation was made with Vps28p (ESCRT-I). In all Clp1p yeast two-hybrid assays, blue colouration was observed for Clp1aa.1-371, except with Vps28p (Figure 3.12).

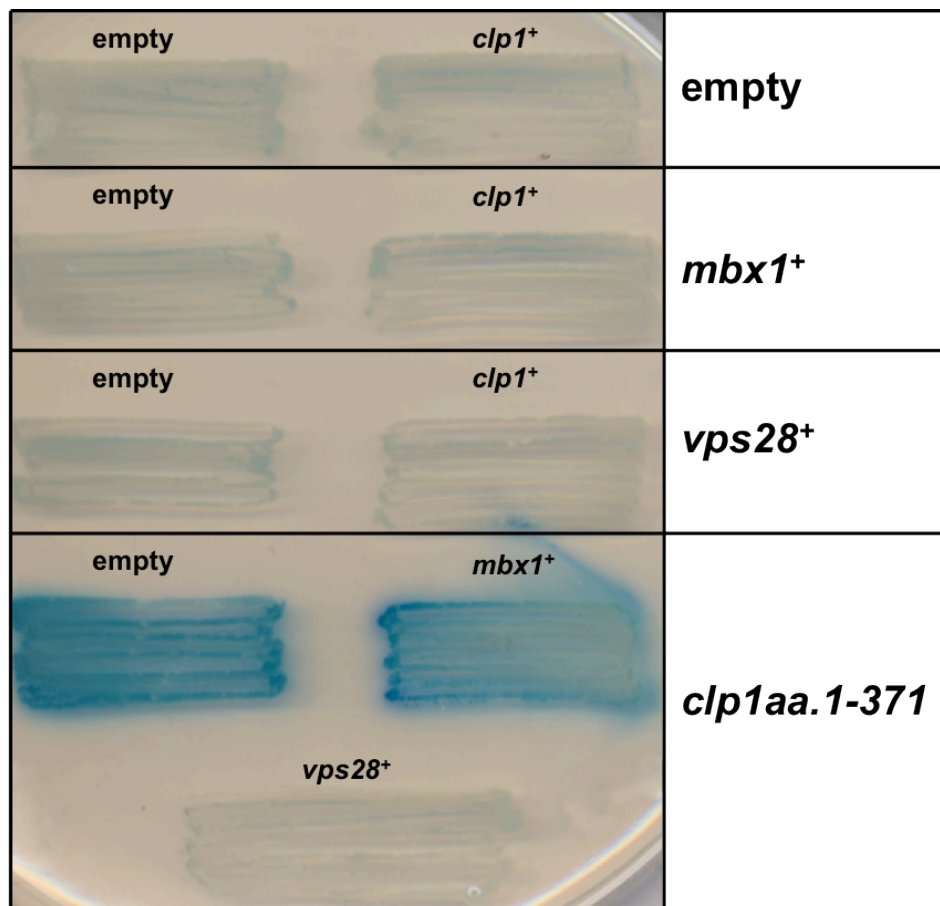


**Figure 3.12: Vps28p and Clp1aa.1-371 results in a negative yeast two-hybrid assay.**

Budding yeast strains were transformed with the yeast two-hybrid bait and prey plasmid constructs indicated. The ESCRT proteins were fused to the prey domain of the GAL4 transcription factor; however, for ease of identification, the bait and prey plasmids have not been labelled consistently. The strains were grown for three days on selective medium when the X-Gal overlay assay was performed.

Clp1aa.1-371 with an empty vector or Mbx1p resulted in deep blue colonies, but in the Vps28p assay alone, Clp1aa.1-371 returned white colonies. This is because Clp1p is itself able to bind DNA (Papadopoulou et al. 2010). Thus, it is apparent that the Clp1aa.1-371 mutant is capable of auto-activating the *gal4* promoter without a binding partner. Therefore, the absence of blue in this assay indicates an interaction between Clp1p and Vps28p, as Vps28p sequesters Clp1p from its DNA-binding function.

Clp1p yeast two-hybrid data are presented in Table 3.5 and a summary of Plo1p and Clp1p yeast two-hybrid interactions with the ESCRT proteins is provided in Table 3.6.

ESCRT	Clp1p	Clp1aa.1-371
Sst4p E-0	X	✓
Sst6aa.20-487 E-I	X	✓
Vps28p E-I	X	X
Vps36p E-II	X	✓
Vps25p E-II	X	✓
Vps20p E-III	X	✓
Vps32p E-III	X	✓
Vps2p E-III	X	✓
Vps4p	X	✓

**Table 3.5: A summary of blue yeast observation in yeast two-hybrid analysis of Clp1p and the ESCRT proteins.**

The table summarises the presence or absence of yeast cells showing a blue colour when each of the ESCRT proteins was assayed with various versions of Clp1p by yeast two-hybrid analysis.

ESCRT	Plo1p	Clp1p
Sst4p E-0	✓	X
Sst6aa.20-487 E-I	X	X
Vps28p E-I	✓	✓
Vps36p E-II	X	X
Vps25p E-II	✓	X
Vps20p E-III	✓	X
Vps32p E-III	✓	X
Vps2p E-III	X	X
Vps4p	X	X

**Table 3.6: A summary of physical interactions between the ESCRT proteins and Plo1p and Clp1p.**

The table summarises protein interactions inferred from yeast two-hybrid analysis between the ESCRT proteins and Plo1p and Clp1p.

To summarise all the yeast two-hybrid data, Plo1p was shown to interact with Sst4p (ESCRT-0), Vps28p (ESCRT-I), Vps25p (ESCRT-II), Vps20p (ESCRT-III), and Vps32p (ESCRT-III), and Clp1p was shown to interact with Vps28p (ESCRT-I).

## 3.3 Concluding remarks

### 3.3.1 Principal findings

In this chapter, it has been shown that ESCRT genes are required for cell separation in fission yeast, implying that the ESCRT machinery has a role in this process (Figure 3.1).

Double mutants of ESCRT chromosomal deletions and mutants of *plo1* or *clp1* revealed defective growth rates, indicating that the *plo1*<sup>+</sup> and *clp1*<sup>+</sup> genes interact with ESCRT genes (Table 3.2).

Furthermore, *plo1* and *clp1* mutants were shown to affect vacuolar sorting in fission yeast (Figure 3.5). Analysis of the double mutants with ESCRT deletions demonstrated phenotypes similar to one or other of the parents, which facilitated characterisation of these genetic interactions (Table 3.3).

Finally, the Plo1p and Clp1p proteins were shown to physically interact with several proteins of the ESCRT machinery (Table 3.6).

### 3.3.2 Summary

These results combined suggest that ESCRT proteins along with Plo1p and Clp1p regulate cytokinesis and septation in fission yeast. The next chapter of this thesis will explore whether similar findings can be observed in human cells.

## **Chapter 4 Plk1 kinase and CDC14A phosphatase interact with ESCRT proteins in humans**

### **4.1 Introduction**

#### **4.1.1 Fission yeast shares a high degree of conservation with higher eukaryotes**

Data presented in *Chapter 3* show that Plo1p and Clp1p genetically and physically interact with members of the ESCRT machinery in fission yeast. As a model organism, fission yeast has allowed the discovery of a large number of genetic and protein interactions, facilitating comprehension of numerous biological processes. Furthermore, fission yeast and human cells share a high degree of similarity, particularly in the events of cell division (Pollard & Wu 2010). Therefore, it was hypothesised that the interactions observed in yeast and presented in *Chapter 3* may be conserved in humans. This two-step approach was employed as yeast allowed the rapid screening of many potential interactions, which then informed which interactions to study in humans, where such analyses are more time-consuming and expensive.

#### **4.1.2 Aims and key findings**

In this study, interactions between human Plk1 (Plo1p) and CDC14A (Clp1p) with ESCRT proteins were investigated. Immunoprecipitation and co-immunoprecipitation methods were employed, whereby a purification of one protein from human cell lysate was undertaken using a selective antibody. This immunoprecipitate was then screened for the presence of co-purifying interacting partners using specific antibodies.

Initially, interactions between Plk1 and ESCRT proteins were screened in HeLa cervical cancer cells that endogenously expressed proteins at wild-type levels. Interactions were not detected, so cell lysates containing over-expressed ESCRT proteins were then analysed. As HeLa cells exhibited low transfection efficiency, ESCRT proteins were instead over-expressed in human embryonic kidney (HEK293) cells. Once a set of conditions in HEK293 cells was determined that allowed observation of interactions, the same conditions were replicated in HeLa cells.

In a different set of experiments, a functional assay was performed to determine if Plk1 kinase inhibition resulted in an ESCRT protein phospho-mobility shift.

Finally, using immunoprecipitation and co-immunoprecipitation methods, interactions between CDC14A and ESCRT proteins were detected in over-expressing HEK293 cells.

## 4.2 Results

### 4.2.1 Investigating interactions between Plk1 and ESCRT proteins in HeLa cells

#### 4.2.1.1 Interactions between Plk1 and FOXM1 were detected in metaphase-arrested cells

Plk1 was immunoprecipitated from HeLa cell lysates. HeLa cells were grown to approximately 90% confluency and harvested (*Materials and Methods 2.3.5.3*). Following quantification of lysate protein content (*Materials and Methods 2.3.6*), 1 mg of lysate was incubated with 13  $\mu$ g anti-Plk1 antibody, or 50 ng IgG from rabbit serum as a control for random protein binding to antibody. To control for false positive cross-reactions with detection antibodies, anti-Plk1 antibody was also incubated in lysis buffer. Following incubation with Protein A sepharose beads to capture the antibodies, the samples were centrifuged briefly to collect the bead-antibody-protein complexes, and the supernatants containing unbound proteins were retained. The beads were extensively washed and then heated in the presence of Laemmli sample buffer to dissociate immunoprecipitated proteins from the bead-antibody complexes. The mixtures were centrifuged, and the supernatant, containing immunoprecipitated Plk1 protein, was retained (*Materials and Methods 2.3.7.1*). The samples were then subjected to SDS-PAGE (*Materials and Methods 2.3.8*) and immunoblotting (*Materials and Methods 2.3.9*) to detect the immunoprecipitation of Plk1 and co-immunoprecipitation of binding partners of Plk1.

Initially, Plk1 was immunoprecipitated from an asynchronous population of untreated HeLa cells. Plk1 was successfully immunoprecipitated, but FOXM1, which has been shown to bind Plk1 using this method (Fu et al. 2008), was not detected (Figure 4.1).

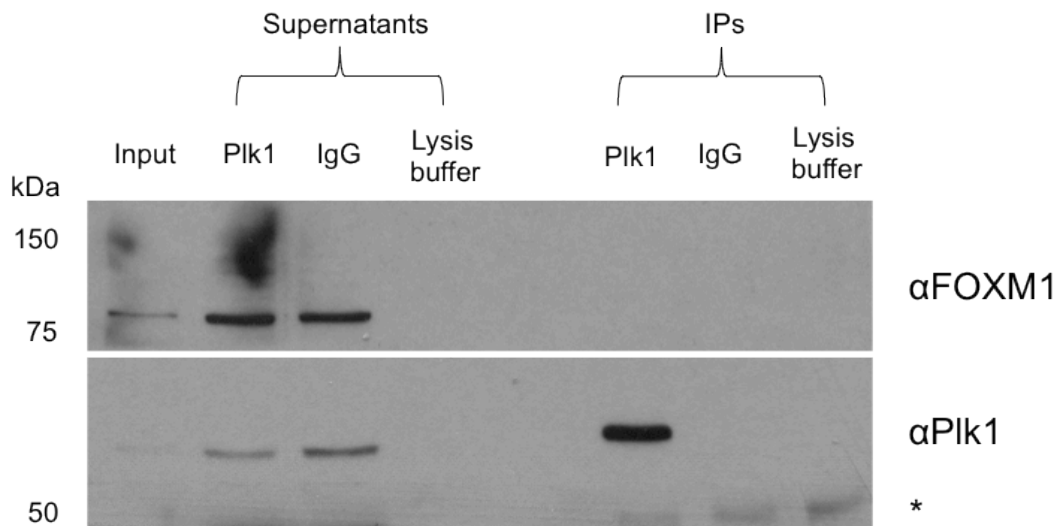


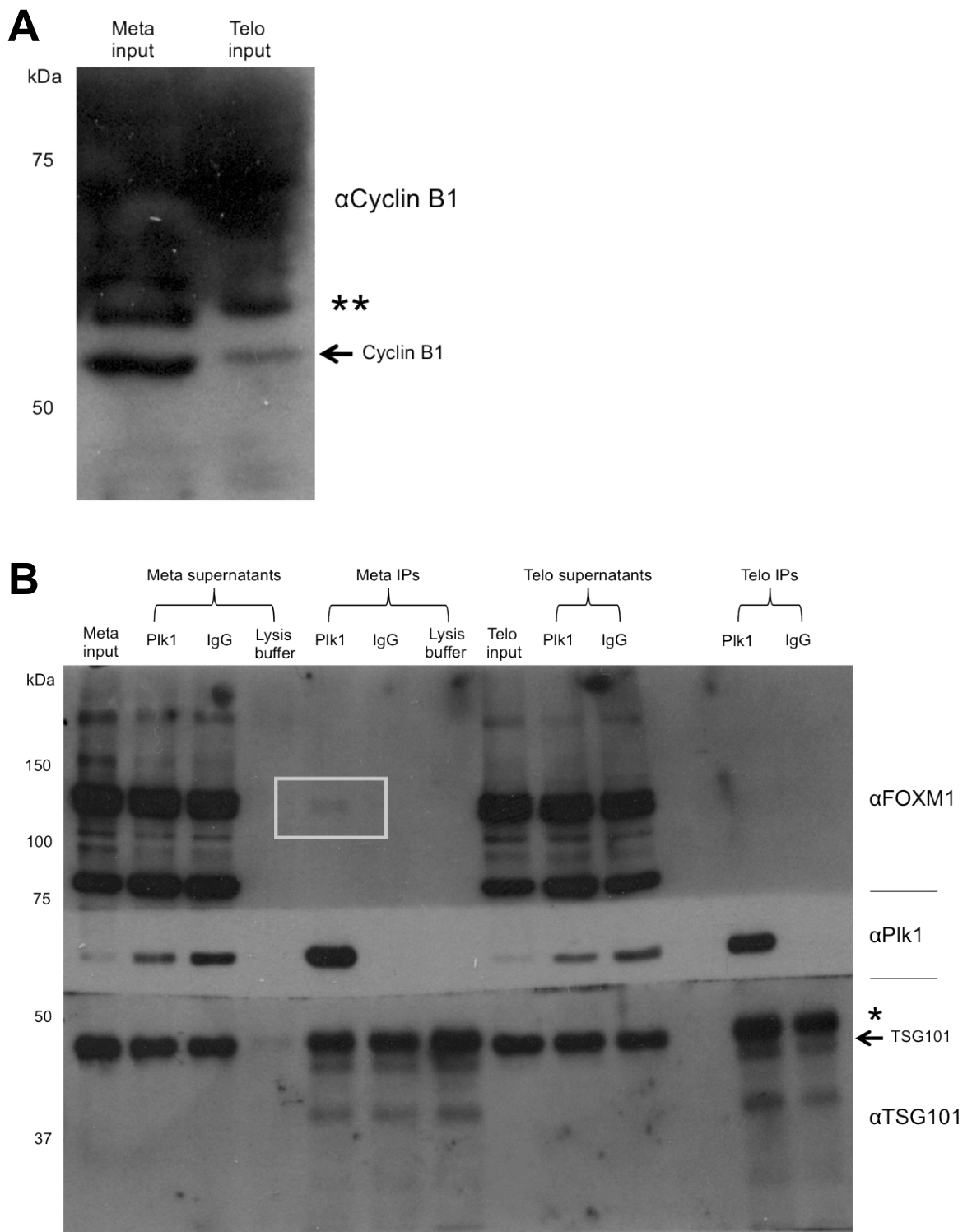
**Figure 4.1: FOXM1 did not co-immunoprecipitate with Plk1 from asynchronous HeLa cell lysates.**

Plk1 was immunoprecipitated from HeLa cell lysate. Either anti-Plk1 antibody (Plk1 in figure) or random rabbit IgG (IgG in figure) was added to cell lysate, and as a further control, anti-Plk1 antibody was added to lysis buffer in the absence of cell lysate. The lysate following incubation with Protein A sepharose beads was retained (*supernatant* in figure: 20 µg was loaded). Complexes were dissociated from beads (*IP*: one quarter was loaded). *Input* refers to the cell lysate that was interrogated: 20 µg was loaded. \*IgG heavy chain. Various exposures are shown of immunoblots derived from a single SDS gel. Experiments were repeated with qualitatively similar results and data from a typical experiment are shown. Molecular weight standards and antibodies used for immunoblotting are indicated.

Immunoblotting with anti-Plk1 antibody revealed that Plk1 was immunoprecipitated (Figure 4.1, bottom panel, right), but that FOXM1 was not co-immunoprecipitated (Figure 4.1, top panel, right). The detection of Plk1 in the supernatant (Figure 4.1, bottom panel, left) indicates the incomplete immunoprecipitation of Plk1 from the input lysate. Immunoprecipitated Plk1 appears to run more slowly most likely due to uneven SDS-PAGE, as indicated by the uneven distribution of IgG heavy chain.

In each immunoprecipitation, 1 mg of protein from cell lysate was used. However, the Plk1 abundance within lysates was not known. Furthermore, Plk1 has roles predominantly in late stages of the cell cycle, during M-phase and cytokinesis, when potential interactions with ESCRT proteins might occur (Lénárt et al. 2007). Therefore, HeLa cells were synchronised to metaphase and telophase to enrich for Plk1 and associated proteins. Published immunoprecipitation of Plk1 and co-immunoprecipitation of FOXM1 has shown a greater abundance of both proteins, and of co-immunoprecipitations, in mitotic cell lysates (Fu et al. 2008).

HeLa cells were arrested in metaphase using thymidine and nocodazole (*Materials and Methods 2.3.5.1*) and interrogated with anti-Plk1 antibody, as described. Using this method, Plk1 was immunoprecipitated from both metaphase- and telophase-arrested cells; FOXM1 was co-immunoprecipitated from metaphase-arrested cells, but none of the assayed ESCRT proteins were detected (Figure 4.2).



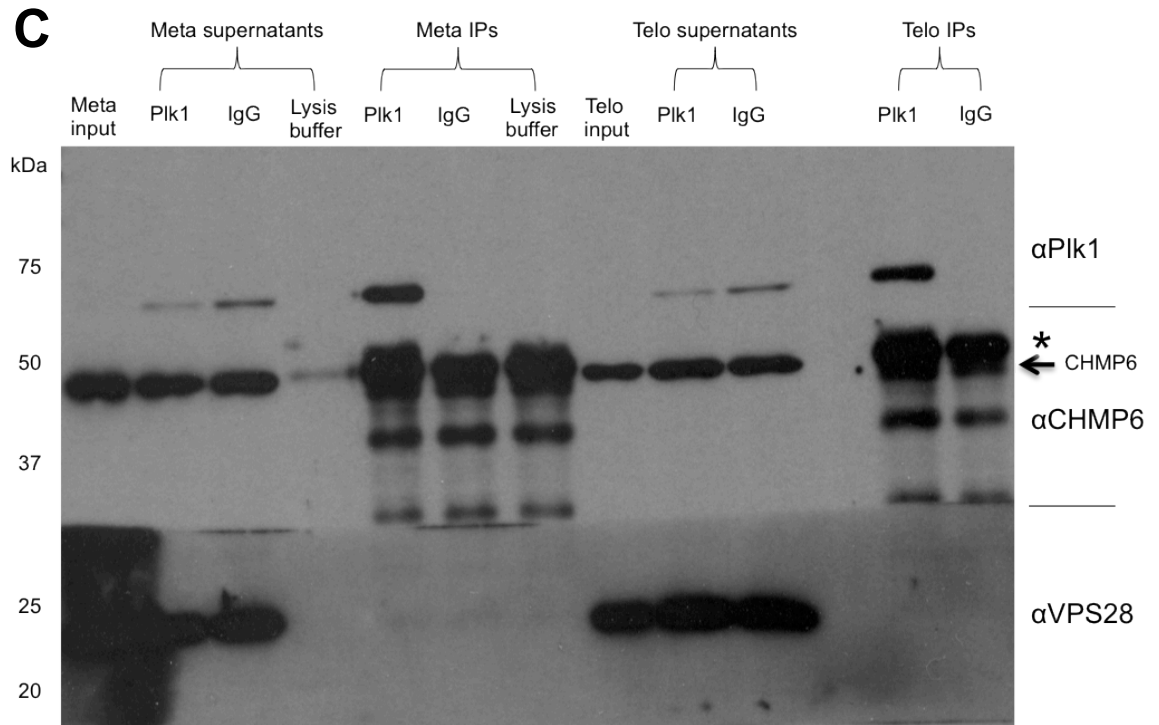


**Figure 4.2: FOXM1 co-immunoprecipitated with Plk1 from metaphase-arrested cell lysates.**

HeLa cells were arrested in metaphase and telophase by thymidine-nocodazole block. (A) Equal amounts of lysates (20  $\mu$ g) were immunoblotted with anti-Cyclin B1 antibody to confirm synchronisation. Non-specific reactive proteins (\*\* in figure) were used as a loading control. Plk1 was immunoprecipitated from (B and C) metaphase- or telophase-arrested HeLa cell lysates. Either anti-Plk1 antibody (Plk1 in figure) or random rabbit IgG (IgG in figure) were added to cell lysate, and as a further control, anti-Plk1 antibody was added to lysis buffer in the absence of cell lysate. The lysate following incubation with Protein A sepharose beads was retained (*supernatant* in figure: 20  $\mu$ g was loaded). Complexes were dissociated from beads (*IP*: one quarter was loaded). *Input* refers to the cell lysate that was interrogated: 20  $\mu$ g was loaded. \*IgG heavy chain. FOXM1 co-immunoprecipitation is highlighted in a box. Membranes were cut to immunoblot using different antibodies then brought back together for ECL developing. Experiments were repeated with qualitatively similar results and data from a typical experiment are shown. Molecular weight standards and antibodies used for immunoblotting are indicated.

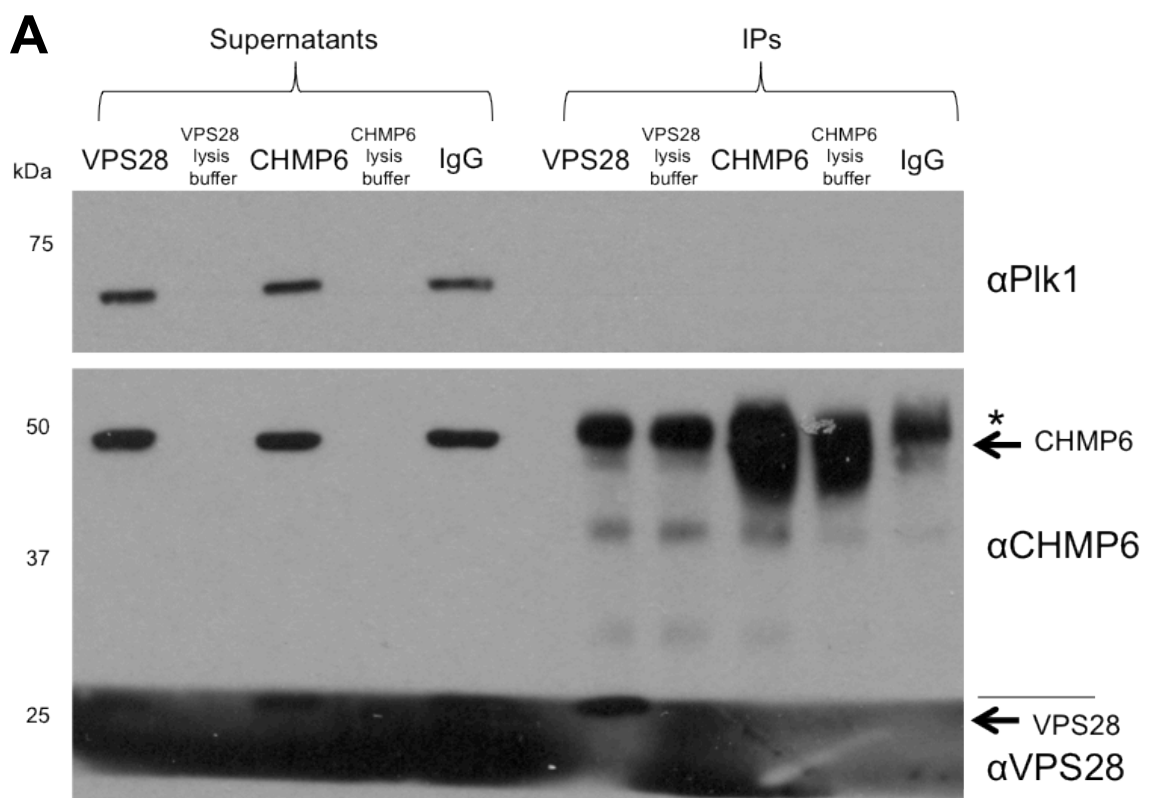
Immunoblotting arrested lysates for Cyclin B1 detection confirmed that cells had arrested in metaphase and telophase (Figure 4.2A), as Cyclin B1 protein levels are downregulated during telophase (Clute & Pines 1999).

Plk1 was immunoprecipitated from HeLa cells arrested in metaphase and telophase. Immunoblotting for FOXM1 detected multiple reactive proteins in input lysates and supernatants. One of these FOXM1 proteins was present in the immunoprecipitation of Plk1, indicating that FOXM1 co-immunoprecipitated with Plk1 from metaphase-arrested cells (Figure 4.2B). Multiple reactive proteins on immunoblotting anti-FOXM1 antibody and co-immunoprecipitation of a single protein are consistent with that which has been published (Fu et al. 2008).

ESCRT proteins TSG101 (fission yeast Sst6p, ESCRT-I) (Figure 4.2B), CHMP6 (Vps20p, ESCRT-III) and VPS28 (Vps28p, ESCRT-I) (Figure 4.2C), did not appear to co-immunoprecipitate with Plk1 from either metaphase- or telophase-arrested cell lysates. However, these observations did not preclude the possibility of detecting an interaction by immunoprecipitating ESCRT proteins and searching for co-immunoprecipitated Plk1.

#### 4.2.1.2 Immunoprecipitation of VPS28 did not yield detection of Plk1

To assay if interactions could be detected when immunoprecipitation was performed in reverse, FOXM1 and ESCRT proteins were immunoprecipitated and then screened to search for co-immunoprecipitated Plk1. Asynchronous and metaphase- and telophase-arrested HeLa cell lysates were all interrogated with antibodies for FOXM1, CHMP6, TSG101 and VPS28 (*Materials and Methods* 2.3.7.2). Of these, VPS28 was successfully immunoprecipitated (Figure 4.3).



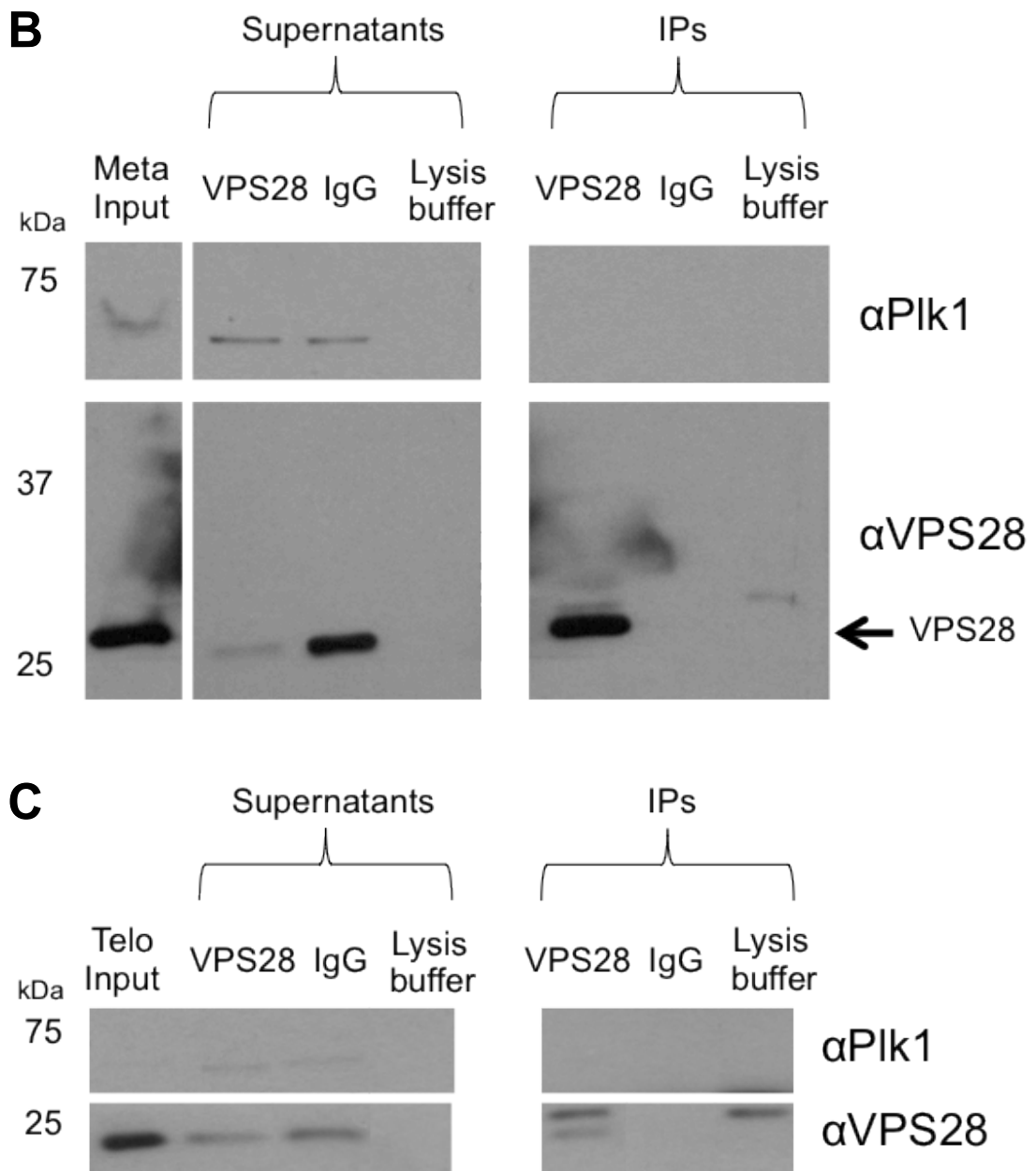


**Figure 4.3: Plk1 did not co-immunoprecipitate with VPS28 from asynchronous or arrested HeLa cell lysates.**

VPS28 was immunoprecipitated from (A) asynchronous HeLa cell lysates, or (B) metaphase-arrested or (C) telophase-arrested lysates from HeLa cells following a thymidine-nocodazole block. Either anti-VPS28 antibody (VPS28 in figure) or random rabbit IgG (IgG in figure) was added to cell lysate and, as a further control, anti-VPS28 antibody was added to lysis buffer in the absence of cell lysate. The lysate following incubation with Protein G sepharose beads was retained (*supernatant* in figure: 20  $\mu$ g was loaded). Complexes were dissociated from beads (*IP*: one quarter was loaded). *Input* refers to the cell lysate that was interrogated: 20  $\mu$ g was loaded, although no lysate remained for immunoblotting in (A). \*IgG heavy chain. Various exposures are shown of immunoblots derived from a single SDS gel. Immunoblot splices used to rearrange lanes are from a single exposure. Experiments were repeated with qualitatively similar results and data from a typical experiment are shown. Molecular weight standards and antibodies used for immunoblotting are indicated.

VPS28 was immunoprecipitated from asynchronous HeLa cell lysates (Figure 4.3A) and from metaphase- and telophase-arrested HeLa cell lysates (Figures

4.3B and C). Plk1 did not co-immunoprecipitate with VPS28 in any of the assayed conditions.

However, endogenous Plk1 has been shown to co-immunoprecipitate over-expressed FOXM1 from HEK293 cells (Fu et al. 2008), so the investigation was directed towards over-expressed cell lysates.

## 4.2.2 Investigating interactions between Plk1 and over-expressed ESCRT proteins in HEK293 cells

The initial investigation in human cells was restricted to asynchronous HeLa cells. When a known binding partner, FOXM1 (Fu et al. 2008), was not detected on immunoprecipitation of Plk1, interactions were then sought in HeLa cell lysates from cells arrested in metaphase and telophase. However, although Plk1 interaction was confirmed with FOXM1 in metaphase-arrested cell lysates, ESCRT interactions remained undetected. Therefore, HeLa cells were transfected with plasmids to over-express individual ESCRT proteins to potentially increase the chance of detecting interactions. However, on assaying transfection efficiency, HeLa cells were found not to transfect effectively: routinely, less than 5% of cells expressed the transfected protein. Therefore, human embryonic kidney (HEK293) cells were instead employed (Fu et al. 2008), as they accepted DNA and over-expressed proteins more efficiently than HeLa cells: expression was routinely observed in 20-30% of HEK293 cells.

### 4.2.2.1 Plk1 interacts with CHMP6 (fission yeast Vps20p, ESCRT-III)

HEK293 cells were grown to a confluency of 90% in antibiotic-free medium. Fresh medium was supplemented with purified CHMP6-GFP DNA (*Materials and Methods 2.3.2*) in complex with transfection reagent, Lipofectamine 2000 (*Materials and Methods 2.3.3*). The medium was replaced the following day and cell lysates were prepared on the third day (*Materials and Methods 2.3.5.3*).

Following quantification of lysate protein content (*Materials and Methods 2.3.6*), 1 mg of lysate was interrogated - first with anti-Plk1 antibody, followed by Protein A sepharose beads - or with beads in the absence of anti-Plk1 antibody. By this method, Plk1 was immunoprecipitated from HEK293 cell lysates (Figure 4.4A) and CHMP6-GFP was co-immunoprecipitated with Plk1 (Figure 4.4B). In addition, to demonstrate that anti-Plk1 antibody did not non-specifically bind to GFP, Plk1 was immunoprecipitated from HEK293 lysates over-expressing either CHMP6-GFP or FIP3-GFP (Figure 4.4C).

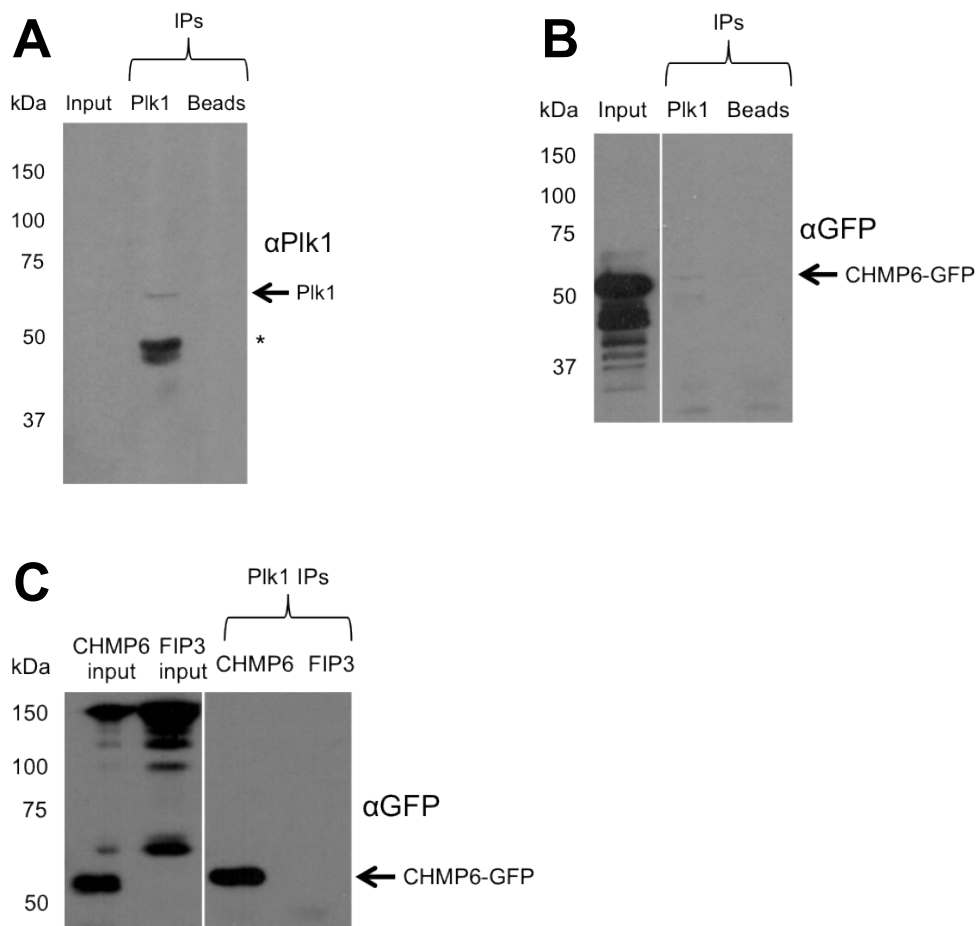


**Figure 4.4: Over-expressed CHMP6 co-immunoprecipitates with Plk1 from HEK293 cell lysates.**

(A) HEK293 cell lysates were prepared and interrogated with anti-Plk1 antibody; a beads-only control was included (10  $\mu$ g input and one-eighth IP were loaded). (B) HEK293 cells were transfected with DNA for CHMP6-GFP. Lysates were prepared and Plk1 was immunoprecipitated. A beads-only control was included (10  $\mu$ g input and one-eighth IP were loaded). (C) HEK293 cells were transfected with DNA for either CHMP6-GFP or FIP3-GFP (5  $\mu$ g input and one-fifteenth IP was loaded). Immunoprecipitated complexes were dissociated from beads. *Input* refers to the cell lysate that was interrogated. \*IgG heavy chain. Various exposures are shown of immunoblots derived from a single SDS gel. Immunoblot splices used to rearrange lanes are from a single exposure. Experiments were repeated with qualitatively similar results and data from a typical experiment are shown. Molecular weight standards and antibodies used for immunoblotting are indicated.

Plk1 was successfully immunoprecipitated from HEK293 cell lysates (Figure 4.4A), although immunoblotting of Plk1 was not robust, presumably because levels of Plk1 in HEK293 cells are low (our unpublished observations). CHMP6 was revealed to co-immunoprecipitate with Plk1 (Figure 4.4B). In the beads-only control, little or no CHMP6-GFP was co-immunoprecipitated. Furthermore, FIP3-GFP was not detected on immunoprecipitation of Plk1, indicating that the co-immunoprecipitation of CHMP6-GFP was not due to an interaction between GFP and anti-Plk1 antibody (Figure 4.4C). However, CHMP6-GFP co-immunoprecipitation with Plk1 would be more robustly demonstrated by

immunoprecipitating, in parallel, Plk1 from lysates over-expressing GFP and CHMP6-GFP, respectively.

#### **4.2.2.2 Plk1 interacts with CHMP6 (Vps20p, ESCRT-III), CHMP4B (Vps32p, ESCRT-III), CHMP3 (Vps24p, ESCRT-III) and CHMP2A (Vps2p, ESCRT-III)**

Following the observation that CHMP6-GFP was co-immunoprecipitated with Plk1, further ESCRT proteins were investigated. Purified DNA for CHMP6-GFP, CHMP4B-YFP, CHMP3-myc and CHMP2A-GFP were individually transfected into HEK293 cells, and lysates were prepared (*Section 4.2.2.1*). One mg of each cell lysate was then interrogated with anti-Plk1 antibody or Protein A sepharose beads alone. Interestingly, immunoblot analysis of lysates and subsequent immunoprecipitated products revealed that the ESCRT proteins co-immunoprecipitated with Plk1 (Figure 4.5).

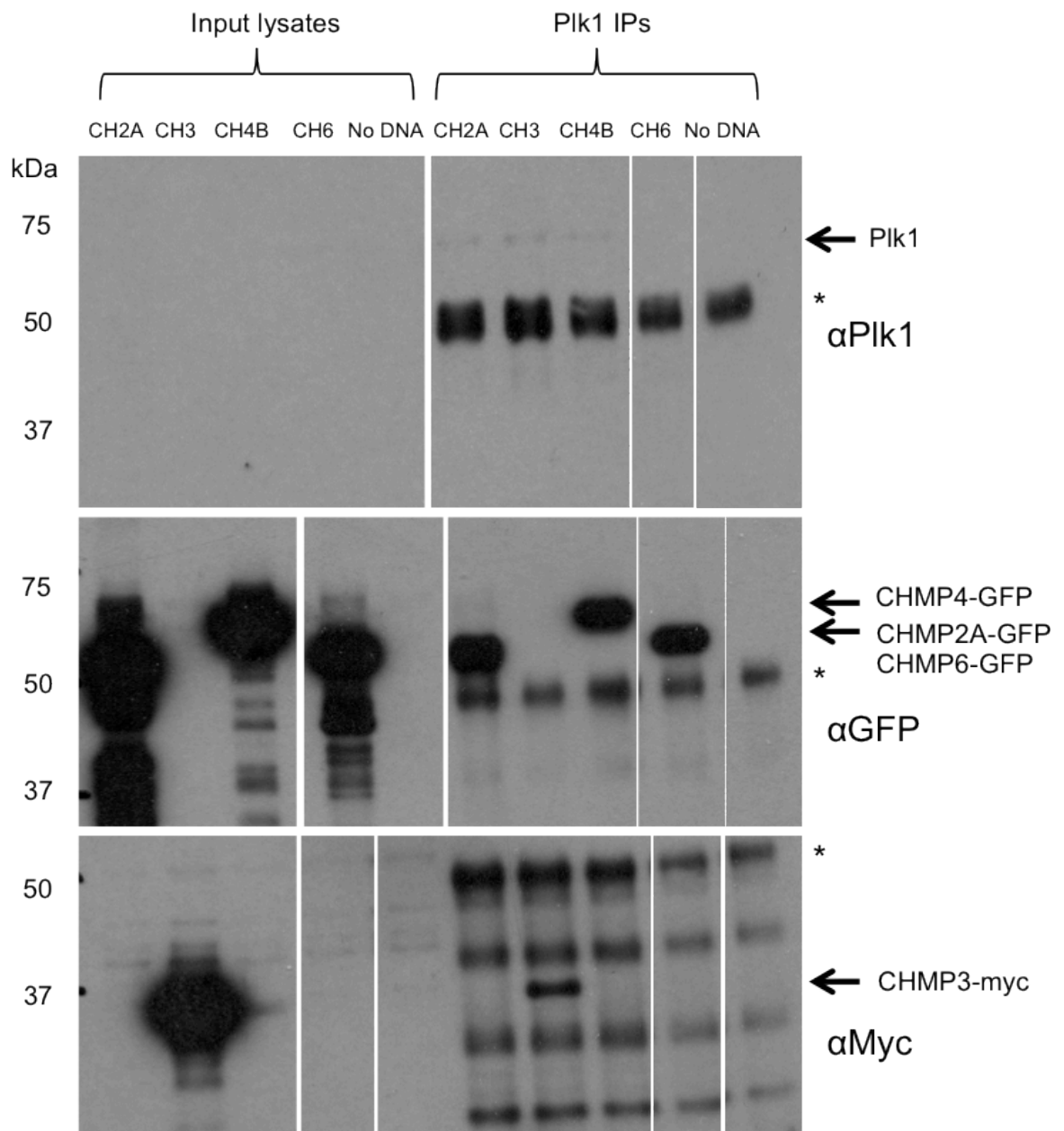


**Figure 4.5: Over-expressed CHMP6, CHMP4B, CHMP3 and CHMP2A co-immunoprecipitate with Plk1 from HEK293 cell lysates.**

HEK293 cells were transfected with DNA for CHMP6-GFP, CHMP4B-YFP, CHMP3-myc, CHMP2A-GFP, or with Lipofectamine 2000 in the absence of transforming DNA. Lysates were prepared and anti-Plk1 antibody (Plk1 in figure) was added to each cell lysate. Complexes were dissociated from beads (*IP*: one-fifteenth was loaded). *Input* refers to the cell lysate that was interrogated: 5  $\mu$ g was loaded. Various exposures are shown of immunoblots derived from a single SDS gel. Immunoblot splices used to rearrange lanes are from a single exposure. \*IgG heavy chain. Experiments were repeated with qualitatively similar results and data from a typical experiment are shown. Molecular weight standards and antibodies used for immunoblotting are indicated.

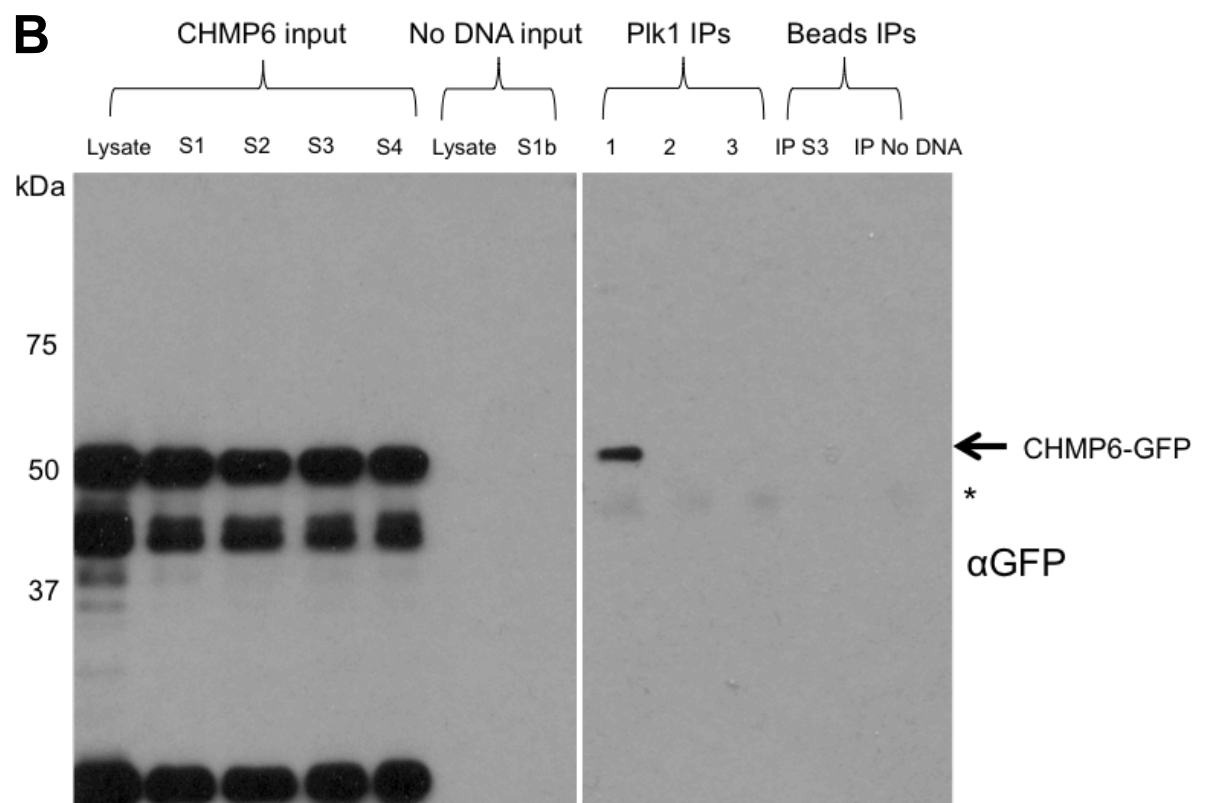
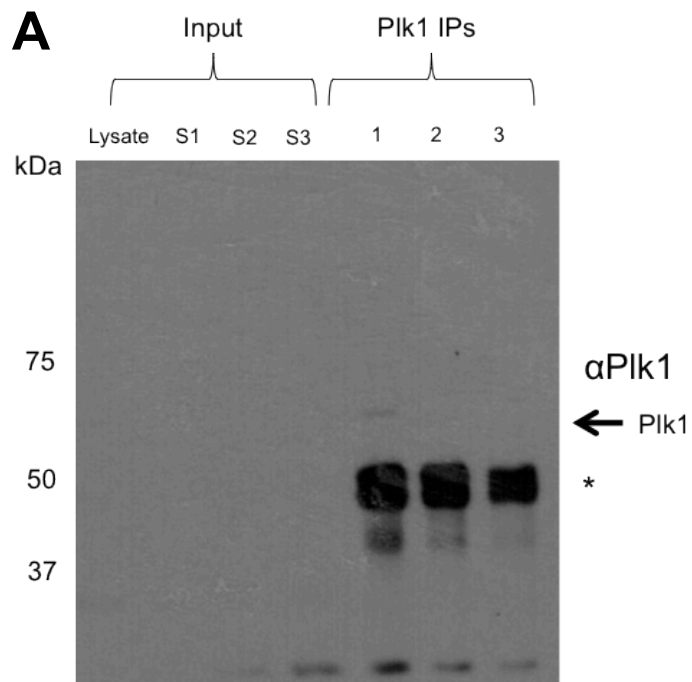
Immunoprecipitation of Plk1 from HEK293 cell lysates over-expressing individual ESCRT proteins revealed interactions between Plk1 and CHMP6, CHMP4B, CHMP3 and CHMP2A. CHMP6-GFP, CHMP4B-YFP and CHMP2A-GFP were all detected in lysates on immunoblotting with anti-GFP antibody and CHMP3-myc was detected

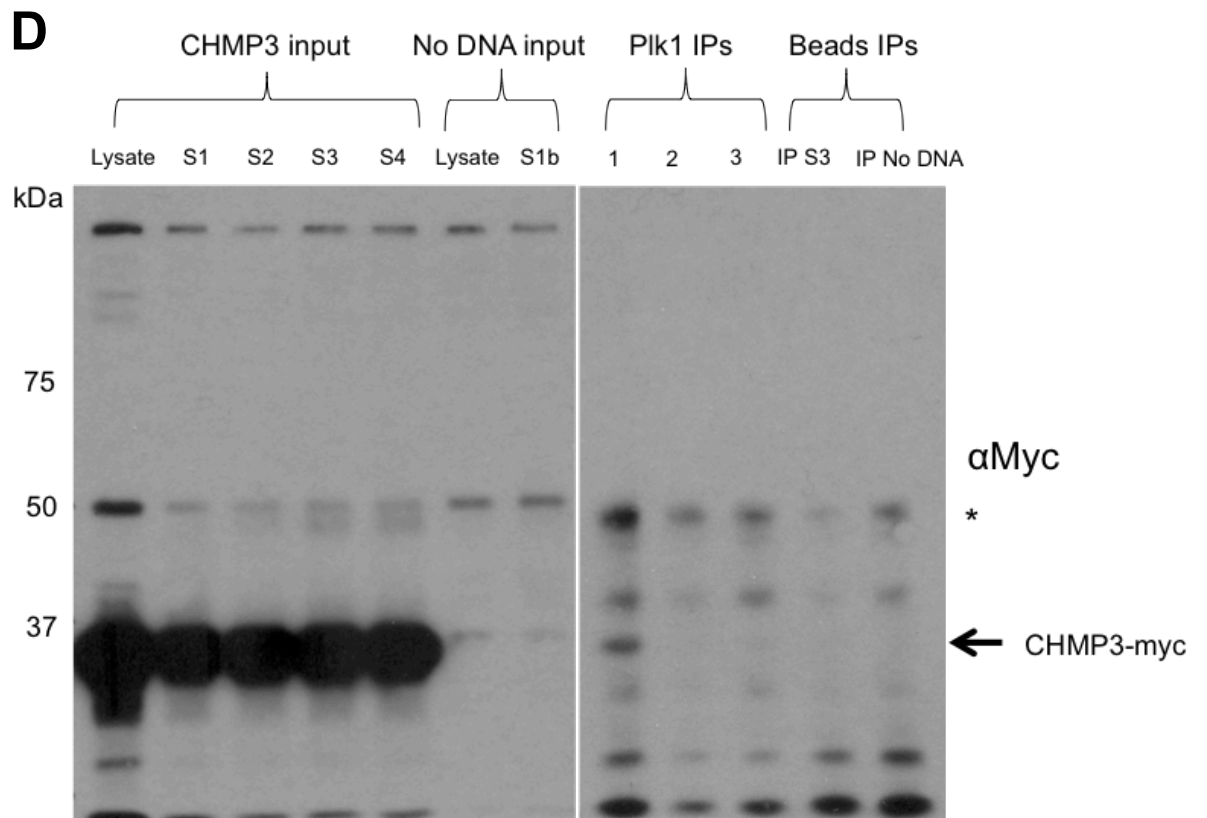
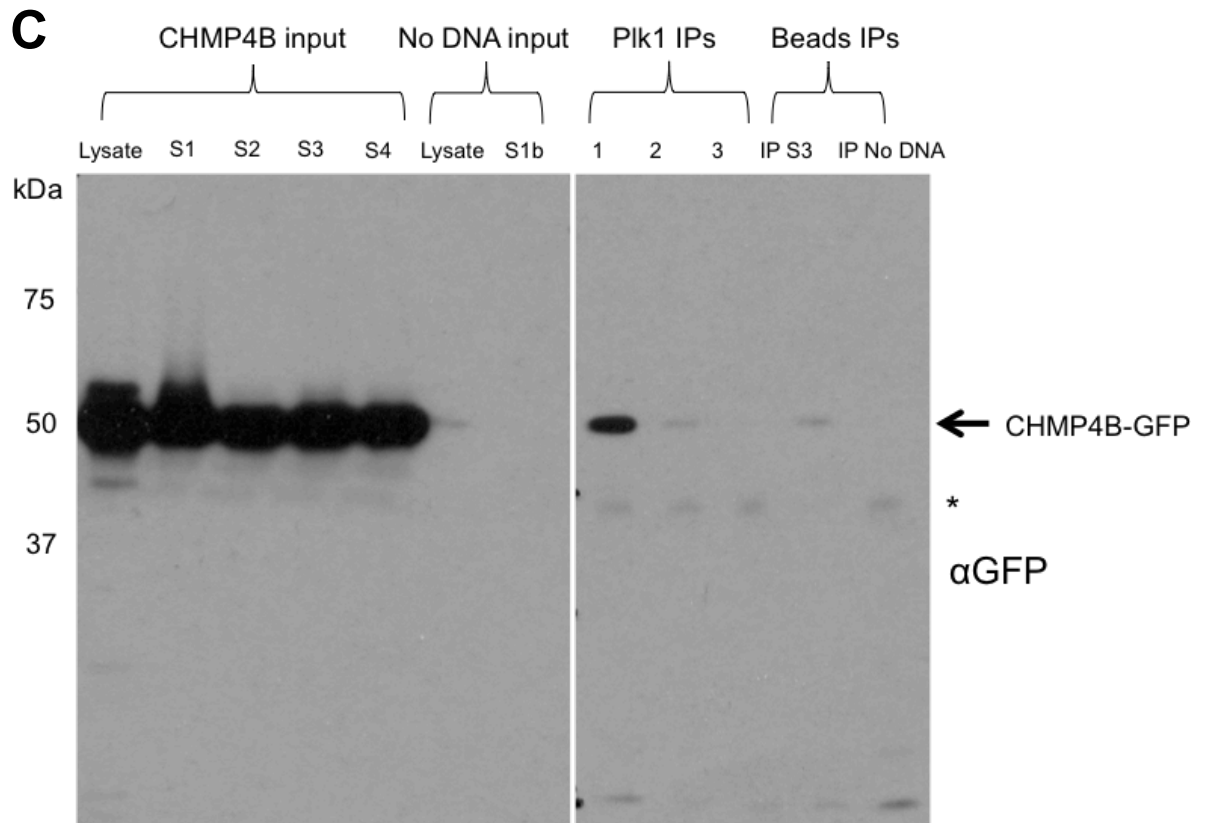
in lysate on immunoblotting with anti-myc antibody. Immunoblotting non-transfected cell lysate revealed the presence of non-specific reactive proteins, including the 50 kDa heavy chain of anti-Plk1 IgG, and facilitated identification of all four ESCRT proteins as co-immunoprecipitated species.

However, Plk1 immunoblotting was irregular, as in Figure 4.5, Plk1 is only clearly detected in three of five immunoprecipitations. There was, therefore, a question over whether ESCRT proteins were actually co-immunoprecipitated by interactions with Plk1. To this end, an experiment was designed to reduce Plk1 levels in cell lysates and thereby assay the impact upon ESCRT co-immunoprecipitation.

#### **4.2.2.3 Sequential immunoprecipitation of Plk1 depletes the co-immunoprecipitation of CHMP6, CHMP4B, CHMP3 and CHMP2A**

Another immunoprecipitation method was employed to demonstrate that the co-immunoprecipitated ESCRT proteins were detected as a result of specific interactions between Plk1 and the ESCRT proteins. HEK293 cell lysates over-expressing individual ESCRT proteins were repeatedly interrogated with anti-Plk1 antibody. Following the addition of anti-Plk1 antibody and incubation with Protein A sepharose beads, lysates were centrifuged and the supernatants removed. Proteins were then purified from the beads by heating in Laemmli sample buffer. However, the supernatants, which represented unbound proteins in lysate, were interrogated a second time with anti-Plk1 antibody. The immunoprecipitation process was performed, sequentially, three times. Immunoblotting each sequential lysate of repeatedly interrogated supernatants and immunoprecipitated products revealed depleted ESCRT co-immunoprecipitation, despite almost no reduction in lysates (Figure 4.6).





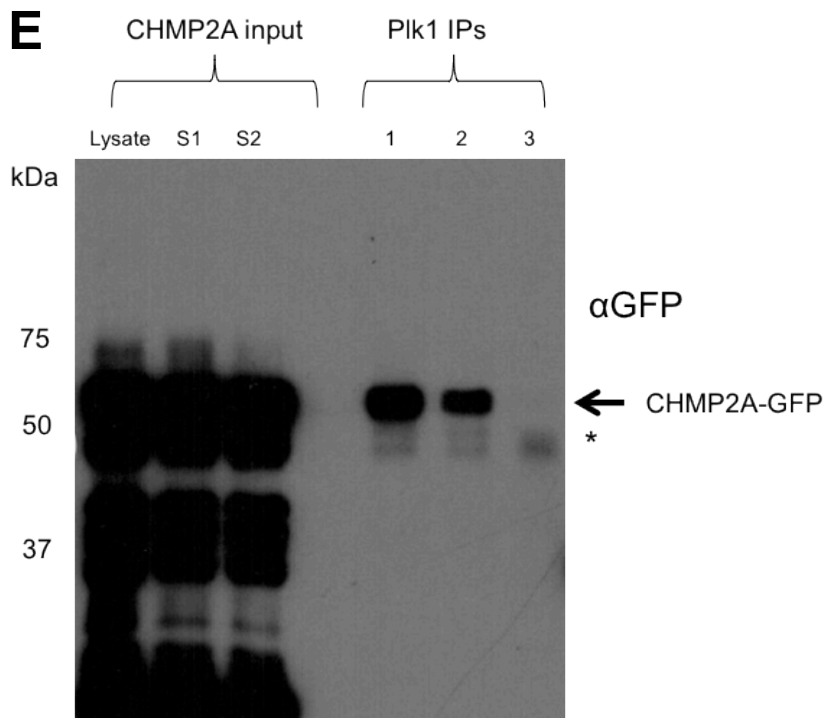


**Figure 4.6: Sequential immunoprecipitation of Plk1 depletes detection of over-expressed ESCRT proteins from anti-Plk1 immunoprecipitations.**

(A) Plk1 was depleted from HEK293 cell lysates by sequential interrogation using anti-Plk1 antibody. HEK293 cells were transfected with DNA for (B) CHMP6-GFP, (C) CHMP4B-YFP, (D) CHMP3-myc, (E) CHMP2A-GFP, or with Lipofectamine 2000 in the absence of transforming DNA. Lysates were prepared and anti-Plk1 antibody (Plk1 in figure) was added to each cell lysate. The lysate following incubation with Protein A sepharose beads was retained (*supernatant* in figure: 5  $\mu$ g was loaded). Anti-Plk1 antibody was re-introduced into the supernatant (S1). Centrifugation following incubation with Protein A sepharose beads resulted in supernatant 2. This was interrogated a third time, resulting in supernatant 3. The third supernatant (S3) resulting from anti-Plk1 interrogation of CHMP2A-transfected supernatant 2 was mistakenly discarded. For (B) CHMP6, (C) CHMP4B and (D) CHMP3, a Protein A sepharose beads-only immunoprecipitation was performed on supernatant 3, resulting in S4. Non-transfected lysates were also interrogated with anti-Plk1 antibody. Complexes were dissociated from beads (*IP*: one-fifteenth was loaded). *Input* refers to the cell lysate that was interrogated: 5  $\mu$ g was loaded. Various exposures are shown of immunoblots derived from a single SDS gel. Immunoblot splices used to rearrange lanes are from a single exposure. \*IgG heavy chain. Molecular weight standards and antibodies used for immunoblotting are indicated.

Sequential immunoprecipitation using anti-Plk1 antibody depleted Plk1 levels in HEK293 cell lysates (Figure 4.6A). Sequential immunoprecipitation of Plk1 depleted the detection of co-immunoprecipitated ESCRT proteins CHMP6 (Figure 4.6B), CHMP4B (Figure 4.6C), CHMP3 (Figure 4.6D) and CHMP2A (Figure 4.6E). However, ESCRT proteins were still detected in the final supernatant following the third anti-Plk1 immunoprecipitation at qualitatively comparable levels to the first supernatant; this final supernatant represents lysate containing unbound proteins.

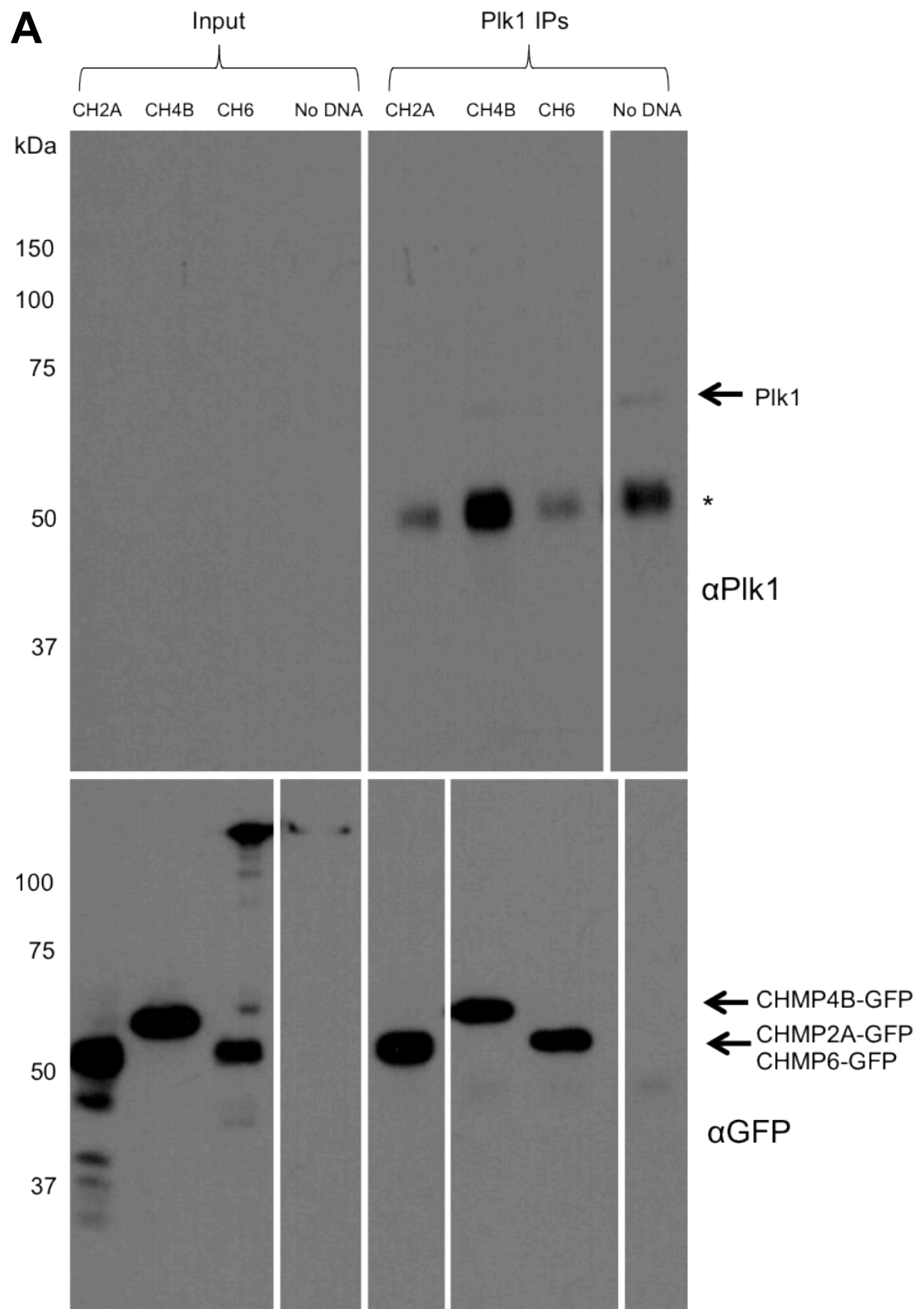
The subsequent beads-only immunoprecipitation of the third supernatant resulted in negligible co-immunoprecipitation of CHMP6 (Figure 4.6B), CHMP4B (Figure 4.6C) and CHMP3 (Figure 4.6D), particularly when compared to the protein levels detected in the final supernatant, S4.

Depleted Plk1 levels within cell lysates resulted in depleted ESCRT co-immunoprecipitation. These data indicate that ESCRT proteins are detected in anti-Plk1 immunoprecipitations due to specific interactions with Plk1. It is also possible that ESCRT proteins are being co-immunoprecipitated due to interactions with an unknown factor binding to either Plk1 or anti-Plk1 antibody; therefore, ESCRT proteins are no longer co-immunoprecipitated on depletion of either Plk1 or the unknown protein.

#### **4.2.2.4 Plk1-ESCRT interactions remained after increasing the detergent in assay conditions**

Experiments presented in *Sections 4.2.2.2 and 4.2.2.3* demonstrate that all of the ESCRT proteins assayed co-immunoprecipitated with Plk1, at least when over-expressed. As the ESCRT proteins are members of a complex (Teis et al. 2009), it is possible that they were co-immunoprecipitating with each other. To overcome this, an experiment was designed in which ESCRT dissociation was attempted using detergent. It was hypothesised that this might allow the co-immunoprecipitation of only certain ESCRT proteins with Plk1, and not others, thus establishing the specific binding partners of Plk1 among the ESCRT proteins.

Purified DNA for CHMP6-GFP, CHMP4B-YFP, CHMP3-myc and CHMP2A-GFP were individually transfected into HEK293 cells and lysates were prepared (*Section 4.2.2.1*). However, in order to disrupt potential interactions between the ESCRT proteins, the Triton X-100 detergent concentration of the lysis buffer was increased tenfold. One mg of each cell lysate was then interrogated with anti-Plk1 antibody or Protein A sepharose beads alone. Immunoblot analysis of the lysates and subsequent immunoprecipitated products revealed no change in the interactions previously observed (Figure 4.7).



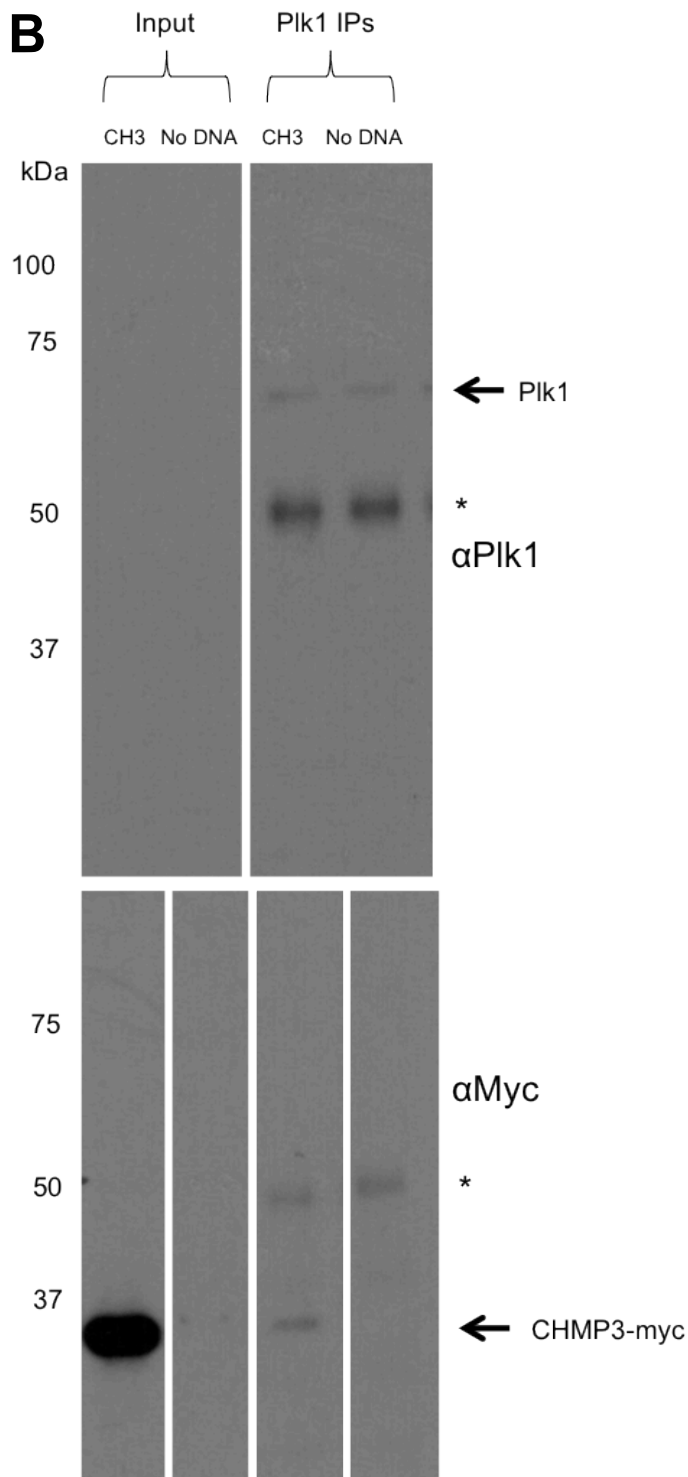


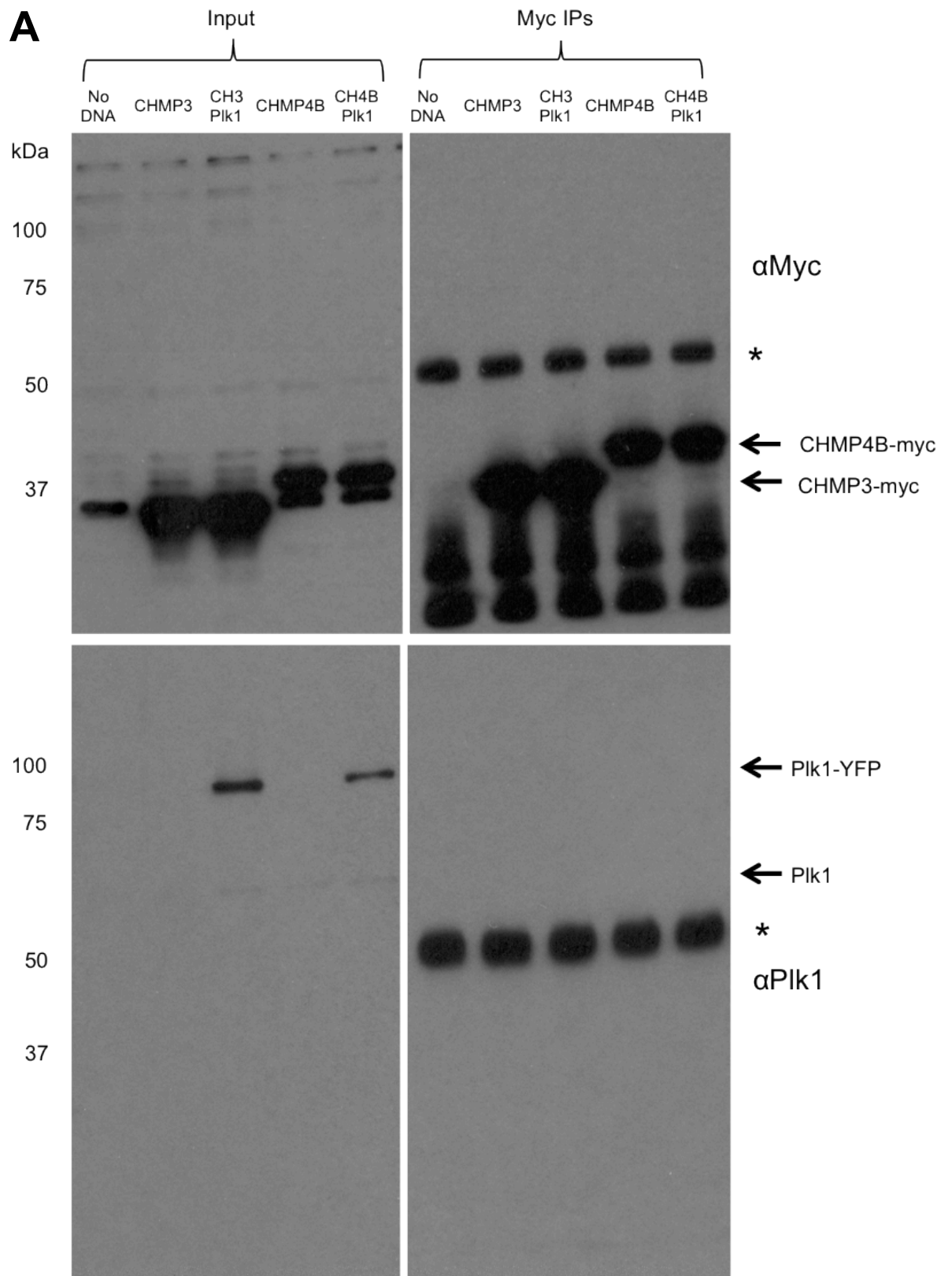
**Figure 4.7: CHMP6, CHMP4B, CHMP3 and CHMP2A co-immunoprecipitate with Plk1 in the presence of increased detergent conditions.**

HEK293 cells were transfected with DNA for (A) CHMP6-GFP, CHMP4B-YFP, CHMP2A-GFP or (B) CHMP3-myc, or with Lipofectamine 2000 in the absence of transforming DNA. Lysates were prepared in buffer with a tenfold higher detergent content. Anti-Plk1 antibody (Plk1 in figure) was added to each cell lysate. Complexes were dissociated from beads (*IP*: one-fifteenth was loaded). *Input* refers to the cell lysate that was interrogated: 5  $\mu$ g was loaded. Various exposures are shown of immunoblots derived from a single SDS gel. Immunoblot splices used to rearrange lanes are from a single exposure. \*IgG heavy chain. Experiments were repeated with qualitatively similar results and data from a typical experiment are shown. Molecular weight standards and antibodies used for immunoblotting are indicated.

CHMP6, CHMP4B, CHMP2A (Figure 4.7A) and CHMP3 (Figure 4.7B) were all detected on over-expression in HEK293 cells and immunoprecipitation of Plk1. Thus, immunoprecipitation of Plk1 from HEK293 lysates prepared with a higher concentration of detergent Triton X-100 did not affect the interactions observed between Plk1 and ESCRT proteins. This suggests that all of the assayed ESCRT proteins interact directly with Plk1. However, this assumes that increasing the Triton X-100 concentration dissociated the ESCRT complex, which was not otherwise assayed.

#### **4.2.2.5 Immunoprecipitation of ESCRT proteins did not result in the co-immunoprecipitation of endogenous or over-expressed Plk1**

Several ESCRT proteins were shown to co-immunoprecipitate with Plk1 (Figure 4.5). To assay whether the observed interactions could be detected when the immunoprecipitation was performed in reverse, ESCRT proteins were immunoprecipitated and screened to detect co-immunoprecipitated Plk1. However, due to the difficulty of detecting Plk1, HEK293 cells were co-transfected with purified DNA for Plk1-YFP and CHMP6-HA, CHMP4B-myc or CHMP3-myc. Cells were also transfected with purified DNA for the individual ESCRT proteins. Lysates were prepared (*Section 4.2.2.1*) and 1 mg of each cell lysate was interrogated with either anti-HA or anti-myc antibody. Immunoblot analysis of lysates and subsequent immunoprecipitated products did not reveal interactions between ESCRT proteins and Plk1-YFP (Figure 4.8).



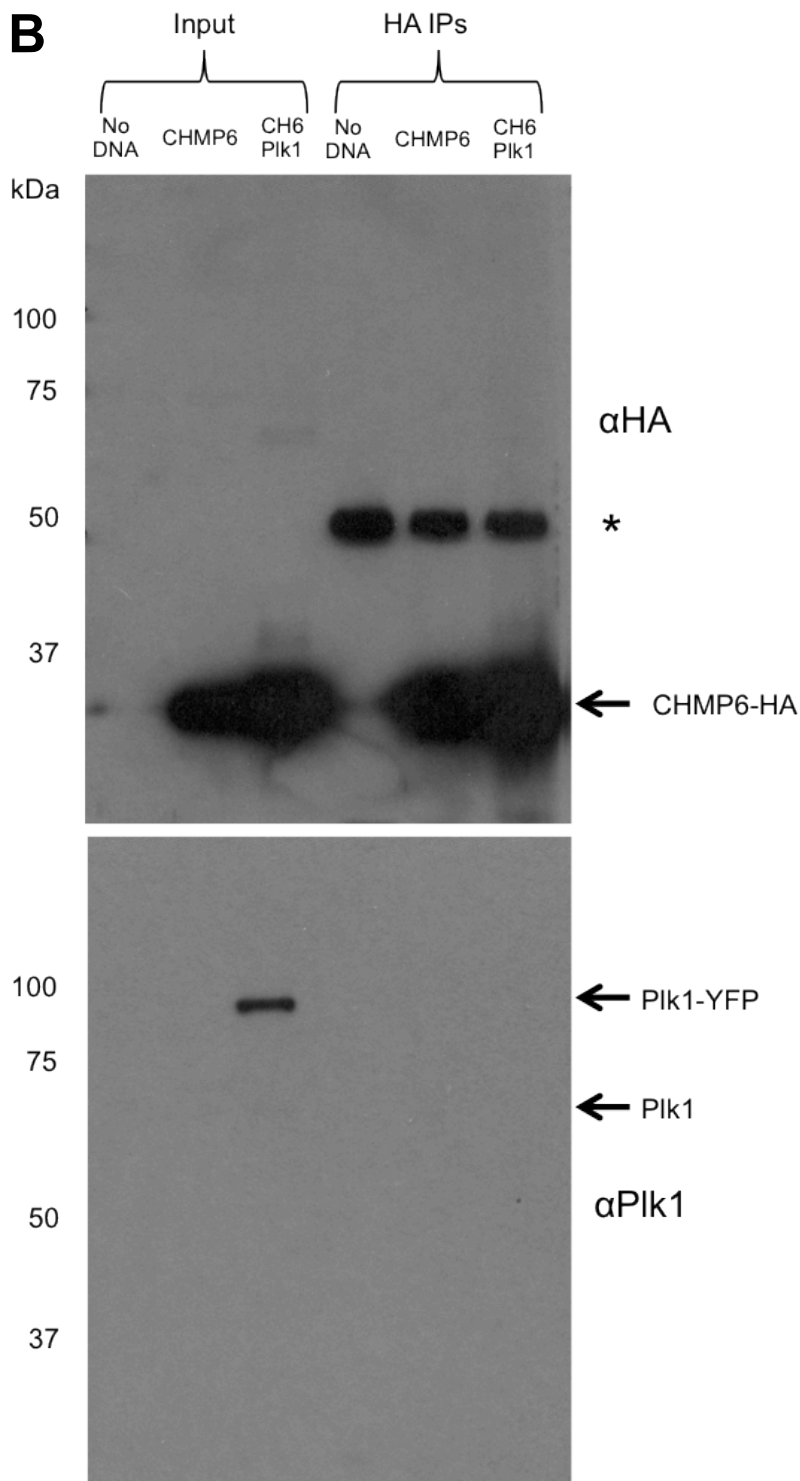


**Figure 4.8: Plk1 was not detected on immunoprecipitation of ESCRT proteins.**

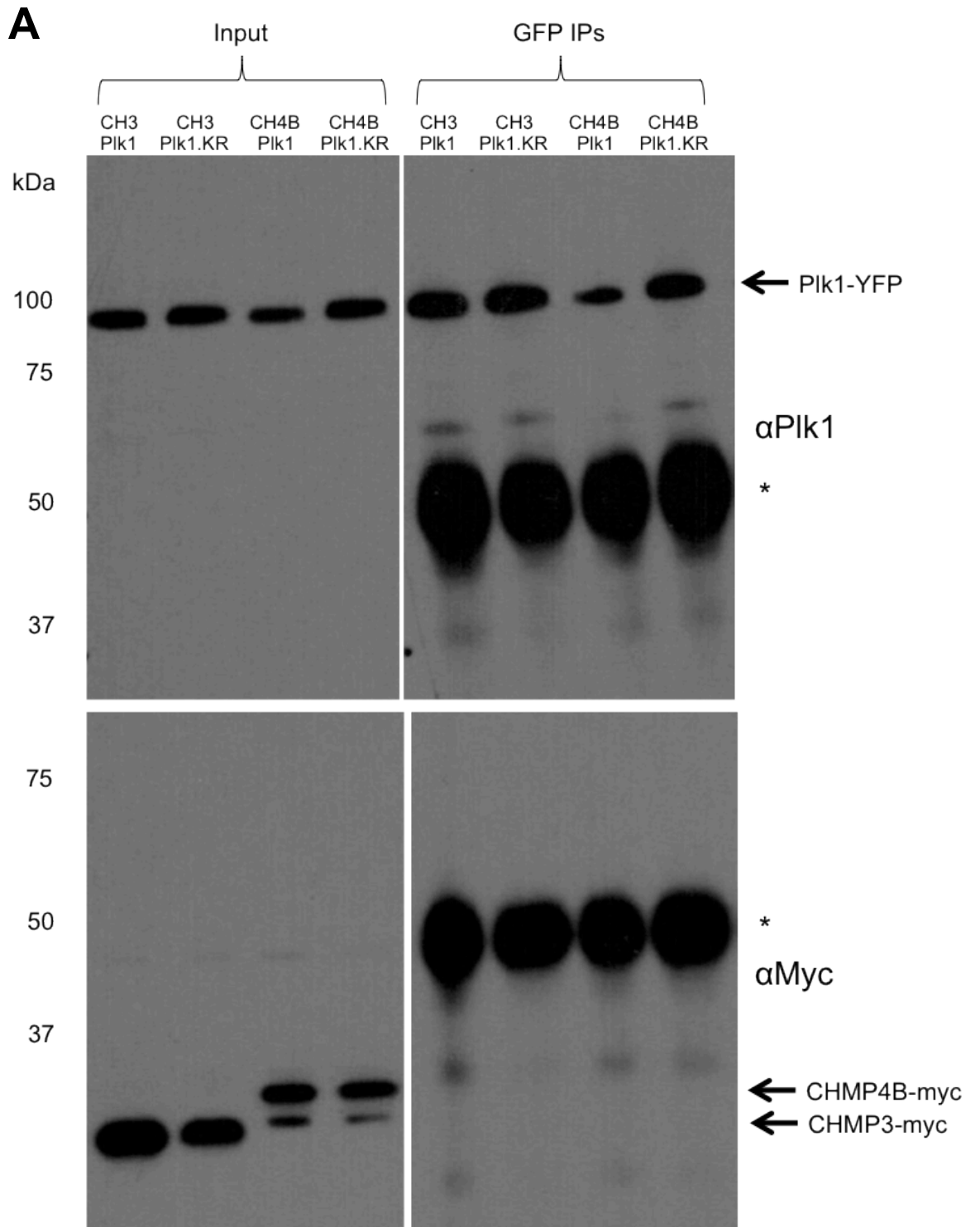
HEK293 cells were transfected with DNA for (A) CHMP4B-myc, CHMP3-myc or (B) CHMP6-HA. Cells were also co-transfected with Plk1-YFP. Lysates were prepared and interrogated with either (A) anti-myc antibody and Protein A sepharose beads, or (B) anti-HA antibody and Protein G sepharose beads. Complexes were dissociated from beads (*IP*: one-fifteenth was loaded). *Input* refers to the cell lysate that was interrogated: 5  $\mu$ g was loaded. Various exposures are shown of immunoblots derived from a single SDS gel. Immunoblot splices used to rearrange lanes are from a single exposure. \*IgG heavy chain. Experiments were repeated with qualitatively similar results and data from a typical experiment are shown. Molecular weight standards and antibodies used for immunoblotting are indicated.

Immunoprecipitation using anti-myc antibody produced purified CHMP3 and CHMP4B from over-expressing HEK293 cell lysates (Figure 4.8A). Several non-specific reactive proteins were detected, and the myc-tagged ESCRT proteins are indicated. However, although endogenous Plk1 and over-expressed Plk1-YFP were detected in lysates, neither was detected on immunoprecipitation of CHMP3 or CHMP4B.

In addition, immunoprecipitation using anti-HA antibody produced purified CHMP6 from over-expressing HEK293 cell lysates (Figure 4.8B). Endogenous Plk1 and Plk1-YFP were detected in lysates, but, again, neither was detected on immunoprecipitation of the ESCRT proteins.

#### **4.2.2.6 Immunoprecipitation of Plk1-YFP did not result in co-immunoprecipitation of ESCRT proteins**

The effect of Plk1.K82R, a kinase-dead form of Plk1 (Golsteyn et al. 1995), upon interactions with ESCRT proteins was investigated. Purified DNA for Plk1-YFP or Plk1.K82R-YFP was co-transfected into HEK293 cells with purified DNA for CHMP6-HA, CHMP4B-myc or CHMP3-myc. Lysates were prepared and immunoprecipitated using anti-GFP antibody (Figure 4.9).



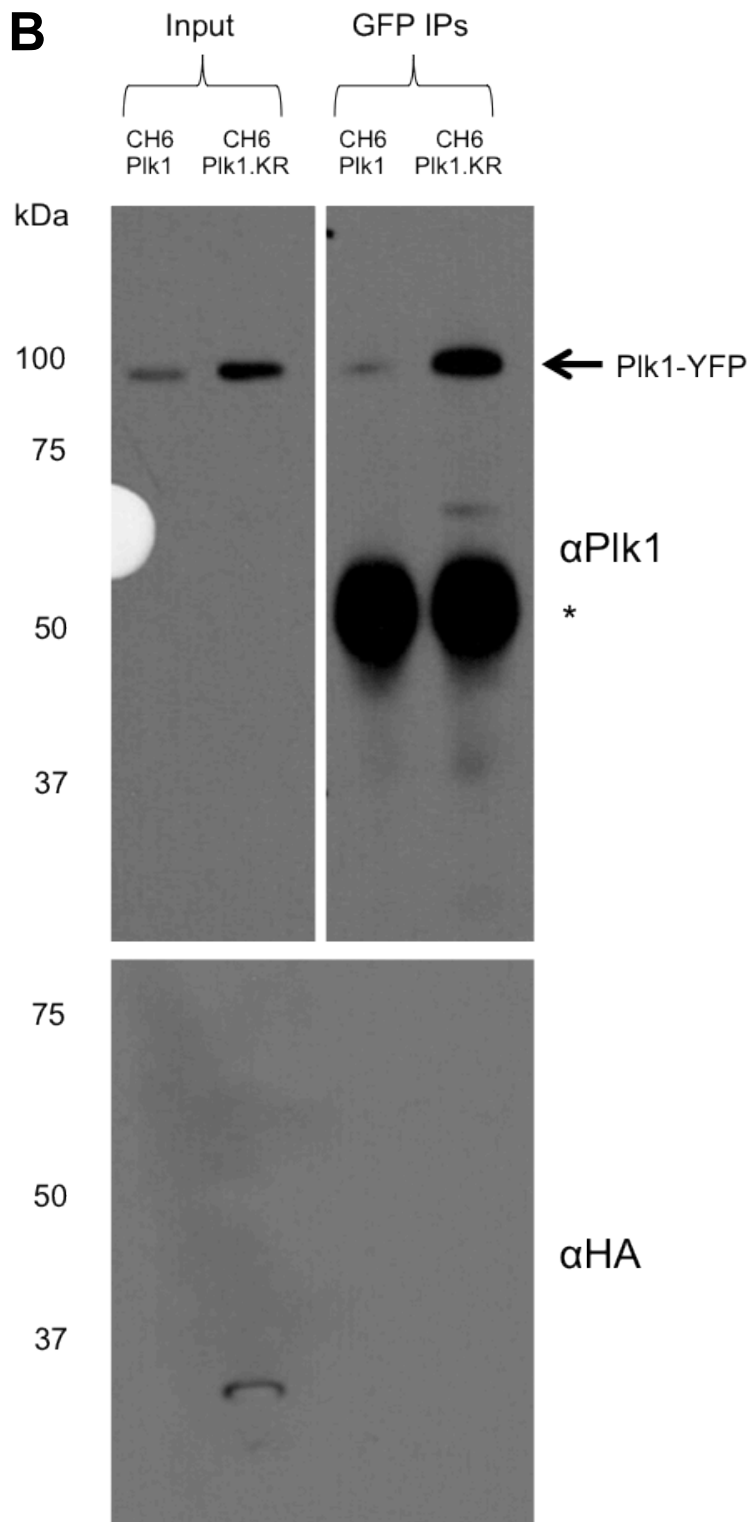


**Figure 4.9: Anti-GFP immunoprecipitation of Plk1-YFP did not result in co-immunoprecipitation of ESCRT proteins.**

HEK293 cells were co-transfected with Plk1-YFP or Plk1.K82R-YFP and (A) CHMP3-myc, CHMP4B-myc or (B) CHMP6-HA. Lysates were prepared and anti-GFP antibody was added to each cell lysate. Complexes were dissociated from Protein A sepharose beads (*IP*: one-fifteenth was loaded). *Input* refers to the cell lysate that was interrogated: 5  $\mu$ g was loaded. No CHMP6+Plk1 lysate remained after immunoprecipitation to analyse via SDS-PAGE. Various exposures are shown of immunoblots derived from a single SDS gel. Immunoblot splices used to rearrange lanes are from a single exposure. \*IgG heavy chain. Experiments were repeated with qualitatively similar results and data from a typical experiment are shown. Molecular weight standards and antibodies used for immunoblotting are indicated.

CHMP3-myc, CHMP4B-myc and CHMP6-HA were over-expressed with Plk1-YFP and Plk1.K82R-YFP in HEK293 cells. Plk1-YFP and Plk1.K82R-YFP were immunoprecipitated using anti-GFP antibody. CHMP3, CHMP4B (Figure 4.9A) and CHMP6 (Figure 4.9B) were detected in lysates, but not in the immunoprecipitation of Plk1-YFP or Plk1.K82R-YFP.

These results suggest that Plk1-YFP did not interact with ESCRT proteins, possibly because Plk1-YFP and ESCRT proteins were expressed in different cells.

#### **4.2.2.7 Immunoprecipitation of ESCRT proteins did not result in detection of Plk1.K82R-YFP**

Plk1-YFP did not co-immunoprecipitate with ESCRT proteins (Figure 4.8). To investigate if Plk1.K82R-YFP could be detected on immunoprecipitation of ESCRT proteins, co-transfected lysates from *Section 4.2.2.6* were interrogated with anti-HA or anti-myc antibody to immunoprecipitate ESCRT proteins. CHMP6-HA, CHMP4B-myc and CHMP3-myc were immunoprecipitated from HEK293 cells co-expressing Plk1-YFP or kinase-dead Plk1.K82R-YFP. Both over-expressed Plk1 species were detected in lysates but neither was co-immunoprecipitated with ESCRT proteins (data not shown).

### **4.2.3 Investigating interactions between Plk1 and over-expressed ESCRT proteins in HeLa cells**

Following observation of interactions between Plk1 and ESCRT proteins in HEK293 cells, HeLa cells were revisited to transfect with purified DNA for ESCRT protein over-expression. Although Plk1-ESCRT interactions were observed in HEK293 cells by immunoprecipitating Plk1, immunoprecipitating ESCRT proteins did not reveal interactions. However, Plk1 had been more readily detected on immunoblotting HeLa cell lysates than HEK293 cell lysates (*Section 4.2.1*), therefore, it was hypothesised that immunoprecipitation of ESCRT proteins could reveal interactions with co-immunoprecipitated Plk1 in HeLa cells.

#### **4.2.3.1 Over-expression of ESCRT proteins in HeLa cells was not robust and did not yield observable interactions**

Purified DNA for CHMP6-GFP was transfected into HeLa cells and lysates were prepared (*Section 4.2.2.1*). One mg of cell lysate was interrogated with anti-Plk1 antibody, or Protein A sepharose beads alone. However, immunoblot analysis of lysates revealed poor expression of CHMP6-GFP, and co-immunoprecipitation was not detected (data not shown).

Transfection method, purified DNA, lysate preparation, immunoprecipitation, SDS-PAGE and immunoblotting were all performed identically for HEK293 and HeLa cells. However, ESCRT proteins were not detected in high abundance in HeLa cell lysates. Fresh HeLa cell stocks were used, but over-expression was never as effective as in HEK293 cells (*Section 4.2.2*).

#### **4.2.3.2 Immunoprecipitation of over-expressed ESCRT proteins did not yield detection of Plk1**

To assay if interactions could be detected when the immunoprecipitation was performed in reverse, ESCRT proteins were immunoprecipitated and screened to detect Plk1. Purified DNA for CHMP6-GFP and CHMP2A-GFP was individually transfected into HeLa cells and lysates were prepared (*Section 4.2.2.1*). One mg of each cell lysate was interrogated with anti-GFP antibody. Immunoblot analysis of lysates and subsequent immunoprecipitated products revealed immunoprecipitation of CHMP6 and CHMP2A, but not co-immunoprecipitation of Plk1 (data not shown).

#### **4.2.4 Investigating an ESCRT protein phospho-mobility shift in the presence of Plk1 kinase inhibition**

Following the observations of interactions between Plk1 and ESCRT proteins, the potential functional consequence of these interactions was examined. As Plk1 is a protein kinase, it controls interacting proteins through phosphorylation. Changes in phosphorylation status of proteins can be detected by SDS-PAGE, as this sometimes results in changes in protein mobility under these conditions, likely due to changes in protein conformation (Wegener & Jones 1984).

Introducing a Plk1 kinase inhibitor to HeLa cells allowed the putative control of Plk1 over the phosphorylation status of ESCRT proteins to be tested. ESCRT protein mobility was then examined by SDS-PAGE before and after treatment to search for changes.

HeLa cells were arrested in metaphase and telophase by thymidine-nocodazole block. Plk1 inhibitor BI 2536 was added to cells (Lénárt et al. 2007). Lysates were prepared and subjected to SDS-PAGE, and the position of CHMP6 (ESCRT-III) was assayed by immunoblotting (Figure 4.10).

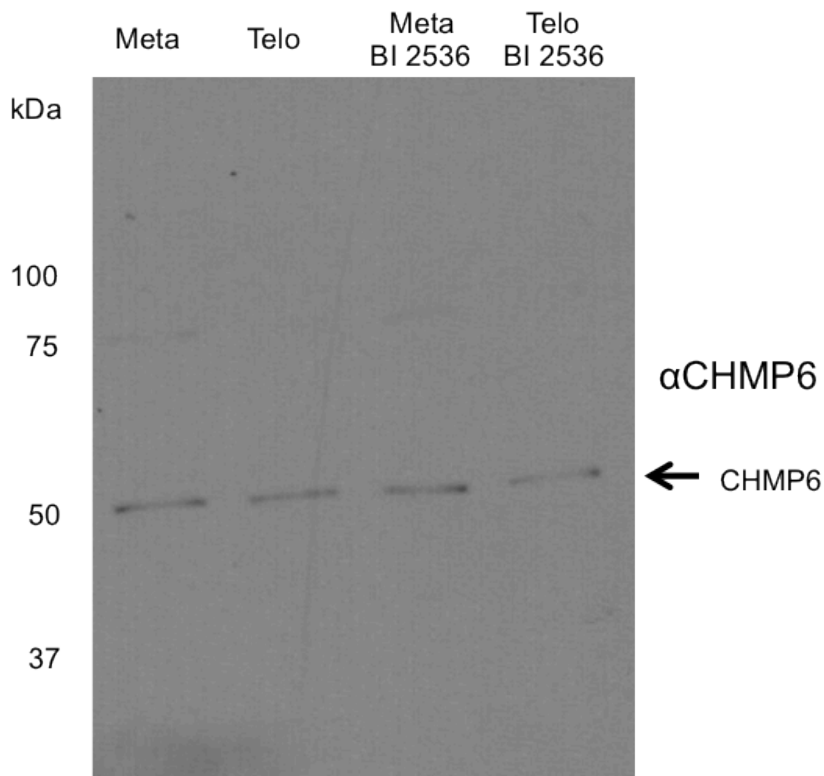


**Figure 4.10: A phospho-mobility shift in the position of CHMP6 was not detected on inhibition of Plk1.**

HeLa cells were arrested in metaphase and telophase by thymidine-nocodazole block. BI 2536 was introduced to inhibit Plk1 kinase. Lysates were prepared and 25  $\mu$ g of each cell lysate was subjected to SDS-PAGE. Experiments were repeated with qualitatively similar results and data from a typical experiment are shown. Molecular weight standards and antibodies used for immunoblotting are indicated.

Immunoblotting Plk1 kinase-inhibited lysates did not reveal a shift in the position of CHMP6 relative to untreated lysates, suggesting that, under these conditions, Plk1 was not influencing the phosphorylation status of CHMP6. However, kinase inhibition was not confirmed in lysates treated with BI 2536. Furthermore, a loading control was not included: this would likely have identified the uneven detection of CHMP6 as an artefact of SDS-PAGE.

A phospho-mobility shift was observed on immunoblotting CHMP3 from Plk1 kinase-inhibited HeLa cell lysates (data not shown). Graduate student Craig Shepherd, whom I supervised, performed this assay; however, as this experiment needs to be repeated to reproduce this result, these data have not been presented.

## **4.2.5 Investigating interactions between CDC14A and ESCRT proteins on over-expressing both in HEK293 cells**

Following the detection of genetic and physical interactions between Plo1p and ESCRT proteins in fission yeast (*Sections 3.2.3 and 3.2.5*) interactions were observed between Plk1 and ESCRT proteins in human cells (*Section 4.2.2*). Since genetic and physical interactions were also detected between Clp1p (CDC14) and ESCRT proteins in fission yeast (*Section 3.2.3 and 3.2.5*), this prompted an investigation into interactions between CDC14 and ESCRT proteins in human cells. HEK293 cells were co-transfected with DNA for both, and assayed by immunoprecipitation and co-immunoprecipitation methods.

### **4.2.5.1 CDC14A phosphatase interacts with CHMP4B (Vps32p, ESCRT-III)**

HEK293 cells were transfected with purified DNA for CHMP4B-YFP alone, and co-transfected with DNA for CDC14A-myc. Lysates were prepared (*Section 4.2.2.1*) and 1 mg of each cell lysate was interrogated with anti-myc antibody. Immunoblot analysis of lysates and subsequent immunoprecipitated products revealed immunoprecipitation of CDC14A and co-immunoprecipitation of CHMP4B (*Figure 4.11*).

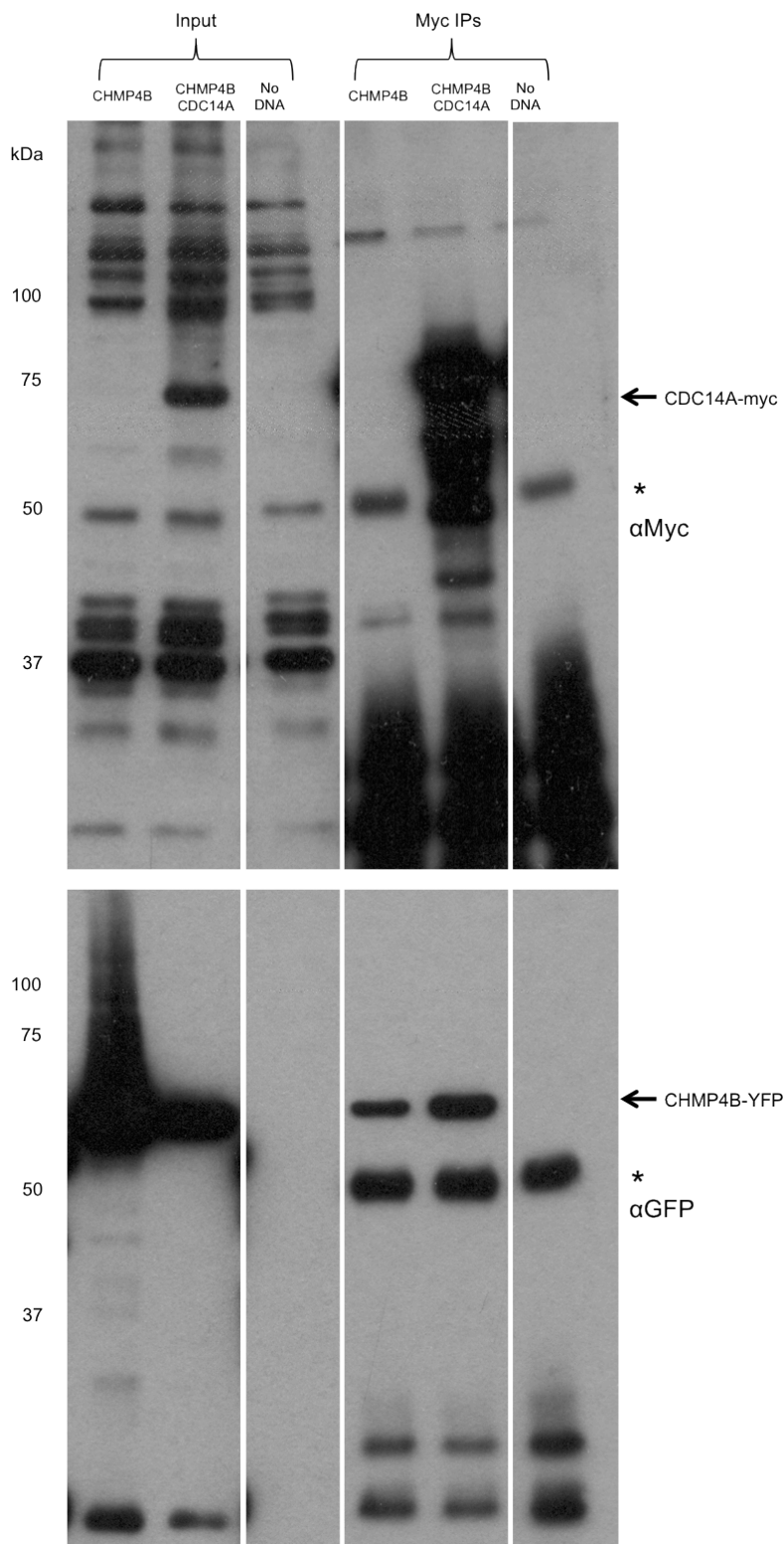


**Figure 4.11: CHMP4B co-immunoprecipitates with CDC14A from HEK293 cell lysates.**

HEK293 cells were transfected with DNA for CHMP4B-YFP or co-transfected with CDC14A-myc. Lysates were also prepared with Lipofectamine 2000 in the absence of transforming DNA. Lysates were interrogated with anti-myc antibody. Complexes were dissociated from beads (*IP*: one-eighth was loaded). *Input* refers to the cell lysate that was interrogated: 10  $\mu$ g was loaded. Various exposures are shown of immunoblots derived from a single SDS gel. Immunoblot splices used to rearrange lanes are from a single exposure. \*IgG heavy chain. Molecular weight standards and antibodies used for immunoblotting are indicated.

CDC14A-myc was detected in lysate co-expressing CHMP4B and subsequent anti-myc immunoprecipitation of this lysate by immunoblotting with anti-myc antibody (Figure 4.11, top panel). Multiple non-specific reactive proteins are detected in all lysates and immunoprecipitations on immunoblotting using anti-myc antibody.

Immunoprecipitation using anti-myc antibody from HEK293 cell lysate over-expressing CHMP4B revealed the presence of CHMP4B in the absence of any myc-tagged partner (Figure 4.11, bottom panel). However, over-expressing CDC14A-myc with CHMP4B resulted in immunoprecipitation of CDC14A and the stronger detection of CHMP4B. This indicates that CHMP4B interacts with CDC14A in human cells. Further ESCRT proteins were then assayed for interactions with CDC14A.

#### **4.2.5.2 CDC14A interacts with CHMP4B (Vps32p, ESCRT-III) and CHMP2A (Vps2p, ESCRT-III)**

HEK293 cells were co-transfected with purified DNA for CDC14A-myc and VPS28-V5, CHMP6-GFP, CHMP4B-YFP, or CHMP2A-GFP. Lysates were prepared (*Section 4.2.2.1*) and 1 mg of each cell lysate was interrogated with anti-myc antibody or Protein A sepharose beads alone. Immunoblot analysis of lysates and subsequent immunoprecipitated products revealed immunoprecipitation of CDC14A and co-immunoprecipitation of CHMP4B and CHMP2A (Figure 4.12).

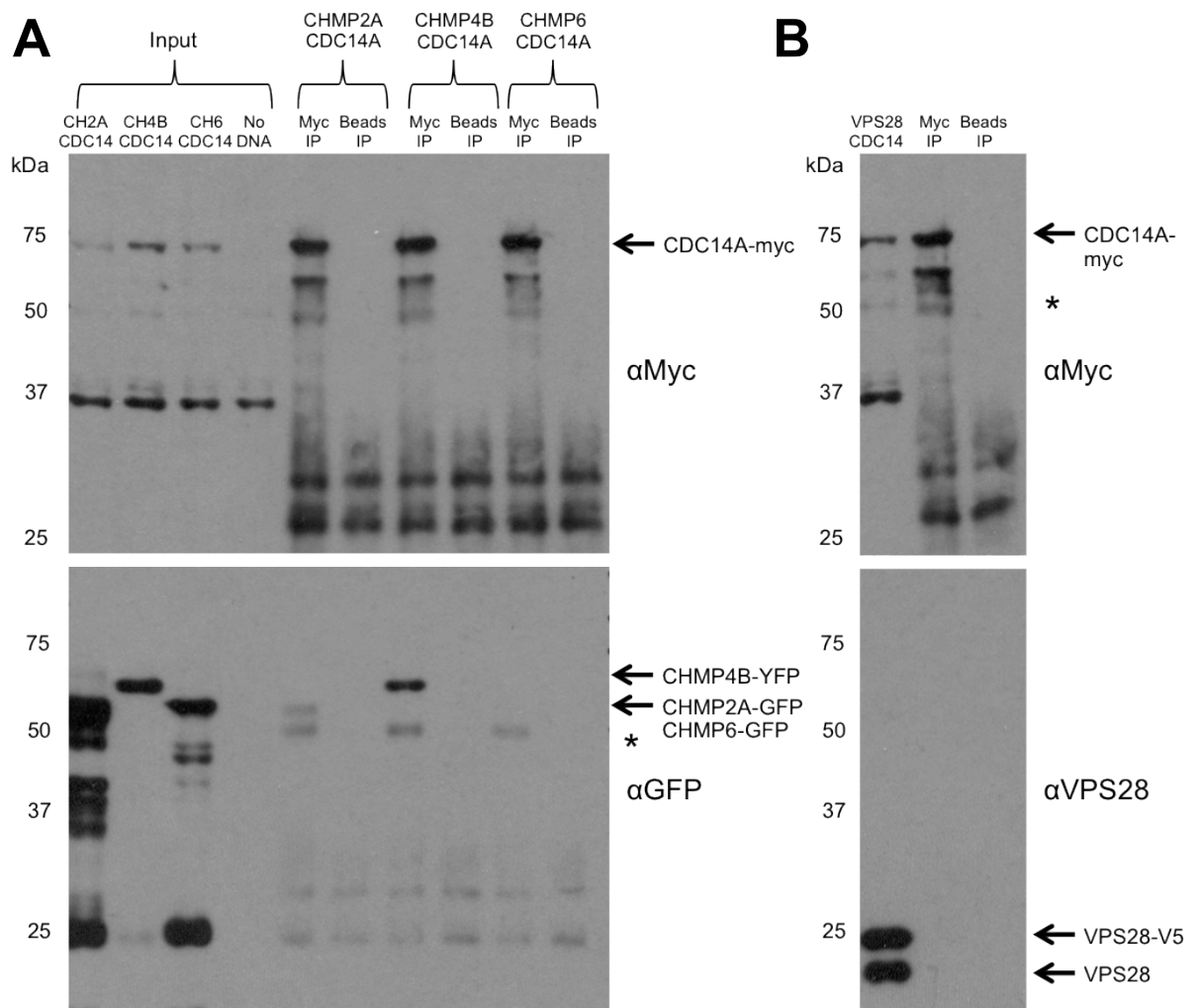


**Figure 4.12: CHMP4B and CHMP2A co-immunoprecipitate with CDC14A from HEK293 cell lysates.**

HEK293 cells were co-transfected with purified DNA for CDC14A-myc and (A) CHMP6-GFP, CHMP4B-YFP, CHMP2A-GFP or (B) VPS28-V5. Lysates were interrogated with anti-myc antibody or with Protein A sepharose beads alone. Complexes were dissociated from beads (*IP*: one-fifteenth was loaded). *Input* refers to the cell lysate that was interrogated: 5  $\mu$ g was loaded. Various exposures are shown of immunoblots derived from a single SDS gel. \*IgG heavy chain. Experiments were repeated with qualitatively similar results and data from a typical experiment are shown. Molecular weight standards and antibodies used for immunoblotting are indicated.

CDC14A-myc was detected in co-expressing lysates and subsequent immunoprecipitations by immunoblotting with anti-myc antibody (Figure 4.12A and B, top panels). CDC14A-myc was not detected in lysate prepared in the absence of transfecting DNA, nor by immunoprecipitating from over-expressing lysates with Protein A sepharose in the absence of anti-myc antibody. CHMP6-GFP, CHMP4B-YFP, CHMP2A-GFP (Figure 4.12A, bottom panel) and VPS28-V5 (Figure 4.12B, bottom panel) were all detected in co-expressing lysates.

Immunoprecipitation of CDC14A resulted in the co-immunoprecipitation of CHMP4B and CHMP2A (Figure 4.12A, bottom panel). CHMP6 (Figure 4.12A, bottom panel) and VPS28 (Figure 4.12B, bottom panel) were not detected on immunoprecipitation of CDC14A.

#### **4.2.5.3 Phosphatase-dead CDC14A.C278S interacts with CHMP4B and CHMP2A**

To investigate whether a phosphatase-dead form of CDC14A affected its interactions with ESCRT proteins, HEK293 cells were co-transfected with purified DNA for CDC14A.C278S-myc (Lanzetti et al. 2007) and VPS28-V5, CHMP6-GFP, CHMP4B-YFP, or CHMP2A-GFP. Lysates were prepared (*Section 4.2.2.1*) and 1 mg of each cell lysate was interrogated with anti-myc antibody or Protein A sepharose beads alone. Immunoblot analysis of lysates and subsequent immunoprecipitated products revealed immunoprecipitation of CDC14A.C278S and co-immunoprecipitation of CHMP4B and CHMP2A (Figure 4.13).

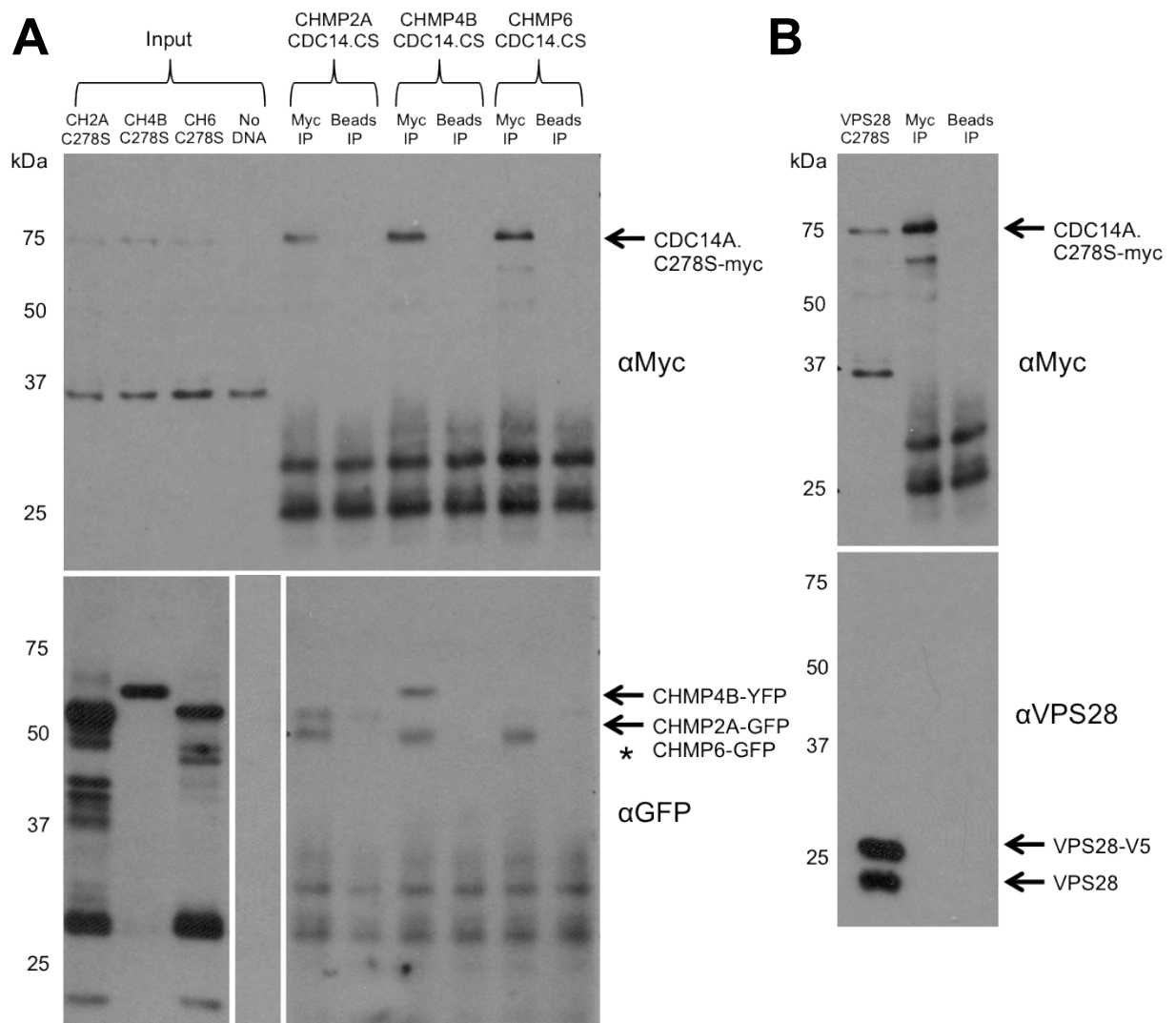


**Figure 4.13: CHMP4B and CHMP2A co-immunoprecipitate with phosphatase-dead CDC14A.C278S from HEK293 cell lysates.**

HEK293 cells were co-transfected with purified DNA for CDC14A.C278S-myc and (A) CHMP6-GFP, CHMP4B-YFP, CHMP2A-GFP or (B) VPS28-V5. Lysates were interrogated with anti-myc antibody or with Protein A sepharose beads alone. Complexes were dissociated from beads (*IP*: one-fifteenth was loaded). *Input* refers to the cell lysate that was interrogated: 5  $\mu$ g was loaded. Various exposures are shown of immunoblots derived from a single SDS gel. Immunoblot splices used to rearrange lanes are from a single exposure. \*IgG heavy chain. Experiments were repeated with qualitatively similar results and data from a typical experiment are shown. Molecular weight standards and antibodies used for immunoblotting are indicated.

CDC14A.C278S-myc was detected in co-expressing lysates and subsequent immunoprecipitations by immunoblotting with anti-myc antibody (Figure 4.13A and B, top panels). CDC14A.C278S-myc was not detected in lysate prepared in the absence of transfecting DNA, nor by immunoprecipitating from over-expressing lysates with Protein A sepharose in the absence of anti-myc antibody. CHMP6-GFP, CHMP4B-YFP, CHMP2A-GFP (Figure 4.13A, bottom panel) and VPS28-V5 (Figure 4.13B, bottom panel) were all detected in co-expressing lysates.

Immunoprecipitation of CDC14A.C278S resulted in the co-immunoprecipitation of CHMP4B and CHMP2A (Figure 4.13A, bottom panel). CHMP6 (Figure 4.13A, bottom panel) and VPS28 (Figure 4.13B, bottom panel) were not detected on immunoprecipitation of CDC14A.C278S.

#### **4.2.5.4 Immunoprecipitation of ESCRT proteins yields detection of CDC14A**

Immunoprecipitation of CDC14A resulted in co-immunoprecipitated ESCRT proteins (Figure 4.12). To investigate if CDC14A could be detected on immunoprecipitation of ESCRT proteins, HEK293 cell lysates from *Section 4.2.5.2* were interrogated with either anti-GFP or anti-VPS28 antibody. Immunoblot analysis of lysates and subsequent immunoprecipitated products revealed immunoprecipitation of ESCRT proteins and co-immunoprecipitation of CDC14A with CHMP4B and CHMP2A (Figure 4.14).

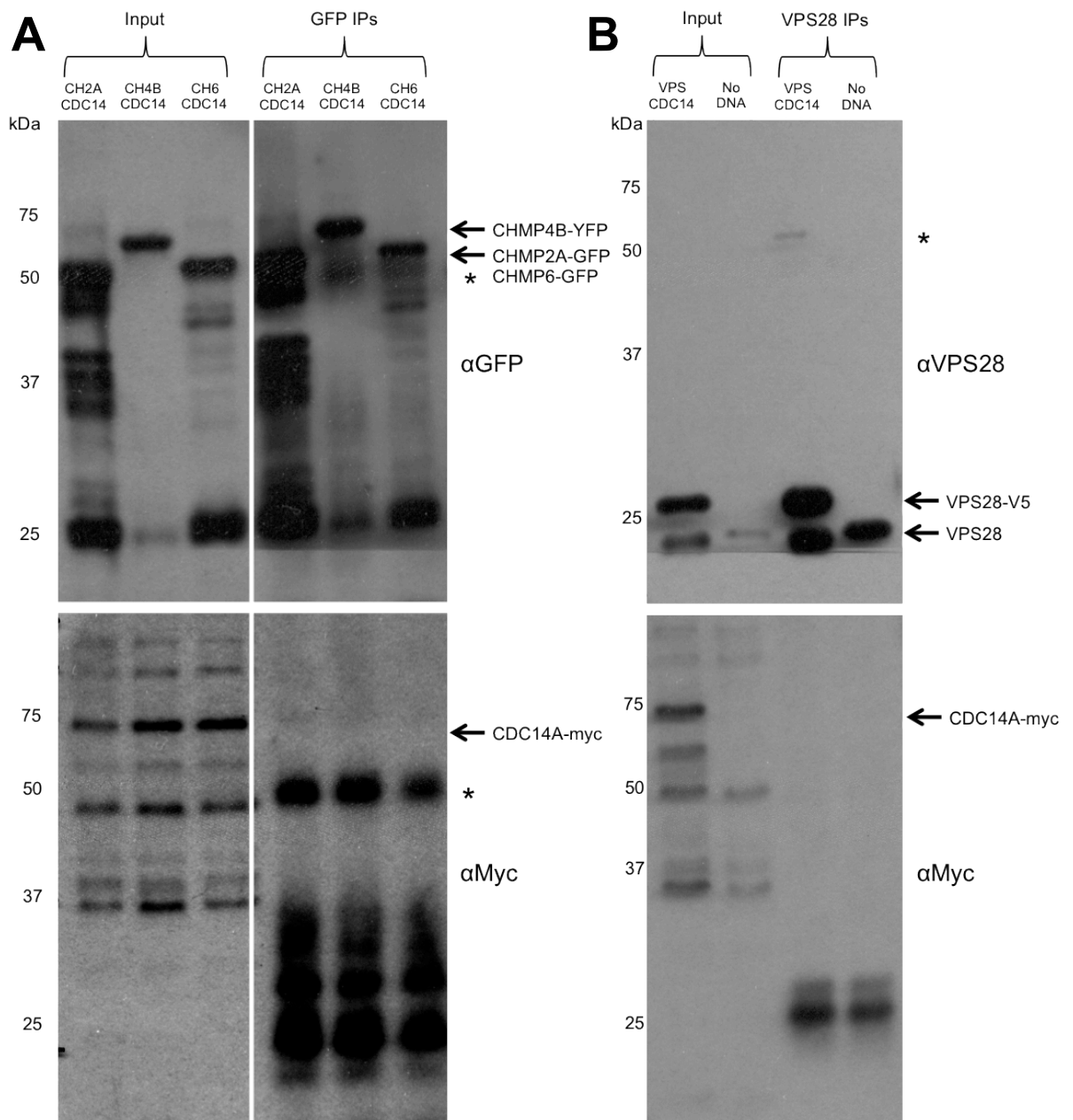


**Figure 4.14: CDC14A co-immunoprecipitates with CHMP4B and CHMP2A.**

HEK293 cells were co-transfected with purified DNA for CDC14A-myc and (A) CHMP6-GFP, CHMP4B-YFP, CHMP2A-GFP or (B) VPS28-V5. Lysates were interrogated with either anti-GFP or anti-VPS28 antibody. Non-transfected HEK293 cell lysates were also interrogated with anti-VPS28 antibody. Complexes were dissociated from beads (*IP*: one-fifteenth was loaded). *Input* refers to the cell lysate that was interrogated: 5  $\mu$ g was loaded. Various exposures are shown of immunoblots derived from a single SDS gel. Immunoblot splices used to rearrange lanes are from a single exposure. \*IgG heavy chain. Molecular weight standards and antibodies used for immunoblotting are indicated.

CHMP6-GFP, CHMP4B-YFP, CHMP2A-GFP (Figure 4.14A, top panel) and VPS28-V5 (Figure 4.14B, top panel) were all detected in co-expressing lysates with CDC14A-myc and subsequent immunoprecipitation with either anti-GFP or anti-VPS28 antibody. CDC14A-myc was detected in co-expressing lysates with ESCRT proteins (Figure 4.14A and B, bottom panels).

Immunoprecipitation of CHMP4B and CHMP2A resulted in the detection of CDC14A, demonstrating that CDC14A co-immunoprecipitated with CHMP4B and CHMP2A (Figure 4.14A, bottom panel). However, this has not presented well here and should be repeated with larger amounts of material to enhance detection.

CDC14A was not detected on immunoprecipitation of either CHMP6 (Figure 4.14A, bottom panel) or VPS28 (Figure 4.14B, bottom panel).

#### **4.2.5.5 Immunoprecipitation of ESCRT proteins did not yield detection of phosphatase-dead CDC14A.C278S**

Immunoprecipitation of CDC14A.C278S resulted in co-immunoprecipitated ESCRT proteins (Figure 4.13). To investigate whether interactions could be detected in reverse, HEK293 cells from *Section 4.2.5.3* were interrogated with either anti-GFP or anti-VPS28 antibody. Immunoblot analysis of lysates and subsequent immunoprecipitated products did not reveal co-immunoprecipitation of CDC14A.C278S with the ESCRT proteins (Figure 4.15).

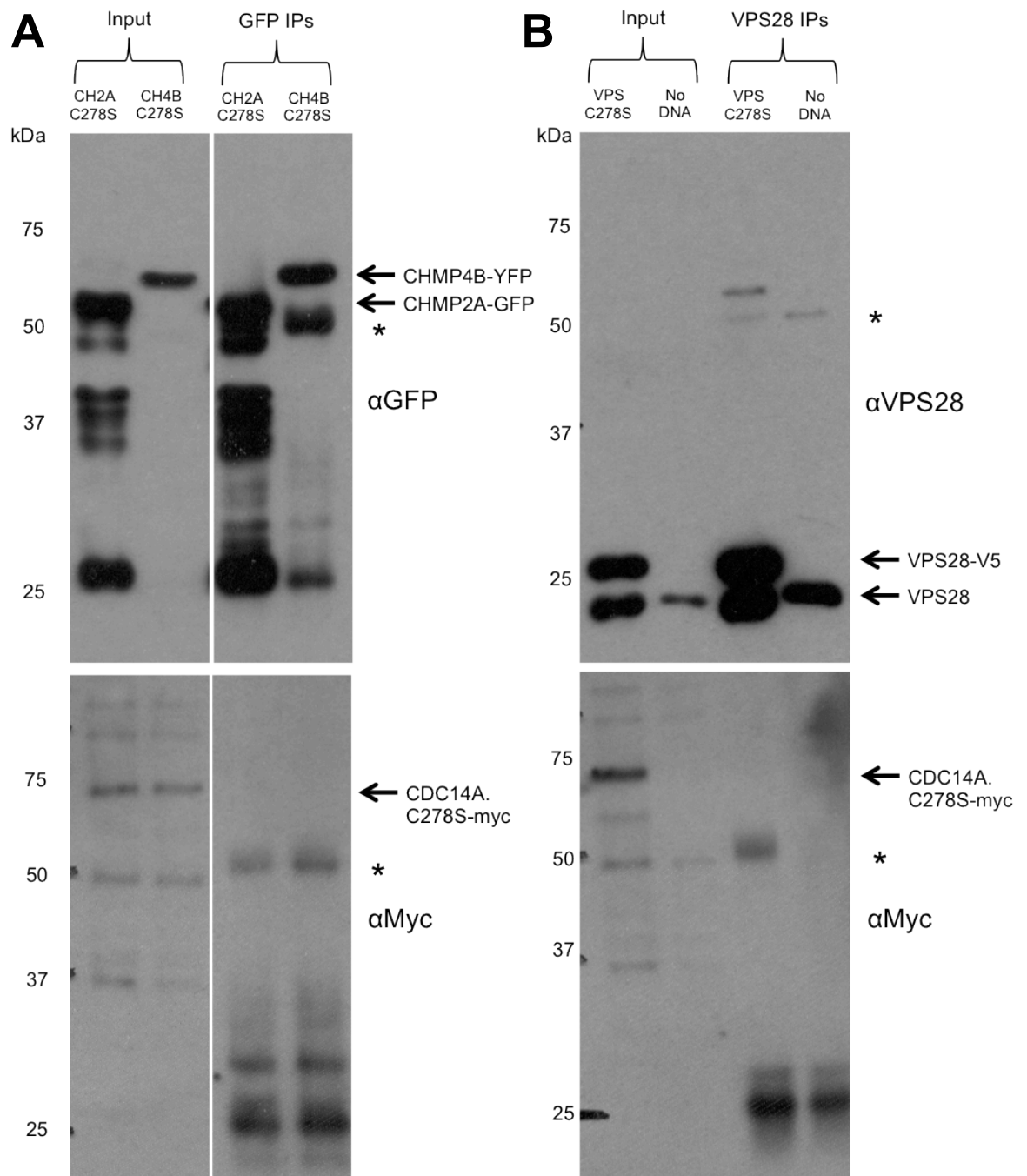


**Figure 4.15: CDC14A.C278S was not detected on immunoprecipitation of VPS28, CHMP4B or CHMP2A.**

HEK293 cells were co-transfected with purified DNA for CDC14A.C278S-myc and (A) CHMP4B-YFP, CHMP2A-GFP or (B) VPS28-V5. Lysates were interrogated with either anti-GFP or anti-VPS28 antibody. Non-transfected HEK293 cell lysates were also interrogated with anti-VPS28 antibody. Complexes were dissociated from beads (*IP*: one-fifteenth was loaded). *Input* refers to the cell lysate that was interrogated: 5  $\mu$ g was loaded. Various exposures are shown of immunoblots derived from a single SDS gel. Immunoblot splices used to rearrange lanes are from a single exposure. \*IgG heavy chain. Molecular weight standards and antibodies used for immunoblotting are indicated.

CHMP4B-YFP, CHMP2A-GFP (Figure 4.15A, top panel) and VPS28-V5 (Figure 4.15B, top panel) were all detected in co-expressing lysates with CDC14A.C278S-myc and subsequent immunoprecipitation with either anti-GFP or anti-VPS28

antibody. CDC14A.C278S-myc was detected in co-expressing lysates with ESCRT proteins (Figure 4.15A and B, bottom panels). Phosphatase-dead CDC14A.C278S was not detected on immunoprecipitation of CHMP4B, CHMP2A (Figure 4.15A, bottom panel) or VPS28 (Figure 4.15B, bottom panel). However, this assay would benefit from being repeated with larger amounts of material.

## 4.2.6 Concluding remarks

### 4.2.6.1 Principal findings

Due to genetic and physical interactions observed between fission yeast counterparts, interactions were investigated in human cells between ESCRT proteins and Plk1 and CDC14A. Immunoprecipitation methods were employed to purify proteins from human cell lysates and to allow detection of co-immunoprecipitated interacting partners.

A published binding partner of Plk1, FOXM1 (Fu et al. 2008), was co-immunoprecipitated from HeLa cells arrested in metaphase (Figure 4.2). However, ESCRT proteins could not be shown to interact with Plk1 in HeLa cells arrested in metaphase or telophase (Figure 4.2). ESCRT-I component, VPS28, was immunoprecipitated from asynchronous HeLa cells and cells arrested in metaphase and telophase, but Plk1 was not shown to interact (Figure 4.3).

ESCRT proteins were next over-expressed in HEK293 cells, due to published observed interactions on immunoprecipitation of Plk1 (Fu et al. 2008). Under these conditions, interactions were detected between Plk1 and ESCRT-III components CHMP6, CHMP4B, CHMP3 and CHMP2A (Figure 4.5). Plk1 was depleted from lysates by sequential immunoprecipitation and ESCRT co-immunoprecipitation significantly diminished, despite almost unchanged expression levels in lysates (Figure 4.6).

However, other experimental conditions did not confirm these interactions. Plk1 was not detected on immunoprecipitation of ESCRT proteins from HEK293 cell lysates (Figure 4.8). Plk1-YFP was co-expressed with ESCRT proteins in HEK293 cells. Immunoprecipitation of Plk1-YFP using anti-GFP antibody did not result in detection of ESCRT proteins (Figure 4.9). This outcome was also shown for kinase-dead Plk1.K82R and ESCRT proteins (Figure 4.9). Furthermore, no reverse interaction was found on immunoprecipitation of ESCRT proteins and screening for Plk1-YFP or Plk1.K82R-YFP (data not shown). ESCRT proteins were over-expressed in HeLa cells less effectively than in HEK293 cells. Interactions were not found between Plk1 and ESCRT proteins in HeLa cells (data not shown).

A functional assay was performed. HeLa cells were arrested in metaphase and telophase and subjected to Plk1 kinase inhibition. A phospho-mobility shift of ESCRT-III protein CHMP6 was not detected (Figure 4.10).

CDC14A and ESCRT proteins were subsequently over-expressed in HEK293 cells. CDC14A was revealed to interact with CHMP4B and CHMP2A (Figure 4.12). Interactions were also shown when the experiment was performed in reverse (Figure 4.14). Phosphatase-dead CDC14A.C278S was also shown to interact with CHMP4B and CHMP2A (Figure 4.13); however, reverse assays did not reveal interactions (Figure 4.15).

#### **4.2.6.2 Summary**

Immunoprecipitation of proteins from human cell lysates was an effective technique in assaying interactions between human proteins. Use of this technique revealed interactions between Plk1 and ESCRT-III proteins CHMP6, CHMP4B, CHMP3 and CHMP2A. Furthermore, CDC14A was also shown to interact with CHMP4B and CHMP2A.

## Chapter 5 Discussion

### 5.1 Plo1p kinase and Clp1 (Cdc14) phosphatase interact with ESCRT proteins in fission yeast

#### 5.1.1 Analysis of the key findings

ESCRT genes were shown in this study to be required for cell division in fission yeast. Analysis of septation in fission yeast revealed an increase in septal defects in fission yeast strains with individual chromosomal deletions of ESCRT genes. Staining newly deposited cell wall with Calcofluor facilitated characterisation of a number of septation phenotypes in fission yeast (Figure 3.1A). These separation defects could be broadly separated into two mechanistic failures: that of septum assembly and separation following septation. In relation to wild-type cells, strains with chromosomal deletions in ESCRT genes *sst4*, *vps20*, *vps24* and *vps4* were shown to have a significant ( $p < 0.05$ ) increase in the *F phenotype*, characterised as delayed separation following septation (Figure 3.1B). The *F phenotype* may be related to a failure to hydrolyse the septum edging material, as mutants in genes required for hydrolysis have been described as having delayed separation, albeit described with the *E phenotype* as characterised in this study (Liu et al 1999; Jin et al. 2008).

Mitchison and Nurse (1985) calculated a delay of 0.12 of a cell cycle between septation and cell separation, so-called *hanging*. The delayed separation *F phenotype* was identified as defective cell separation on the basis of its higher frequency among fission yeast with deleted ESCRT genes. However, were this phenotype to be characterised further, it would be worthwhile to subject stained yeast suspensions to brief sonication before visualisation. This has been employed to disrupt hanging following septation (Mitchison & Nurse 1985). By this method, it may be possible to distinguish between typical hanging and delayed separation following septation.

Fission yeast double mutants were generated by crossing strains containing individual deletions of ESCRT genes with a temperature-sensitive mutant strain of *plo1*, *plo1-ts35*, and various mutants of *clp1*. Genetic interactions may be inferred by synthetic lethality among offspring (Papadopoulou et al. 2010),

however, all double mutants in this study were found to be viable. Subtle synthetic interactions were inferred by assaying growth rates among parent and offspring strains on rich and minimal solid media at various temperatures. In several instances, such as in the double mutant *plo1-ts35 vps20Δ*, growth rate defects were noted at 30°C, indicating that the restrictive temperature of *plo1-ts35*, 36°C, had been lowered. This principle has been shown previously between *plo1<sup>+</sup>* and *clp1<sup>+</sup>*, whereby *clp1.D257A* reduced the restrictive temperature of *plo1-ts35*, indicative of exacerbated cell stress as a result of genetic interactions (Papadopoulou et al. 2010). Defective growth rates were observed among double mutants with mutant *plo1* and *clp1* from every class of ESCRT gene (0, I, II and III), as well as *vps4* (Table 3.2). Thus, it has been shown that *plo1<sup>+</sup>* and *clp1<sup>+</sup>* interact genetically with ESCRT genes. Furthermore, an increased prevalence of septal defects was observed in double mutants of fission yeast strains with individual ESCRT gene deletions and *plo1-ts35*, *clp1Δ*, a deletion mutant of *mid1*, as well as two temperature-sensitive mutants of Aurora B kinase, *ark1-T8* and *ark1-T11* (Appendix 6.2).

Genetic interactions between *plo1<sup>+</sup>*, *clp1<sup>+</sup>* and ESCRT genes were further analysed by investigating vacuolar sorting in fission yeast; the cellular distributions of GFP-labelled receptor Ub-GFP-*SpCPS* and vacuolar stain FM 4-64 were analysed. Using this method, the ESCRT machinery was confirmed to be required for downregulation of ubiquitin-labelled receptors via the multivesicular body pathway, and the requirement of individual ESCRT genes for correct sorting was demonstrated (Figure 3.4; Iwaki et al. 2007).

The cellular distributions of Ub-GFP-*SpCPS* and FM 4-64 were then characterised in fission yeast with mutations in *plo1* and *clp1* to test the hypothesis that Plo1p and Clp1p are required for vacuolar sorting. Fission yeast strains with mutations in *plo1* and *clp1* exhibited defective sorting, but with distinct phenotypes to those observed in ESCRT deletion strains (Figure 3.5). Cells containing the temperature-sensitive *plo1* mutant, *plo1-ts35*, exhibited a uniform array of vacuoles at permissive temperature, with Ub-GFP-*SpCPS* precisely co-localised to the vacuolar periphery. In contrast, cells with a chromosomal deletion of the *clp1* gene, *clp1Δ*, exhibited a luminal pattern of Ub-GFP-*SpCPS* localisation. Cells with loss-of-function mutation *clp1.D257A* were similar to wild-type cells in their Ub-GFP-*SpCPS* and vacuolar distributions. Finally, cells with gain-of-function *clp1*

mutation *clp1.3A* were phenotypically intermediate between the distribution reported for wild-type cells (Iwaki et al. 2007) and the *plo1-ts35* distribution patterns reported here. Examining Ub-GFP-*SpCPS* and FM 4-64 localisation patterns in double mutants of ESCRT deletions with *clp1.D257A* and *clp1.3A* may provide further definition of the functions of these *clp1* mutants in fission yeast vacuolar sorting.

Similar defective sorting phenotypes to budding yeast strains with ESCRT deletions were identified in a deletion mutant of the endosomal ion exchanger *nhx1* (Kallay et al. 2011). However, these findings showed that Nhx1 functioned independently to the ESCRT proteins, despite the observation of synthetic phenotypes in double mutants of *nhx1Δ* and a number of ESCRT deletions.

The observations reported here indicate novel functions for *plo1*<sup>+</sup> and *clp1*<sup>+</sup> in vacuolar sorting in fission yeast. However, the phenotypes observed in strains with mutations in *plo1* and *clp1* were distinct to the punctate phenotype observed in strains with single deletions in ESCRT genes. There are two potential ways to explain this difference: firstly, that Plo1p and Clp1p regulate vacuolar sorting independently of the ESCRT machinery; or secondly, that Plo1p and Clp1p regulate vacuolar sorting through more than one ESCRT protein.

To investigate the dependency of ESCRT proteins on Plo1p and Clp1p in controlling vacuolar sorting, double mutants of *plo1-ts35* and *clp1Δ* with ESCRT deletions were examined. Ub-GFP-*SpCPS* and FM 4-64 distributions were characterised in fission yeast strains with double mutants of *plo1-ts35* and individual ESCRT deletions. Double mutant phenotypes were more similar to *plo1-ts35*, although the converse was noted for *plo1-ts35 vps4Δ* (Figure 3.6). Analysis of double mutants of *clp1Δ* and individual ESCRT deletions revealed phenotypes more similar to each respective ESCRT single deletion mutant (Figure 3.7). These epistasis experiments suggest that *plo1*<sup>+</sup> functions upstream of ESCRT genes in controlling vacuolar sorting and that *clp1*<sup>+</sup> functions downstream of ESCRT genes. These data are consistent with a model of regulation whereby Plo1p and Clp1p interact with ESCRT proteins, respectively, before and after ESCRT functions in vacuolar sorting. In particular, the similarity between the *plo1-ts35* and *clp1.3A* mutant strains may indicate that increased Clp1p activity conferred by this gain-of-function mutation reverses Plo1p

phosphorylation to maintain ESCRT proteins in a hypophosphorylated form, thus trapping Ub-GFP-*SpCPS* upon the peripheral membrane. The genetic dependency of ESCRT genes upon *plo1*<sup>+</sup> and *clp1*<sup>+</sup> may be further characterised by producing yeast strains with multiple deletions in ESCRT genes. Epistasis experiments of this type may allow identification of the specific genetic pathway involving these genes in vacuolar sorting.

Previous studies have demonstrated the translation of genetic interactions into protein interactions (Papadopoulou et al. 2010). In this study, the yeast two-hybrid assay was used to further analyse the genetic interactions observed between *plo1*<sup>+</sup>, *clp1*<sup>+</sup>, and ESCRT genes. Plo1p was shown to physically interact with Sst4p (ESCRT-0), Vps28p (ESCRT-I), Vps25p (ESCRT-II), Vps20p and Vps32p (both ESCRT-III) (Table 3.6).

Wild-type Plo1p did not exhibit interactions with Sst4p or Vps25p. Instead, interactions were observed between kinase-dead Plo1.K69R and Sst4p and Vps25p. These observations allude to the possible nature of the interactions between Plo1p and these ESCRT proteins. The yeast two-hybrid assay allows detection of *in vivo* protein-protein interactions, but is sometimes insensitive to transient interactions (Brückner et al. 2009). Therefore, interactions observed after mutating one of the binding partners indicates stability conferred by the mutation. Interactions have been shown in yeast two-hybrid using ‘substrate-trap’ phosphatase-dead mutants (Fukada et al. 2005). In the present study, as kinase function has been inactivated in Plo1.K69R, these interactions suggest that Plo1p binds to and phosphorylates Sst4p and Vps25p; these interactions may be characterised as being transient and to occur in a manner that requires phosphorylation prior to dissociation.

Clp1p was shown to interact with just Vps28p (ESCRT-I) (Figure 3.12). Yeast two-hybrid assays investigating interactions with Clp1p proved difficult due to the *in vivo* transcriptional activity of Clp1p (Papadopoulou et al. 2010), although this ultimately proved advantageous in the identification of a solitary interaction. The interaction between Clp1p and Vps28p was identified on the basis of inhibited auto-activation of the *gal4* promoter by truncation mutant Clp1aa.1-371 in the presence of Vps28p. However, this observation does not necessitate a negative interaction assay for the remaining ESCRT proteins with Clp1p.

Nevertheless, in light of this result with Vps28p, negative interactions were scored for the remaining ESCRT proteins. It may be possible to clarify ESCRT protein interactions with Clp1p by utilising different transcriptional readouts in the yeast two-hybrid assay, such as auxotrophic markers (Brückner et al. 2009). Alternatively, assaying  $\beta$ -galactosidase activity in liquid cultures would allow calculation of a baseline value for transcription. It may then be possible to quantitatively identify increased transcription when assaying Clp1p yeast two-hybrid with ESCRT proteins. Quantifying  $\beta$ -galactosidase activity was attempted in this study (data not shown), and although published values for interactions between Plo1p, Clp1p and Mbx1p were replicated (Papadopoulou et al. 2008), subsequent assay of ESCRT proteins with Plo1p resulted in irreproducible values. The  $\beta$ -galactosidase assay was eventually discarded to focus on assaying interactions in human cells.

### **5.1.2 A model for ESCRT regulation by Plo1p and Clp1p**

Plo1p physically interacts with proteins in ESCRT classes 0, I, II and III. Clp1p physically interacts with Vps28p, a member of ESCRT-I. Current views of cytokinesis in human cells describe roles for ESCRT-I and -III in abscission (Elia et al. 2012). However, ESCRT classes 0-III have also been implicated in MVB formation (Wollert & Hurley 2010). Therefore, if ESCRT subunit function is conserved between fission yeast and humans, these findings suggest that Plo1p regulates the ESCRT proteins in vacuolar sorting and cytokinesis (Figure 5.1). Similarly, the observation of interactions between Clp1p and an ESCRT-I subunit, combined with the epistasis data on vacuolar sorting, suggest that Clp1p is regulating ESCRT proteins in cytokinesis, and possibly in vacuolar sorting (Figure 5.1).

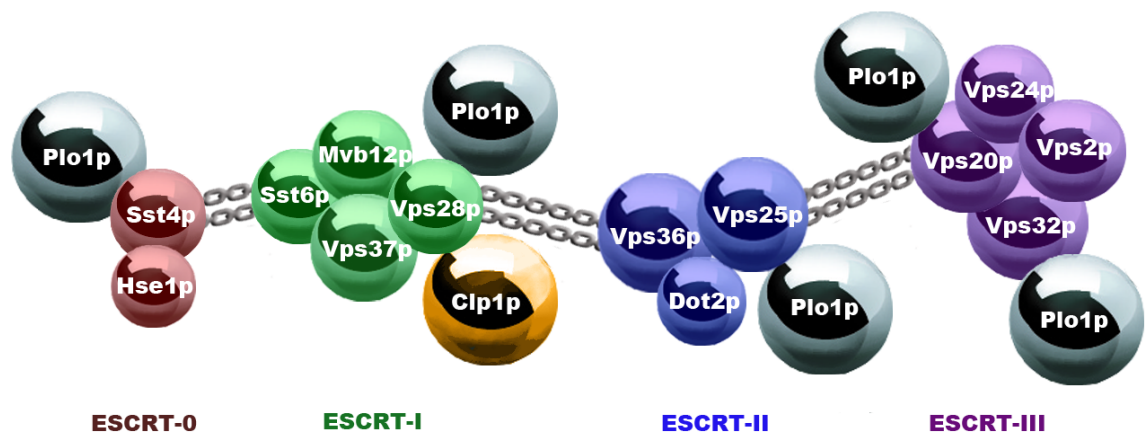


**Figure 5.1: Plo1p and Clp1p interact with members of the ESCRT machinery in fission yeast.**

This model illustrates proteins of each fission yeast ESCRT subunit and the linkers between each subunit. Plo1p and Clp1p are shown interacting with members of the ESCRT machinery.

The implication of this model is that Plo1p and Clp1p regulate ESCRT proteins via their phosphorylation state. In particular, the *vps4Δ* vacuolar sorting phenotype was quite dissimilar to the primary ESCRT genes. Furthermore, although synthetic growth phenotypes were noted, epistasis experiments provided little information about *vps4<sup>+</sup>* interactions with *plo1<sup>+</sup>* and *clp1<sup>+</sup>*, and yeast two-hybrid indicated that these proteins do not interact. Taken together, these data suggest a model for ESCRT function in vacuolar sorting whereby Plo1p phosphorylates ESCRT proteins to elicit some conformational change, perhaps to allow association with other ESCRT components, cargo, lipids, or other proteins; Vps4p then redistributes ESCRT-III, then Clp1p dephosphorylates ESCRT proteins to reverse Plo1p-mediated conformational changes.

## 5.2 Plk1 kinase and CDC14A phosphatase interact with ESCRT proteins in humans

### 5.2.1 Analysis of the key findings

Following the observation of genetic and physical interactions between Plo1p, Clp1p and ESCRT proteins, human homologues Plk1 and CDC14A were investigated using immunoprecipitation and co-immunoprecipitation methods. HeLa cells were initially used due to their ease of manipulation and synchronisation. Furthermore, a known binding partner of Plk1, FOXM1, has been shown to co-immunoprecipitate with Plk1 from asynchronous and mitotic HeLa cell lysates (Fu et al. 2008) and could therefore be used as a positive control. In this study, FOXM1 was successfully co-immunoprecipitated with Plk1 from metaphase-arrested HeLa cells (Figure 4.2B); however, ESCRT proteins were not shown to co-immunoprecipitate. To overcome the possibility that this negative result was due to low abundance of ESCRT proteins preventing detection, ESCRT proteins were over-expressed to seek interactions with Plk1. As HeLa cells did not efficiently accept transfecting DNA to over-express proteins, HEK293 cells were used instead, as they have been used previously to observe interactions between endogenous Plk1 and over-expressed binding partners (Fu et al. 2008).

Over-expressed ESCRT-III protein CHMP6 was co-immunoprecipitated with Plk1 from HEK293 cells (Figure 4.4). FIP3-GFP was used to show that CHMP6-GFP was co-immunoprecipitated due to interactions between Plk1 and CHMP6, rather than via GFP. However, it should be noted that, formally, GFP may bind to anti-Plk1 antibody in a manner blocked by fusion to FIP3. Therefore, a more appropriate control would be to over-express cells with un-fused GFP, or to incubate lysates with recombinant GFP. If these lysates then immunoprecipitated Plk1 with anti-Plk1 antibody, but not GFP, this would indicate that CHMP6-GFP does not co-immunoprecipitate due to interactions between GFP and anti-Plk1 antibody. A further control to include in this immunoprecipitation assay would be to incubate anti-Plk1 antibody with the purified epitope of the Plk1 motif that binds to the antibody to block the antibody sites. If CHMP6 does not co-immunoprecipitate in these conditions, this would indicate that CHMP6 co-immunoprecipitates due to interactions with Plk1, rather than anti-Plk1 antibody. The combination of these controls would more

robustly demonstrate that ESCRT proteins co-immunoprecipitate from human cell lysates due to interactions with Plk1. However, on the basis of the subsequent results obtained, it would seem unlikely that non-specific interactions with anti-Plk1 antibody underlie the interactions observed.

ESCRT proteins CHMP6, CHMP4B, CHMP3 and CHMP2A were shown to co-immunoprecipitate with Plk1 (Figure 4.5). Immunoblotting Plk1 from HEK293 cell lysates was often not robust. However, the sequential immunoprecipitation of Plk1 from these lysates demonstrated, firstly, that Plk1 immunoprecipitated from lysates and, secondly, that the ESCRT proteins co-immunoprecipitated due to direct interactions with Plk1 (Figure 4.6). This experiment was analogous to an RNAi knockdown assay of Plk1, but rather than using RNAi, which can be costly, complex to achieve, and may affect other cell processes, the levels of Plk1 within lysates were gradually reduced. Repeated immunoprecipitation of human cell lysates with anti-Plk1 antibody resulted in the loss of co-immunoprecipitated ESCRT proteins. However, the supernatants resulting from the final immunoprecipitation were qualitatively shown to still express ESCRT proteins to a degree almost indistinguishable to the first lysate before immunoprecipitation. These data are strong indicators that the ESCRT proteins interact with Plk1, rather than with anti-Plk1 antibody - neither directly, nor by their respective tags. However, as a further consideration, it is possible that ESCRT proteins are co-immunoprecipitated due to interactions with an unknown protein, which binds to either Plk1 or anti-Plk1 antibody. Nevertheless, the data gathered in yeast imply the veracity of the interactions observed in human cells.

The consensus motif for Plk1 substrate phosphorylation was determined as [(D/E)-X<sub>aa</sub>-(S/T)-Φ-X<sub>aa</sub>-(D/E), Φ=hydrophobic] (Nakajima et al. 2003), while the substrate binding motif for the polo box domain has been described as [S-(pT/pS)-(P/X<sub>aa</sub>)] (Elia et al. 2003). The kinase motif is present within many ESCRT proteins, several of which have co-immunoprecipitated with Plk1 in this study: TSG101 and VPS28 (ESCRT-I), EAP45 and EAP20 (ESCRT-II), CHMP6 and CHMP4B (ESCRT-III), as well as in VPS4B. Variations of the Plk1 substrate-binding motif are present within almost all ESCRT proteins. Interestingly, although both motifs are found within CEP55, a phospho-substrate of Plk1, CEP55 is phosphorylated on Ser436 within NESLVE (Bastos & Barr 2010), which lacks full fidelity with the target motif (Nakajima et al. 2003). This indicates that Plk1

exerts flexibility in substrate phosphorylation with respect to a non-canonical substrate motif and may phosphorylate certain substrates in a distributive mode (Park et al. 2010).

All of the ESCRT proteins assayed co-immunoprecipitated with Plk1. One explanation for this observation is that ESCRT proteins are pulled down in a complex; therefore, interaction with one ESCRT protein allows detection of the rest. Attempts were made to address this by increasing the detergent concentration within the buffer conditions to disrupt the complex. Triton X-100 was increased in concentration tenfold, yet ESCRT proteins continued to co-immunoprecipitate with Plk1 (Figure 4.7). However, when compared to previous assays (Figure 4.5), the co-immunoprecipitation of CHMP3 in the presence of higher Triton X-100 appeared to be reduced. Subsequent attempts to dissociate the ESCRT proteins from their complex should be analysed by SDS-PAGE alongside basal immunoprecipitation conditions to detect subtle changes; a loading control may be required for this experiment. It should be noted that ESCRT complex dissociation was not shown. Future experiments to dissociate ESCRT proteins may be designed around changes in salt and pH conditions (Eisele et al. 2011). An important consideration in attempting to dissociate the ESCRT complex is that the interactions between the ESCRT proteins and Plk1 must remain extant. Whatever the means employed, a balance would need to be reached for this to be achieved. Given the yeast two-hybrid data suggesting transient interactions between Plo1p and Sst4p and Vps25p, there may be a high likelihood of disrupting kinase-substrate interactions.

However, it may not be necessary to dissociate ESCRT proteins from their complex. Although all assayed ESCRT proteins were co-immunoprecipitated with Plk1, not all co-immunoprecipitated with CDC14A. VPS28 and CHMP6 did not appear to interact with CDC14A (Figure 4.12); were the ESCRT proteins still in complex, it would be reasonable to expect that these proteins would be detected on immunoprecipitation of CDC14A. Assaying immunoprecipitated Plk1 for co-immunoprecipitated over-expressed VPS28 may reveal a similar result to that observed for CDC14A. Finally, although this was not attempted, immunoblotting ESCRT immunoprecipitations for different ESCRT proteins may confirm whether ESCRT proteins immunoprecipitate individually or in complex.

Yeast two-hybrid data revealed that certain interactions between Plo1p and ESCRT proteins were only observed in assays with kinase-dead Plo1.K69R. In this study, there were no ESCRT proteins that over-expressed well in HEK293 cells that were not subsequently co-immunoprecipitated with Plk1. Therefore, ESCRT proteins were expected to co-immunoprecipitate with kinase-dead Plk1.K82R. However, it was observed that anti-GFP immunoprecipitation of Plk1-YFP and Plk1.K82R-YFP from lysates over-expressed with ESCRT proteins produced effective immunoprecipitation of tagged species of Plk1, yet no co-immunoprecipitation of ESCRT proteins (Figure 4.9). One interpretation of these results is that Plk1-YFP and ESCRT proteins were co-expressed within a population, but not within individual cells, which may not result in interactions. Future assays should include confirmation of co-expression, or otherwise, within individual cells; this could be achieved by fluorescence microscopy of fixed cells following co-transfection performed in parallel with co-transfection for lysate preparation. Time prevented further exploration of this hypothesis.

Following observation of interactions between Plk1 and ESCRT proteins in HEK293 cells, CDC14A and ESCRT proteins were over-expressed in HEK293 cells to detect interactions using immunoprecipitation and co-immunoprecipitation methods. Over-expressed ESCRT-III proteins CHMP4B-YFP and CHMP2A-GFP were shown to co-immunoprecipitate with CDC14A-myc from HEK293 cell lysates (Figure 4.12); these interactions remained when assayed with phosphatase-dead CDC14A.C278S (Figure 4.13). Interactions were also shown by co-immunoprecipitating CDC14A with CHMP4B and CHMP2A (Figure 4.14). To more robustly demonstrate these interactions, anti-myc immunoprecipitations should be performed in cell lysates over-expressing ESCRT proteins in the absence of CDC14A-myc. Furthermore, a larger volume of material analysed by SDS-PAGE may clarify the CDC14A co-immunoprecipitation. The CHMP6 reverse immunoprecipitation was not performed as Protein A sepharose beads were mistakenly omitted from the incubated cell lysate-antibody mixture. To complete these assays, this CHMP6 reverse immunoprecipitation should be performed.

CHMP6 and, perhaps surprisingly, VPS28, did not co-immunoprecipitate with CDC14A (Figure 4.12 and 4.13). In the yeast two-hybrid screen of fission yeast protein-protein interactions, fission yeast Vps28p was the only protein regarded

to interact with Clp1p (CDC14) (Figure 3.12). This observation may necessitate a reinterpretation of the yeast two-hybrid data in light of the immunoprecipitation data, or it may simply reflect variances in the conservation of interactions between these two species.

### 5.2.2 Refining the model

Plk1 interacts with ESCRT-III proteins CHMP6, CHMP4B, CHMP3 and CHMP2A. Furthermore, CDC14A interacts with ESCRT-III proteins CHMP4B and CHMP2A. These observations are consistent with ESCRT functions in cytokinesis (Guizetti et al. 2011). This model suggests, therefore, that Plk1 and CDC14A interact with ESCRT-III proteins in cytokinesis to control their phosphorylation state (Figure 5.2).

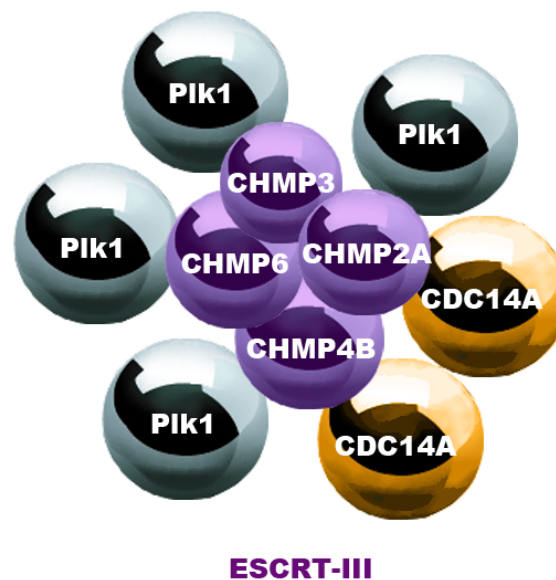


**Figure 5.2: Plk1 and CDC14A interact with members of the ESCRT machinery in human cells.**

This model illustrates proteins of ESCRT-III. Plk1 and CDC14A are shown interacting with members of ESCRT-III in human cells.

The genetic and physical interactions revealed in this study are summarised in Table 5.1.

Species	ESCRT-0		ESCRT-I		ESCRT-II		ESCRT-III													
	Sst4p	HRS	Sst6p	TSG101	Vps28p	VPS28	Vps36p	EAP45	Vps25p	EAP20	Vps20p	CHMP6	Vps32p	CHMP4B	Vps24p	CHMP3	Vps2p	CHMP2A	Vps4p	VPS4
Polo kinase	Genetic interaction with <i>plo1-ts35</i>	✓	✓	✓	✓	✓	X	✓	✓	✓	✓	✓	ND	ND	ND	✓	✓	✓	✓	✓
	Y2H interaction with Plo1p	✓	X	✓	✓	✓	X	✓	✓	✓	✓	✓	✓	✓	✓	ND	X	X	X	X
	CoIP with PIK1	ND	ND	ND	ND	ND	ND	ND	ND	ND	✓	✓	✓	✓	✓	✓	✓	✓	ND	ND
Cdc14 phosphatase	Genetic interaction with <i>cip1</i>	✓	ND	✓	✓	✓	✓	✓	X	X	✓	✓	ND	ND	ND	ND	✓	✓	✓	✓
	Y2H interaction with Cip1p	X	X	X	✓	✓	X	X	X	X	X	X	ND	ND	ND	ND	X	X	X	X
	CoIP with CDC14A	ND	ND	ND	X	✓	ND	ND	ND	ND	X	✓	✓	✓	✓	ND	ND	✓	✓	ND

**Table 5.1: Genetic and physical interactions were observed between ESCRT proteins, polo kinase and Cdc14 phosphatase in fission yeast and humans.**  
The table summarises the genetic and physical interactions observed in this study. Y2H, yeast two-hybrid; CoIP, co-immunoprecipitation; ND, not determined.

### 5.3 Future work

The observations of genetic interactions between ESCRT genes and the Aurora kinase *ark1*<sup>+</sup> and the anillin *mid1*<sup>+</sup> require further study. In both cases, yeast two-hybrid could be used to examine if the encoded proteins interact and immunoprecipitation experiments used to detect physical interactions in human cells. Furthermore, vacuolar sorting using Ub-GFP-*SpCPS* could be investigated in *ark1* and *mid1* mutants. Experiments are ongoing with *ark1*<sup>+</sup> using yeast-two hybrid. Preliminary data suggests an interaction between VPS4B and anillin in human cells (GW Gould pers. comm.), and *vps4* and *mid1* deletion mutants show synthetic lethality in fission yeast (CJ McInerny pers. comm.). Temperature-sensitive mutant, *ark1-T8*, also appears to affect vacuolar sorting in fission yeast (CJ McInerny pers. comm.).

Mid1p has a prominent role in fission yeast controlling the deposition of the contractile ring that determines the site of septation and is known to interact with both Plo1p and Clp1p (Almonacid et al. 2011; Clifford et al. 2008), so it possible that it also plays a role in controlling ESCRT function during cytokinesis in fission yeast. Similarly, Ark1p controls late cell cycle events (Petersen & Hagan 2003), and thus the genetic experiments presented here suggest that it too may play a role in controlling ESCRT function.

The yeast two-hybrid system was used to assay interactions between fission yeast proteins. This assay could also be used to study interactions between human homologues. Wild-type and catalytically inactive forms of *PLK1* and *CDC14A* genes were amplified from plasmid vectors and cloned into the intermediate StrataClone vector used in the cloning throughout this study. It was hoped that these would be cloned into appropriate bait and prey vectors for inclusion in a yeast two-hybrid screen against human ESCRT proteins. Although this was not completed within the timeframe of this project, this assay should complement the observations made in this study.

A yeast two-hybrid screen for interactions between human proteins would be advantageous for several reasons. Firstly, the assay would deliver rapid results in comparison to immunoprecipitation assays. Secondly, as proved elusive with Plk1, a yeast two-hybrid screen would be particularly useful for identifying

differences in interactions between ESCRT proteins and the catalytically inactive forms of Plk1 and CDC14A. Indeed, stable interactions have been demonstrated in yeast two-hybrid screens of CDC14A.C278S, in which screens of wild-type CDC14A were negative (Lanzetti et al. 2007); and this was similarly observed using kinase-dead fission yeast Plo1.K69R (*Section 3.2.5*). Finally, a yeast two-hybrid screen of human ESCRT proteins would resolve the question of ESCRT proteins remaining in complex; this is because amplifying ESCRT genes using specific primers would eliminate the possibility of other proteins remaining in complex with the amplified ESCRT.

This study focused on interactions between Plk1, CDC14A and ESCRT proteins, with a brief attempt to investigate functional relevance. Plk1 kinase inhibitor BI 2536 was added to mitotic HeLa cells. Lysates were then immunoblotted for CHMP6 to seek a mobility shift on SDS-PAGE (Figure 4.10). This experiment could be repeated with several modifications. Firstly, future use of BI 2536 should include detection of a marker for inhibition. For instance, immunoblotting BubR1 should reveal a mobility shift on treating HeLa cells with BI 2536 (Lénárt et al. 2007). Secondly, untreated and Plk1-inhibited lysates should be run in parallel. Thirdly, a loading control, such as GAPDH, should be used as a control for conditions that may result in aberrant protein positions during SDS-PAGE.

As a further consideration, the mobility shift may be exacerbated by addition of reagent Phos-Tag™ to the SDS gel. Phos-Tag™ selectively binds phosphorylated proteins (Kinoshita et al. 2004) and can be used to retard them during SDS-PAGE (Kinoshita et al. 2006). Use of Phos-Tag™ while subjecting untreated and Plk1 kinase-inhibited cell lysates to SDS-PAGE and immunoblotting for ESCRT proteins may elucidate whether Plk1 activity results in phosphorylation of ESCRT proteins. Combined with the results of immunoprecipitation and co-immunoprecipitations, Phos-Tag™ SDS-PAGE could provide compelling evidence that Plk1 phosphorylates ESCRT proteins. Equivalent experiments could also be performed using the competitive inhibitor of CDC14A, sodium tungstate (Lanzetti et al. 2007). However, performing *in vitro* kinase assays could provide definitive evidence of ESCRT phosphorylation by Plk1.

*In vitro* kinase assays have been performed by incubating [ $\gamma$ -<sup>32</sup>P]ATP with substrate protein Tau and various kinases (Kinoshita-Kikuta et al. 2007). Silver-

staining subsequent Phos-Tag™ SDS gels produced multiple phospho-species and autoradiography showed that kinase reactions proceeded correctly. Similar assays with recombinant Plk1 could show that Plk1 phosphorylates ESCRT proteins. Furthermore, subsequent incubation of kinase reactions with CDC14A could show, generally, that CDC14A dephosphorylates ESCRT proteins, and specifically, that CDC14A dephosphorylates ESCRT proteins following phosphorylation by Plk1.

*In vitro* kinase assays performed with Plk1 have confirmed that Plk1 binding to FOXM1 is required for substrate phosphorylation (Fu et al. 2008). Furthermore, *in vitro* kinase assays could be performed with ESCRT proteins. ESCRT-III protein CHMP4C was shown to be phosphorylated by Aurora B kinase (Carlton et al. 2012); phosphorylation was revealed to have an inhibitory role, and further insights into ESCRT function were therefore revealed (Carlton et al. 2012). These approaches would have the advantage of allowing estimation of the stoichiometry of phosphorylation, thus revealing the effectiveness of a particular ESCRT subunit as a substrate for Plk1.

This research by the Martin-Serrano group raises potential future dimensions to this study (Carlton et al. 2012). Further to ESCRT binding and mapping studies, the functional impact of Plk1 and CDC14A activity upon ESCRT proteins requires elucidation. Is binding of Plk1 and CDC14A to ESCRT proteins required for mediating phosphorylation status? Which ESCRT residues are phosphorylated? Examining ESCRT sequences for Plk1 binding motifs provides clues (*Section 5.2.1*); mutating these residues may abolish binding and phosphorylation by Plk1. Do the ESCRT proteins require modification or phosphorylation prior to Plk1 binding? Do alterations in phosphorylation state elicit ESCRT conformational changes that regulate interactions with other ESCRT subunits, proteins or even lipids? Finally and most crucially, determining the functional significance of controlling ESCRT phosphorylation status may provide insights into future methods of manipulating abscission in instances of uncontrolled cell division.

## 5.4 Conclusion

ESCRT proteins are required for cell division in humans (Morita et al. 2007). This study has shown that ESCRT proteins are required for septation and cell separation in fission yeast. Genetic interactions were observed between ESCRT genes and *plo1*<sup>+</sup>, *clp1*<sup>+</sup>, *mid1*<sup>+</sup> and *ark1*<sup>+</sup>. Furthermore, novel roles were demonstrated for Plo1p and Clp1p in vacuolar sorting in fission yeast, and genetic analysis facilitated characterisation of a genetic pathway in vacuolar sorting for *plo1*<sup>+</sup>, ESCRT genes and *clp1*<sup>+</sup>. Yeast two-hybrid analysis of fission yeast proteins revealed physical interactions between Plo1p and ESCRT proteins from classes 0, I, II and III. Physical interactions were also observed between Clp1p and ESCRT-I. Immunoprecipitation and co-immunoprecipitation analyses in human cell lysates revealed physical interactions between Plk1, CDC14A and ESCRT-III proteins.

These findings provide evidence for ESCRT regulation by polo kinase and Cdc14 phosphatase during cytokinesis in fission yeast and humans. It is proposed that mediating ESCRT phosphorylation status may elicit conformational changes, such as ESCRT-III nucleation, that drive abscission (Elia et al. 2011). Consistent with this model, Plk1 has recently been shown to reappear at the midbody following initial downregulation (Hu et al. 2012). Therefore, future characterisation of these interactions and their functional significances may provide useful insights towards manipulating ESCRT proteins in controlling cell division in disease processes.

## Chapter 6 Appendices

### 6.1 Strains list

#### 6.1.1 *Schizosaccharomyces pombe* strains

Lab no.	Genotype	Source
GG 1146	<i>h<sup>+</sup> clp1 ::ura4<sup>+</sup> ura4-D18 leu1-32 ade6-210</i>	(Trautmann et al. 2001)
GG 1167	<i>h<sup>+</sup> plo1-ts35 ura4-D18 leu1-32</i>	(Anderson et al. 2002)
GG 1171	<i>h<sup>-</sup> plo1-ts35 leu1-32</i>	(Anderson et al. 2002)
GG 1191	<i>h<sup>-</sup> clp1.D257A-13myc:kanR ura4-D18 leu1-32 ade6-210</i>	(Wolfe et al. 2006)
GG 1193	<i>h<sup>-</sup> clp1.3A-13myc:kanR ura4-D18 leu1-32 ade6-216</i>	(Wolfe et al. 2006)
GG 1202	<i>h<sup>+</sup> clp1.D257A-13myc:kanR cdc25-22 leu1-32 ura4-D18 ade6-210</i>	(Wolfe et al. 2006)
GG 1204	<i>h<sup>+</sup> clp1.3A-13myc:kanR cdc25-22 leu1-32 ura4-D18 ade6-216</i>	(Wolfe et al. 2006)
GG 1279	975 <i>h<sup>+</sup></i>	Laboratory stock
GG 1306	<i>h<sup>-</sup> clp1::kanR leu1-32 ura4-D18</i>	(Trautmann et al. 2001)
GG 1307	<i>h<sup>+</sup> clp1 ::kanR leu1-32 ura4-D18</i>	(Trautmann et al. 2001)
GG 1455	<i>h<sup>-</sup> leu1-32</i>	Laboratory stock
GG 1554	<i>h<sup>+</sup> dmf1::kanMX4 ura4-D18 leu1-32 ade6-216</i>	(Celton-Morizur et al. 2004)
GG 1615	<i>h90 sst6::ura4<sup>+</sup> leu1-32 ura4-D18 ade6-M210</i>	(Iwaki et al. 2007)
GG 1616	<i>h90 vps28::ura4<sup>+</sup> leu1-32 ura4-D18 ade6-M210</i>	(Iwaki et al. 2007)
GG 1617	<i>h<sup>-</sup> vps36::ura4<sup>+</sup> leu1-32 ura4-D18</i>	(Iwaki et al. 2007)
GG 1618	<i>h<sup>-</sup> vps25::ura4<sup>+</sup> leu1-32 ura4-D18</i>	(Iwaki et al. 2007)
GG 1619	<i>h90 vps20::ura4<sup>+</sup> leu1-32 ura4-D18 ade6-M210</i>	(Iwaki et al. 2007)
GG 1620	<i>h<sup>-</sup> vps24::ura4<sup>+</sup> leu1-32 ura4-D18 ade6-M210</i>	(Iwaki et al. 2007)

GG 1622	<i>h<sup>-</sup> vps4::ura4<sup>+</sup> leu1-32 ura4-D18</i>	(Iwaki et al. 2007)
GG 1623	<i>h<sup>-</sup> sst4::ura4<sup>+</sup> leu1-32 ura4-D18</i>	(Iwaki et al. 2007)
GG 1637	<i>h90 vps28::ura4<sup>+</sup> clp1 ::kanR leu1-32 ura4-D18</i>	This study
GG 1646	<i>h<sup>+</sup> vps2::LEU2 clp1 ::kanR leu1-32 ura4-C190T / ura4-D18</i>	This study
GG 1649	<i>h90 vps20::ura4<sup>+</sup> clp1 ::kanR leu1-32 ura4-D18</i>	This study
GG 1654	<i>h<sup>+</sup> vps36::ura4<sup>+</sup> clp1 ::kanR leu1-32 ura4-D18</i>	This study
GG 1657	<i>h<sup>-</sup> vps25::ura4<sup>+</sup> clp1 ::kanR leu1-32 ura4-D18</i>	This study
GG 1660	<i>h<sup>+</sup> sst4::ura4<sup>+</sup> clp1 ::kanR leu1-32 ura4-D18</i>	This study
GG 1663	<i>h<sup>+</sup> vps4::ura4<sup>+</sup> clp1 ::kanR leu1-32 ura4-D18</i>	This study
GG 1666	<i>h<sup>+</sup> sst4::ura4<sup>+</sup> plo1-ts35 leu1-32 ura4-D18</i>	This study
GG 1676	<i>h<sup>-</sup> vps36::ura4<sup>+</sup> plo1-ts35 leu1-32 ura4-D18</i>	This study
GG 1679	<i>h<sup>+</sup> vps25::ura4<sup>+</sup> plo1-ts35 leu1-32 ura4-D18</i>	This study
GG 1682	<i>h90 vps28::ura4<sup>+</sup> plo1-ts35 leu1-32 ura4-D18</i>	This study
GG 1688	<i>h90 sst6::ura4<sup>+</sup> plo1-ts35 leu1-32 ura4-D18 ade6-M210</i>	This study
GG 1691	<i>h90 vps20::ura4<sup>+</sup> plo1-ts35 leu1-32 ura4-D18 ade6-M210</i>	This study
GG 1694	<i>h<sup>+</sup> vps2::LEU2 plo1-ts35 leu1-32 ura4-C190T</i>	This study
GG 1705	<i>h<sup>-</sup> vps4::ura4<sup>+</sup> clp1.D257A-13myc:kanR cdc25-22 leu1-32 ura4-D18 ade6-210</i>	This study
GG 1706	<i>h<sup>-</sup> sst4::ura4<sup>+</sup> clp1.D257A-13myc:kanR leu1-32 ura4-D18 ade6-210</i>	This study
GG 1714	<i>h<sup>+</sup> sst6::ura4<sup>+</sup> cdc25-22 leu1-32 ura4-D18 ade6-M210</i>	This study
GG 1717	<i>h90 vps28::ura4<sup>+</sup> clp1.D257A-13myc:kanR leu1-32 ura4-D18 ade6-M210</i>	This study
GG 1725	<i>h<sup>-</sup> vps4::ura4<sup>+</sup> plo1-ts35 leu1-32 ura4-D18</i>	This study
GG 1760	<i>h<sup>+</sup> vps36::ura4<sup>+</sup> clp1.D257A-13myc:kanR leu1-32 ura4-D18 ade6-210</i>	This study
GG 1765	<i>h<sup>-</sup> vps25::ura4<sup>+</sup> clp1.D257A-13myc:kanR leu1-32 ura4-D18 ade6-210</i>	This study
GG 1785	<i>h90 vps20::ura4<sup>+</sup> clp1.D257A-13myc:kanR leu1-32 ura4-D18 ade6-M210</i>	This study
GG 1791	<i>h<sup>-</sup> vps2::LEU2 clp1.D257A-13myc:kanR leu1-32 ura4-D18/ura4-C190T</i>	This study

GG 1805	<i>h? vps28::ura4<sup>+</sup> clp1.3A-13myc:kanR leu1-32 ura4-D18 ade6-M21X</i>	This study
GG 1809	<i>h? vps36::ura4<sup>+</sup> clp1.3A-13myc:kanR leu1-32 ura4-D18</i>	This study
GG 1826	<i>h? vps25::ura4<sup>+</sup> clp1.3A-13myc:kanR leu1-32 ura4-D18</i>	This study
GG 1832	<i>h? vps4::ura4<sup>+</sup> clp1.D257A-13myc:kanR leu1-32 ura4-D18 ade6-210</i>	This study
GG 1836	<i>h? vps4::ura4<sup>+</sup> clp1.3A-13myc:kanR leu1-32 ura4-D18 ade6-216</i>	This study
GG 1842	<i>h? sst4::ura4<sup>+</sup> clp1.3A-13myc:kanR leu1-32 ura4-D18 ade6-216</i>	This study
GG 1844	<i>h? vps20::ura4<sup>+</sup> clp1.3A-13myc:kanR leu1-32 ura4-D18 ade6-M21X</i>	This study
GG 1850	<i>h? vps2::LEU2 clp1.3A-13myc:kanR leu1-32 ura4-D18/ura4-C190T ade6-216</i>	This study
GG 2127	<i>pREP41:Ub-GFP-SpCPS h<sup>-</sup> leu1-32</i>	This study
GG 2132	<i>pREP41:Ub-GFP-SpCPS h<sup>+</sup> clp1 ::ura4<sup>+</sup> ura4-D18 leu1-32 ade6-210</i>	This study
GG 2139	<i>pREP41:Ub-GFP-SpCPS h<sup>+</sup> sst6::ura4<sup>+</sup> ura4-D18 leu1-32 ade6-210</i>	This study
GG 2142	<i>pREP41:Ub-GFP-SpCPS h<sup>+</sup> vps20::ura4<sup>+</sup> ura4-D18 leu1-32 ade6-210</i>	This study
GG 2145	<i>pREP41:Ub-GFP-SpCPS plo1-ts35 leu1-32</i>	This study
GG 2184	<i>pREP41:Ub-GFP-SpCPS h<sup>-</sup> sst4::ura4<sup>+</sup> leu1-32 ura4-D18</i>	This study
GG 2187	<i>pREP41:Ub-GFP-SpCPS h90 vps28::ura4<sup>+</sup> leu1-32 ura4-D18 ade6-M210</i>	This study
GG 2190	<i>pREP41:Ub-GFP-SpCPS h<sup>-</sup> vps36::ura4<sup>+</sup> leu1-32 ura4-D18</i>	This study
GG 2193	<i>pREP41:Ub-GFP-SpCPS h<sup>-</sup> vps4::ura4<sup>+</sup> leu1-32 ura4-D18</i>	This study
GG 2196	<i>pREP41:Ub-GFP-SpCPS h<sup>+</sup> clp1 ::ura4<sup>+</sup> ura4-D18 leu1-32 ade6-210</i>	This study
GG 2206	<i>pREP41:Ub-GFP-SpCPS h<sup>-</sup> plo1-ts35 leu1-32</i>	This study
GG 2216	<i>pREP41:Ub-GFP-SpCPS h<sup>+</sup> sst4::ura4<sup>+</sup> clp1 ::kanR leu1-32 ura4-D18</i>	This study
GG 2219	<i>pREP41:Ub-GFP-SpCPS h90 vps28::ura4<sup>+</sup> clp1 ::kanR leu1-32 ura4-D18</i>	This study
GG 2222	<i>pREP41:Ub-GFP-SpCPS h<sup>+</sup> vps36::ura4<sup>+</sup> clp1 ::kanR leu1-32 ura4-D18</i>	This study
GG 2225	<i>pREP41:Ub-GFP-SpCPS h90 vps20::ura4<sup>+</sup> clp1 ::kanR leu1-32 ura4-D18</i>	This study
GG 2228	<i>pREP41:Ub-GFP-SpCPS h<sup>+</sup> vps4::ura4<sup>+</sup> clp1 ::kanR leu1-32 ura4-D18</i>	This study
GG 2239	<i>pREP41:Ub-GFP-SpCPS h<sup>+</sup> sst4::ura4<sup>+</sup> plo1-ts35 leu1-32 ura4-D18</i>	This study

GG 2242	<i>pREP41:Ub-GFP-SpCPS h90 vps28::ura4<sup>+</sup> plo1-ts35 leu1-32 ura4-D18</i>	This study
GG 2245	<i>pREP41:Ub-GFP-SpCPS h90 vps20::ura4<sup>+</sup> plo1-ts35 leu1-32 ura4-D18 ade6-M210</i>	This study
GG 2248	<i>pREP41:Ub-GFP-SpCPS h<sup>-</sup> vps4::ura4<sup>+</sup> plo1-ts35 leu1-32 ura4-D18</i>	This study
GG 2251	<i>pREP41:Ub-GFP-SpCPS h<sup>-</sup> vps36::ura4<sup>+</sup> plo1-ts35 leu1-32 ura4-D18</i>	This study
GG 2275	<i>pREP41:Ub-GFP-SpCPS h<sup>-</sup> clp1.3A-13myc:kanR ura4-D18 leu1-32 ade6-216</i>	This study
GG 2296	<i>pREP41:Ub-GFP-SpCPS h<sup>-</sup> clp1.3A-13myc:kanR ura4-D18 leu1-32 ade6-216</i>	This study
GG 2299	<i>pREP41:Ub-GFP-SpCPS h<sup>+</sup> clp1 ::ura4<sup>+</sup> ura4-D18 leu1-32 ade6-210</i>	This study
GG 2302	<i>pREP41:Ub-GFP-SpCPS h<sup>-</sup> clp1.D257A-13myc:kanR ura4-D18 leu1-32 ade6-210</i>	This study
GG 2412	<i>h<sup>+</sup> ark1-T11&lt;&lt;kanR leu1-32</i>	(Koch et al. 2011)
GG 2423	<i>h<sup>-</sup> ark1-T11&lt;&lt;kanR vps2::LEU2 leu1-32</i>	Graduate student, Brinta Roy
GG 2426	<i>h<sup>+</sup> ark1-T8-GFP-flag-His&lt;&lt;kanR ura4-D18 leu1-32 ade6-210</i>	Laboratory stock
GG 2451	<i>h<sup>+</sup> ark1-T11&lt;&lt;kanR ura4-C190T leu1-32</i>	Graduate student, Brinta Roy
GG 2452	<i>h<sup>-</sup> ark1-T11&lt;&lt;kanR ura4-C190T leu1-32</i>	Graduate student, Brinta Roy
GG 2453	<i>h<sup>+</sup> sst6::ura4<sup>+</sup> ark1-T8-GFP-flag-His&lt;&lt;kanR ura4-D18 leu1-32 ade6-210</i>	Graduate student, Brinta Roy
GG 2458	<i>h<sup>+</sup> sst6::ura4<sup>+</sup> ark1-T11&lt;&lt;kanR ura4-D18/C190T leu1-32</i>	Graduate student, Brinta Roy
GG 2462	<i>h<sup>+</sup> ark1-T11&lt;&lt;kanR ura4-C190T</i>	Graduate student, Brinta Roy
GG 2466	<i>h<sup>-</sup> vps4::ura4<sup>+</sup> ark1-T8-GFP-flag-His&lt;&lt;kanR ura4-D18 leu1-32 ade6-210</i>	Graduate student, Brinta Roy
GG 2471	<i>h<sup>-</sup> vps4::ura4<sup>+</sup> ark1-T11-GFP-flag-His&lt;&lt;kanR ura4-D18 leu1-32</i>	Graduate student, Brinta Roy
GG 2476	<i>h<sup>-</sup> sst4::ura4<sup>+</sup> ark1-T8-GFP-flag-His&lt;&lt;kanR ura4-D18 leu1-32 ade6-210</i>	Graduate student, Brinta Roy
GG 2481	<i>h<sup>+</sup> sst4::ura4<sup>+</sup> ark1-T11-GFP-flag-His&lt;&lt;kanR ura4-D18 leu1-32</i>	Graduate student, Brinta Roy

GG 2486	<i>h90 vps28::ura4<sup>+</sup> ark1-T8-GFP-flag-His&lt;&lt;kanR ura4-D18 leu1-32 ade6-M210</i>	Graduate student, Brinta Roy
GG 2491	<i>h<sup>+</sup> ark1-T11&lt;&lt;kanR vps28::ura4<sup>+</sup> ura4-D18/C190T leu1-32</i>	Graduate student, Brinta Roy
GG 2496	<i>h<sup>-</sup> ark1-T8-GFP-flag-His&lt;&lt;kanR vps36::ura4<sup>+</sup> ura4-D18 leu1-32 ade6-210</i>	Graduate student, Brinta Roy
GG 2501	<i>h<sup>+</sup> ark1-T11&lt;&lt;kanR vps36::ura4<sup>+</sup> ura4-D18/C190T leu1-32</i>	Graduate student, Brinta Roy
GG 2506	<i>h<sup>+</sup> ark1-T8-GFP-flag-His&lt;&lt;kanR vps25::ura4<sup>+</sup> ura4-D18 leu1-32</i>	Graduate student, Brinta Roy
GG 2511	<i>h<sup>-</sup> ark1-T11&lt;&lt;kanR vps25::ura4<sup>+</sup> ura4-D18 /ura4-C190T leu1-32</i>	Graduate student, Brinta Roy
GG 2516	<i>h90 ark1-T8-GFP-flag-His&lt;&lt;kanR vps20::ura4<sup>+</sup> ura4-D18 leu1-32 ade6-M210/ade6-210</i>	Graduate student, Brinta Roy
GG 2521	<i>h90 ark1-T11&lt;&lt;kanR ura4-C190T vps20::ura4<sup>+</sup> ura4-D18 leu1-32 ade6-M210</i>	Graduate student, Brinta Roy
GG 2526	<i>h<sup>+</sup> ark1-T8-GFP-flag-His&lt;&lt;kanR vps2::LEU2 leu1-32</i>	Graduate student, Brinta Roy
GG 2531	<i>h90 vps32:ura4<sup>+</sup> leu1-32 ura4-D18 ade6-M210</i>	(Iwaki et al. 2007)
GG 2559	<i>h? vps32:ura4<sup>+</sup> plo1-ts35 ura4-D18 leu1-32 ade6-M210</i>	Graduate student, Brinta Roy
GG 2562	<i>h? vps32:ura4<sup>+</sup> clp1 ::kanR leu1-32 ura4-D18 ade6-M210</i>	Graduate student, Brinta Roy
GG 2566	<i>h? vps32:ura4<sup>+</sup> ark1-T11&lt;&lt;kanR leu1-32 ura4-D18/C190T ade6-M210</i>	Graduate student, Brinta Roy
GG 2571	<i>h? vps32:ura4<sup>+</sup> dmf1::kanMX4 ura4-D18 leu1-32 ade6-216 /210</i>	Graduate student, Brinta Roy
GG 2575	<i>h? vps32:ura4<sup>+</sup> ark1-T8-GFP-flag-His&lt;&lt;kanR ura4-D18 leu1-32 ade6-210</i>	Graduate student, Brinta Roy

## 6.1.2 *Saccharomyces cerevisiae* strains

Lab no.	Genotype	Source
GGBY 138	<i>MATa URA3::lexA-lacZ met- his3 ade2 trp1 leu2 gal4-D gal80-D</i>	(Reynolds & Ohkura 2003)
GGBY 171	<i>MATa trp1-190 leu2-3, 112, ura 3-52 his 3-200 gal4 delete gal80 delete LYS2 replaced by GAL1-HIS3 GAL2-ADE2 met2 replaced by GAL-lacZ</i>	(James et al. 1996)
GGBY 173	<i>pGBT9:clp1<sup>+</sup> PJ69-4A</i>	(James et al. 1996)
GGBY 174	<i>pGBT9:clp1aa 1-371 PJ69-4A</i>	(James et al. 1996)
GGBY 208	<i>pBTM116:plo1<sup>+</sup> and pACT2:vps20<sup>+</sup></i>	This study
GGBY 211	<i>pBTM116:plo1<sup>+</sup> and pACT2:sst6aa.97-1503</i>	This study
GGBY 214	<i>pGBT9:clp1<sup>+</sup> and pACT2:sst6aa.97-1503</i>	This study
GGBY 217	<i>pBTM116 empty bait vector and pACT2:sst6aa.97-1503</i>	This study
GGBY 220	<i>pBTM116 empty bait vector and pACT2:vps20<sup>+</sup></i>	This study
GGBY 221	<i>pGBT9 empty bait vector and pACT2 empty prey vector</i>	This study
GGBY 224	<i>pGBT9 empty bait vector and pACT2:vps20<sup>+</sup></i>	This study
GGBY 226	<i>pGBT9 empty bait vector and pACT2:sst6aa.97-1503</i>	This study
GGBY 229	<i>pBTM116 empty bait vector and pACT2:vps20<sup>+</sup></i>	This study
GGBY 231	<i>pBTM116 empty bait vector and pACT2:mbx1<sup>+</sup></i>	This study
GGBY 234	<i>pGBT9:clp1<sup>+</sup> and pACT2:mbx1<sup>+</sup></i>	This study
GGBY 237	<i>pGBT9:clp1<sup>+</sup> and pACT2:vps20<sup>+</sup></i>	This study
GGBY 239	<i>pBTM116:plo1.K69R and pACT2:vps20<sup>+</sup></i>	This study
GGBY 242	<i>pBTM116:plo1.K69R and pACT2:sst6aa.97-1503</i>	This study

GGBY 245	<i>pBTM116-plo1.472-684 and pACT2:vps20<sup>+</sup></i>	This study
GGBY 248	<i>pBTM116-plo1.472-684 and pACT2:sst6aa.97-1503</i>	This study
GGBY 251	<i>pBTM116-plo1.DHK625AAA and pACT2:vps20<sup>+</sup></i>	This study
GGBY 254	<i>pBTM116-plo1.DHK625AAA and pACT2:sst6aa.97-1503</i>	This study
GGBY 257	<i>pGBT9:clp1aa 1-371 and pACT2:sst6</i>	This study
GGBY 260	<i>pGBT9:clp1aa 1-371 and pACT2:vps20<sup>+</sup></i>	This study
GGBY 261	<i>pBTM116 empty bait vector and pACT2:sst4<sup>+</sup></i>	This study
GGBY 263	<i>pBTM116:plo1<sup>+</sup> and pACT2:sst4<sup>+</sup></i>	This study
GGBY 265	<i>pBTM116:plo1.K69R and pACT2:sst4<sup>+</sup></i>	This study
GGBY 267	<i>pBTM116-plo1.472-684 and pACT2:sst4<sup>+</sup></i>	This study
GGBY 269	<i>pBTM116-plo1.DHK625AAA and pACT2:sst4<sup>+</sup></i>	This study
GGBY 271	<i>pBTM116 empty bait vector and pACT2:vps28<sup>+</sup></i>	This study
GGBY 273	<i>pBTM116:plo1<sup>+</sup> and pACT2:vps28<sup>+</sup></i>	This study
GGBY 275	<i>pBTM116:plo1.K69R and pACT2:vps28<sup>+</sup></i>	This study
GGBY 277	<i>pBTM116-plo1.472-684 and pACT2:vps28<sup>+</sup></i>	This study
GGBY 279	<i>pBTM116-plo1.DHK625AAA and pACT2:vps28<sup>+</sup></i>	This study
GGBY 281	<i>pBTM116 empty bait vector and pACT2:vps36<sup>+</sup></i>	This study
GGBY 283	<i>pBTM116:plo1<sup>+</sup> and pACT2:vps36<sup>+</sup></i>	This study
GGBY 285	<i>pBTM116:plo1.K69R and pACT2:vps36<sup>+</sup></i>	This study
GGBY 287	<i>pBTM116-plo1.472-684 and pACT2:vps36<sup>+</sup></i>	This study
GGBY 289	<i>pBTM116-plo1.DHK625AAA and pACT2:vps36<sup>+</sup></i>	This study

GGBY 291	<i>pGBT9 empty bait vector and pACT2:ssst4<sup>+</sup></i>	This study
GGBY 293	<i>pGBT9:clp1<sup>+</sup> and pACT2:ssst4<sup>+</sup></i>	This study
GGBY 295	<i>pGBT9:clp1aa 1-371 and pACT2:ssst4<sup>+</sup></i>	This study
GGBY 297	<i>pGBT9 empty bait vector and pACT2:vps28<sup>+</sup></i>	This study
GGBY 299	<i>pGBT9:clp1<sup>+</sup> and pACT2:vps28<sup>+</sup></i>	This study
GGBY 301	<i>pGBT9:clp1aa 1-371 and pACT2:vps28<sup>+</sup></i>	This study
GGBY 303	<i>pGBT9 empty bait vector and pACT2:vps36<sup>+</sup></i>	This study
GGBY 305	<i>pGBT9:clp1<sup>+</sup> and pACT2:vps36<sup>+</sup></i>	This study
GGBY 307	<i>pGBT9:clp1aa 1-371 and pACT2:vps36<sup>+</sup></i>	This study
GGBY 353	<i>pBTM116-plo1.DHK625AAA and pACT2-vps25<sup>+</sup></i>	This study
GGBY 359	<i>pBTM116-plo1.DHK625AAA and pACT2-<sup>-</sup></i>	This study
GGBY 361	<i>pBTM116-empty and pACT2-vps2<sup>+</sup></i>	This study
GGBY 363	<i>pBTM116-plo1<sup>+</sup> and pACT2-vps2<sup>+</sup></i>	This study
GGBY 365	<i>pGBT9-clp1<sup>+</sup> and pACT2-vps25<sup>+</sup></i>	This study
GGBY 367	<i>pGBT9-clp1aa.1-371 and pACT2-vps25<sup>+</sup></i>	This study
GGBY 369	<i>pGBT9-empty and pACT2-vps2<sup>+</sup></i>	This study
GGBY 371	<i>pGBT9-clp1<sup>+</sup> and pACT2-vps2<sup>+</sup></i>	This study
GGBY 373	<i>pGBT9-clp1aa.1-371 and pACT2-vps2<sup>+</sup></i>	This study
GGBY 375	<i>pGBT9-empty and pACT2-vps25<sup>+</sup></i>	This study
GGBY 377	<i>pBTM116-empty and pACT2-vps25<sup>+</sup></i>	This study
GGBY 379	<i>pBTM116-plo1<sup>+</sup> and pACT2-vps25<sup>+</sup></i>	This study

GGBY 381	<i>pBTM116-plo1.K69R and pACT2-vps25<sup>+</sup></i>	This study
GGBY 383	<i>pBTM116-plo1.472-684 and pACT2-vps25<sup>+</sup></i>	This study
GGBY 385	<i>pBTM116-plo1.K69R and pACT2-vps2<sup>+</sup></i>	This study
GGBY 387	<i>pBTM116-plo1.472-684 and pACT2-vps2<sup>+</sup></i>	This study
GGBY 389	<i>pBTM116-empty and pACT2-vps32<sup>+</sup></i>	This study
GGBY 391	<i>pBTM116-plo1<sup>+</sup> and pACT2-vps32<sup>+</sup></i>	This study
GGBY 393	<i>pBTM116-plo1.K69R and pACT2-vps32<sup>+</sup></i>	This study
GGBY 395	<i>pBTM116-plo1.472-684 and pACT2-vps32<sup>+</sup></i>	This study
GGBY 397	<i>pBTM116-plo1.DHK625AAA and pACT2-vps32<sup>+</sup></i>	This study
GGBY 399	<i>pGBT9-empty and pACT2-vps32<sup>+</sup></i>	This study
GGBY 401	<i>pGBT9-clp1<sup>+</sup> and pACT2-vps32<sup>+</sup></i>	This study
GGBY 403	<i>pGBT9-clp1aa.1-371 and pACT2-vps32<sup>+</sup></i>	This study
GGBY 405	<i>pBTM116-empty and pACT2-vps4<sup>+</sup></i>	This study
GGBY 407	<i>pBTM116-plo1<sup>+</sup> and pACT2-vps4<sup>+</sup></i>	This study
GGBY 409	<i>pBTM116-plo1.K69R and pACT2-vps4<sup>+</sup></i>	This study
GGBY 411	<i>pBTM116-plo1.472-684 and pACT2-vps4<sup>+</sup></i>	This study
GGBY 413	<i>pBTM116-plo1.DHK625AAA and pACT2-vps4<sup>+</sup></i>	This study
GGBY 415	<i>pGBT9-empty and pACT2-vps4<sup>+</sup></i>	This study
GGBY 417	<i>pGBT9-clp1<sup>+</sup> and pACT2-vps4<sup>+</sup></i>	This study
GGBY 419	<i>pGBT9-clp1aa.1-371 and pACT2-vps4<sup>+</sup></i>	This study

## 6.2 Septation defects in mutants of *plo1*, *clp1*, *mid1* and *ark1*

### 6.2.1 Single mutants *plo1-ts35*, *clp1* $\Delta$ , *mid1* $\Delta$ , *ark1-T8* and *ark1-T11* exhibit septation defects

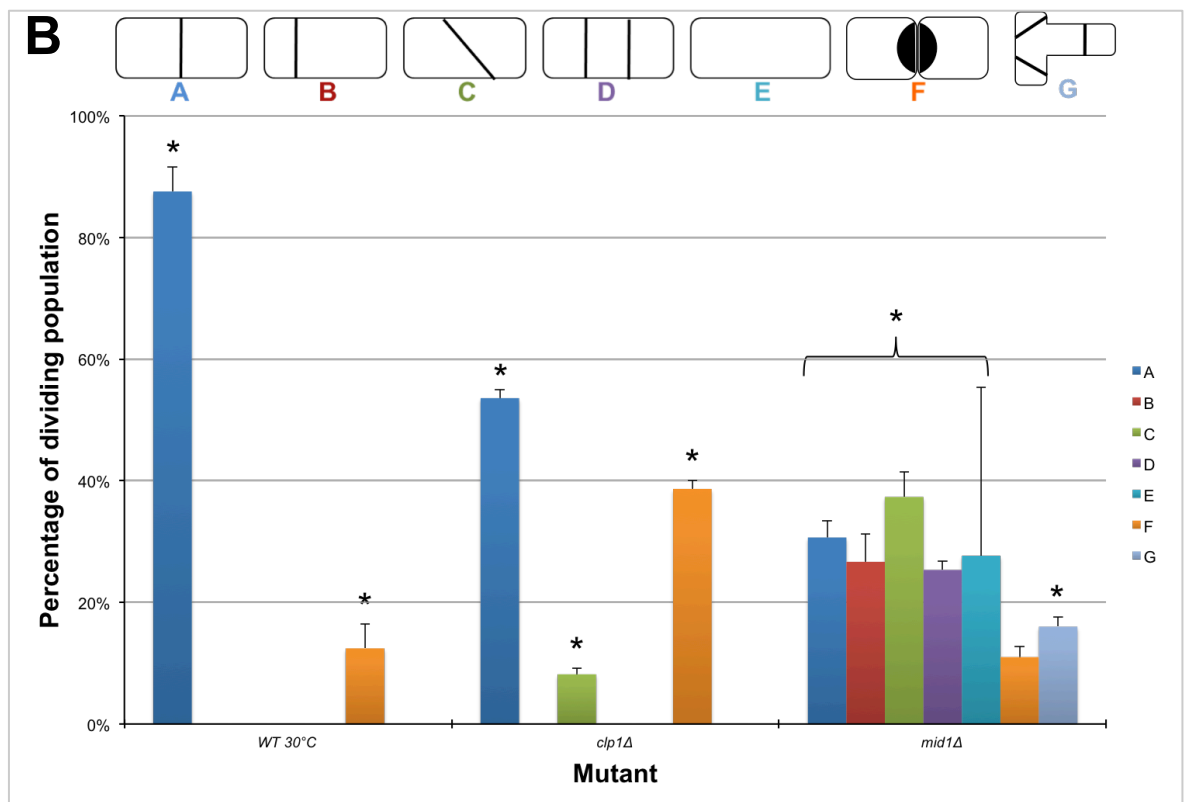
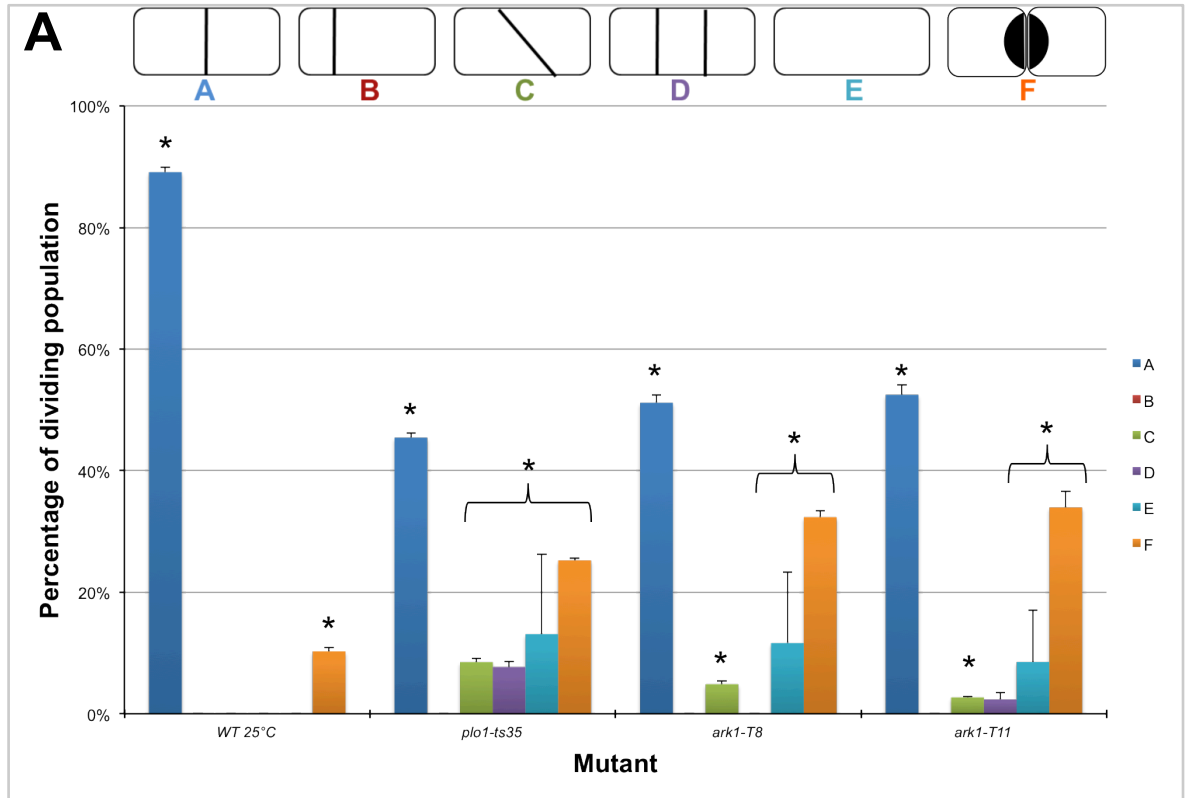


**Figure 6.1: Fission yeast with mutants in *plo1*, *ark1*, *clp1* and *mid1* exhibit septal defects.**

Wild-type fission yeast were grown in rich liquid medium to mid-exponential phase at either (A) 25°C along with strains with temperature-sensitive mutations *plo1-ts35*, *ark1-T8* or *ark1-T11*, or (B) 30°C along with strains with chromosomal deletions *clp1Δ* or *mid1Δ*. Cells were harvested and stained with Calcofluor white and visualised by fluorescence microscopy. The graph represents the frequency of phenotypes A-F among various single and double mutant strains (400 cells, n=3): (A) a normal septum, (B) a misaligned septum, (C) a non-perpendicular septum, (D) multiple septa, (E) no septal formation, and (F) failed separation of daughter cells following septation, and (G) branched cells with multiple septa. Data was collected by graduate student Brinta Roy.

### 6.2.2 Septation defects in *plp1-ts35* double mutants

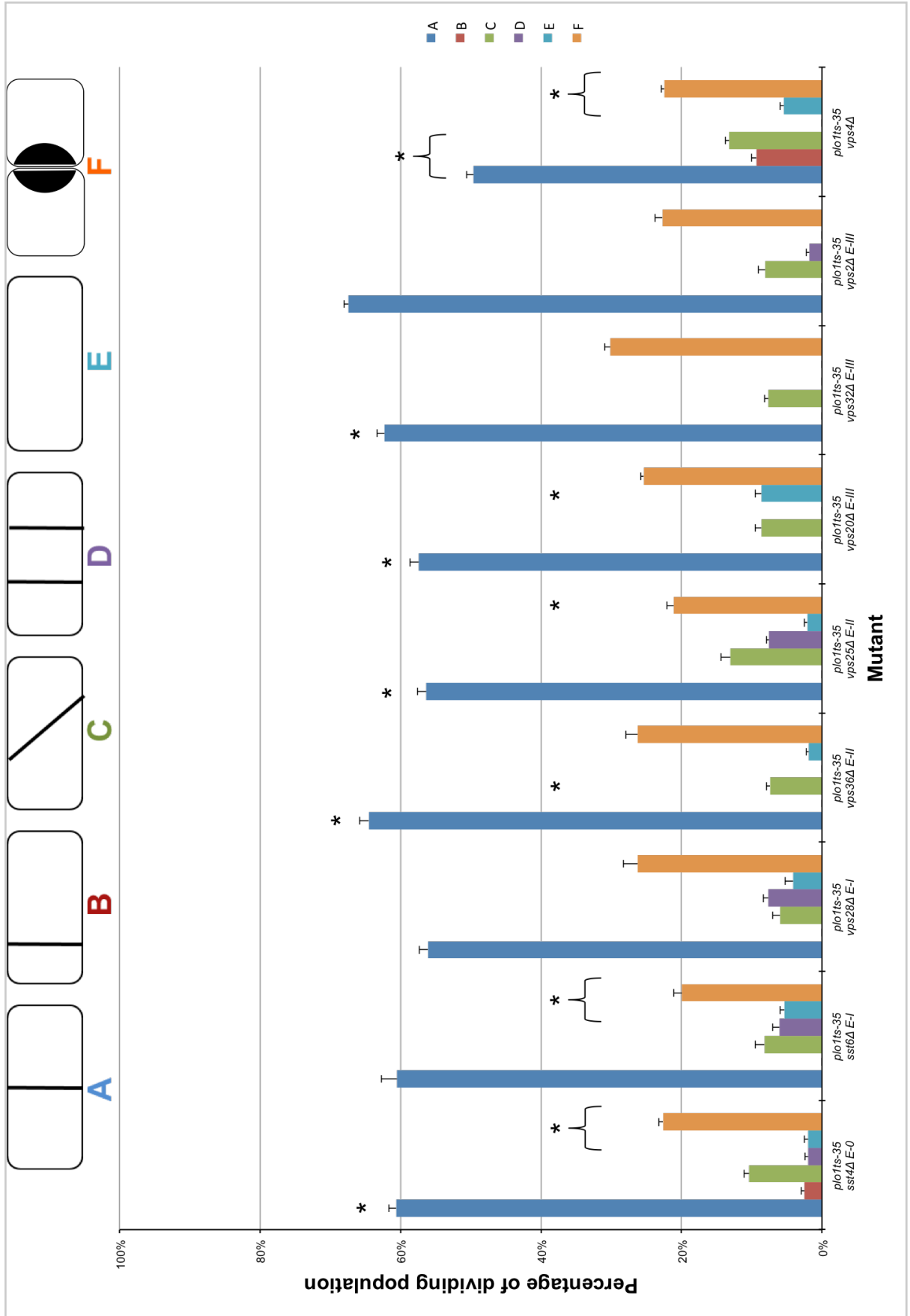


**Figure 6.2: Double mutants of ESCRT deletions and *plo1-ts35* exhibit septation defects in fission yeast.**

Fission yeast with temperature-sensitive *plo1* mutation *plo1-ts35* combined with individual ESCRT deletions were grown in rich liquid medium to mid-exponential phase and harvested. Cells were stained with Calcofluor white and visualised by fluorescence microscopy. The graph represents the frequency of phenotypes A-F among various single and double mutant strains (400 cells, n=3): (A) a normal septum, (B) a misaligned septum, (C) a non-perpendicular septum, (D) multiple septa, (E) no septal formation, and (F) failed separation of daughter cells following septation. Each of the ESCRT genes labels is accompanied by its respective ESCRT subunit (E-0-III). Data was collected by graduate student Brinta Roy.

### 6.2.3 Septation defects in *clp1Δ* double mutants

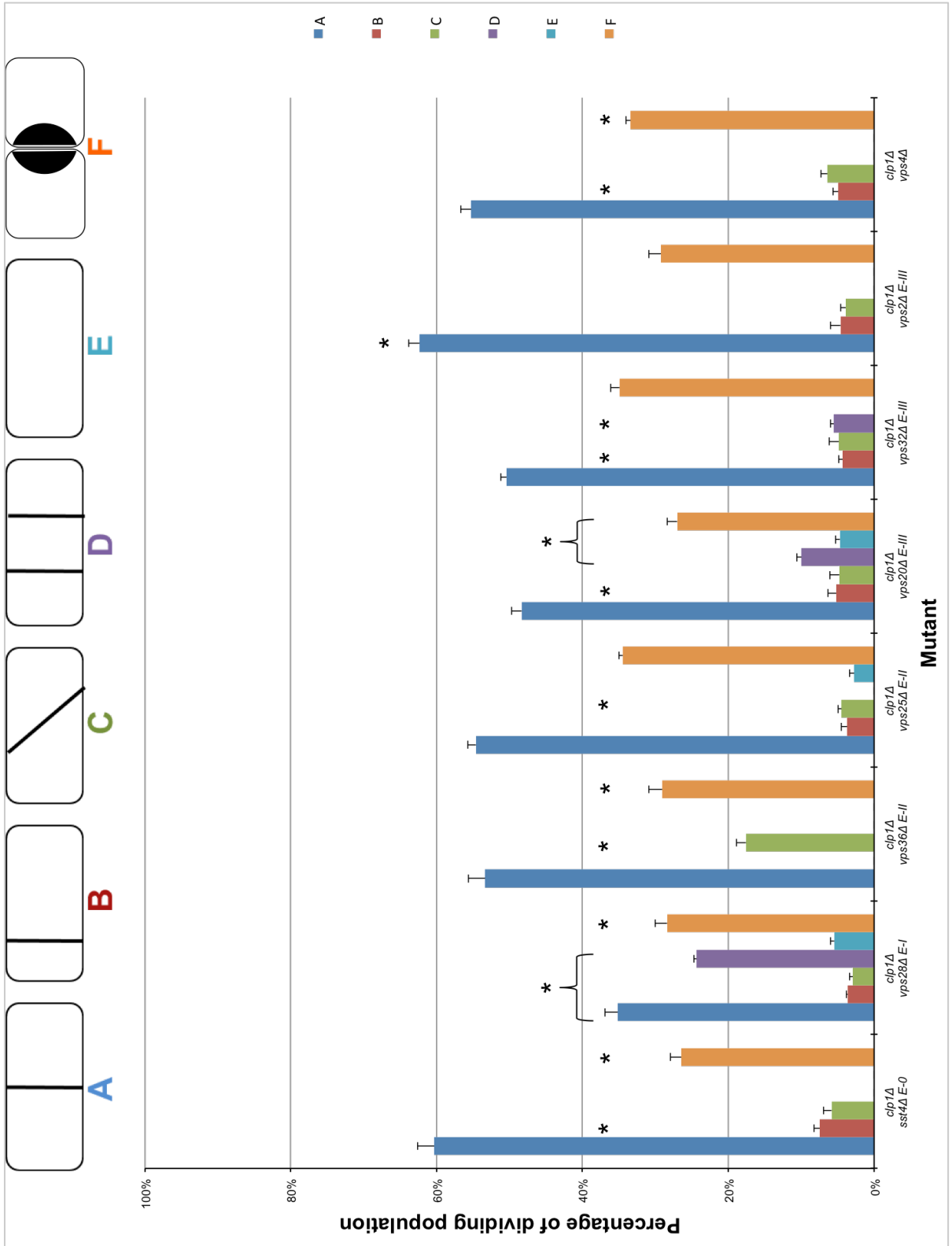


**Figure 6.3: Double mutants of ESCRT deletions and *clp1Δ* exhibit septation defects in fission yeast.**

Fission yeast with *clp1* chromosomal deletion mutation *clp1Δ* combined with individual ESCRT deletions were grown in rich liquid medium to mid-exponential phase and harvested. Cells were stained with Calcofluor white and visualised by fluorescence microscopy. The graph represents the frequency of *phenotypes A-F* among various single and double mutant strains (400 cells, n=3): (A) a normal septum, (B) a misaligned septum, (C) a non-perpendicular septum, (D) multiple septa, (E) no septal formation, and (F) failed separation of daughter cells following septation. Each of the ESCRT genes labels is accompanied by its respective ESCRT subunit (*E-0-III*). Data was collected by graduate student Brinta Roy.

## 6.2.4 Septation defects in *mid1Δ* double mutants

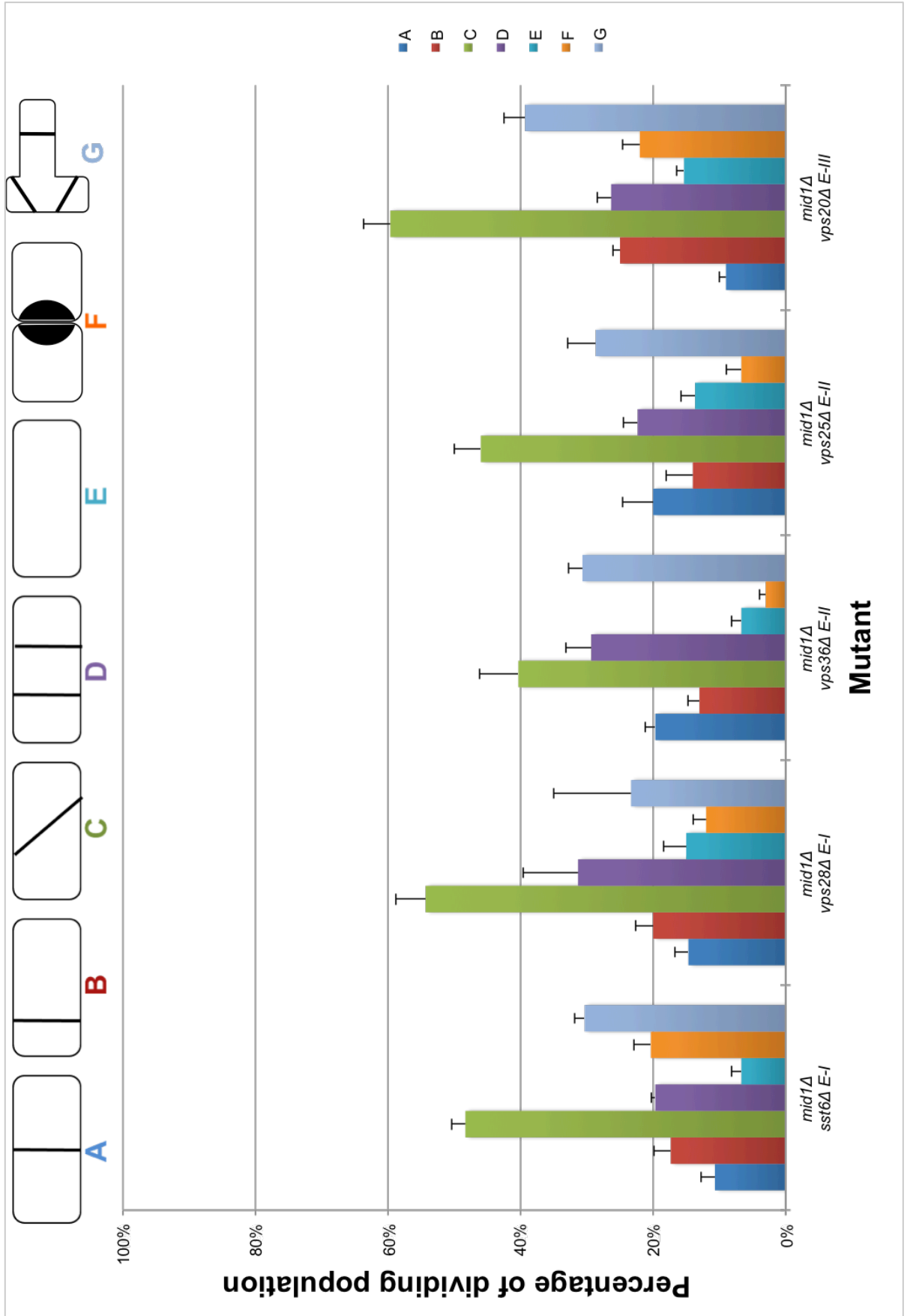


**Figure 6.4: Double mutants of ESCRT deletions and *mid1Δ* exhibit septation defects in fission yeast.**

Fission yeast with *mid1* chromosomal deletion mutation *mid1Δ* combined with individual ESCRT deletions were grown in rich liquid medium to mid-exponential phase and harvested. Cells were stained with Calcofluor white and visualised by fluorescence microscopy. The graph represents the frequency of phenotypes A-F among various single and double mutant strains (400 cells, n=3): (A) a normal septum, (B) a misaligned septum, (C) a non-perpendicular septum, (D) multiple septa, (E) no septal formation, (F) failed separation of daughter cells following septation, and (G) branched cells with multiple septa. Each of the ESCRT genes labels is accompanied by its respective ESCRT subunit (*E-0-III*). Data was collected by graduate student Brinta Roy.

## 6.2.5 Septation defects in *ark1ts* double mutants

### 6.2.5.1 Septation defects in *ark1-T8* double mutants

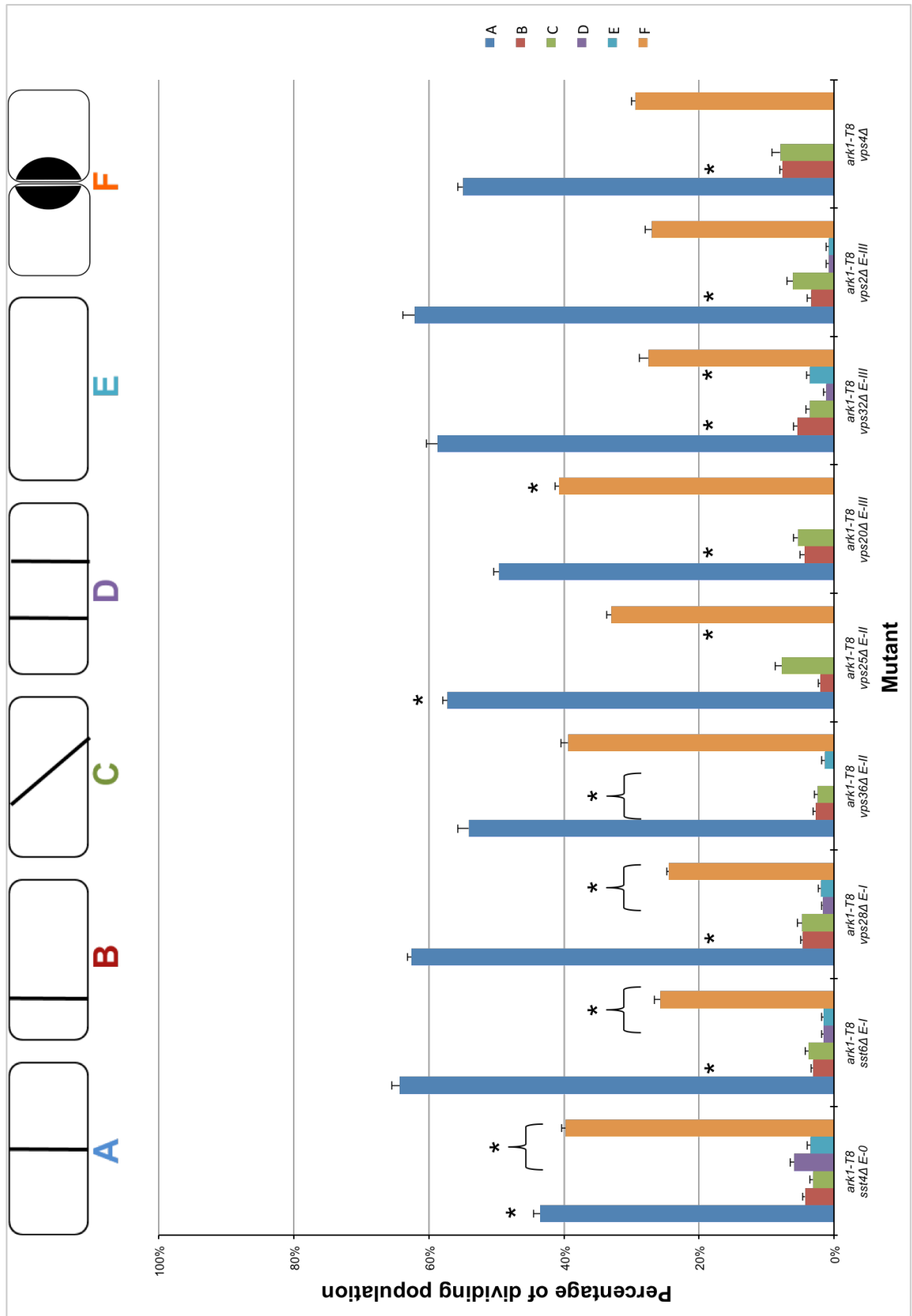


**Figure 6.5: Double mutants of ESCRT deletions and *ark1-T8* exhibit septation defects in fission yeast.**

Fission yeast with temperature-sensitive *ark1* mutation *ark1-T8* combined with individual ESCRT deletions were grown in rich liquid medium to mid-exponential phase and harvested. Cells were stained with Calcofluor white and visualised by fluorescence microscopy. The graph represents the frequency of phenotypes A-F among various single and double mutant strains (400 cells, n=3): (A) a normal septum, (B) a misaligned septum, (C) a non-perpendicular septum, (D) multiple septa, (E) no septal formation, and (F) failed separation of daughter cells following septation. Each of the ESCRT genes labels is accompanied by its respective ESCRT subunit (E-0-III). Data was collected by graduate student Brinta Roy.

6.2.5.2 Septation defects in *ark1-T11* double mutants

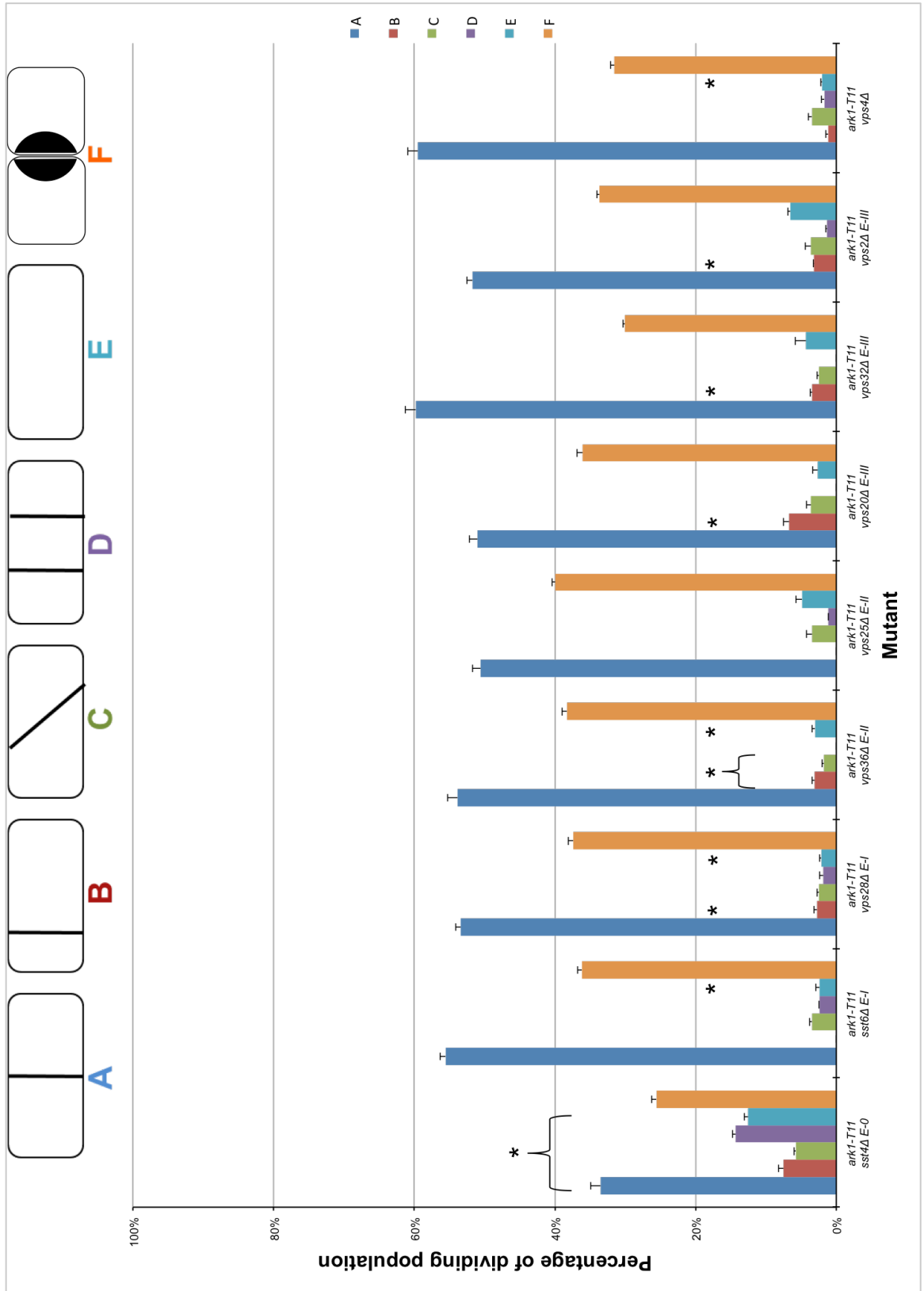


**Figure 6.6: Double mutants of ESCRT deletions and *ark1-T11* exhibit septation defects in fission yeast.**

Fission yeast with temperature-sensitive *ark1* mutation *ark1-T8* combined with individual ESCRT deletions were grown in rich liquid medium to mid-exponential phase and harvested. Cells were stained with Calcofluor white and visualised by fluorescence microscopy. The graph represents the frequency of phenotypes A-F among various single and double mutant strains (400 cells, n=3): (A) a normal septum, (B) a misaligned septum, (C) a non-perpendicular septum, (D) multiple septa, (E) no septal formation, and (F) failed separation of daughter cells following septation. Each of the ESCRT genes labels is accompanied by its respective ESCRT subunit (E-0-III). Data was collected by graduate student Brinta Roy.

## List of References

- Agromayor, M. & Martin-Serrano, J., 2006. Interaction of AMSH with ESCRT-III and deubiquitination of endosomal cargo. *J Biol Chem*, 281(32), pp.23083-91.
- Almonacid, M., Celton-Morizur, S., Jakubowski, J.L., et al., 2011. Temporal control of contractile ring assembly by Plo1 regulation of Myosin II recruitment by Mid1/Anillin. *Curr Biol*, 21(6), pp.473-9.
- Anderson, M., Ng, S.S., Marchesi, V., et al., 2002. *plo1*<sup>+</sup> regulates gene transcription at the M-G<sub>1</sub> interval during the fission yeast mitotic cell cycle. *EMBO J*, 21(21), pp.5745-55.
- Asakawa, K. & Toh-e, A., 2002. A defect of Kap104 alleviates the requirement of mitotic exit network gene functions in *Saccharomyces cerevisiae*. *Genetics*, 162(4), pp.1545-56.
- Babst, M., Wendland, B., Estepa, E.J. et al., 1998. The Vps4p AAA ATPase regulates membrane association of a Vps protein complex required for normal endosome function. *EMBO J*, 17(11), pp.2982-93.
- Bähler, J., Steever, A.B., Wheatley, S. et al., 1998. Role of polo kinase and Mid1p in determining the site of cell division in fission yeast. *J Cell Biol*, 143(6), pp.1603-16.
- Balasubramanian, M.K., Bi, E. & Glotzer, M., 2004. Comparative analysis of cytokinesis in budding yeast, fission yeast and animal cells. *Curr Biol*, 14(18), R806-18.
- Barr, F.A., Silljé, H.H. & Nigg, E.A., 2004. Polo-like kinases and the orchestration of cell division. *Nat Rev Mol Cell Biol*, 5(6), pp.429-40.
- Bastos, R.N. & Barr, F.A., 2010. Plk1 negatively regulates Cep55 recruitment to the midbody to ensure orderly abscission. *J Cell Biol*, 191(4), pp.751-60.

- Bembenek, J. & Yu, H., 2001. Regulation of the anaphase-promoting complex by the dual specificity phosphatase human Cdc14a. *J Biol Chem*, 276(51), pp.48237-42.
- Bi, E., 2001. Cytokinesis in budding yeast: the relationship between actomyosin ring function and septum formation. *Cell Struct Funct*, 26(6), pp.529-37.
- Brückner, A., Polge, C., Lentze, N. et al., 2009. Yeast two-hybrid, a powerful tool for systems biology. *Int J Mol Sci*, 10(6), pp.2763-88.
- Burgess, D.R. & Chang, F., 2005. Site selection for the cleavage furrow at cytokinesis. *Trends Cell Biol*, 15(3), pp.156-62.
- Carlton, J.G., Caballe, A., Agromayor, M. et al., 2012. ESCRT-III governs the Aurora B-mediated abscission checkpoint through CHMP4C. *Science*, 336(6078), pp.220-5.
- Cascone, I., Selimoglu, R., Ozdemir, C. et al., 2008. Distinct roles of RalA and RalB in the progression of cytokinesis are supported by distinct RalGEFs. *EMBO J*, 27(18), pp.2375-87.
- Celton-Morizur, S., Bordes, N., Fraissier, V. et al., 2004. C-terminal anchoring of mid1p to membranes stabilizes cytokinetic ring position in early mitosis in fission yeast. *Mol Cell Biol*, 24(24), pp.10621-35.
- Chen, C.-T., Feoktistova, A., Chen, J.-S. et al., 2008. The SIN kinase Sid2 regulates cytoplasmic retention of the Cdc14-like phosphatase Clp1 in *S. pombe*. *Curr Biol*, 18(20), pp.1594-9.
- Clifford, D.M., Wolfe, B.A., Roberts-Galbraith, R.H. et al., 2008. The Clp1/Cdc14 phosphatase contributes to the robustness of cytokinesis by association with anillin-related Mid1. *J Cell Biol*, 181(1), pp.79-88.
- Clute, P. & Pines, J., 1999. Temporal and spatial control of cyclin B1 destruction in metaphase. *Nat Cell Biol*, 1(2), pp.82-7.

Eisele, K.-H., Fink, K., Vey, M. et al., 2011. Studies on the dissociation of botulinum neurotoxin type A complexes. *Toxicon*, 57(4), pp.555-65.

Elia, A.E., Cantley, L.C. & Yaffe, M.B., 2003. Proteomic screen finds pSer/pThr-binding domain localizing Plk1 to mitotic substrates. *Science*, 299(5610), pp.1228-31.

Elia, N., Fabrikant, G., Kozlov, M.M. et al., 2012. Computational model of cytokinetic abscission driven by ESCRT-III polymerization and remodeling. *Biophys J*, 102(10), pp.2309-20.

Elia, N., Sougrat, R., Spurlin, T.A. et al., 2011. Dynamics of endosomal sorting complex required for transport (ESCRT) machinery during cytokinesis and its role in abscission. *PNAS*, 108(12), pp.4846-51.

Estey, M.P., Ciano-Oliveira, C., Froese, C.D. et al., 2010. Distinct roles of septins in cytokinesis: SEPT9 mediates midbody abscission. *J Cell Biol*, 191(4), pp.741-9.

Fendrych, M., Synek, L., Pecenková, T. et al., 2010. The Arabidopsis exocyst complex is involved in cytokinesis and cell plate maturation. *Plant Cell*, 22(9), pp.3053-65.

Fielding, A.B., Schonteich, E., Matheson, J. et al., 2005. Rab11-FIP3 and FIP4 interact with Arf6 and the exocyst to control membrane traffic in cytokinesis. *EMBO J*, 24(19), pp.3389-99.

Fields, S. & Song, O., 1989. A novel genetic system to detect protein-protein interactions. *Nature*, 340(6230), pp.245-6.

Fisher, R.D., Chung, H.Y., Zhai, Q. et al., 2007. Structural and biochemical studies of ALIX/AIP1 and its role in retrovirus budding. *Cell*, 128(5), pp.841-52.

Forsburg, S.L. & Nurse, P., 1991. Cell cycle regulation in the yeasts *Saccharomyces cerevisiae* and *Schizosaccharomyces pombe*. *Annu. Rev. Cell Biol.*, 7, pp.227-56.

Fu, Z., Malureanu, L., Huang, J. et al., 2008. Plk1-dependent phosphorylation of FoxM1 regulates a transcriptional programme required for mitotic progression. *Nat Cell Biol*, 10(9), pp.1076-82.

Fukada, M., Kawachi, H., Fujikawa, A. et al., 2005. Yeast substrate-trapping system for isolating substrates of protein tyrosine phosphatases: isolation of substrates for protein tyrosine phosphatase receptor type z. *Methods*, 35(1), pp.54-63.

Golsteyn, R.M., Mundt, K.E., Fry, A.M. et al., 1995. Cell cycle regulation of the activity and subcellular localization of Plk1, a human protein kinase implicated in mitotic spindle function. *J Cell Biol*, 129(6), pp.1617-28.

Goss, J.W. & Toomre, D.K., 2008. Both daughter cells traffic and exocytose membrane at the cleavage furrow during mammalian cytokinesis. *J Cell Biol*, 181(7), pp.1047-54.

Gould, G.W. & Lippincott-Schwartz, J., 2009. New roles for endosomes: from vesicular carriers to multi-purpose platforms. *Nat Rev Mol Cell Biol*, 10(4), pp.287-92.

Gromley, A., Yeaman, C., Rosa, J. et al., 2005. Centriolin anchoring of exocyst and SNARE complexes at the midbody is required for secretory-vesicle-mediated abscission. *Cell*, 123(1), pp.75-87.

Guizetti, J., Schermelleh, L., Mäntler, J. et al., 2011. Cortical constriction during abscission involves helices of ESCRT-III-dependent filaments. *Science*, 331(6024), pp.1616-20.

Guizetti, J. & Gerlich, D.W., 2010. Cytokinetic abscission in animal cells. *Semin Cell Dev Biol*, 21(9), pp.909-16.

Hachet, O. & Simanis, V., 2008. Mid1p/anillin and the septation initiation network orchestrate contractile ring assembly for cytokinesis. *Genes Dev*, 22(22), pp.3205-16.

Harper, J.V., 2005. Synchronization of cell populations in G1/S and G2/M phases of the cell cycle. *Methods Mol Biol*, 296, pp.157-66.

Hayles, J., Fisher, D., Woollard, A. et al., 1994. Temporal order of S phase and mitosis in fission yeast is determined by the state of the p34cdc2-mitotic B cyclin complex. *Cell*, 78(5), pp.813-22.

Hinshaw, J.E., 2000. Dynamin and its role in membrane fission. *Annu Rev Cell Dev Biol*, 16, pp.483-519.

Hu, C.-K., Ozlü, N., Coughlin, M. et al., 2012. Plk1 negatively regulates PRC1 to prevent premature midzone formation before cytokinesis. *Mol Biol Cell*, 23(14), pp.2702-11.

Hu, C.-K., Coughlin, M. & Mitchison, T.J., 2012. Midbody assembly and its regulation during cytokinesis. *Mol Biol Cell*, 23(6), pp.1024-34.

Hurley, J.H. & Emr, S.D., 2006. The ESCRT complexes: structure and mechanism of a membrane-trafficking network. *Annu Rev Biophys Biomol Struct*, 35, pp.277-98.

Hurley, J.H. & Hanson, P.I., 2010. Membrane budding and scission by the ESCRT machinery: it's all in the neck. *Nat Rev Mol Cell Biol*, 11(8), pp.556-66.

Iwaki, T., Onishi, M., Ikeuchi, M. et al., 2007. Essential roles of class E Vps proteins for sorting into multivesicular bodies in *Schizosaccharomyces pombe*. *Microbiology*, 153(Pt 8), pp.2753-64.

James, P., Halladay, J. & Craig, E.A., 1996. Genomic libraries and a host strain designed for highly efficient two-hybrid selection in yeast. *Genetics*, 144(4), pp.1425-36.

Jang, Y.-J., Lin, C.Y., Ma, S. et al., 2002. Functional studies on the role of the C-terminal domain of mammalian polo-like kinase. *PNAS*, 99(4), pp.1984-9.

Jin, Q.-W., Zhou, M., Bimbo, A. et al., 2006. A role for the septation initiation network in septum assembly revealed by genetic analysis of *sid2-250* suppressors. *Genetics*, 172(4), pp.2101-12.

Johnson, B.F., Yoo, B.Y. & Calleja, G.B., 1973. Cell division in yeasts: movement of organelles associated with cell plate growth of *Schizosaccharomyces pombe*. *J Bacteriol*, 115(1), pp.358-66.

Kaiser, B.K., Zimmerman, Z.A., Charbonneau, H. et al., 2002. Disruption of centrosome structure, chromosome segregation, and cytokinesis by misexpression of human Cdc14A phosphatase. *Mol Biol Cell*, 13(7), pp.2289-300.

Kallay, L.M., Brett, C.L., Tukaye, D.N. et al., 2011. Endosomal Na<sup>+</sup> (K<sup>+</sup>)/H<sup>+</sup> exchanger Nhx1/Vps44 functions independently and downstream of multivesicular body formation. *J Biol Chem*, 286(51), pp.44067-77.

Kinoshita, E., Kinoshita-Kikuta, E., Takiyama, K. et al., 2006. Phosphate-binding tag, a new tool to visualize phosphorylated proteins. *Mol Cell Proteomics*, 5(4), pp.749-57.

Kinoshita, E., Takahashi, M., Takeda, H. et al., 2004. Recognition of phosphate monoester dianion by an alkoxide-bridged dinuclear zinc(II) complex. *Dalton Trans*, 21(8), pp.1189-93.

Kinoshita-Kikuta, E., Aoki, Y., Kinoshita, E. et al., 2007. Label-free kinase profiling using phosphate affinity polyacrylamide gel electrophoresis. *Mol Cell Proteomics*, 6(2), pp.356-66.

Koch, A., Krug, K., Pengelley, S. et al., 2011. Mitotic substrates of the kinase aurora with roles in chromatin regulation identified through quantitative phosphoproteomics of fission yeast. *Sci signal*, 4(179), rs6.

Koepp, D.M., Harper, J.W. & Elledge, S.J., 1999. How the cyclin became a cyclin: regulated proteolysis in the cell cycle. *Cell*, 97(4), pp.431-4.

Krapp, A., Gulli, M.-P. & Simanis, V., 2004. SIN and the art of splitting the fission yeast cell. *Curr Biol*, 14(17), R722-30.

Lanzetti, L., Margaria, V., Melander, F. et al., 2007. Regulation of the Rab5 GTPase-activating protein RN-tre by the dual specificity phosphatase Cdc14A in human cells. *J Biol Chem*, 282(20), pp.15258-70.

Laoukili, J., Kooistra, M.R., Brás, A. et al., 2005. FoxM1 is required for execution of the mitotic programme and chromosome stability. *Nat Cell Biol*, 7(2), pp.126-36.

Lata, S., Schoehn, G., Jain, A. et al., 2008. Helical structures of ESCRT-III are disassembled by VPS4. *Science*, 321(5894), pp.1354-7.

Lee, M.G. & Nurse, P., 1987. Complementation used to clone a human homologue of the fission yeast cell cycle control gene *cdc2*. *Nature*, 327(6117), pp.31-5.

Lénárt, P., Petronczki, M., Steegmaier, M. et al., 2007. The small-molecule inhibitor BI 2536 reveals novel insights into mitotic roles of polo-like kinase 1. *Curr Biol*, 17(4), pp.304-15.

Lin, Y., Kimpler, L.A., Naismith, T.V. et al., 2005. Interaction of the mammalian endosomal sorting complex required for transport (ESCRT) III protein hSnf7-1 with itself, membranes, and the AAA+ ATPase SKD1. *J Biol Chem*, 280(13), pp.12799-809.

Lindon, C. & Pines, J., 2004. Ordered proteolysis in anaphase inactivates Plk1 to contribute to proper mitotic exit in human cells. *J Cell Biol*, 164(2), pp.233-41.

Liu, J., Wang, H., McCollum, D. et al., 1999. Drc1p/Cps1p, a 1,3-beta-glucan synthase subunit, is essential for division septum assembly in *Schizosaccharomyces pombe*. *Genetics*, 153(3), pp.1193-203.

Mailand, N., Lukas, C., Kaiser, B.K. et al., 2002. Deregulated human Cdc14A phosphatase disrupts centrosome separation and chromosome segregation. *Nat Cell Biol*, 4(4), pp.317-22.

Martín-Cuadrado, A.B., Morrell, J.L., Konomi, M. et al., 2005. Role of septins and the exocyst complex in the function of hydrolytic enzymes responsible for fission yeast cell separation. *Mol Biol Cell*, 16(10), pp.4867-81.

Martin-Serrano, J., Yarovoy, A., Perez-Caballero, D. et al., 2003. Divergent retroviral late-budding domains recruit vacuolar protein sorting factors by using alternative adaptor proteins. *PNAS*, 100(21), pp.12414-9.

Maundrell, K., 1993. Thiamine-repressible expression vectors pREP and pRIP for fission yeast. *Gene*, 123, pp.127-30.

McDonald, B. & Martin-Serrano, J., 2009. No strings attached: the ESCRT machinery in viral budding and cytokinesis. *J Cell Sci*, 122(13), pp.2167-77.

McMurray, M.A., Stefan, C.J., Wemmer, M. et al., 2011. Genetic interactions with mutations affecting septin assembly reveal ESCRT functions in budding yeast cytokinesis. *Biol Chem*, 392(8-9), pp.699-712.

Mitchison, J.M. & Nurse, P., 1985. Growth in cell length in the fission yeast *Schizosaccharomyces pombe*. *J Cell Sci*, 75, pp.357-76.

Mitra, P., Zhang, Y., Rameh, L.E. et al., 2004. A novel phosphatidylinositol(3,4,5)P3 pathway in fission yeast. *J Cell Biol*, 166(2), pp.205-11.

Mocciaro, A. & Schiebel, E., 2010. Cdc14: a highly conserved family of phosphatases with non-conserved functions? *J Cell Sci*, 123(17), pp.2867-76.

Moreno, S., Klar, A. & Nurse, P., 1991. Molecular genetic analysis of fission yeast *Schizosaccharomyces pombe*. *Methods Enzymol*, 194, pp.795-823.

Morgan, D.O., 1995. Principles of CDK Regulation. *Nature*, 374(6518), pp.131-4.

Morita, E., Sandrin, V., Chung, H.Y. et al., 2007. Human ESCRT and ALIX proteins interact with proteins of the midbody and function in cytokinesis. *EMBO J*, 26(19), pp.4215-27.

Morita, E., Colf, L.A., Karren, M.A. et al., 2010. Human ESCRT-III and VPS4 proteins are required for centrosome and spindle maintenance. *PNAS*, 107(29), pp.12889-94.

Morita, E. & Sundquist, W.I., 2004. Retrovirus budding. *Annu Rev Cell Dev Biol*, 20, pp.395-425.

Muziol, T., Pineda-Molina, E., Ravelli, R.B. et al., 2006. Structural basis for budding by the ESCRT-III factor CHMP3. *Dev Cell*, 10(6), pp.821-30.

Nakajima, H., Toyoshima-Morimoto, F., Taniguchi, E. et al., 2003. Identification of a consensus motif for Plk (Polo-like kinase) phosphorylation reveals Myt1 as a Plk1 substrate. *J Biol Chem*, 278(28), pp.25277-80.

Neef, R., Preisinger, C., Sutcliffe, J. et al., 2003. Phosphorylation of mitotic kinesin-like protein 2 by polo-like kinase 1 is required for cytokinesis. *J Cell Biol*, 162(5), pp.863-75.

Neto, H., Collins, L.L. & Gould, G.W., 2011. Vesicle trafficking and membrane remodelling in cytokinesis. *Biochem J*, 437(1), pp.13-24.

Neto, H. & Gould, G.W., 2011. The regulation of abscission by multi-protein complexes. *J Cell Sci*, 124(19), pp.3199-207.

Ng, S.S., Papadopoulou, K. & McNerny, C.J., 2006. Regulation of gene expression and cell division by Polo-like kinases. *Curr Genet*, 50(2), pp.73-80.

Ohkura, H., Hagan, I.M. & Glover, D.M., 1995. The conserved *Schizosaccharomyces pombe* kinase plo1, required to form a bipolar spindle, the actin ring, and septum, can drive septum formation in G1 and G2 cells. *Genes & Development*, 9(9), pp.1059-73.

Okazaki, K., Okazaki, N., Kume, K. et al., 1990. High-frequency transformation method and library transducing vectors for cloning mammalian cDNAs by trans-complementation of *Schizosaccharomyces pombe*. *Nucleic Acids Res*, 18(22), pp.6485-9.

Papadopoulou, K., Chen, J.S., Mead, E. et al., 2010. Regulation of cell cycle-specific gene expression in fission yeast by the Cdc14p-like phosphatase Clp1p. *J Cell Sci*, 123(24), pp.4374-81.

Papadopoulou, K., Ng, S.S., Ohkura, H. et al., 2008. Regulation of gene expression during M-G1-phase in fission yeast through Plo1p and forkhead transcription factors. *J Cell Sci*, 121(1), pp.38-47.

Park, J.-E., Soung, N.K., Johmura, Y. et al., 2010. Polo-box domain: a versatile mediator of polo-like kinase function. *Cell Mol Life Sci*, 67(12), pp.1957-70.

Pereira, G. & Schiebel, E., 2003. Separase regulates INCENP-Aurora B anaphase spindle function through Cdc14. *Science*, 302(5653), pp.2120-4.

Petersen, J. & Hagan, I.M., 2003. *S. pombe* Aurora kinase/survivin is required for chromosome condensation and the spindle checkpoint attachment response. *Curr Biol*, 13(7), pp.590-7.

Petronczki, M., Glotzer, M., Kraut, N. et al., 2007. Polo-like kinase 1 triggers the initiation of cytokinesis in human cells by promoting recruitment of the RhoGEF Ect2 to the central spindle. *Dev Cell*, 12(5), pp.713-25.

Pollard, T.D. & Wu, J.-Q., 2010. Understanding cytokinesis: lessons from fission yeast. *Nat Rev Mol Cell Biol*, 11(2), pp.149-155.

Raymond, C.K., Howald-Stevenson, I., Vater, C.A. et al., 1992. Morphological classification of the yeast vacuolar protein sorting mutants: evidence for a prevacuolar compartment in class E vps mutants. *Mol Biol Cell*, 3(12), pp.1389-402.

Reynolds, N. & Ohkura, H., 2003. Polo boxes form a single functional domain that mediates interactions with multiple proteins in fission yeast polo kinase. *J Cell Sci*, 116(7), pp.1377-87.

Saito, R.M., Perreault, A., Peach, B. et al., 2004. The CDC-14 phosphatase controls developmental cell-cycle arrest in *C. elegans*. *Nat Cell Biol*, 6(8), pp.777-83.

Sambrook, J., Fritsch, E.F. & Maniatis, T., 2001. *Molecular Cloning: a laboratory manual*. Cold Spring Harbor Laboratory, Cold Spring Harbor, NY.

Samson, R.Y. & Bell, S.D., 2009. Ancient ESCRTs and the evolution of binary fission. *Trends Microbiol*, 17(11), pp.507-13.

Schiel, J.A. & Prekeris, R., 2010. Making the final cut - mechanisms mediating the abscission step of cytokinesis. *ScientificWorldJournal*, 10, pp.1424-34.

Schiel, J.A., Park, K., Morphew, M.K. et al., 2011. Endocytic membrane fusion and buckling-induced microtubule severing mediate cell abscission. *J Cell Sci*, 124(9), pp.1411-24.

Schwab, M., Lutum, A.S. & Seufert, W., 1997. Yeast Hct1 is a regulator of Clb2 cyclin proteolysis. *Cell*, 90(4), pp.683-93.

Seki, A., Coppinger, J.A., Jang, C.Y. et al., 2008. Bora and the kinase Aurora a cooperatively activate the kinase Plk1 and control mitotic entry. *Science*, 320(5883), pp.1655-8.

Skop, A.R., Liu, H., Yates, J. 3<sup>rd</sup> et al., 2004. Dissection of the mammalian midbody proteome reveals conserved cytokinesis mechanisms. *Science*, 305(5680), pp.61-6.

Sohrmann, M., Fankhauser, C., Brodbeck, C. et al., 1996. The *dmf1/mid1* gene is essential for correct positioning of the division septum in fission yeast. *Genes Dev*, 10(21), pp.2707-19.

Sumara, I., Vorlaufer, E., Stukenberg, P.T. et al., 2002. The dissociation of cohesin from chromosomes in prophase is regulated by Polo-like kinase. *Mol Cell*, 9(3), pp.515-25.

Sunkel, C.E. & Glover, D.M., 1988. *polo*, a mitotic mutant of *Drosophila* displaying abnormal spindle poles. *J Cell Sci*, 89(1), pp.25-38.

Sztul, E. & Lupashin, V., 2006. Role of tethering factors in secretory membrane traffic. *Am J Physiol Cell Physiol*, 290(1), C11-26.

Tanaka, K., Petersen, J., MacIver, F. et al., 2001. The role of Plo1 kinase in mitotic commitment and septation in *Schizosaccharomyces pombe*. *EMBO J*, 20(6), pp.1259-70.

Taniguchi, E., Toyoshima-Morimoto, F. & Nishida, E., 2002. Nuclear translocation of plk1 mediated by its bipartite nuclear localization signal. *J Biol Chem*, 277(50), pp.48884-8.

Teis, D., Saksena, S. & Emr, S.D., 2008. Ordered assembly of the ESCRT-III complex on endosomes is required to sequester cargo during MVB formation. *Dev Cell*, 15(4), pp.578-89.

Teis, D., Saksena, S. & Emr, S.D., 2009. SnapShot: the ESCRT machinery. *Cell*, 137(1), pp.182-182.e1.

Toyoshima-Morimoto, F., Taniguchi, E., Shinya, N. et al., 2001. Polo-like kinase 1 phosphorylates cyclin B1 and targets it to the nucleus during prophase. *Nature*, 410(6825), pp.215-20.

Toyoshima-Morimoto, F., Taniguchi, E. & Nishida, E., 2002. Plk1 promotes nuclear translocation of human Cdc25C during prophase. *EMBO Rep*, 3(4), pp.341-8.

Trautmann, S., Wolfe, B.A., Jorgensen, P. et al., 2001. Fission yeast Clp1p phosphatase regulates G2/M transition and coordination of cytokinesis with cell cycle progression. *Curr Biol*, 11(12), pp.931-40.

Trautmann, S., Rajagopalan, S. & McCollum, D., 2004. The *S. pombe* Cdc14-like phosphatase Clp1p regulates chromosome biorientation and interacts with Aurora kinase. *Dev Cell*, 7(5), pp.755-62.

Vavylonis, D., Wu, J.Q., Hao, S. et al., 2008. Assembly mechanism of the contractile ring for cytokinesis by fission yeast. *Science*, 319(5859), pp.97-100.

Visintin, R., Craig, K., Hwang, E.S. et al., 1998. The phosphatase Cdc14 triggers mitotic exit by reversal of Cdk-dependent phosphorylation. *Mol Cell*, 2(6), pp.709-18.

Visintin, R., Hwang, E.S. & Amon, A., 1999. Cfi1 prevents premature exit from mitosis by anchoring Cdc14 phosphatase in the nucleolus. *Nature*, 398(6730), pp.818-23.

Watanabe, N., Arai, H., Nishihara, Y. et al., 2004. M-phase kinases induce phospho-dependent ubiquitination of somatic Wee1 by SCFbeta-TrCP. *PNAS*, 101(13), pp.4419-24.

Wegener, A.D. & Jones, L.R., 1984. Phosphorylation-induced mobility shift in phospholamban in sodium dodecyl sulfate-polyacrylamide gels. Evidence for a protein structure consisting of multiple identical phosphorylatable subunits. *J Biol Chem*, 259(3), pp.1834-41.

Whitley, P., Reaves, B.J., Hashimoto, M. et al., 2003. Identification of mammalian Vps24p as an effector of phosphatidylinositol 3,5-bisphosphate-dependent endosome compartmentalization. *J Biol Chem*, 278(40), pp.38786-95.

Wilson, G., Fielding, A.B., Simon, G.C. et al., 2005. The FIP3-Rab11 protein complex regulates recycling endosome targeting to the cleavage furrow during late cytokinesis. *Mol Biol Cell*, 16(2), pp.849-60.

Wolfe, B.A., McDonald, W.H., Yates, J.R. 3<sup>rd</sup> et al., 2006. Phospho-regulation of the Cdc14/Clp1 phosphatase delays late mitotic events in *S. pombe*. *Dev Cell*, 11(3), pp.423-30.

Wollert, T., Wunder, C., Lippincott-Schwartz, J. et al., 2009. Membrane scission by the ESCRT-III complex. *Nature*, 458(7235), pp.172-7.

Wollert, T. & Hurley, J.H., 2010. Molecular mechanism of multivesicular body biogenesis by ESCRT complexes. *Nature*, 464(7290), pp.864-9.

Wu, J.-Q., Kuhn, J.R., Kovar, D.R. et al., 2003. Spatial and temporal pathway for assembly and constriction of the contractile ring in fission yeast cytokinesis. *Dev Cell*, 5(5), pp.723-34.

Yamano, H., Kitamura, K., Kominami, K. et al., 2000. The spike of S phase cyclin Cig2 expression at the G1-S border in fission yeast requires both APC and SCF ubiquitin ligases. *Mol Cell*, 6(6), pp.1377-87.

Yang, D., Rismanchi, N., Renvoisé, B. et al., 2008. Structural basis for midbody targeting of spastin by the ESCRT-III protein CHMP1B. *Nat Struct Mol Biol*, 15(12), pp.1278-86.

Yorikawa, C., Shibata, H., Waguri, S. et al., 2005. Human CHMP6, a myristoylated ESCRT-III protein, interacts directly with an ESCRT-II component EAP20 and regulates endosomal cargo sorting. *Biochem J*, 387(1), pp.17-26.

Zhao, W., Seki, A. & Fang, G., 2006. Cep55, a microtubule-bundling protein, associates with centralspindlin to control the midbody integrity and cell abscission during cytokinesis. *Mol Biol Cell*, 17(9), pp.3881-96.